Helical Polymers: Synthesis, Structures, and Functions

Eiji Yashima,*,† Katsuhiro Maeda,‡ Hiroki Iida,† Yoshio Furusho,† and Kanji Nagai†,§

Department of Molecular Design and Engineering, Graduate School of Engineering, Nagoya University, Chikusa-ku, Nagoya 464-8603, Japan, and Graduate School of Natural Science and Technology, Kanazawa University, Kakuma-machi, Kanazawa 920-1192, Japan

Received April 23, 2009

Contents

1. Introduction

The helix is the central structural motif in biological macromolecules, such as DNA and proteins, and is also the ubiquitous object in nature from microscopic to macroscopic points of view. Most importantly, the helical conformation is inherently chiral, and right- and left-handed helices are exactly mirror images of each other; therefore, they cannot be superimposed. Accordingly, if one of the helices could be selectively synthesized, induced, or constructed for molecules, supramolecules, oligomers, or polymers, they should be optically active without any additional configurationally chiral components. Inspired by sophisticated biological helices that are of key importance for their elaborate functions in living systems involving molecular recognition, replication, and catalytic activity, chemists have been challenged to develop artificial helical polymers, supramolecules, and oligomers with a controlled handedness, not only to mimic biological helices and functions but also for their potential applications in materials science, such as ferroelectric liquid crystals (LCs) and nonlinear optical materials, sensing specific molecules, the separation of enantiomers, and asymmetric catalysis.

The history of helical polymers extends back to the 1950s, when Pauling and Watson and Crick discovered the right-

* E-mail: yashima@apchem.nagoya-u.ac.jp.
† Nagoya University.
‡ Kanazawa University.
§ Present address: Department of Applied Chemistry, Graduate School of Engineering, Nagoya University.

10.1021/cr900162q CCC: $71.50
Published on Web 11/11/2009

Eiji Yashima received his B.S. (1982), M.S. (1984), and Ph.D. (1988) degrees from Osaka University in the group of Prof. Yoshio Okamoto. In 1986, he joined Kagoshima University, working with Prof. Mitsuru Akashi as Assistant Professor. After spending one year at UMass with Prof. David A. Tirrell, he moved to Nagoya University and was promoted to a full Professor in 1998. He was the project leader of the ERATO Project (JST) on "Yashima Super-structured Helix" (2002−2007). He received the Wiley Polymer Science Award from the SPSJ in 2000, the Japan IBM Science Award in 2001, the Molecular Chirality Award in 2005, the Thomson Scientific Research Front Award in 2007, and the Award of the Society of Polymer Science, Japan, in 2008. His current research interests are in the design and synthesis of helical molecules, supramolecules, and polymers with novel functions.

Katsuhiro Maeda received his B.S. (1993), M.S. (1995), and Ph.D. (1998) degrees from Nagoya University in the group of Prof. Yoshio Okamoto. In 1998, he joined the faculty at Nagoya University and was promoted to Associate Professor in 2002. After spending six months at MIT with Prof. Tim Swager, he moved to Kanazawa University in 2008.

handed α-helix for proteins[1] and the right-handed double-stranded helix for DNA[2] in 1951 and 1953, respectively. After the discovery of these biological helical structures, remarkable progress has been made in molecular biology, and their amazing functions have been elucidated at a molecular level.[3,4] It cannot be overemphasized, however, that at the same time as the discovery of these biological helices, Natta in 1955 found that the highly isotactic polypropylene synthesized by the Ziegler−Natta catalyst possessed a helical conformation in the crystalline state.[5] Although the isotactic helical polypropylene exists in an equal mixture of right- and left-handed helices in the solid state and the polypropylene cannot maintain its helical conformation, thus instantly changing to a random conformation once dissolved in solvents, this was a significant milestone in the field of synthetic helical polymers, through which a number of isotactic vinyl polymers have been prepared and their helical structures in the crystalline state have been revealed.[6]

Hiroki Iida received his B.S. (2000), M.S. (2002), and Ph.D. (2005) degrees from Osaka University in the group of Prof. Takeshi Naota. After spending one year and five months at University of Texas at Austin, working with Prof. Michael J. Krische, he joined the group of Prof. Eiji Yashima at Nagoya University as Assistant Professor in 2007.

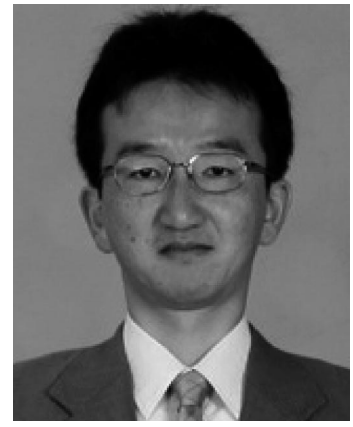

Yoshio Furusho received his B.S. (1991), M.S. (1993), and Ph.D. degrees (1998) from the University of Tokyo in the group of Prof. Takuzo Aida. In 1995, he joined Osaka Prefecture University as an Assistant Professor, working with Prof. Toshikazu Takata. After spending one year in Strasbourg, working with Prof. Jean-Pierre Sauvage, he joined the ERATO Project as a Group Leader in 2003, and he accepted his Associate Professor position at Nagoya University in 2008.

Kanji Nagai received his B.S. (2004), M.S. (2006), and Ph.D. (2009) degrees from Nagoya University in the group of Prof. Eiji Yashima. Currently, he is an Assistant Professor in the group of Prof. Masami Kamigaito at Nagoya University.

Pino et al. systematically investigated the structural and chiroptical properties of a series of optically active isotactic vinyl polymers prepared by the polymerization of α-olefins bearing optically active substituents in the 1960s and, for

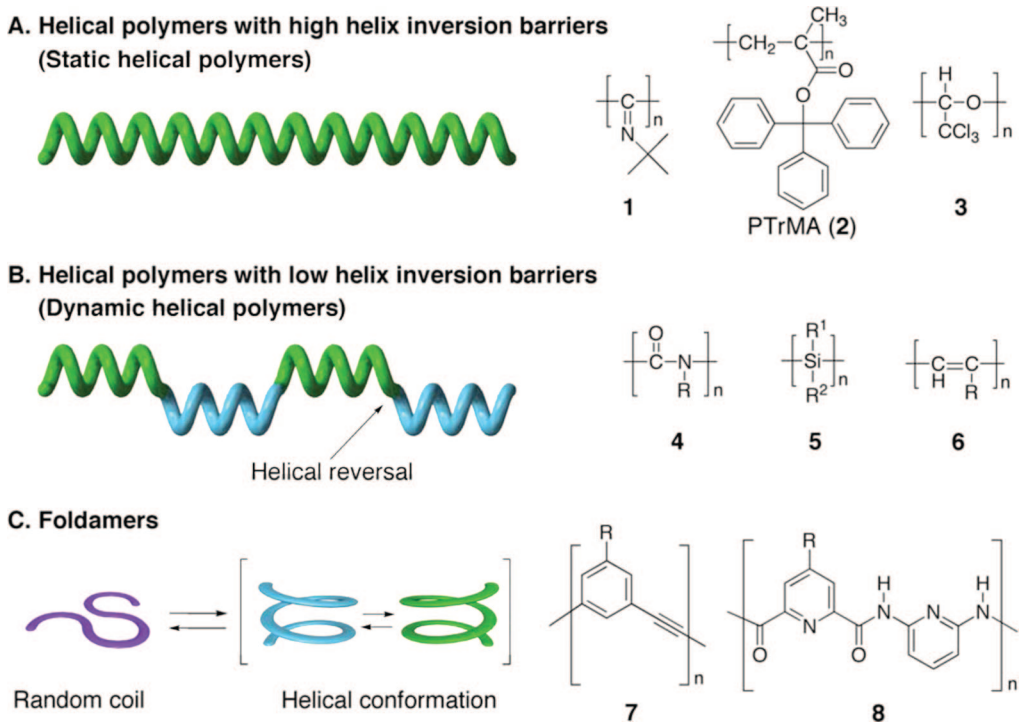

Figure 1. Three types of helical polymers and their representative structures.

the first time, revealed the helical conformation of synthetic vinyl polymers with an excess one-handed helical sense in solution,[7] although the helical polyolefins are totally dynamic and composed of very short helical segments separated by frequently occurring helical reversals among disordered, random coil conformations, as later pointed out by Green et al.[8] Therefore, the helical polymers, in particular, helical vinyl polymers stable in solution, had been considered difficult to synthesize at that time.[9,10]

Since the 1970s, however, significant progress in developing synthetic helical polymers that retain their helical conformations in solution has been achieved by the groups of Nolte, Okamoto, Green, Fujiki, and others. The details of their pioneering studies have been thoroughly reviewed elsewhere,[10−21] but a brief overview is described here (Figure 1).

Nolte and Drenth et al. successfully resolved poly(*tert*-butyl isocyanide) (**1**) into enantiomeric right- and left-handed helices by chiral chromatography in 1974.[22] Later, Okamoto and Yuki et al., for the first time, synthesized an optically active helical vinyl polymer (PTrMA, **2**) by the helix-sense-selective polymerization of an achiral monomer, triphenylmethyl methacrylate (TrMA), using chiral anionic initiators in 1979, which produced an excess single-handed, fully isotactic helical polymer with a large specific rotation.[23] These findings clearly provide convincing evidence that a helical conformation that is stable in solution can be synthesized when bulky substituents are introduced as the pendant groups of specific polymers. In addition, the one-handed helical **2** shows a significant chiral recognition ability for a wide variety of racemic compounds, affording a practically useful chiral stationary phase (CSP) for high-performance liquid chromatography (HPLC).[24] This was a significant breakthrough in the field of synthetic helical polymers, through which a number of optically active polymers have been prepared and applied to CSPs in HPLC. Isotactic polychloral (**3**) was also proposed to be helical in the solid state by Vogl et al. in 1980,[25] which has been confirmed by NMR and X-ray crystallographic analyses of the uniform chloral oligomers.[26,27]

On the other hand, Green and co-workers discovered in 1988 another type of helical polymer, i.e., the dynamic helical polyisocyanates (**4**),[28] and experimentally and theoretically revealed their characteristic helical structures that consist of interconvertible right- and left-handed helical conformations separated by rarely occurring helical reversals. Green et al. have further demonstrated the unique feature of chiral amplification in polyisocyanates by a small chiral bias through covalent or noncovalent bonding interactions with a high cooperativity, resulting in a large helical sense excess of the entire polymer chains.[17] This discovery is one of the key studies in helical polymers, in recognition of the fact that a large number of optically active polymers that involve polysilanes (**5**),[18] polyacetylenes (**6**),[19,20,29,30] and others (see section 2) belong to this category.

Based on these pioneering studies, the already prepared synthetic helical polymers exhibiting an optical activity solely due to their macromolecular helicity can be basically classified into two categories with respect to their helix inversion barriers. As a result, the optically active **1**−**3** have a rigid helical structure with a sufficiently high helix inversion barrier (static helical polymers). Therefore, optically active helical polymers **1**−**3** with a one helical sense excess can be prepared by the helix-sense-selective polymerization of the corresponding achiral monomers with chiral catalysts or initiators under kinetic control (Figure 1A). On the other hand, the dynamic helical polymers, such as **4**−**6**, possess a very low helix inversion barrier, and therefore, a predominantly one-handed helical conformation can be induced in the presence of a small amount of chiral residue at the pendant or terminal ends or stimulant, and their helical senses are determined under thermodynamic control (Figure 1B). Certain helical polymers, however, exhibit both features depending on the structures of the repeating monomer units; in other words, the boundary between the static and dynamic

Scheme 1. Helix-Sense-Selective Anionic Polymerization of TrMA

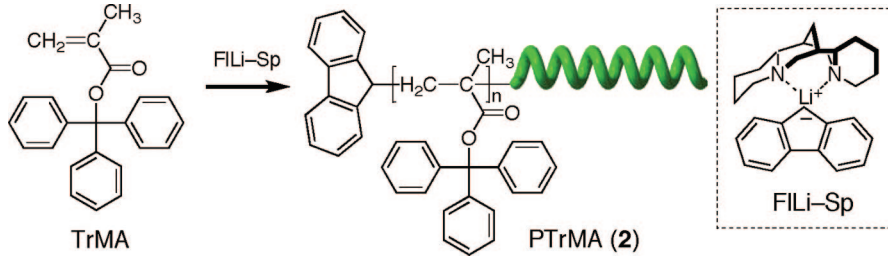

helical conformations is totally dependent on the helix inversion barrier.

Foldamers, which were first defined by Gellman[31] as "any polymer with a strong tendency to adopt a specific compact conformation", have become one of the emerging research areas in supramolecular chemistry, and foldamer motifs (**7** and **8**), which fold into a preferred-handed helical conformation developed by Moore et al.[32] and Hamilton,[33] Lehn,[34] and Huc et al.,[35] have been applied to the design and synthesis of novel helical polymers with a controlled helical sense. Such foldamer-based helical polymers may be regarded as a kind of dynamic helical polymer in terms of cooperativity during an excess single-handed helix formation through intra- and/or intermolecular noncovalent bonding interactions but differ from typical dynamic helical polymers (Figure 1B) in random conformational preferences under certain experimental conditions (Figure 1C).

In 2001, Nakano and Okamoto,[15] and Rowan, Nolte, Sommerdijk, and co-workers[16] reported the comprehensive reviews of synthetic helical polymers, while Moore et al. reviewed foldamers[32] in this journal. Here, the complete progress in the synthesis of helical polymers, their unique properties, structures, and functions mostly since 2001 along with historically important research studies will be described. Remarkable progress that has been achieved in synthetic double-stranded helical polymers and oligomers that resemble the DNA double helix in terms of structure and function has also been demonstrated in this review. The vast areas of helical assemblies of small molecules and oligomers[19,36−43] and biorelated helical polymers and oligomers, such as peptide nucleic acids (PNAs),[44] α-, *β*-, and *γ*-peptides,[45,46] and peptoids[47] are not included in this review but have been reviewed elsewhere.[48]

2. Synthesis of Helical Polymers

2.1. Helical Polymers with High Helix Inversion Barriers (Static Helical Polymers)

In principle, optically active static helical polymers can be synthesized by either the polymerization of optically active monomers or the helix-sense-selective polymerization of achiral or prochiral monomers using chiral initiators or catalysts, when the helix inversion barriers are sufficiently high. For these synthetic methods, the helical structures of the polymers, such as the helical sense and helical pitch, are determined by chiral substituents covalently bonded to the polymer backbones or by the chirality of chiral ligands or initiators under kinetic control during the polymerization. Figure 1A shows typical synthetic, static helical polymers that exhibit an optical activity mainly due to their preferred-handed helical conformations. These helical conformations are stable even in solution because of the sufficiently large steric repulsion between the bulky side groups.

2.1.1. Polymethacrylates and Polymethacrylamides

Helical PTrMA (**2**) has been, for the first time as a vinyl polymer, prepared by the helix-sense-selective polymerization of an achiral (prochiral) monomer, triphenylmethyl methacrylate (TrMA), using anionic initiators such as 9-fluorenyllithium (FlLi) complexed with chiral ligands such as (−)-sparteine (Sp),[49] which results in a single-handed, fully isotactic helical polymer showing a large optical rotation ($[\alpha]_D$ *ca.* +380°) (Scheme 1).[15,23] The chiral sparteine ligand controls the main-chain configuration as well as the helical sense of the polymer. Most importantly, the bulky triphenylmethyl groups prevent the polymer from unfolding the helical conformation produced through the polymerization process. Therefore, the optical activity of PTrMA disappears when the bulky triphenylmethyl groups are removed from the polymer chain. The helical structure of PTrMA has been further clarified by the optical resolution of an optically inactive PTrMA prepared by achiral anionic initiators with chiral chromatography, which affords two fractions showing opposite optical rotations. The optically active helical PTrMA is a practically useful chiral packing material for HPLC, showing a remarkable chiral recognition for a variety of racemic compounds, as briefly described in section 5.1.

Since the discovery of the helix-sense selection during the polymerization of TrMA, Okamoto et al. have prepared a series of analogous helical poly(triarylmethyl methacrylate)s by the helix-sense-selective polymerization of bulky methacrylates (**9**−**12**, Chart 1) and have investigated their helical structures, chiroptical properties, and chiral recognition abilities as well as the mechanism of the helix-sense-selective polymerization.[15] Although anionic polymerization techniques have often been used for the synthesis of the helical polymethacrylates, free-radical polymerization has proven to be an alternative and more versatile way to produce a helical polymethacrylate from **11**.[50] An almost perfect isotactic polymer with an excess one-handedness has been prepared by the free-radical polymerization of **11** with 1,1′-azobisisobutyronitrile (AIBN) in the presence of chiral chain transfer agents or cobalt(II) complexes (**13**, **14**) that interact with the growing radical[51] or in chiral solvents.[15]

The isotacticity (*mm*) of PTrMA obtained by radical polymerization ranges from 64 to 99% and depends on the monomer concentrations, temperatures, and solvents. The reason was not clear but was considered to be due to changes in the kinetic and thermodynamic control.[52] The fact that the isotacticity increases with the decreasing monomer concentration suggests the possibility of preparing stereogradient polymers by giving the chains a living nature. Kamigaito et al. have recently demonstrated the formation of stereogradient polymers by the reversible addition−fragmentation chain transfer (RAFT) polymerization of TrMA, in which the isospecificity gradually increased with a decrease in the monomer concentrations.[53] This is most likely caused

Chart 1

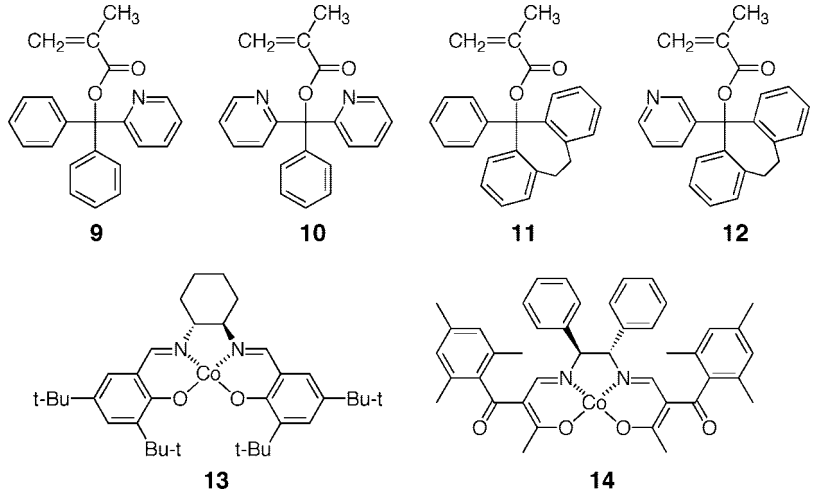

Chart 2

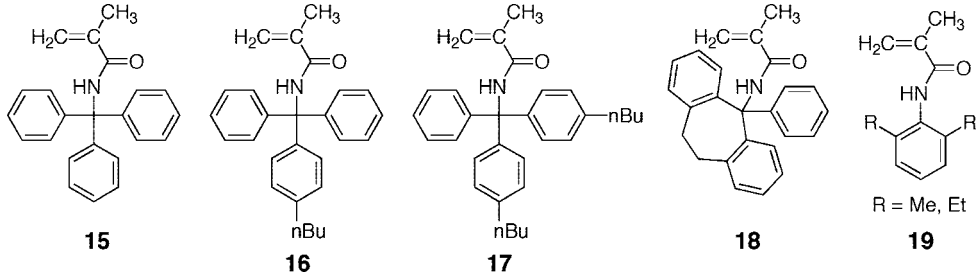

by the propagation−depropagation equilibrium, which can convert a less stable growing PTrMA terminal with the *r* conformation into the more stable *m* form, especially at a lower monomer concentration.

The radical polymerization of bulky *N*-triphenylmethyl methacrylamides (**15**—**18**, Chart 2) in the presence of (+)- and (−)-menthol also produces highly isotactic, optically active helical polymers, although the helix-sense excess of the polymers seems lower than that of PTrMA.[54] In the case of the radical polymerization of *N*-phenyl methacrylamides in L- or D-menthol, only the 2,6-disubstituted derivatives, such as **19**, produce optically active polymers.[55] On the other hand, the anionic polymerization of *N*-triphenylmethyl methacrylamides with *n*-butyllithium does not proceed due to the presence of its acidic NH proton. However, the chiral anionic initiator system consisting of the organozincates with chiral additives, such as *n*-Bu_4ZnLi_2/2,3,4,6-tetra-*O*-acetyl-α-D-galactopyranosyl bromide, allows the helix-sense-selective anionic polymerization of the bulky methacrylamide **16** to afford the highly isotactic, optically active helical polymer.[56]

Chen et al. have developed the helix-sense-selective coordination polymerization of *N*,*N*-diphenyl acrylamides (**20**) using the optically active (*R*,*R* or *S*,*S*)-*ansa*-zirconocenium ester enolate catalyst (**21**) (Chart 3) at room temperature and successfully obtained optically active helical poly(*N*,*N*-diphenyl acrylamide)s (poly-**20**) and their block copolymers using methyl methacrylate (MMA).[57,58] The magnitude of the specific rotation of poly-**20b** obtained with (*R*,*R*)-**21** ($[\alpha]_D$ +180°) seems to be comparable or greater than that obtained by the helix-sense-selective anionic polymerization with FlLi-Sp ($[\alpha]_{365}$ −657°) at −98 °C.[59]

Poly(dibenzofulvene) is a vinyl polymer but has no stereogenic centers in its polymer backbone. Poly-**22** obtained by the anionic polymerization of 2,7-di-*n*-pentyldibenzofulvene (**22**) using the complexes of FlLi with chiral ligands, such as Sp, shows a significant CD signal in the film state but almost no CD in solution (Scheme 2A).[60] A π-stacked structure is indicated for poly-**22** based on a significantly high hypochromicity in the absorption and exclusive dimer emission of the fluorescence spectra. Therefore, the observed CD for the poly-**22** film has been considered to be due to the helical conformation of

Chart 3

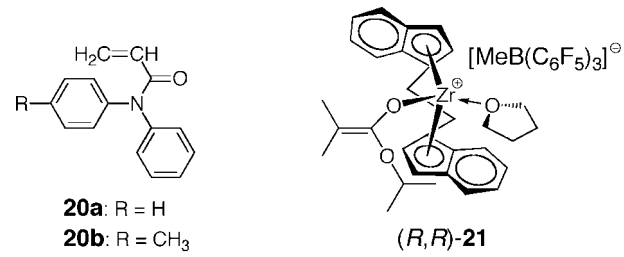

Scheme 2

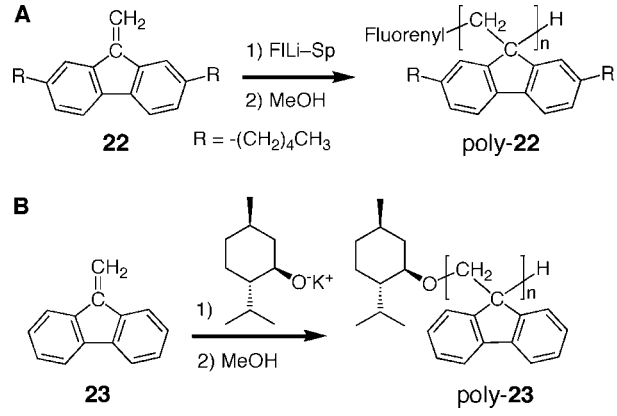

Table 1. Estimated Activation Energy Values for the Helix-Sense Inversion of Various Helical Polymers

polymer		activation energy (kJ mol^{-1})	method[a]	ref
polymethacrylate	poly-**9**	$E_a = 96$	A	64
polycrotonate	poly-**24**	$\Delta H^{\neq} = 119$[b]	B	65
oligochloral	**305a** ($n = 3$)	$\Delta G^{\neq}_{-98} = 34.3$	C	27
	305b ($n = 4$)	$\Delta G^{\neq}_{4} = 53.2$	C	26, 27
	305c ($n = 5$)	$\Delta G^{\neq}_{72} = 68.6$	C	26, 27
	305d ($n = 6$)	$\Delta G^{\neq}_{140} = 82.0$	C	27
oligoquinoxaline	oligo-**53a′** ($n = 6$)	$E_a = 100$	A	104
	oligo-**53b′** ($n = 5$)	$E_a = 106$	A	104
	oligo-**53c′** ($n = 6$)	$E_a = 133$	A	104
polyisocyanate	**63**	$\Delta G^{\neq}_{100} = 79.5$	C	118
polyacetylene	**93c**	$\Delta G^{\neq}_{110} = 77.4$[c]	C	190
oligopeptide	**247**−**249**	$\Delta G^{\neq}_{20} = 86.6$[d]	B	384

[a] A, Arrhenius plots of the rate constants; B, Eyring plots of the kinetic data; C, dynamic ^{1}H NMR spectroscopy. [b] The activation enthalpy value for the helix-sense inversion. [c] The observed value may be underestimated because, at elevated temperature, unavoidable *cis*-to-*trans* isomerization took place in part to reduce the stereoregularity of the polymer. [d] The effect of guest (**249**) binding on the rate of helix inversion could be negligible.

poly-**22** with a helix-sense bias. In contrast, the poly-**22** hardly shows any chiroptical properties in solution, suggesting that the polymer may possess a cryptochiral property.[61] The preferred-handed helical conformation of the poly-**22** induced during the polymerization may be amplified and stabilized in the solid state as a result of intermolecular cooperative effects. An optically active poly(dibenzofulvene) bearing a chiral terminal group (poly-**23**) has also been synthesized by the anionic polymerization of **23** with potassium L-menthoxide as the initiator (Scheme 2B).[62] The obtained poly-**23** exhibits CD bands in the absorption region of the fluorenyl units, which indicates a preferred-handed helical conformation induced to the stacked main-chain by the chiral terminal group. The CD intensity was reversibly changed by heating or cooling, suggesting that the helix-sense bias is dependent on the temperature. The chiral influence of the terminal group decreased as the chain length increased, and the influence seems to be especially significant on the first three monomeric units from the chain terminal. Based on the theoretical CD calculations, a left-handed helical conformation is postulated for the poly-**23** with the twist angle of *ca.* 10−20° between neighboring monomeric units.

An unprecedented inversion of the macromolecular helicity (see section 2.8) in solution has been observed for a low molecular weight, one-handed helical poly(diphenyl-2-pyridyl methacrylate) (poly-**9**) prepared from **9**, accompanied by a gradual decrease in the optical rotation with time. This change in the optical rotation is ascribed to the helix−helix transition of the main-chain (helix inversion), that is, the change from the one-handed helix to a mixture of right- and left-handed helices, which has been further evidenced by the chromatographic separation into two fractions showing

Scheme 4

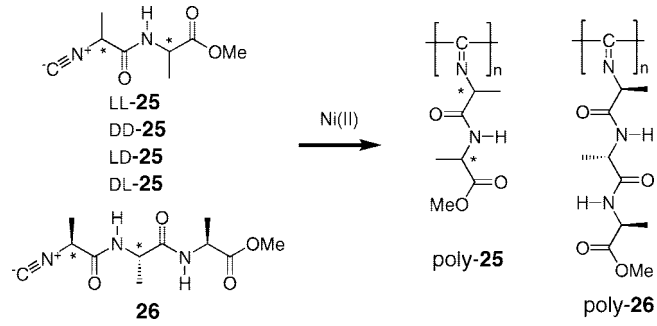

opposite optical rotations.[63] The activation energy (E_a) for the helix-sense inversion (racemization) of poly-**9** has been estimated to be 96 kJ mol^{-1} (Table 1).[64]

The polymerization of triphenylmethyl crotonate (**24**), which is a constitutional isomer of TrMA, with FlLi complexed with (*S*,*S*)-(+)-2,3-dimethoxy-1,4-bis(dimethylamino)butane (DDB) affords an optically active and highly threodiisotactic poly(triphenylmethyl crotonate) (poly-**24**) (Scheme 3). The optical rotation of poly-**24** gradually and irreversibly decreased at 60 °C, which may be ascribed to the helix−helix transition of the main-chain. From the rate constant at 50 and 60 °C, the activation enthalpy ($\Delta H^{\neq}$) for the inversion of helicity of poly-**24** has been determined to be 119 kJ mol^{-1} (Table 1).[65]

2.1.2. Polyisocyanides

Polyisocyanides with a bulky side group are considered to possess a stable 4/1 helical conformation even in solution. This helical structure was first proposed by Millich[66] and confirmed by Nolte et al. through the direct resolution of poly(*tert*-butyl isocyanide) (**1**) into enantiomeric helices by liquid chromatography using a CSP composed of an optically active polyisocyanide.[22] The resolved polymer with a positive rotation was assumed to have a left-handed helix based on a CD spectral analysis.[67] The stable helical conformation of the polyisocyanides has further been revealed by the helix-sense-selective polymerization of achiral bulky isocyanides by Nolte[68] and Novak.[69]

Since the discovery of the helical polyisocyanides, Nolte and co-workers and other groups have further synthesized a wide variety of functional polyisocyanides with a controlled helical architecture.[16,70,71] Recent progress in the synthesis, structures, and chiroptical properties of helical polyisocyanides is described below.

A series of helical polyisocyanides bearing chiral peptide pendants, such as poly-**25** and poly-**26** (Scheme 4), called "poly(isocyanopeptide)s", have been prepared by the polymerization of the corresponding α-amino acid-bound isocyanide monomers with a Ni(II) catalyst. They form very stable β-helical architectures stabilized by the intramolecular

Scheme 3

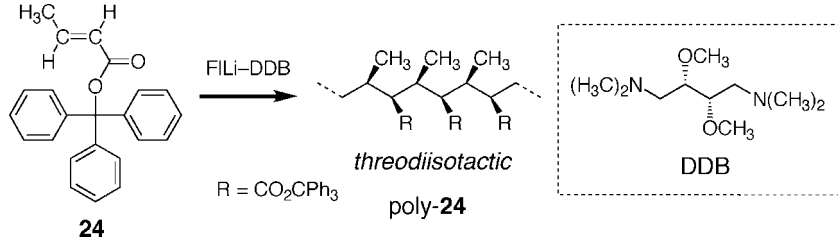

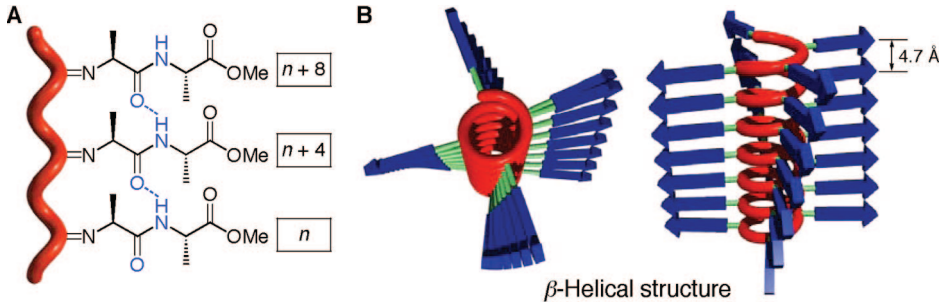

Figure 2. (A) Schematic representation of the intramolecular hydrogen bond formation between the amide groups in side chains *n* and (*n* + 4) of helical poly(isocyanopeptide)s. (B) Schematic model showing a 4/1 helical backbone (red) and the β-strands (blue). Side (right) and top (left) view highlighting the stacked arrangement of the β-strands.

Chart 4

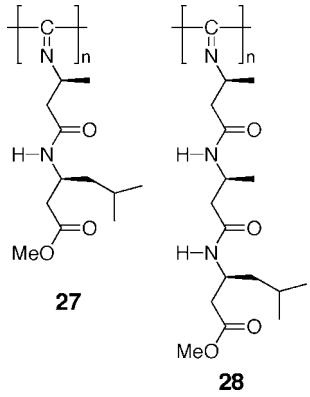

hydrogen bonding networks formed between the peptide side chains *n* and (*n* + 4) parallel to the polymer backbone (Figure 2).[72,73] Analogous to the denaturation of proteins, disruption of the hydrogen bonds in these poly(isocyano-α-peptide)s is anticipated to lead to unfolding of the helical structure. However, the unfolding takes place only when using strong acids, such as trifluoroacetic acid (TFA), but not with hydrogen bond breaking solvents, such as methanol and dimethyl sulfoxide (DMSO), thereby demonstrating the robust helical scaffold assisted by hydrogen bond arrays.[74] Moreover, the secondary network makes the array rigid, resulting in extremely stiff helical polymers (persistence length (*q*) = 76 nm), which prevents the unwinding of the helix in polar solvents.[74,75]

Nolte et al. further synthesized helical poly(isocyanopeptide)s derived from β-amino acids (**27**, **28**, Chart 4).[76] The resulting poly(isocyano-β-peptide)s also possess a preferred-handed helical conformation stabilized by an internal hydrogen-bonding network along the polymeric backbone. In sharp contrast to their poly(isocyano-α-peptide) counterparts, the helical structures of the poly(isocyano-β-peptide)s are dynamic in nature and their helical conformations initially formed during the polymerization readily convert into another helix with time and also to a nonhelical conformation in the presence of TFA, presumably due to rather flexible β-peptide side arms. In particular, the CD spectral pattern of **27** dramatically and irreversibly changed with time, and the Cotton effect sign became inverted and accompanied by a change in its specific rotation value from −87.5 to 27.8°. Such inversions of the Cotton effect and optical rotation signs have been ascribed to helix inversion (see section 2.8). In the present case, however, a change in the arrangement of the hydrogen-bonded amide groups coupled to a possible change in the helical pitch of the preferred-handed helical polyisocyanide has been taken into consideration based on the IR measurement results. Unexpectedly, the altered helical conformation of the poly(isocyano-β-peptide)s turned out to be much more stable than that of their poly(isocyano-α-peptide) counterparts upon heating. Upon the addition of TFA, both the original and altered poly(isocyano-β-peptide)s completely lost their chiroptical activity, indicating the unfolding into a nonhelical conformation. When the solutions were subsequently neutralized, only the energetically more favorable altered conformation of the polymers was regained. As a consequence, polyisocyanides are not completely a static helical polymer but possess a dynamic helical feature depending on the pendant groups, as demonstrated for the helicity induction and memory effect observed in the poly(4-carboxyphenyl isocyanide) (see section 2.7.1).

The TFA-initiated polymerization of isocyanopeptides has been found to produce extremely long polymers with lengths up to 14 μm.[77] For the polymerization of LD-**25** at the low TFA concentration of 1 mM, a large entropy of activation (−170 J mol^{-1} K^{-1}) has been revealed by kinetic studies, indicating a very high degree of organization in the transition state (route A in Figure 3). At higher TFA concentrations, however, conversion of the monomer into the corresponding formamide takes place instead of polymerization (route B). Based on these results, a TFA-initiated polymerization mechanism has been proposed; first a helical oligomer is formed, acting as a helical template for the incorporation of subsequent monomer units through a supramolecular complex (route A).[77] In the case of high TFA concentrations, the template is likely disrupted and destroyed by the TFA and no further polymerization takes place (route B). The fact that LL-**25** itself cannot be polymerized with TFA demonstrates that LL-**25** may not be able to form such an active helical template due to the higher steric repulsion between the monomeric units in the helix.

Quite interestingly, the TFA-initiated polymerization of diastereomeric and enantiomeric isocyanopeptides **25** proceeds in a highly stereospecific manner.[77] Poly-LD-**25** prepared by TFA maintains its polymerization activity and can be used as a macroinitiator for the further block copolymerizations of **25**. Upon the addition of LD-**25**, the block copolymerization takes place as expected, while no further block copolymerization proceeded in the presence of the enantiomeric DL-**25** and even with 1% DL-**25**, indicating that propagation of the macroinitiator poly-LD-**25** was completely blocked with a trace amount of DL-**25**. A similar perfect enantiomer-selective block copolymerization turned out to be possible for LL-**25** and DD-**25**; poly-LD-**25** favorably copolymerized LL-**25**, whereas its enantiomeric counterpart, DD-**25**, was never copolymerized with the macroinitiator poly-LD-**25**. These extremely high enantiomer and diastere-

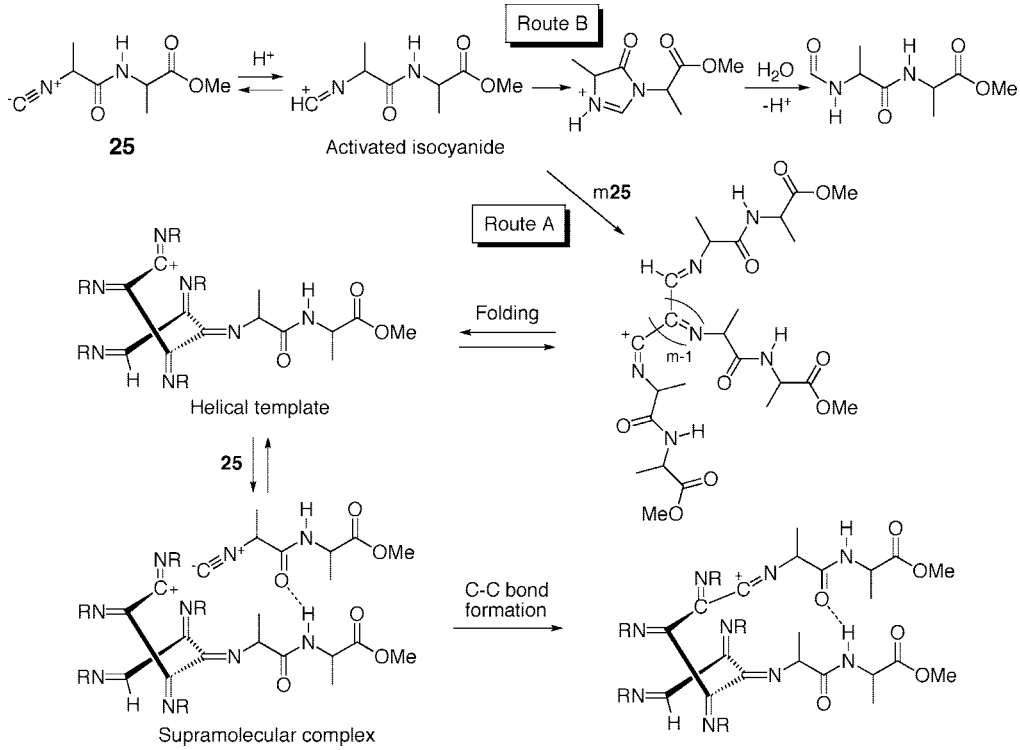

Figure 3. Proposed initiation and propagation of the acid-initiated polymerization of isocyanopeptides **25** (route A) and a side reaction forming the formamide via a cyclic imidazolone (route B).

Chart 5

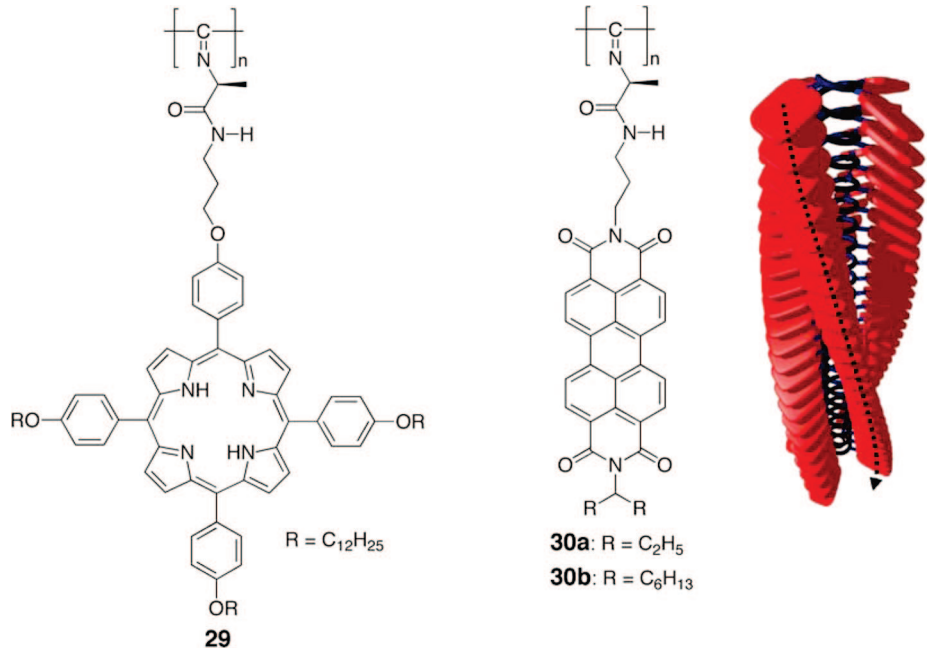

omer selectivities in the block copolymerization processes demonstrate the critical effect of the absolute configuration of the first stereogenic center of the monomers **25** on the block copolymerization by poly-LD-**25**. Most importantly, all of the above monomer combinations could readily be copolymerized with a Ni(II) catalyst. These results together with no polymerizability of LL-**25** with TFA suggest that the TFA-initiated stereospecific and enantiomer-selective polymerization of isocyanopeptides appears to be specific and exclusive, and a highly organized supramolecular complex likely plays an important role.

A unique rigid-rod helical polyisocyanide architecture has been employed as an attractive scaffold for organizing functional chromophores into a one-handed helical array along the polymer backbone (Chart 5). A rigid helical poly(isocyanopeptide) (**29**) bearing well-defined arrays of porphyrins assisted by an intramolecular hydrogen-bonded network has been synthesized, and its physical and optical properties have been studied.[78] Each polymer strand contains four columns of around 200 stacked porphyrins and has an overall length of 87 nm. The porphyrin rings are arranged in a left-handed helical fashion along the helical backbone.

Scheme 5

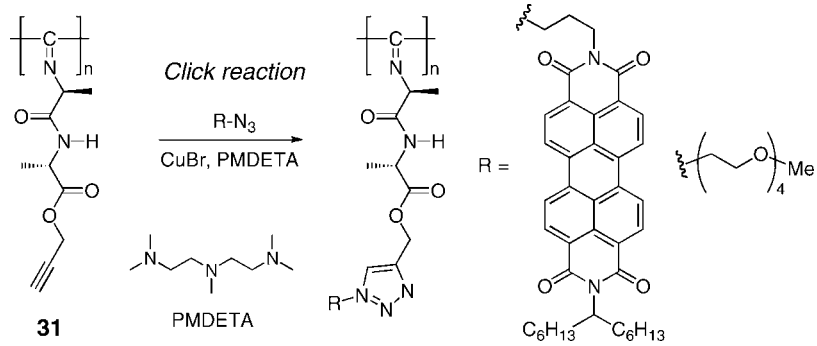

Photophysical studies showed that at least 25 porphyrins within one column are exceptionally coupled.

The perylenediimide functionalized polyisocyanides (**30**) have also been synthesized as a synthetic antenna system, which could be possibly applied as n-type materials in organic photovoltaics.[79−82] The fluorescence decay of the monomer is monoexponential with a characteristic lifetime value (τ) of 3.9 ns, while the polymer showed a lifetime value of 19.9 ns, a typical value for excimer-like species.[81] When blended with an electron-donor system, such as regioregular poly(3-hexylthiophene), **30b** demonstrated a relative improvement in charge generation and diffusion as compared to the monomeric, aggregated perylenediimide.[79] Atomic force microscopy (AFM) investigations revealed that the two polymers form interpenetrating bundles with a nanophase-segregated character, featuring a high density of contact points between the two different phases. Kelvin probe force microscopy on submonolayer-thick films visualized the relationship between the architecture and the photovoltaic efficiency,[79] thus allowing the direct visualization of the photovoltaic activity occurring in a nanoscale phase-segregated ultrathin film at a true nanoscale spatial resolution, which enables a study of the correlation between function and architecture at a nanoscale resolution.

As described above, the preparation of polyisocyanides with the desired chromophoric pendants arranging in a preferred-handed helical array requires the synthesis of the chromophore-containing isocyanide monomers before the polymerization, which often encounters laborious synthetic procedures. In order to overcome this problem, the copper-catalyzed click reaction (see section 2.3.1)[83] of a novel helical poly(isocyanopeptide) containing acetylene groups on the side arms as a scaffold (**31**), with a variety of azides, has been employed (Scheme 5).[84] A chromophoric water-soluble polymeric nanowire was obtained by the click reaction of **31** with ethylene glycol azide and perylene azide. The potential to incorporate multiple chromophores has also been demonstrated by the reaction of **31** with perylene azide and azidocoumarin dyes. A helical poly(isocyanopeptide) bearing the coumarin moieties showed a blue-shifted emission from the coumarin due to the interaction with the coupled perylene molecules.

An unprecedented helix-sense-controlled polymerization has been found for the polymerization of one enantiomer of phenyl isocyanide (L-**32**) bearing an L-alanine pendant with a long *n*-decyl chain through an amide linkage with an achiral nickel catalyst ($NiCl_2$), which produced both diastereomeric right- and left-handed helical polyisocyanides (poly-L-**32**) whose helical sense can be controlled by the polymerization solvent and temperature (Figure 4).[85] The CD spectra of the poly-L-**32**s obtained by the polymerization of L-**32** at ambient temperature in nonpolar solvents, such as CCl_4 (poly-L-**32a**) and toluene (poly-L-**32b**), exhibited the positive first Cotton effects, which are opposite to those of the polymers prepared in polar tetrahydrofuran (THF) (poly-L-**32c**) (Figure 4B). This suggests that the helix-senses of poly-L-**32a** and poly-L-**32c** are opposite to each other, although all of these polymers have the same L-alanine pendants. Moreover, the resulting helical polyisocyanides with the opposite helix-sense form lyotropic, cholesteric LCs with the opposite twist-senses (Figure 4C and D). This unusual change in the helical sense of the poly-L-**32**'s depending on the polymerization solvent can be ascribed to the "on−off" fashion of the intermolecular hydrogen bonds between the pendant amide residues of the growing chain end and L-**32** during the propagation reaction, which may force the poly-L-**32** into either a right- or left-handed helical structure. In nonpolar solvents, the polymerization proceeds under predominantly kinetic control because of the strong hydrogen bonds, while in polar solvents, such as THF, however, such hydrogen bonding will be hampered, resulting in a thermodynamically favorable helical conformation. This speculation is supported by the NMR and IR spectra of L-**32** measured in polar and nonpolar solvents[86] and also by the fact that polymerization of an analogous isocyanide in which the amide linkage is replaced by an ester one produces a helical polyisocyanide with the same handedness independent of the polymerization conditions.[86] The helical structures of the diastereomeric helical polyisocyanides including helical pitch and handedness have been determined by direct observations of the diastereomeric helical polyisocyanides by high-resolution AFM (see section 3.2.2).

On the other hand, the polymerization of the enantiomerically pure L-**32** with the Pt−Pd μ-ethynediyl complex (**33**) as the initiator, which is known to promote the living polymerization of aryl isocyanides,[87,88] simultaneously produced diastereomeric right- and left-handed helices with different molecular weights and narrow molecular weight distributions (Figure 5A).[89] Each single-handed, rodlike helical poly-L-**32** with a controlled length and handedness (poly-L-**32g** and poly-L-**32h**) can be separated by solvent fractionation with acetone, thus showing the Cotton effects with mirror images to each other (Figure 5B). The fractionated poly-L-**32**'s with narrow length distributions exhibit well-defined two-dimensional (2D) and three-dimensional (3D) smectic orderings on a graphite substrate (see section 3.2.2.1) and in an LC state, as revealed by high-resolution AFM and polarized optical micrographs (POMs) (Figure 5C and D), respectively.

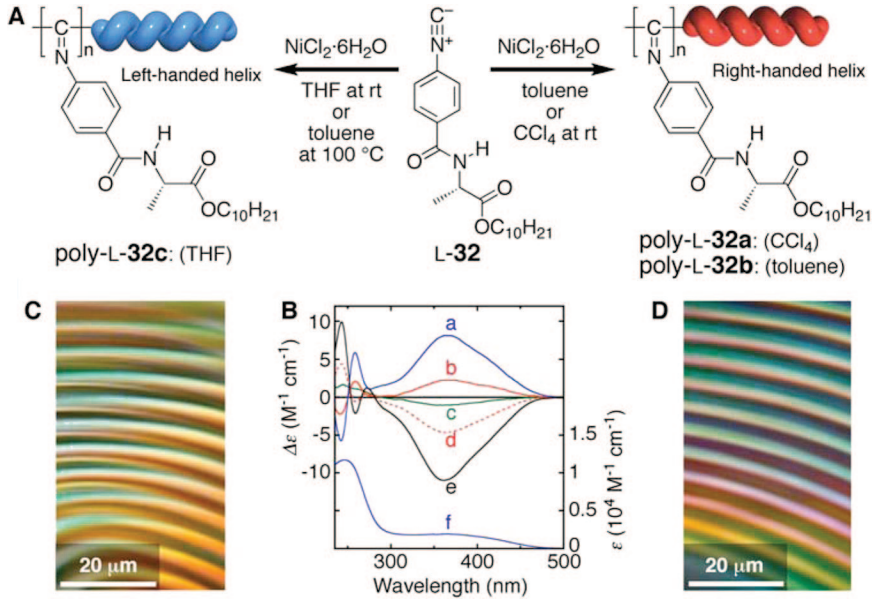

Figure 4. (A) Schematic illustration of diastereomeric helical polyisocyanides produced by the helix-sense-controlled polymerization of L-**32**. The helix-sense can be controlled by the solvent polarity and temperature during the polymerization, resulting in the formation of diastereomeric helical polyisocyanides. (B) CD spectra of poly-L-**32a** (a, blue line), poly-L-**32b** (b, red solid line), and poly-L-**32c** (c, green line) polymerized in CCl_4, toluene, and THF, respectively, at ambient temperature; poly-L-**32d** (d, red dotted line) polymerized in toluene at 100 °C; and poly-L-**32e** (e, black line) after poly-L-**32d** annealed in toluene at 100 °C for 6 days. The absorption spectrum of poly-L-**32a** (f) is also shown. (C, D) Polarized optical micrographs of cholesteric LC phases of poly-L-**32a** (D) and poly-L-**32e** (C) in chloroform (15 wt %). (Reproduced with permission from ref 85. Copyright 2006 American Chemical Society.)

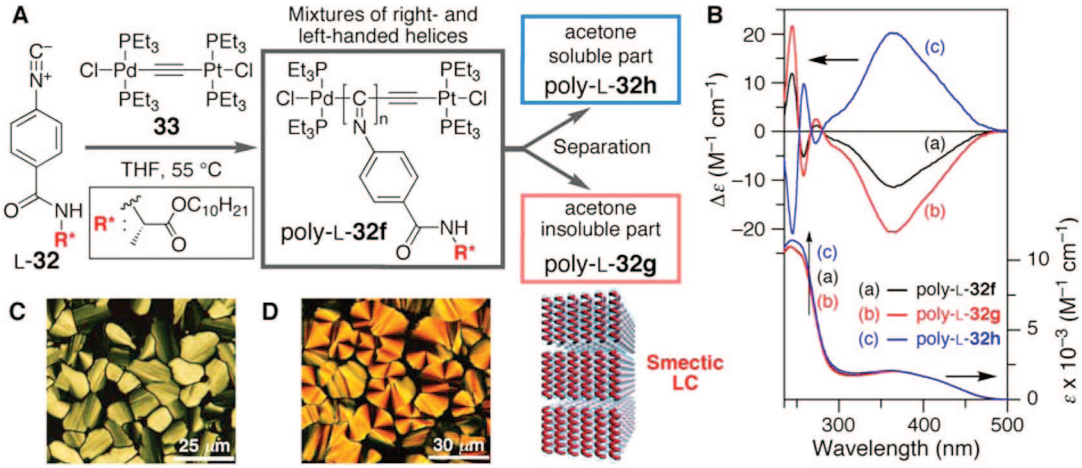

Figure 5. (A) Schematic illustration of the helix-sense-selective living polymerization of L-**32** with μ-ethynediyl Pt−Pd complex (**33**), yielding a mixture of diastereomeric, right- and left-handed helical poly-L-**32f** with different molecular weights and a narrow molecular weight distribution, which can be further separated into each single-handed helical poly-L-**32**. (B) CD and absorption spectra of poly-L-**32f** (a), poly-L-**32g** (b), and poly-L-**32h** (c) in chloroform at 25 °C. (C, D) Polarized optical micrographs of poly-L-**32h** (C) and poly-L-**32g** (D) in *ca.* 15 wt % chloroform solution taken at ambient temperature and schematic illustration of smectic ordering of the one-handed helical poly-L-**32**'s in the LC state. (Reproduced with permission from ref 89. Copyright 2008 American Chemical Society.)

Takahashi and Onitsuka et al. have reported that the Pt−Pd μ-ethynediyl complex can promote the living polymerization of aryl isocyanides.[87,88] This living polymerization system has been successfully applied to the precise synthesis of two- and three-armed polyisocyanides (**37**, **38**) by using the multifunctional initiators (**34**, **35**) containing Pd−Pt μ-ethynediyl units (Scheme 6).[90] The cleavage of the polymer chains from the multiarmed polymers as well as kinetic studies revealed that all the Pd−Pt μ-ethynediyl units in the multifunctional initiators produced the multiarmed polyisocyanides with the same arm length. The polymerization of the isocyanide monomer possessing a chiral ester group (**36c**) gives the multiarmed helical polymers (**37c**, **38c**) with an excess handedness, as evidenced by large specific rotations and distinct Cotton effects, although there is no attractive interaction among the polymer pendants. This method can be applicable to the precise synthesis of star-shaped polyisocyanides composed of more than three arms.

The arylrhodium complex **39** can also effectively initiate the living polymerization of phenyl isocyanides possessing bulky substituents at the *ortho* position,[91,92] while the Pt−Pd μ-ethynediyl complex (**33**) did not because of its steric hindrance. The helix-sense-selective polymerization using the arylrhodium complex **39** has been performed for bulky aryl isocyanides bearing *tert*-butyl groups at the *ortho* position and chiral ester or amide groups at the *para* position (**40**), and the chiroptical properties of the obtained polymers (poly-**40**) have been investigated (Scheme 7).[92] Comparison with analogous poly(aryl isocyanide)s having no substituents at

Scheme 6

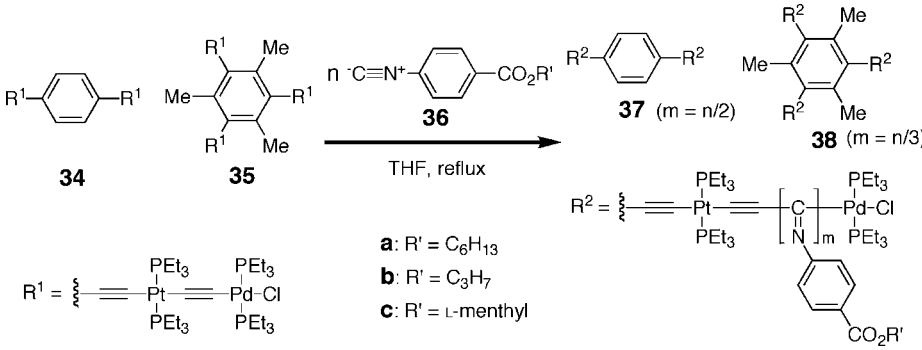

Scheme 7

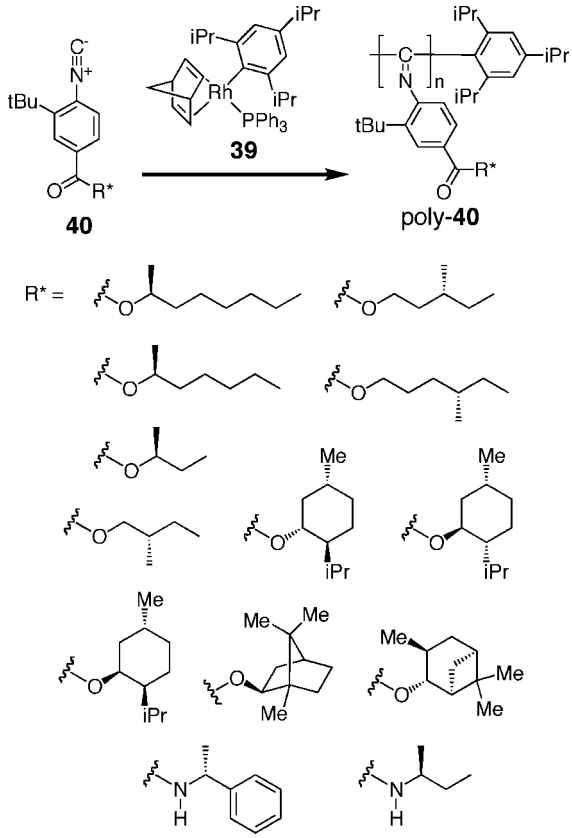

Chart 6

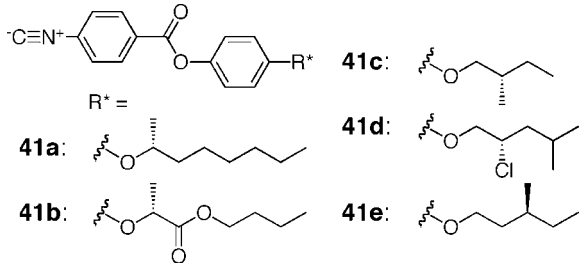

the *ortho* position suggests that the *tert*-butyl group enhances the selectivity of the preferred-handed helical conformation.

Amabilino and Veciana et al. have reported that helical polyisocyanides with either an excess right- or left-handed helical conformation can be obtained by the polymerization of aromatic isocyanides with a stereogenic center positioned far from the polymer backbone (**41a**—**e**, Chart 6).[70,93] The steric effect between the neighboring phenyl benzoate moieties has been considered to be one reason for this long-range chirality transfer from the side chains to the polymer backbones. The helicity induction process shows odd—even effects with respect to the position of the chiral substituent. Furthermore, a series of optically active poly(phenyl isocyanide)s bearing a stereogenic center separated by various rodlike spacers (poly-**42a**—**g**) have been prepared by the polymerization of the corresponding chiral phenyl isocyanides (**42a**—**g**) using a $NiCl_2 \cdot 6H_2O$ catalyst (Scheme 8), and the effects of the length, constitution, and conformation of the rodlike spacers between an isocyanide group and a chiral substituent on the helical sense preference during the polymerization of these monomers have been studied.[94] The most efficient chirality transfer from the stereogenic center to the polymer backbone has been observed for the polyisocyanide bearing a benzoate moiety. The chiral moiety separated from the polymer main-chain through a rodlike spacer by as far as 21 Å could induce a predominant screw-sense in the main-chain during the polymerization process.[70,94]

Polyisocyanides bearing achiral dendronized pendant groups (**43**) were prepared by Iyoda and co-workers, and their thermotropic LC properties and the formation of supramolecular nanostructures have been reported.[95] A series of novel optically active phenyl isocyanides bearing mono-, di-, or tri-(*S*)-alkoxy chains with a stereogenic center at a different position as the pendants have also been prepared.[96] The chiroptical properties of the resulting poly(phenyl isocyanide)s (**44**—**46**, Chart 7) investigated by CD showed a significant dependence on the number of alkoxy chains and the position of the stereogenic center. The polyisocyanides with a single alkoxy chain (**44**) showed no Cotton effect in the polymer backbone regions regardless of the position of the stereogenic center, while the polyisocyanides bearing dialkoxy chains with a stereogenic center located close to the phenyl group (**45**) exhibited an apparent but relatively weak Cotton effect. In contrast, the polyisocyanides bearing fan-shaped, bulky trialkoxy chains (**46**) efficiently biased the helical sense and showed intense Cotton effects, and **46a** showed a thermotropic LC formation. A clear odd—even effect with respect to the position of the stereogenic center has also been observed for the polyisocyanides with di- and trialkoxy chains.

A redox-switchable poly(phenyl isocyanide) bearing a tetrathiafulvalene (TTF) pendant with two stereocenters located at the end of the semirigid part (**47**) has been designed and synthesized (Figure 6).[70,97] CD studies revealed a long-range chiral induction into the polymer backbone, although the helix-sense selectivity during the polymerization reaction is lower than that of the other examples with a similar distance between the chiral units and the isocyanide group. The redox properties of the polyisocyanide are similar to

Scheme 8

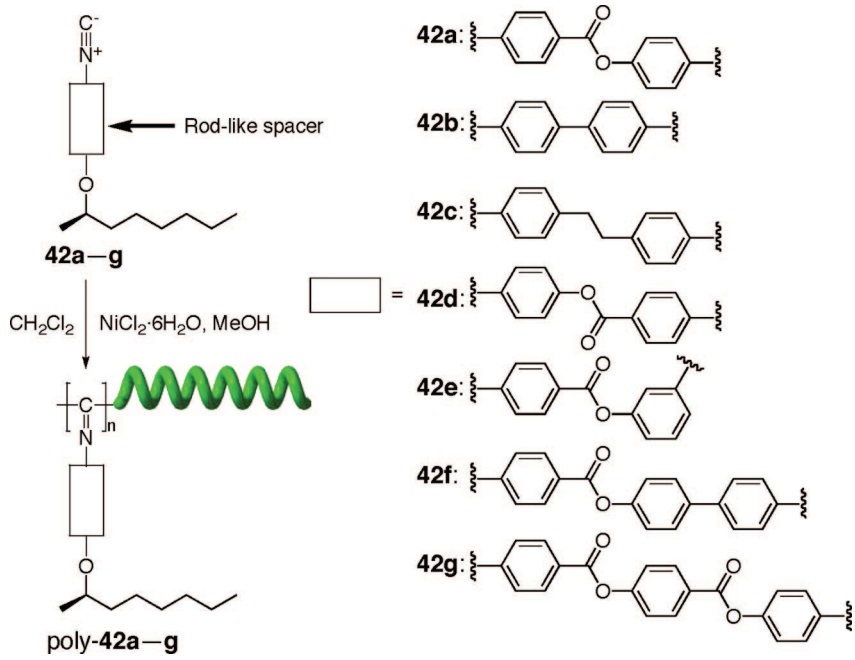

Chart 7

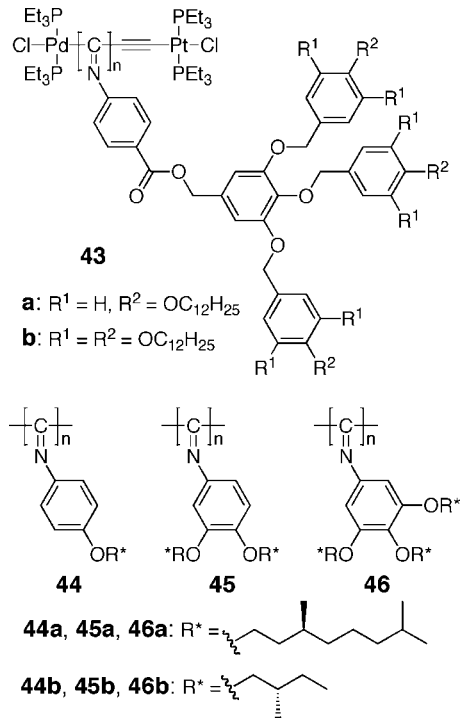

those of small molecule TTFs. Two sequential waves were observed at 0.61 and 0.93 V versus Ag/AgCl, corresponding to formation of the cation radical and dication, respectively. The chemical oxidation has also been performed using bromine or iron(III) perchlorate, allowing observation of the three extreme oxidation states (all neutral, cation radical, and dication), and the two intermediate ones (with mixtures of neutral and cation radical and of cation radical and dication) by both absorption and CD spectroscopies. Each of the redox states has a distinct and characteristic set of Cotton effects. The polymer backbone is considered to be essential for this property, since the monomer does not show such features. In addition, the process is reversible. Thus, the polyisocyanide can act as a platform for a multistate redox-switchable organic system.

An optically active helical poly(phenyl isocyanide) bearing a ferrocenyl group as the pendant (**48**) has also been synthesized by the polymerization of the corresponding chiral monomer with the living catalyst **33**. The structure of **48** is reversibly controlled from a helical conformation to a disordered one in response to the oxidation and reduction of the ferrocenyl pendants (Figure 7).[98]

The thermal stability of helical polyisocyanides (**49**) derived from phenylalanine has been investigated (Scheme 9).[99] **49a** takes a stable helical conformation independent of the polymerization temperature, while the helical conformation of **49b** with slightly smaller side groups was thermally less stable. The specific rotation and CD intensity of **49b** prepared at temperatures higher than 40 °C were considerably low in comparison with the values for **49b** prepared at or below room temperature. In addition, **49b** exhibited a reversible temperature-dependent change in its specific rotation and CD spectrum, whereas **49a** showed only slight changes. These results suggest a temperature-dependent dynamic behavior of the polyisocyanide **49b**, and its helical conformation alters from tightly to loosely coiled helices at low and high temperatures, respectively.

Kobayashi et al. have synthesized a series of glycosylated poly(phenyl isocyanide)s (**50**, Chart 8) in an attempt to elucidate the effect of the three-dimensionally regulated saccharide arrays along the helical polymer backbones on molecular recognition (see section 5.1).[100] Poly(phenyl isocyanide)s bearing α-D-glucose, β-D-glucose, β-D-galactose, and β-D-lactose units (**50**) have been obtained by polymerization of the corresponding acetylated glycosyl phenyl isocyanides with a Ni(II) catalyst and subsequent deacetylation. The CD spectroscopic study along with molecular dynamics (MD) calculations demonstrated that the polymers take an excess of a one-handed helical conformation, and the saccharide arrays are spatially regulated. Their binding affinity toward lectins investigated by inhibition of hemagglutination and fluorescence spectroscopy revealed that the rigid cylindrical phenyl isocyanide glycopolymers contribute

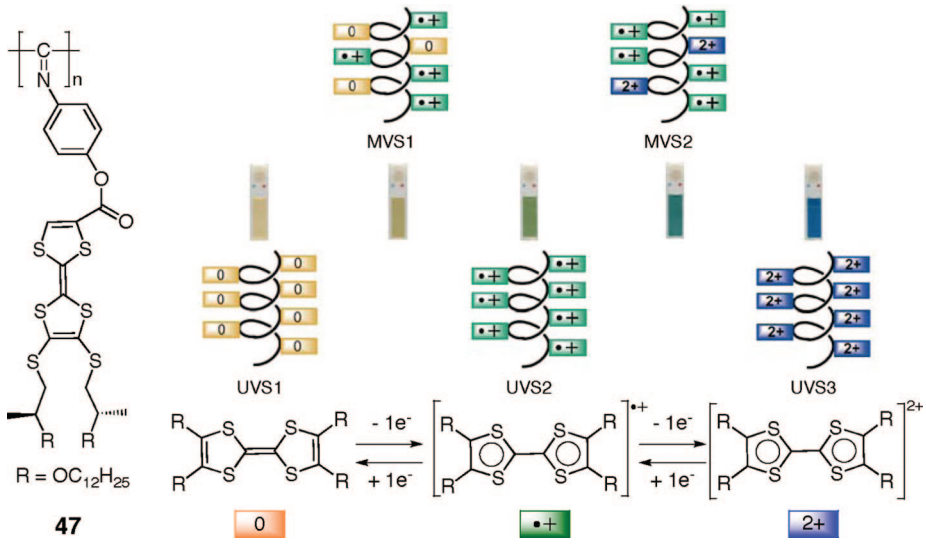

Figure 6. Schematic representation of the redox states of **47** with TTF units in the pendants and the colors of the corrsponding polymer solutions: univalent states with all neutral (UVS1), all cation radical (UVS2), or all dication (UVS3) TTF units, and the intermediate mixed-valence states (MVS1 and MVS2). (Reproduced with permission from ref 97. Copyright 2005 Wiley-VCH.)

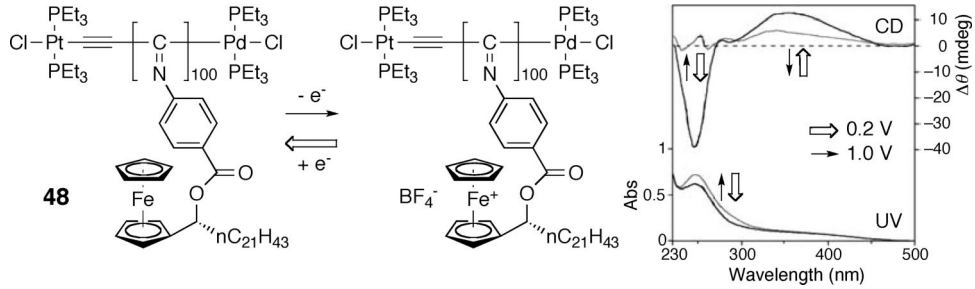

Figure 7. CD and absorption spectral changes of **48** in the oxidation and reduction states. (Reproduced with permission from ref 98. Copyright 2003 Wiley-VCH.)

Scheme 9

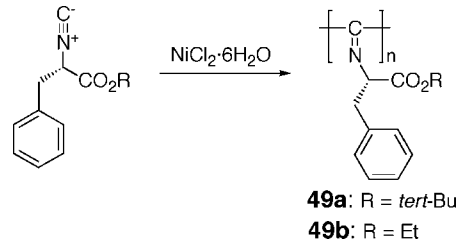

Chart 8

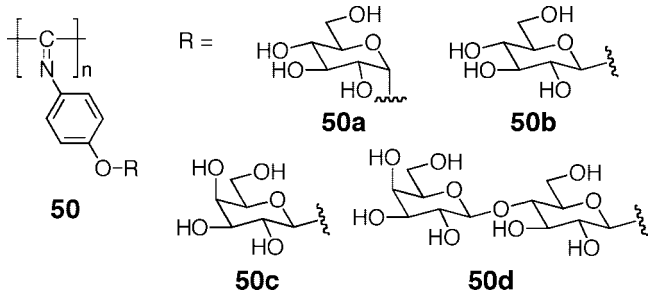

to small specific interactions with lectins, in contrast to the highly specific interactions of the multivalent glycoclusters along flexible polyacrylamide glycopolymers. This suggests that the compatibility of the orientation and spacing of clustered saccharide chains of glycopolymers is essential for the specific molecular recognition by lectins.[100] Multilayer

Scheme 10

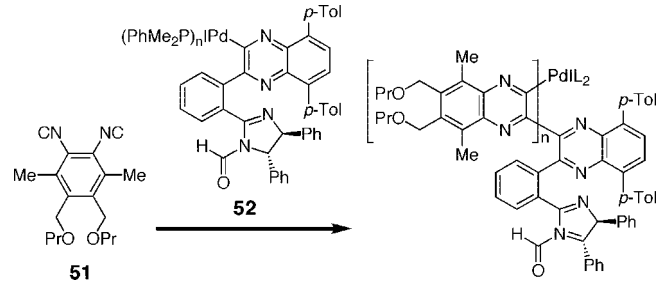

thin films prepared from **50a** are found to orient horizontally and two-dimensionally on hydrophilic surfaces in an aqueous solution.[101]

2.1.3. Poly(quinoxaline-2,3-diyl)s

A bifunctional isocyanide, 1,2-diisocyanobenzene (**51**), has been polymerized using an organopalladium complex with an optically active imidazoline group (**52**) as the initiator, which produces right-handed helical poly(quinoxaline-2,3-diyl)s. The polymerization proceeds with an almost 100% helix-sense selectivity through a living and cyclopolymerization mechanism (Scheme 10).[102,103] In sharp contrast to other living polymerization systems, the active growing chains complexed with the palladium can be isolated, and the subsequent helix-sense-selective living block polymerization occurs.[102]

The racemization process of oligoquinoxalines has been investigated in detail.[104] The diastereomerically pure pen-

Scheme 11

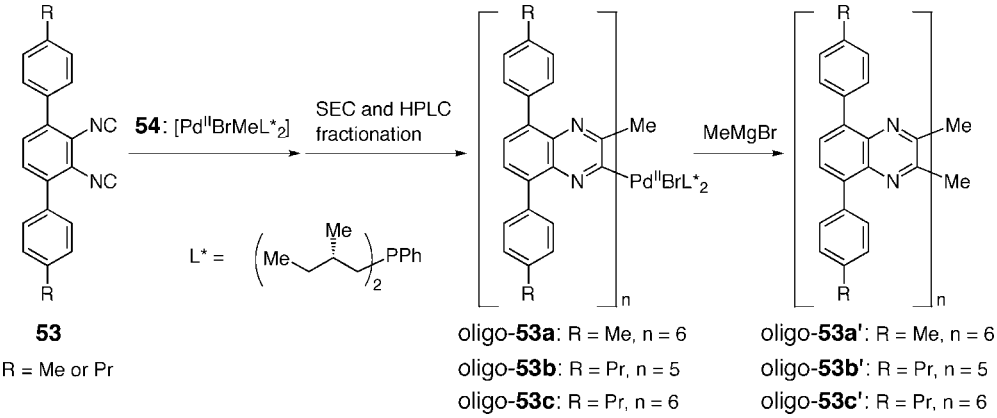

Scheme 12

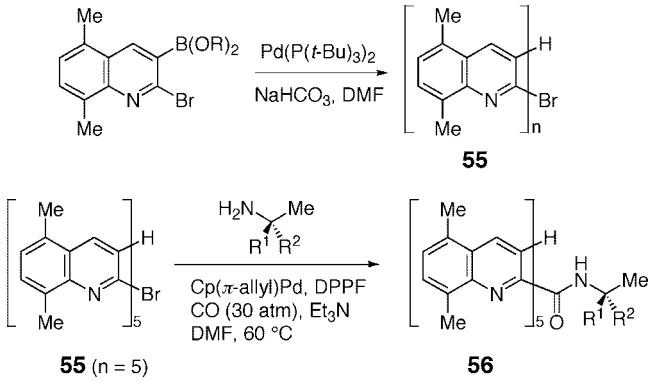

tameric and hexameric oligoquinoxalinylpalladiums (oligo-**53a**−**c**) were first prepared by the oligomerization of 1,2-diisocyanobenzene bearing *para*-tolyl groups at the 3- and 6-positions (**53**) in the presence of the chiral palladium complex **54** followed by isolation with preparative size-exclusion chromatography (SEC) and HPLC. Further treatment with MeMgBr affords the optically active oligoquinoxalines (oligo-**53a′**−**c′**), in which both chain ends are terminated with methyl groups (Scheme 11). Among the three optically active oligomers, only oligo-**53c′** is tolerant toward racemization at room temperature, whereas the others undergo racemization at room temperature. The racemization process obeys first-order kinetics, and the activation energies (E_a) for the racemization of oligo-**53a′**, -**53b′**, and -**53c′** have been calculated to be 100, 106, and 133 kJ mol^{-1}, respectively, on the basis of their Arrhenius plots (Table 1). The stability of the helical conformation significantly depends on the chain length and on the 5,8-substituent of the oligomers.

Oligo(quinoline-2,3-diyl)s, in which quinoline units are linked at their 2- and 3-positions, are structurally similar aromatic oligomers to oligo(quinoxaline-2,3-diyl)s. Suginome et al. have synthesized oligo(quinoline-2,3-diyl)s possessing a terminal bromo group (**55**) by the Suzuki−Miyaura coupling of the 5,8-disubstituted 2-bromoquinolin-3-ylboronic acid derivatives and have investigated their helical structures in detail (Scheme 12).[105] A single-crystal X-ray analysis revealed that the pentamer **55** adopts a 5/2 helix with an average dihedral angle of 127° between the adjacent quinoline rings (see also section 3.1.1). Moreover, the predominantly one-handed helix is successfully induced in the oligoquinolines (**56**) by introduction of optically active amide groups at the termini of the oligomers via a palladium-catalyzed reaction of **55** with optically pure primary amines under a carbon monoxide atmosphere.[105]

2.1.4. Polyguanidines

Polyguanidines (poly(carbodiimide)s) prepared by the polymerization of carbodiimides were previously considered to be an interesting class of dynamic helical polymers, which undergo a very rapid helix inversion (Figure 8A) (see section 2.5.2). Novak et al. have found that an optically active polyguanidine (poly-**57**) just after the polymerization has a specific rotation identical to that of its monomer ([α]$_D$ +7.5°), which, however, significantly increased in solution and reached a plateau value ([α]$_D$ −157.5°) upon annealing at elevated temperature.[106] This unusual behavior is irreversible and ascribed to the conformational change from a kinetically formed structure to a thermodynamically stable helical one with an excess of one helical sense upon heating. A helix-sense bias is induced for an optically inactive polyguanidine (poly-**58**) upon treatment with a catalytic amount of optically active camphorsulfonic acid (CSA).[106] A static helical polyguanidine (poly-**59**) stable in solution has been synthesized by the polymerization of the corresponding optically active bulky carbodiimide (**59**) using an achiral titanium(IV) catalyst. Poly-**59** showed a large specific rotation ([α]$_D$ +791°) due to a regular one-handed helical conformation, which remained constant after annealing at a high temperature for a long time (>34 h).[107] Optically active helical polyguanidines have also been synthesized by the helix-sense-selective polymerization of achiral carbodiimides (**60** and **61**) with a chiral binaphthol-based titanium(IV) catalyst (Figure 8B).[108−110] The anthracene-containing helical poly-**61** has no chiral substituents and slowly racemizes in toluene at 80 °C, suggesting a high helix inversion barrier. However, surprisingly, the polyguanidine exhibits a reversible, thermodriven and solvent-driven chiroptical switch due to a reversible and cooperative change in the orientation of the pendant anthracene rings below the racemization temperature in toluene, as supported by electronic and vibrational CD (VCD) measurements (Figure 9), while the main-chain helical conformation kinetically produced during the helix-sense-selective polymerization is considered to remain unchanged.[109,110]

2.2. Helical Polymers with Low Helix Inversion Barriers (Dynamic Helical Polymers)

Since the pioneering work by Green and co-workers on the detailed structural and chiroptical investigations of

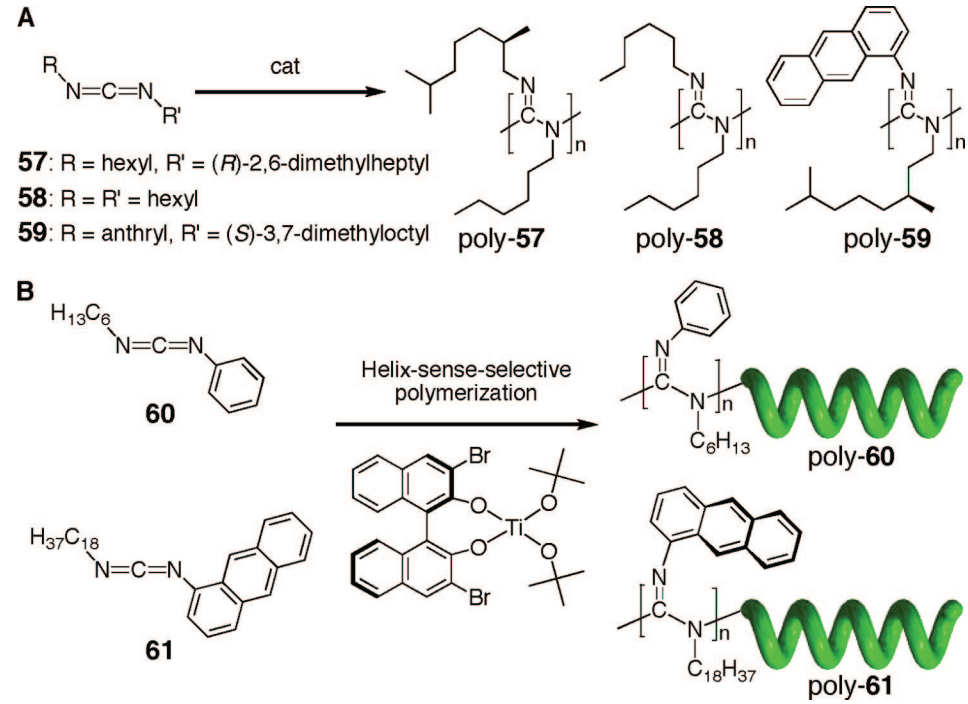

Figure 8. (A) Synthetic scheme of polyguanidines (poly-**57**—poly-**59**). (B) Schematic illustration of the helix-sense-selective polymerization of achiral guanidines (**60**, **61**) using a chiral Ti catalyst resulting in excess of one-handed helical polyguanidines (poly-**60**, poly-**61**).

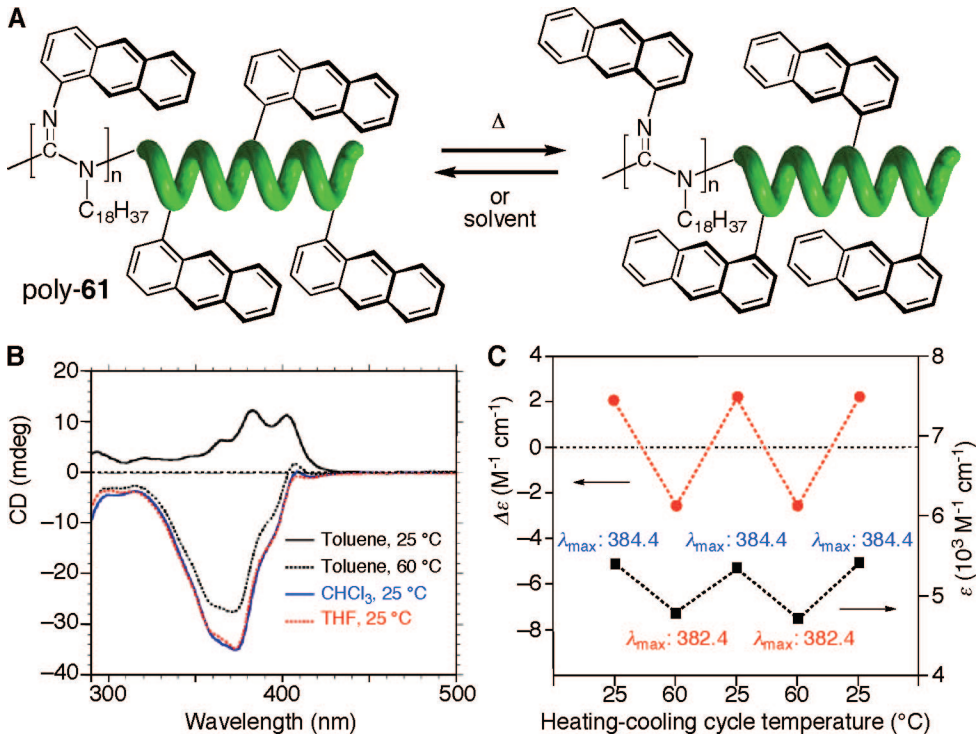

Figure 9. (A) Schematic representation of reversible switching of the orientation of the pendant anthracene rings. (B) CD spectra of poly-**61** in toluene at 25 and 60 °C, in chloroform at 25 °C, and in THF at 25 °C. (C) Heating−cooling thermal cycles of poly-**61** in toluene; the wavelength for $\Delta\varepsilon$ is 382.0 nm. (Reproduced with permission from ref 109. Copyright 2005 Wiley-VCH.)

polyisocyanates, a stiff rodlike helical polymer with a long persistent length (q), the significant feature of the dynamic macromolecular helicity of polyisocyanates, has been experimentally and theoretically revealed.[17,111] An extremely high sensitivity to a chiral environment is the most important characteristic of dynamic helical polyisocyanates, and polysilanes, polyacetylenes, and some foldamer-based helical polymers (section 2.3) belong to this category. A small chiral bias can induce a main-chain conformational change with a large amplification through covalent or noncovalent bonding with a high cooperativity, resulting in a large helical sense excess of the helical polymers (see section 2.6). Therefore, such systems can provide the basis for constructing novel chiral materials. The underlying principle observed in dynamic helical polyisocyanates has been proved to be universal and applicable to other polymeric and supramolecular helical systems.

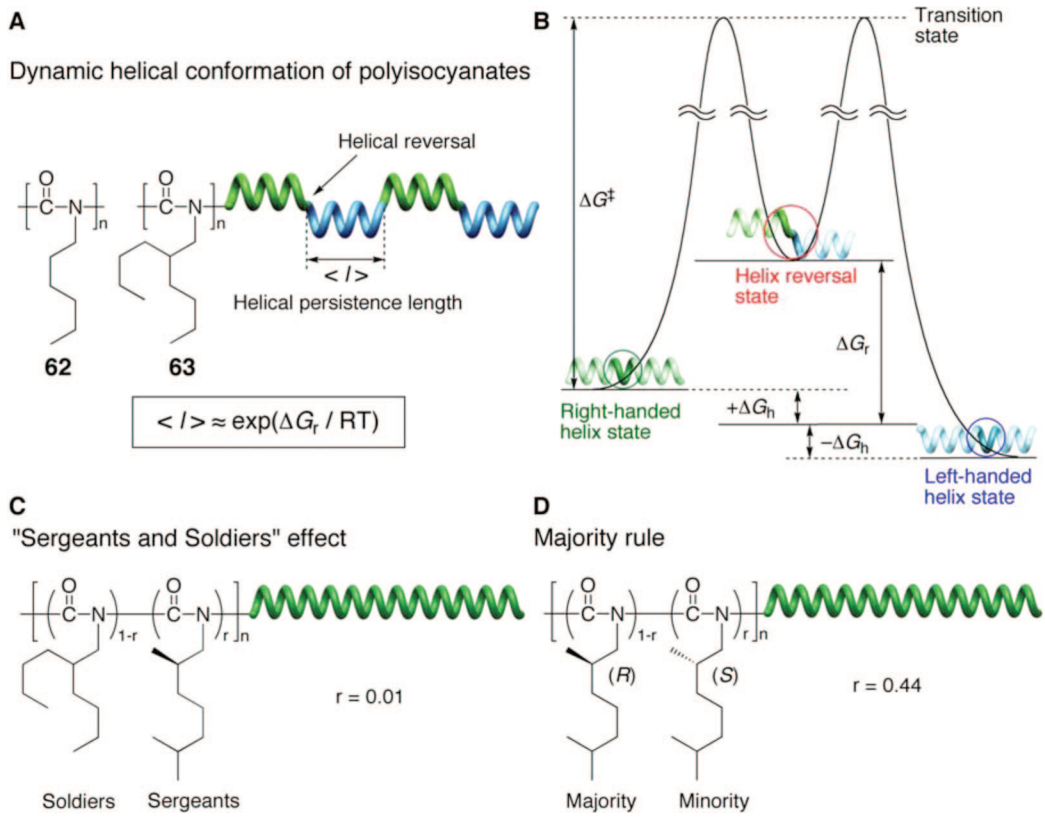

Figure 10. Schematic illustration of dynamic helical conformation of polyisocyanates (A), energy diagram of dynamic helical polymers (B), "sergeants and soldiers" effect (C), and majority rule (D).

2.2.1. Polyisocyanates

Polyisocyanates are composed of an *N*-substituted amide repeating unit (nylon-1) and take a 8/3 helical conformation rather than a restricted coplanar conformation. The stiffness of polyisocyanates is attributable to the conjugated, partial double-bonded nature of the amide backbones. Poly(*n*-hexyl isocyanate) (**62**, $q = 20-40$ nm) and poly(2-butylhexyl isocyanate) (**63**) have no stereogenic centers and are absolutely optically inactive, but they consist of an equal mixture of interconvertible right- and left-handed helical segments separated by the rarely occurring helical reversals that readily move along the polymer backbone (Figure 10A). Therefore, helical polyisocyanates in dynamic equilibrium are inherently chiral (or dynamically racemic) macromolecules.

However, due to the extremely low helix inversion barrier, helical polyisocyanates with an excess one-handedness can be obtained through the copolymerization of an achiral isocyanate with a small amount of an optically active isocyanate (less than 1 mol %)[112,113] or polymerization of achiral isocyanates with optically active initiators.[114] This is a typical and excellent example of the chiral amplification of covalent systems in a polymer. This highly cooperative amplification phenomenon is called the "sergeants and soldiers" effect; the chiral units are sergeants and the achiral units soldiers (Figure 10C and see also section 2.6.1 for other examples). The underlying principle for this unique chiral amplification has been theoretically and quantitatively interpreted using a statistical theory, in which each monomer unit in the helical polymer chains can take either a right-handed helical state, left-handed helical state, or helix reversal state.[17,111,115] According to Lifson, Green, Teramoto, and coworkers, the helical sense excess of the preferred helical state in helical homopolymers of isocyanates, such as a deuterium-substituted polyisocyanate (poly-**64**) (Figure 11A), can be calculated as a function of the thermodynamic stability parameters, the free energy difference between the right- and left-handed helical states ($2\Delta G_h$), the excess free energy of the helical reversal state (ΔG_r) (per monomer unit), the degree of polymerization (N), and the absolute temperature (Figure 10B).[116] The key energy parameters ($2\Delta G_h$ and ΔG_r) for poly-**64b** have been estimated to be 3.1 J mol^{-1} and 16.3 kJ mol^{-1} on a monomer unit basis in hexane at 25 °C, respectively (Table 2).[117] Importantly, the former value is about 3 orders of magnitude smaller than the latter. The $2\Delta G_h$ value indicates that poly-**64b** favorably takes the right-handed helix over the left-handed counterpart only by 0.12%, while, for the longer polymer chain of poly-**64b** ($N = 2000$), this extremely small helical sense excess is significantly amplified in a cooperative fashion to 67:33, resulting in the appearance of intense Cotton effects in the polymer backbone region as well as a large optical rotation (Figure 11B).[28] Moreover, the helix reversal costs 16.3 kJ mol^{-1} and appears only once in every 762 monomer units on average. This long helical persistence length (l) based on the relatively large ΔG_r value directly contributes to the observed chiral amplification in polyisocyanates, since the chiral bias $2\Delta G_h$ is multiplied by the number of monomer units between the helical reversals (l). Therefore, many monomer units can take the same helical sense within the polymer chain, through which the small chiral bias of each unit of the polymer chain is remarkably amplified.[111,116]

Based on the variable-temperature NMR experiments of **63**, Ute et al. have estimated the activation energy ($\Delta G^{\neq}_{100}$) for the interconversion process between the right- and left-handed helical conformations ($2\Delta G_h = 0$ in this case) of **63** to be 79.5 kJ mol^{-1} (Table 1). This value is significantly greater than the thermodynamic excess energy of the helical reversal ($\Delta G_r = 21$ kJ mol^{-1}),[118] which supports the fact

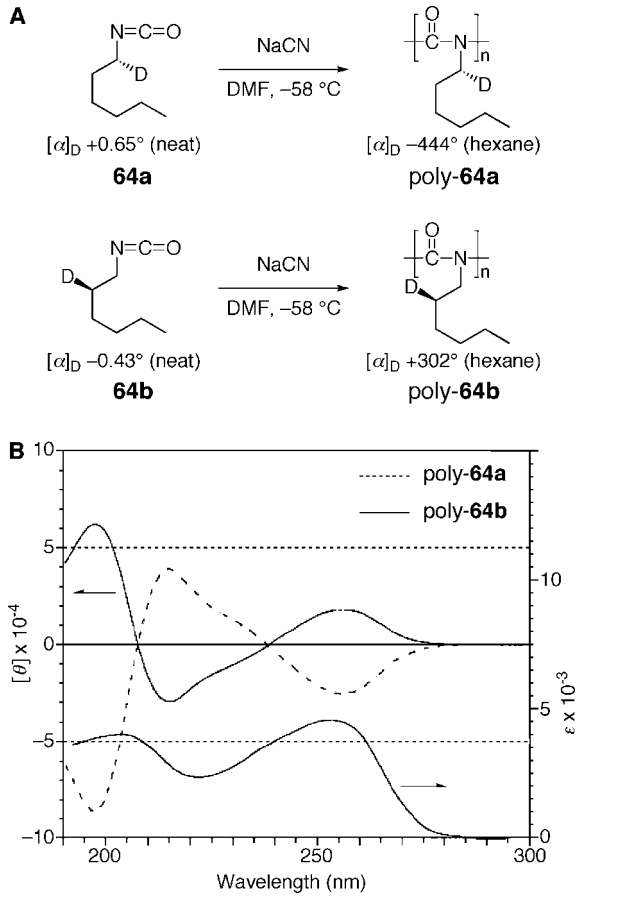

Figure 11. (A) Structures and changes in optical activities in the conversion of the monomers (**64a**, **64b**) into polymers (poly-**64a**, poly-**64b**). (B) CD and absorption spectra of poly-**64a** and poly-**64b** in hexane. (Reproduced with permission from ref 28. Copyright 1988 American Chemical Society.)

Table 2. $2\Delta G_h$ and ΔG_r Values of Dynamic Helical Polymers

polymer		$2\Delta G_h$ (J/mol)	ΔG_r (kJ/mol)	solvent	temp (°C)	ref
polyacetylenes	**87a**	−4.6	15.5	THF	[a]	192
	87b	−4.8	15.5	THF	[a]	192
	93c		6.7	toluene	22	190
	109	0.1	16.7	THF	20	192
	110	−5.0	15.5	DMSO/MeOH (1/9, v/v)	[a]	192
	111		14.2[b]		20−25	193
polyisocyanates	poly-**64a**	−5.9	15.9	hexane	20	195
		−8.4	15.2	1-chlorobutane	20	195
		−10.9	13.6	CH_2Cl_2	20	195
	poly-**64b**	3.1	16.3	hexane	25	117
		4.1	14.7	1-chlorobutane	20	117
		3.6	13.5	CH_2Cl_2	20	117
	112	473	12.3	chloroform	25	194
	113	−19.0[c]	13.2	THF	20	196
		19.6[c]	9.6	THF	−65	196
		9.7	13.6	CH_2Cl_2	20	196
polysilanes	**67**	59.5	7.4	isooctane	25	197
	70	−42[c]	12.1	isooctane	25	198
		44[c]	11.6	isooctane	−30	198

[a] $2\Delta G_h$ and ΔG_r values are assumed to be independent of temperature.[192] [b] Estimated on the basis of the direct observation of the helical reversals in individual polymer chains obtained from the high-resolution AFM (see section 3.2.2.1).[193] [c] Temperature-induced helix inversion took place, and therefore, the $2\Delta G_h$ sign is inverted by changing the temperature.

that inversion of the helix readily occurs at ambient temperature. Therefore, detecting such dynamic interconvertible helical segments and rarely occurring helical reversals may be extremely difficult using conventional spectroscopic methods (see Figure 76 for the direct observation of helical reversals by AFM). Chiral solvation, though its chiral bias ($2\Delta G_h$) appears to be very weak (0.17 J mol^{-1}), can also be used to induce a preferred-handed helical conformation in the dynamically racemic poly(*n*-hexyl isocyanate) (**62**) in optically active solvents.[119]

Scheme 13

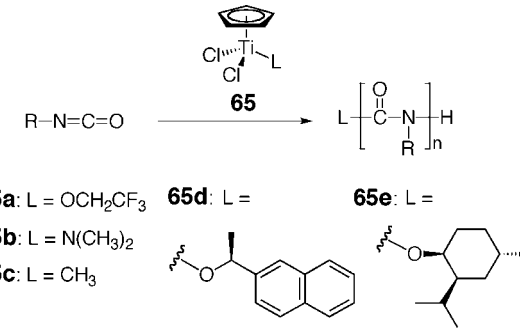

Green et al. further discovered another intriguing amplification of chirality in the copolymers of the isocyanates consisting of a mixture of (*R*)- and (*S*)-enantiomers with a small enantiomeric excess (ee) that also form a predominantly one-handed helical conformation (Figure 10D); only a 12% ee is sufficient to produce a single-handed helical polymer for poly(2,6-dimethylheptyl isocyanate).[120] The minority units obey the helical sense of the majority units in order to avoid introducing energetic helical reversals. This phenomenon is called the "majority rule" (see section 2.6.1 for other polymeric and supramolecular helical systems).

Usually, anionic initiators, such as sodium cyanide and metal alkoxides, naphthalenide, and amides, are used to polymerize isocyanates, but the polymerization proceeds so fast and is accompanied with side reactions, such as trimerization through backbiting, that it was difficult to control the molecular weight and molecular weight distribution. Organotitanium(IV) complexes (**65**) developed by Novak et al. are versatile catalysts for the living coordination polymerization of alkyl isocyanates, producing poly(alkyl isocyanate)s with a controlled molecular weight and narrow molecular weight distribution (Scheme 13).[121,122] When chiral (**65d** and **65e**) and achiral (**65a**) alkoxy-bound titanium catalysts are used, the alkoxy groups initiate the polymerization. Lee et al. have ensured the living character of polymerization of alkyl isocyanates with sodium naphthalenide as the initiator using additives, such as 15-crown-5[123] and sodium tetraphenylborate,[124] which prevent the formation of cyclic trimers or other side reactions as a result of the high reactivity of the naphthalenide carbanion. Sodium benzanilide (Na-BA) also works as a unique initiator for the polymerization of isocyanates to serve the dual function of the controlled initiation and efficient protection of the living chain-ends (Scheme 14),[125] thus providing a useful method to prepare helical polyisocyanates with controlled molecular weights.

2.2.2. Polysilanes

Polysilanes (**66**−**70**, Chart 9) also belong to a class of dynamic helical polymers such as polyisocyanates with essentially a 7/3 helical structure, but they are different from polyisocyanates with respect to their unique chromophoric and fluorophoric Si σ-conjugated backbones. Starting with the pioneering work by Fujiki and Matyjaszewski on

Scheme 14

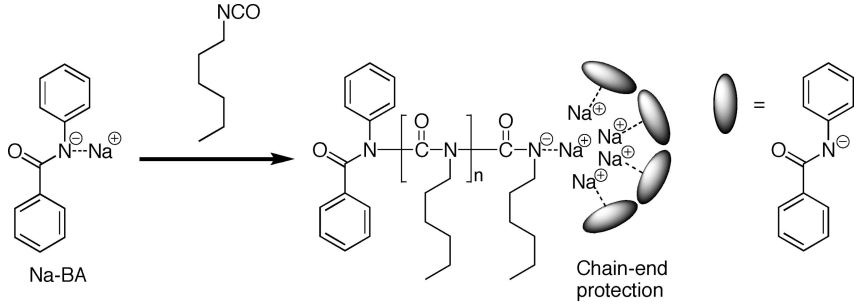

Chart 9

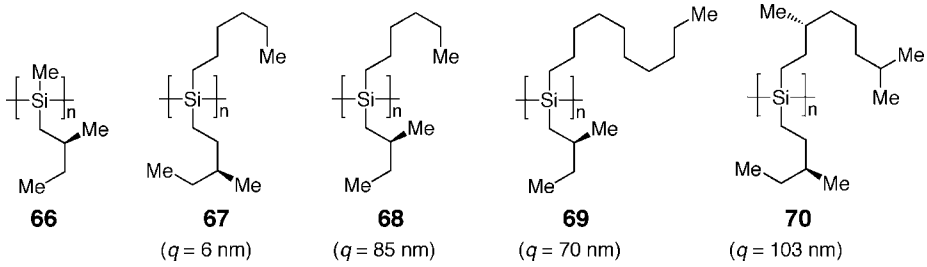

chiroptical investigation of polysilanes,[126−128] Fujiki and coworkers have synthesized a wide variety of optically active polysilanes bearing chiral alkyl or aromatic side groups and copolymers with achiral monomers.[18,129] The rigidity of the polymer backbones (q = 6 (**67**), 70 (**69**), 85 (**68**), and 103 nm (**70**): see also Table 3 in section 3.1) depends on the structures of the pendant groups, in particular, the chain length and position of the branching methyl group at the chiral center, which also significantly influence the thermodynamic stability of the helical conformations and their electric properties, including the absorption, CD, and fluorescence spectral profiles. The chiroptical properties of helical polysilanes obey the sergeants and soldiers effect and the majority rule.[129,130]

Fujiki et al. have found the intramolecular cooperative C−F···Si weak interaction that affects the rigidity of the polysilanes, leading to their stable helical conformation.[131] The replacement of the *n*-propyl group with the 3,3,3-trifluoropropyl group does not affect the helical conformation of the polysilanes with the chiral β-branched alkyl substituent (**71**), but it brings about a significant variation in the helical conformation of the polysilanes with the chiral γ-branched alkyl substituent (**72**). The absorption, fluorescence, and CD spectra of **72a** showed typical characteristics of a stable helical chain having a preferential screw-sense with a g_{abs} ($\Delta\varepsilon/\varepsilon$) value of 1.09×10^{-4} and a narrow full width at half-maximum (fwhm) of 13.6 nm in THF at 20 °C, while those of **72b** exhibited a negligibly weak Cotton effect and broad absorption (Figure 12). This helical sense bias in **72a** can be attributed to the chain stiffness induced by the intramolecular weak interaction between the pendant fluorine atoms and the Si backbone. The β-branches in **71a** may prevent the interaction by steric hindrance, while the γ-branches in **72a** located at the same radial distance as the fluorine atom from the Si backbone can facilitate the interaction.

A semiflexible polysilane copolymer bearing 3,3,3-trifluoropropyl and *n*-decyl side chains (**73**, Chart 10) forms an organogel in nonpolar organic solvents,[132] probably due to the weak C−F···Si intermolecular interactions between the Si main-chain and the fluoropropyl side chain, which act as noncovalent cross-links. In addition, the relatively rigid main-chain is also responsible for the gelation ability of the copolymer. The C−F···Si interchain interactions have been

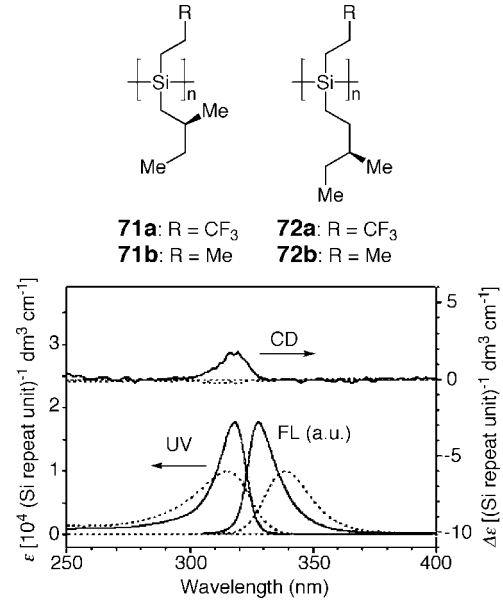

Figure 12. Absorption, CD, and fluorescence spectra of **72a** (solid line) and **72b** (dashed line) in THF at 20 °C. (Reproduced with permission from ref 131. Copyright 2004 The Royal Society of Chemistry.)

Chart 10

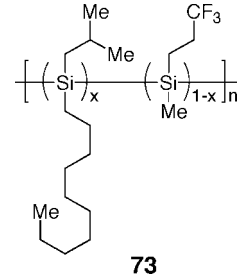

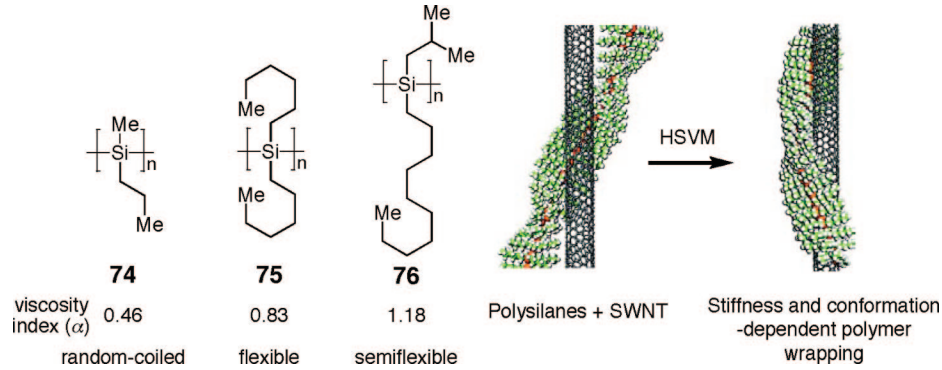

Figure 13. Structures of poly(dialkylsilane)s with different main-chain stiffness (**74**−**76**) and schematic illustrations of stiffness-dependent polymer wrapping behavior onto SWNT by the high-speed vibration milling (HSVM) method. (Reproduced with permission from ref 133. Copyright 2008 American Chemical Society.)

Chart 11

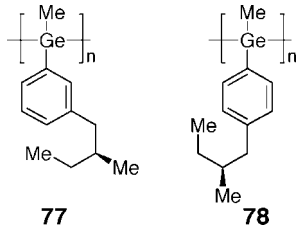

demonstrated by careful IR measurements and analysis using a model silane molecule.

The main-chain stiffness of poly(dialkylsilane)s can be tailored by the well-established molecular designs of silane monomers.[18] The effect of the main-chain stiffness and conformational flexibility of dynamic helical poly(dialkylsilane)s on the wrapping behaviors around single-walled carbon nanotubes (SWNTs) has been investigated by employing three kinds of poly(dialkylsilane)s with a different stiffness and thereby different viscosity index values: random-coiled (**74**), flexible (**75**), and semiflexible (**76**) main chains (Figure 13).[133] Complexes of poly(dialkylsilane) and SWNTs were prepared using a mechanochemical high-speed vibration milling (HSVM) technique. Interestingly, random-coiled (**74**) and flexible (**75**) poly(dialkylsilane)s can be wrapped onto small bundles of SWNTs through their conformational change to fit the surface curvatures of the SWNTs, whereas semiflexible poly(dialkylsilane) (**76**) cannot form a complex with the SWNTs and its conformation remains unchanged even after the same HSVM process. The random-coiled and flexible poly(dialkylsilane)s spontaneously wrap onto the SWNT surface via an induced-fit mechanism, driven by subtle but sufficiently strong CH−π interactions between the alkyl side chains of the poly(dialkylsilane)s and the SWNT surface.

Optically active polygermanes (**77**, **78**, Chart 11), which possess the σ-delocalized polymer backbone like polysilanes, have been synthesized by the demethanative coupling of the corresponding optically active aryldimethylgermanes catalyzed by a ruthenium complex.[134] These polymers adopt a helical conformation with a predominant helix-sense in solution, as evidenced by the appearance of CD signals in the main-chain chromophore region. By comparing the g_{abs} ($\Delta\varepsilon/\varepsilon$) values, it is concluded that the polygermanes likely have a lower helix-sense preference than the corresponding polysilanes, resulting from the longer Ge−Ge bond than the Si−Si one, which may reduce the favorable steric interactions between the chiral pendants for induction of one particular helical sense.

2.2.3. Polyacetylenes

Since the pioneering work by Ciardelli et al. (**79**−**82**),[135−139] a large number of π-conjugated, dynamic helical polyacetylenes with optical activities have also been prepared in the past decade by the polymerization of optically active phenylacetylenes (**83**−**92**, Chart 12),[140−155] propiolic esters (**93**),[156] propargyl esters (**94**),[157] *N*-propargylamides (**95**),[158−163] and aliphatic acetylene (**96**, **97**) (Chart 13)[164−167] or by the copolymerization with achiral acetylenes. Rhodium catalysts, such as $[Rh(nbd)Cl]_2$ (nbd: norbornadiene), are often used to obtain stereoregular (*cis*−*transoidal*) polyacetylenes,[168−171] resulting in the formation of a helical structure with a helical sense bias. The control of the main-chain stereoregularity is essential for induction of a specific handed helical conformation.[168,172,173]

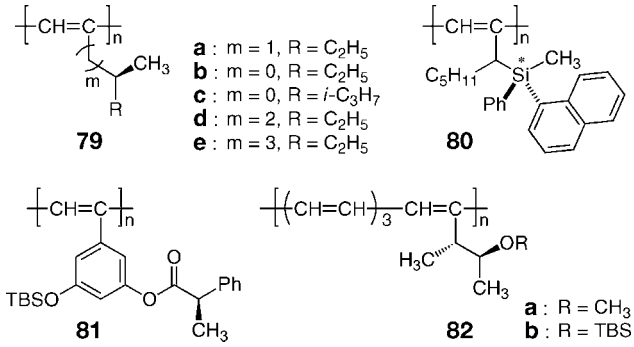

Percec and co-workers have prepared a series of *cis*-poly(phenylacetylene)s (PPAs) bearing self-assembling dendrons and minidendrons (**98**−**108**, Chart 14)[174−183] with chiral or achiral peripheral alkyl chains, and investigated their thermal stabilities, steric effects of chiral peripheral alkyl chains on a preferred-handed helix formation, and helical structures (see section 3.1.2).

The PPA derivatives prepared so far are more or less thermally unstable in solution, especially in chloroform, and undergo *cis*−*trans* isomerization, and irreversible intramolecular 6π-electrocyclization of the 1,3-*cis*-5-hexatriene sequences in the polymer backbone takes place followed by chain cleavage and subsequent release of the 1,3,5-triphenylbenzene derivatives.[184−189] However, the dendronized *cis*-PPAs, such as **98**−**103** and **108**, showed an unprecedented thermal stability even at 100 °C in the solid state due to the steric demand of the bulky self-assembling dendrons that eliminate the intramolecular 6π-electrocyclization in the bulk.[176,177,179]

Chart 12

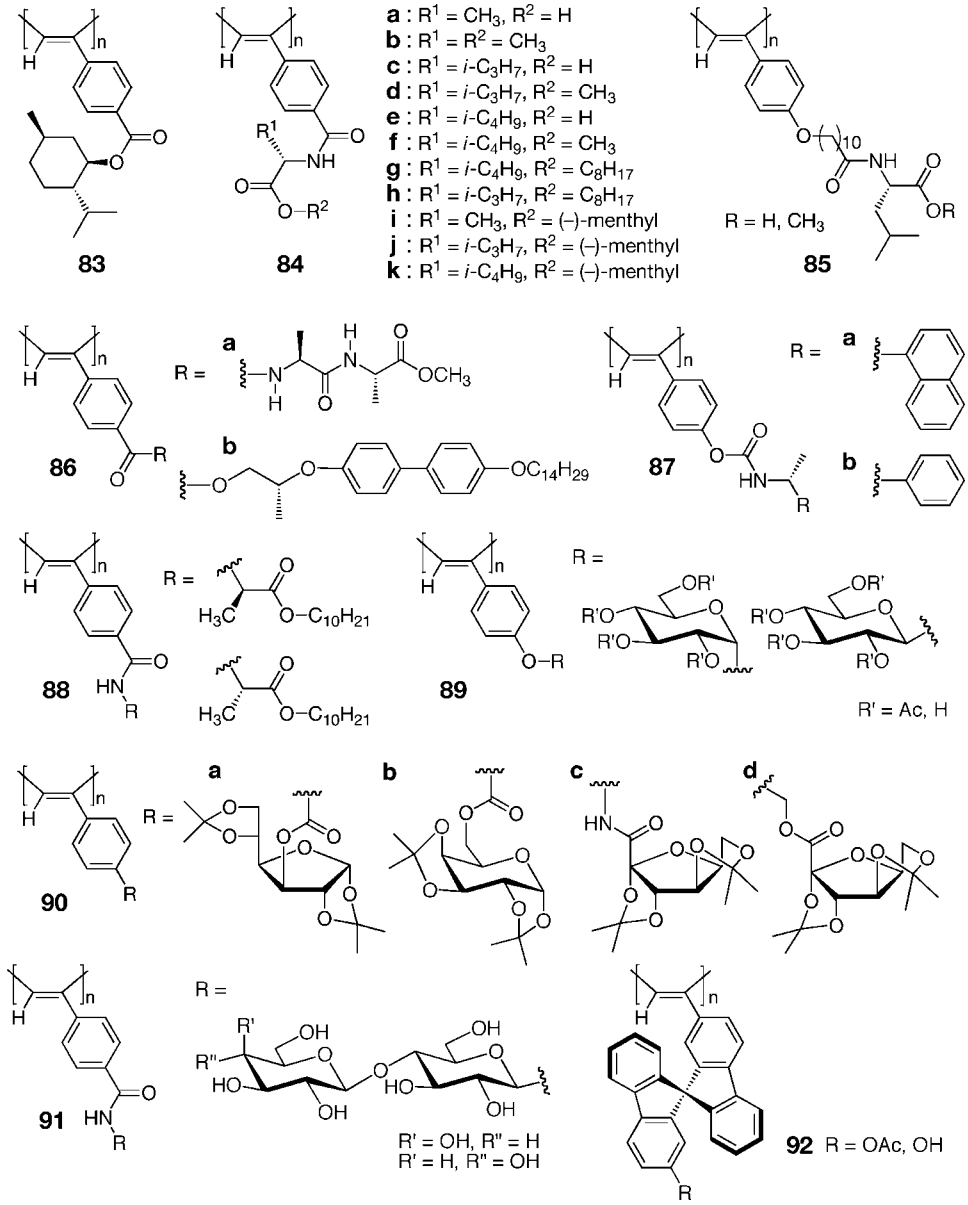

Dendronized *cis*-PPAs are a class of dynamic helical polymers, and therefore, chiral peripheral alkyl chains with very weak chiral bias can induce a preferred-handed helical conformation in the polymer backbones via amplification of the chirality. In fact, most of the dendronized *cis*-PPAs with optically active peripheral alkyl chains (**100f**, **102b**, **104b**, **105b**, **107b**, **108a**) exhibited an ICD in the main-chain chromophore regions in spite of the stereogenic centers located away from the polyene backbones. This long-range effect of chirality transfer from the chiral peripheral alkyl chains to the polymer backbones has been ascribed to the steric communication of the chiral peripheral alkyl chains. Variable-temperature CD spectra revealed a typical dynamic helical behavior in solution, and the CD intensities decreased with the increasing temperature. The CD intensities of the dendronized *cis*-PPAs that reflect their helical sense excesses are significantly dependent on the dendron structures. The dendronized poly(ethynylcarbazole)s (**104b** and **105b**)[174] and **106**[178] displayed an exceptionally rather intense CD, while other dendronized *cis*-PPAs (**100f** and **107b**)[176,181] showed a weak CD even at low temperature. Due to the close proximity of the stereogenic center to the polymer backbone, **106** exhibited intense split-type Cotton effects at low temperature.[178] On the basis of the exciton coupling analysis, **106** was tentatively assigned to have a right-handed helix.[178]

The activation energy value ($\Delta G^{\neq}_{110}$) of the helix−helix interconversion for a poly(propiolic ester) has been experimentally estimated on the basis of the variable-temperature NMR results of **93c** to be *ca.* 77.4 kJ mol^{-1},[190] which is comparable to that for the polyisocyanate **63** (Table 1).[118]

In contrast to stiff rodlike helical polyisocyanates and polysilanes, helical polyacetylenes were considered to be flexible, and their reported short persistence length (q) values are 8.6 and 13.5 nm for a helical poly((4-carboxyphenyl)-acetylene) (**148** in Figure 19) induced by chiral amines[191] and poly(*N*-propargyl-2-ethylhexanamide) (**95c**),[160] respectively (see Table 3). However, the temperature dependent changes in the ICD intensities of a series of homopolymers (**87a**, **87b**, **109**−**111**) and copolymers of phenylacetylenes and *N*-propargylamides revealed that their ΔG_r values (*ca.* 16 kJ mol^{-1}) are close to or slightly greater than those for polyisocyanates (poly-**64a**, poly-**64b**, **112**, **113**) and poly-(dialkylsilane)s (**67**, **70**) (Table 2).[117,190,192−198] These results

Chart 13

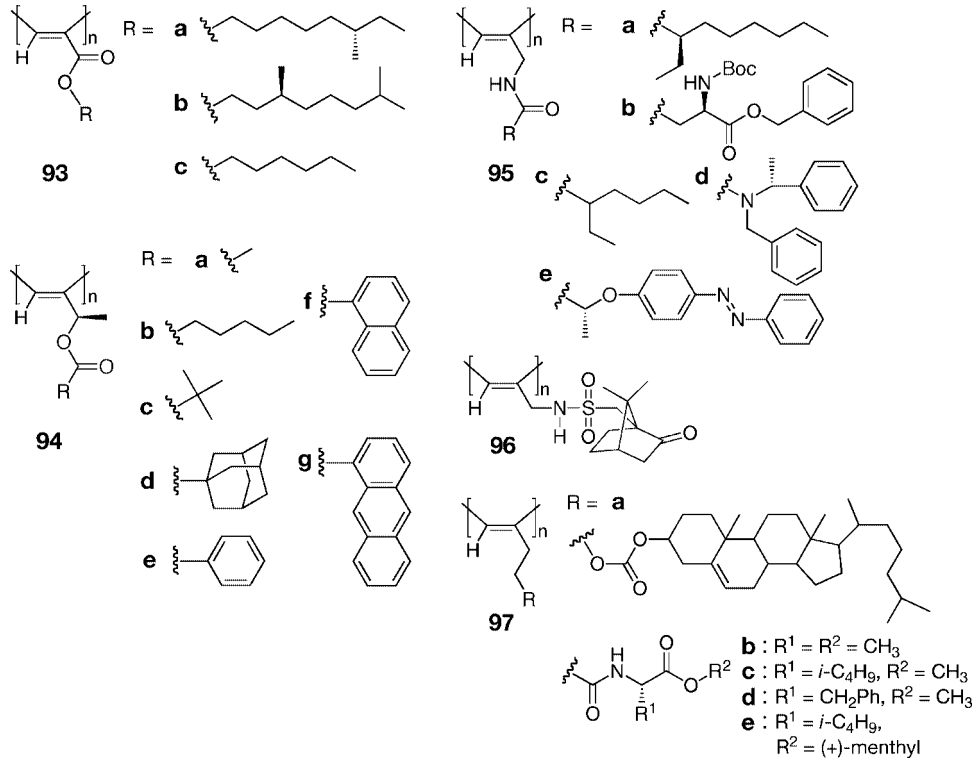

suggest that the semirigid helical polyacetylenes are also composed of long one-helical sense domains, probably *ca.* 660 monomer units, separated by rarely occurring helical reversals.[192,199] Therefore, a similar chiral amplification (sergeants and soldiers effect and majority rule) observed in rigid-rod polyisocyanates and polysilanes also occurs in polyacetylenes (see section 2.6.1).[29,30,156,199]

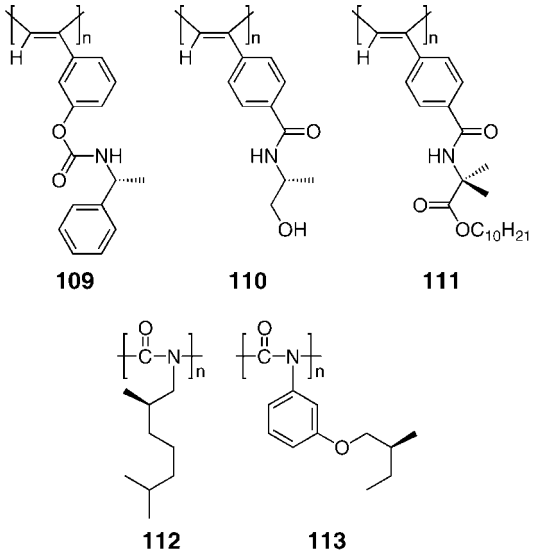

Helical polyacetylenes bearing various amino acids and peptide residues at the pendants have been prepared by Tang et al. and Masuda et al., and their chiroptical properties including their helical conformations and inversion of helicity (see section 2.8) have been investigated.[150,159,190] The intramolecular hydrogen bond networks formed between the neighboring amide groups play a critical role to induce and stabilize the preferred-handed helical conformation. Nevertheless, the hydrogen-bonded poly(*N*-propargylamide) (**95c**) is not rigid, judging from its short persistence length (q = 13.5 nm) in chloroform.[160] An exceptionally rigid rodlike helical PPA has been prepared by the polymerization of phenylacetylenes having an L- or D-alanine residue with a long *n*-decyl chain as the pendant (**88**). As anticipated, the *cis*−*transoidal* PPAs formed a lyotropic cholesteric LC phase in concentrated organic solvents based on the main-chain stiffness, as confirmed by their long q values of *ca.* 40 nm in chloroform.[151] Interestingly, the helical sense of L- or D-**88** was inverted in polar and nonpolar solvents, accompanied with a remarkable change in its q value from 135 nm in CCl_4 to 19 nm in THF. This inversion of the helicity process is generally followed by CD but can be directly proved by high-resolution AFM (see section 3.2.2).

The PPAs decorated with the pendants of naturally occurring amino acids (**84a**)[144] and sugars (**90b**)[153] (Chart 12) show cytocompatibility to living HeLa cells that were survived in the presence of **84a**, while **90b** stimulated the growth of living cells.

In order to prepare optically active helical polyacetylenes, the synthesis of optically active monomers and subsequent polymerization are required. Recently, a unique and versatile method to synthesize an optically active, helical PPA starting from a racemic phenylacetylene bearing a secondary alcohol residue (*rac*-**114**) has been developed (Figure 14).[200] Lipase efficiently catalyzes the kinetic resolution of *rac*-**114** in the presence of isopropenyl acetate as an acetylating agent to give optically active monomers bearing an alcohol ((*S*)-**114**) and ester group ((*R*)-**115**) as the pendants. Subsequent copolymerization of the monomers with a rhodium catalyst without further purification and isolation produced an optically active copolymer, which exhibited a split-type ICD in the polymer backbone region due to an excess one-handed helix formation, even though the starting monomer was racemic. A small chiral bias in the pendants generated by the enzyme-assisted resolution was transformed into a main-

Chart 14

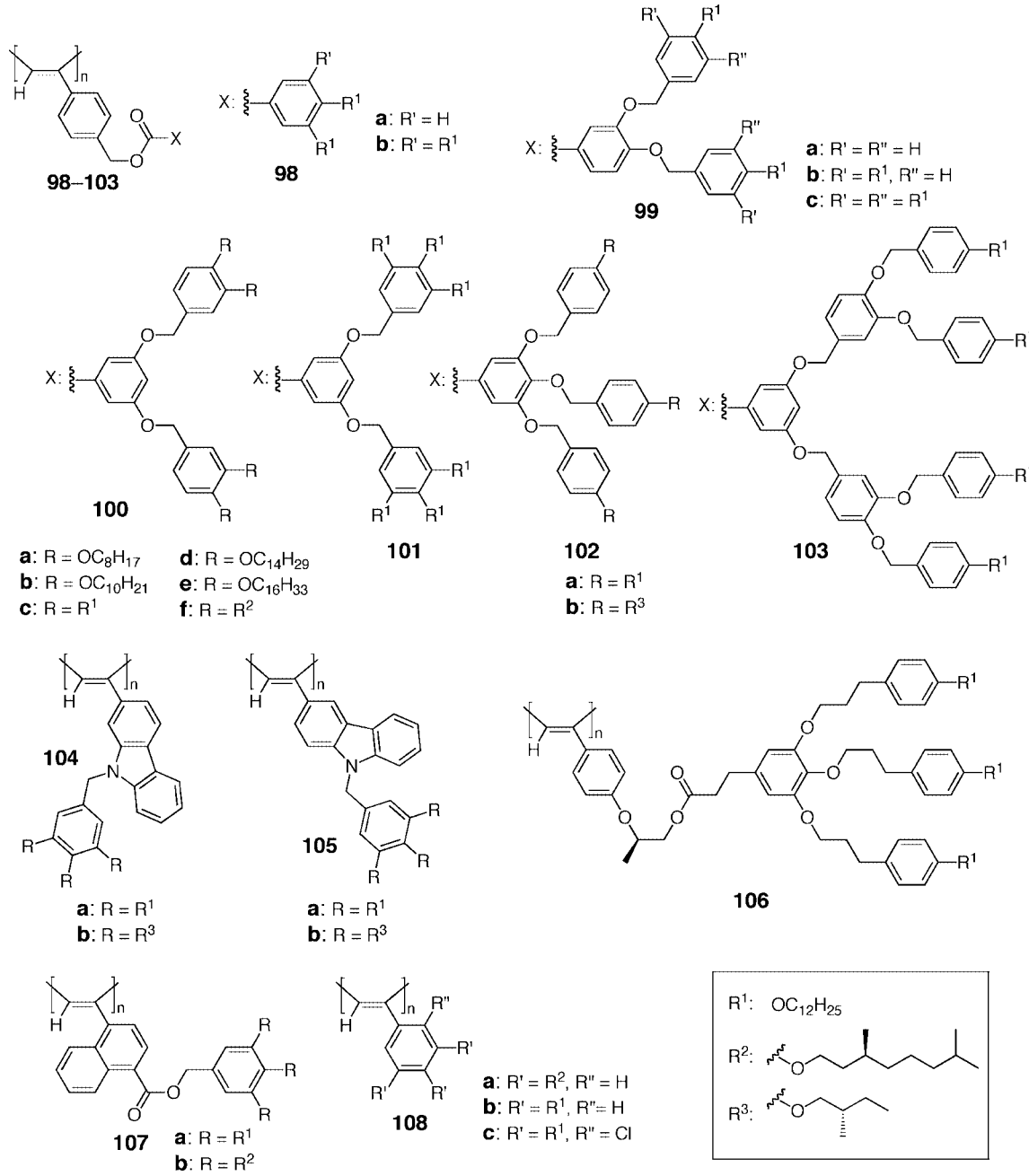

chain conformational change with a large amplification, resulting in the formation of an excess of the preferred helical sense. Interestingly, the helical sense of the copolymer underwent inversion from one helix to another by further modification of the pendant hydroxy groups with achiral bulky isocyanates and an acid chloride.

Achiral phenylacetylenes bearing two hydroxy groups on the phenyl residue (**116** and **117**) gave optically active PPAs when polymerized with a rhodium catalyst in the presence of (*S*)- or (*R*)-1-phenylethylamine (**118**, PEA) (Scheme 15).[201−204] The resulting optically active polymers exhibited an ICD, probably due to an excess of the preferred helical sense stabilized by intramolecular hydrogen bonds, and are stable in chloroform at high temperatures, but the ICD disappeared in the presence of DMSO.[201] The chain length of the alkyl groups of **116** was found to play an important role in achieving helix-sense-selective polymerization.[204] Such a helix-sense-selective polymerization of achiral phenylacetylenes is also possible for achiral and bulky phenylacetylenes (**119** and **120**) to afford optically active helical PPAs kinetically stabilized by the bulky side groups instead of intramolecular hydrogen bonds like the case of PTrMA.[205,206] Optically active helical polyradicals with a high spin concentration were successfully prepared by oxidation of the helical PPAs obtained from **117**[202] and **120**.[206] Recently, Hayashi, Masuda, and co-workers have succeeded in a helix-sense-selective polymerization of **116b** using an optically active rhodium complex bearing C_2-symmetric optically active norbornene ligands.[203]

Polymerization of an optically active phenylacetylene bearing an L-valinol residue and two hydroxy groups using a rhodium catalyst in the presence of (*S*)- or (*R*)-**118** produces diastereomeric helical polymers (**121**, Scheme 15) with an opposite helical sense to each other.[207] The PPA prepared using a rhodium catalyst in the absence of **118** exhibited an ICD whose CD spectral pattern was similar to that obtained

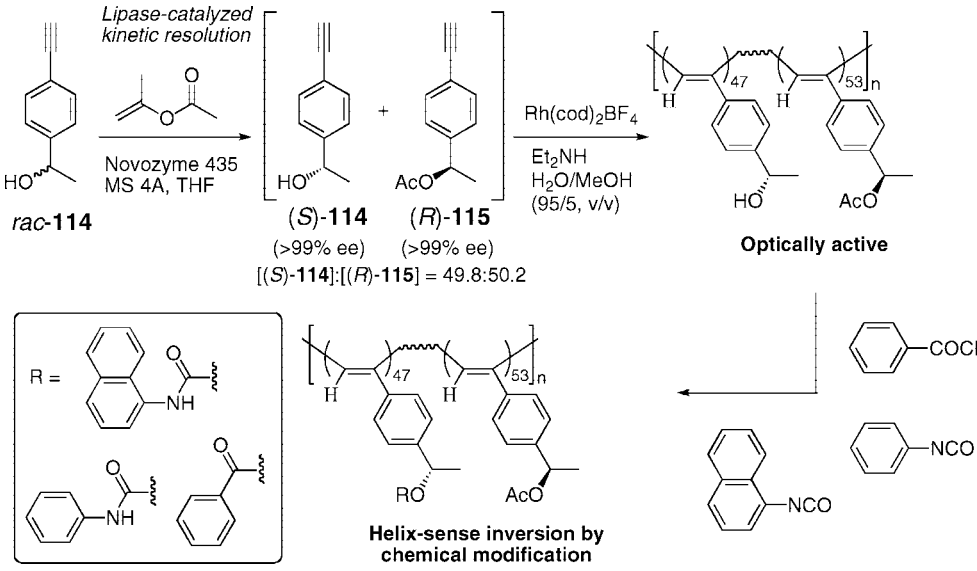

Figure 14. Schematic illustration of the synthesis of optically active helical PPAs by the enzymatic enantioselective transesterification of a racemic phenylacetylene bearing a secondary alcohol moiety followed by the subsequent copolymerization of the obtained optically active phenylacetylenes in one pot and macromolecular helicity inversion by chemical modofication of the pendant.

Scheme 15. Helix-Sense-Selective Polymerization of Phenylacetylenes

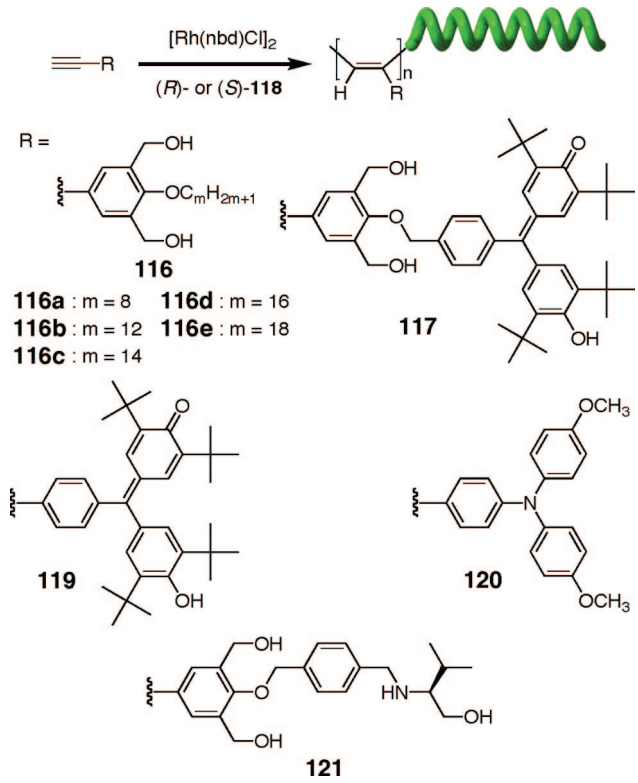

in the presence of (*S*)-**118**, suggesting that the helical sense of **121** can be controlled not only by the chirality of the pendant group but also by the cocatalyst chirality, **118**, during the polymerization of the single enantiomeric phenylacetylene monomer under kinetic control. This observation resembles the helix-sense-controlled polymerization of the enantiomerically pure **32** with an achiral nickel catalyst (Figure 4).[85]

In-situ polymerization of phenylacetylenes catalyzed by WCl_6/Ph_4Sn and $[Rh(nbd)Cl]_2$ in the presence of multiwalled carbon nanotubes (MWNTs) produces PPA/MWNT hybrids in which the MWNTs are helically wrapped by the PPA chains.[208] The pyrene-functionalized PPA/MWNT hybrids are electronically more conjugated and efficiently emit brighter blue-green light than their parent polymers upon the photoexcitation.[209]

2.3. Foldamer-Based Helical Polymers

The π-conjugated oligo(*m*-phenylene ethynylene)s, a typical class of foldamers such as **122** (Chart 15) developed by Moore et al. in 1997, possess a strong tendency to fold into a right- and/or left-handed helical conformation in certain solvents or in the presence of specific guests (for foldamers that exhibit an optical activity due to a preferred-handed helicity induced by noncovalent or covalent bonding with chiral guests or chiral substituents attached at the terminal, see sections 2.5.3 and 2.6.2, respectively).[32,210−213] This foldamer motif has been applied to the design and synthesis of helical polymers with a controlled helix-sense, and several poly(*m*-phenylene ethynylene) derivatives bearing chiral pendant groups have been prepared (Chart 15). A water-soluble **123** bearing L-alanine-derived pendant groups folds into a preferred handedness of the helical conformation, resulting in the appearance of a strong bisignated CD in methanol, water, and their mixtures.[214] The helical polymer is assumed to interact in a manner similar to DNA with the metallointercalator $[Ru(bpy)_2(dppz)]^{2+}$ (bpy = 2,2-bipyridine and dppz = dipyrido[3,2-*a*:2′,3′-*c*]phenazine), such that the dppz ligand intercalates within adjacent π-stacked phenylene ethynylene residues in the helical conformation. The helical polymer also serves as a template for the formation of supramolecular helical aggregates of achiral cationic cyanine dyes, driven by an electrostatic interaction in water, as evidenced by an ICD signal.

An optically active poly(*m*-phenylene ethynylene)-based polyradical (**124b**) bearing galvinoxyl and chiral pinanyl pendant groups has been prepared from the hydrogalvinoxyl precursor polymer (**124a**) by the treatment with PbO_2.[215] **124b** showed a weak but characteristic CD due to the *m*-phenylene ethynylene chromophore regions in a methanol/chloroform mixture, while Cotton effects were hardly observed in chloroform, THF, and benzene. Poly(phenylene ethynylene)s bearing L-menthyl groups (**125**) showed a weak

Chart 15

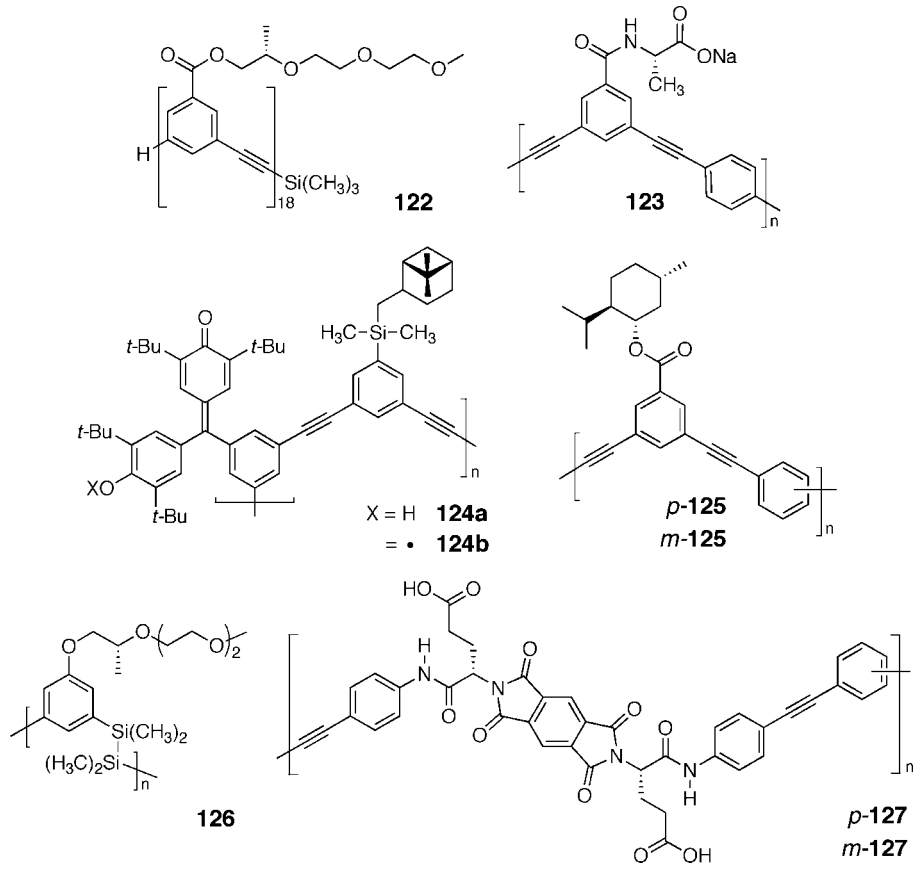

but apparent CD in the main-chain chromophore region, and the CD intensities slightly changed in the presence of L- and D-menthol by responding to the chirality of menthol.[216]

An analogous $\sigma_{(Si-Si)}-\pi$ conjugated polymer, poly(*m*-phenylenedisilanylene) (**126**), has been synthesized by the sodium coupling of the chlorosilane monomer.[217] The methanol solution of **126** showed positive Cotton effects in the absorption region ascribed to the $\sigma-\pi$ conjugation of the main-chain, while no Cotton effects were observed in dichloromethane. Interestingly, the helical handedness of **126** can be biased through the complexation with appropriate metal ions even in dichloromethane. The positive Cotton effects appeared upon the addition of Li^+, whereas the opposite, negative Cotton effects appeared in the presence of Na^+, K^+, Cu^{2+}, or Zn^{2+}. Optically active polymers composed of the *m*- or *p*-phenyleneethynylene skeleton linked by an L-glutamic acid-derived benzenetetracarboxylic diimide residue (*p*-**127** and *m*-**127**)[218] exhibited an ICD whose intensity was not sensitive to temperature and solvent compositions (DMF and water), but *p*-**127** is quite sensitive to KOH and lost its optical activity in the presence of an excess of KOH. In contrast, *m*-**127** maintains its CD signal with the addition of KOH.

Meijer and co-workers have designed and synthesized a series of novel helical polymers consisting of a ureidophthalimide backbone (**128**) that folds into a helical architecture with a pitch of *ca.* 6−8 units in which the urea linker adopts a *cisoid* conformation assisted by intramolecular imide-urea hydrogen bonding (Figure 15).[219−221] A poly(ureidophthalimide) bearing chiral alkyl side chains (**128a**) showed an intense CD in THF but was CD silent in chloroform. An analogous poly(ureidophthalimide) bearing hydrophilic chiral oligo(ethylene oxide) groups (**128b**) also exhibited an apparent Cotton effect in THF and water. Due to strong hydrophobic forces and $\pi-\pi$ stacking interactions in water, the helical structure of **128b** is noticeably stable in water, and the CD intensity hardly changed even at 90 °C. In sharp contrast, the CD intensity in THF decreased upon heating and completely disappeared at 55 °C, suggesting the dynamic nature of its helical conformation in THF. Interestingly, the Cotton effect signs of **128b** in THF and water are opposite to each other, indicating a solvent-induced helix inversion (see also section 2.8.2).[220] This foldamer architecture has been further employed as a scaffold for organizing oligo(*p*-phenylene vinylene) (OPV) chromophores into a one-handed helical array along the polymer backbone (**128c**), as evidenced by the appearance of CDs in the OPV and main-chain chromophore regions in THF, although no Cotton effect was observed in chloroform because of its unfolding into a random coil in this solvent.[221] The polymer retains the previous history of its helical and random coil conformations in solution, so that the CD reappeared in heptane when **128c** was recovered from the THF solution.

Taking advantage of the *cis* conformation preference of *N*-alkylated aromatic amides,[222,223] a series of helical poly(*p*-benzamide)s (**129a**) bearing chiral side chains have been prepared by a chain-growth polycondensation which affords poly(*p*-benzamide)s with well-defined molecular weights and narrow molecular weight distributions (Chart 16).[224] The dispersion-type CD signals of **129a** observed in several organic solvents, such as acetonitrile, chloroform, and methanol, are highly temperature- and chain-length-dependent, suggesting that the polymers possess a dynamic helical structure. The secondary structure of **129a** has been determined to be a right-handed helix, as revealed by the X-ray crystallographic analysis of the corresponding uniform oli-

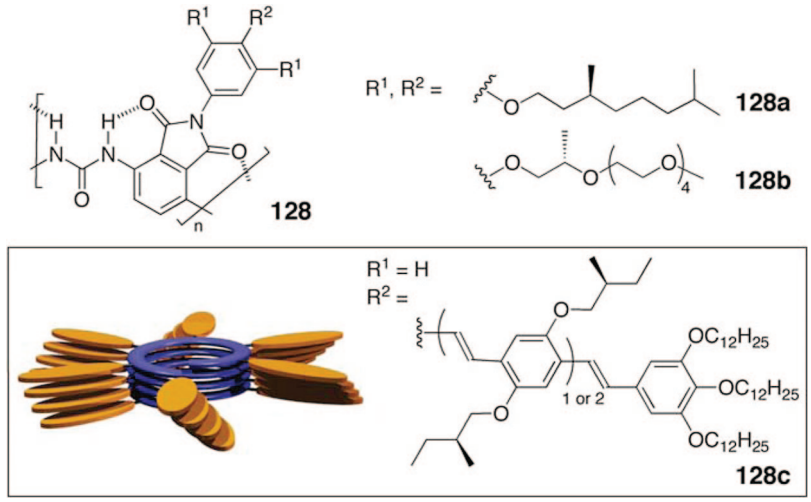

Figure 15. Optically active helical polymers consisting of an ureidophthalimide backbone. (Reproduced with permission from ref 221. Copyright 2006 American Chemical Society.)

Chart 16

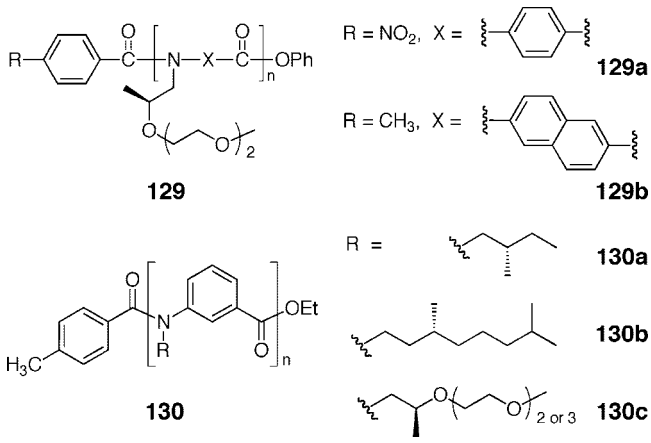

gomers as well as the exciton model analysis of the absorption and CD spectra of **129a**, as described in sections 3.1.1 and 3.2.1. An analogous poly(naphthalenecarboxamide) with the same chiral side chain (**129b**) has also been synthesized to examine its secondary structure in solution.[225] In contrast to **129a**, the right-handed helical folding of **129b** was enhanced by a solvophobic effect in water/methanol mixed solvents.

Poly(*m*-benzamide)s (**130**, Chart 16) having hydrophobic or hydrophilic chiral side chains have also been synthesized by the chain-growth polycondensation method. They exhibited a temperature-dependent CD in methanol and chloroform, suggesting a dynamic behavior in their helical conformations.[226]

Combined with the foldamer concept together with the click reaction and the regioselective ring-closing reaction, helical polymers with novel backbones have been prepared.

2.3.1. Click Polymerization

The Cu-catalyzed 1,3-dipolar cycloaddition of azides and alkynes, known as the "click reaction", has become very popular in polymer chemistry, and a variety of functional polymers with unique architectures have been developed,[227−230] but only few examples have been reported regarding the synthesis of helical polymers using the click reaction. Optically active triazole-pyridine/benzene copolymers (**131**) prepared by the step-growth click polymerization of amphiphilic 2,6-diethynylpyridine with chiral aromatic diazide (Scheme 16)[231] adopt a helical conformation with a biased helical sense assisted by a preference for the kinked *anti-anti* conformation of the 2,6-bis(1,2,3-triazol-4-yl)pyridine subunits, as supported by an intense bisignated Cotton effect in polar and nonpolar solvents. The addition of transition metal ions, such as Zn^{2+}, Fe^{2+}, and Eu^{3+}, to the polymer solutions produced a physical gel through coordinative cross-linking of the polymer backbones.

Similar to this, an optically active monomer **132** bearing both azide and acetylene groups within the molecule has been click homopolymerized (Scheme 17).[232] The polymer poly-**132a** exhibited a weak CD in DMF and DMSO, but upon the addition of poor solvents, such as chloroform and methanol, the CD intensity in the π-conjugated main-chain region significantly increased, accompanied by a fluorescence color change due to the formation of π-stacked supramolecular chiral aggregates. Interestingly, the monomer can be chain polymerized with a rhodium catalyst, giving an optically active helical PPA poly-**132b**. Since poly-**132b** has azide groups at the side chain, further modification of the azide pendant via the "click" polymer reaction is possible using optically active acetylenes, thus producing diverse optically active PPAs poly-**132c** (Scheme 17).

2.3.2. Ring-Closing Reaction

An interesting approach to constructing a distinct helicene-like ladder polymer with a controlled helical sense from a rather flexible linear polymer has been reported.[233] The key step for this purpose is a quantitative and regioselective intramolecular ring-closing reaction. The prepolymer, an optically active alkylsulfoxide-substituted poly(1,3-phenylene) bearing chiral substituents (**133**) prepared by quantitative oxidation of the corresponding alkylthio-substituted poly(1,3-phenylene) ($M_n = 1.1 \times 10^4$ and $M_w/M_n = 1.2$), showed no Cotton effect in good solvents such as chloroform but exhibited an apparent CD in the presence of acetonitrile, a poor solvent. The CD intensity significantly decreased with temperature in the range from 25 to 50 °C, indicating a typical helix formation driven by solvophobic forces in the presence of poor solvents. The intramolecular ring-closing condensation of the helical prepolymer with triflic acid can fix its preferred-handed helical conformation solvophobically induced in a chloroform and acetonitrile mixture to produce

Scheme 16. Synthesis of 131 via the Step-Growth Click Polymerization

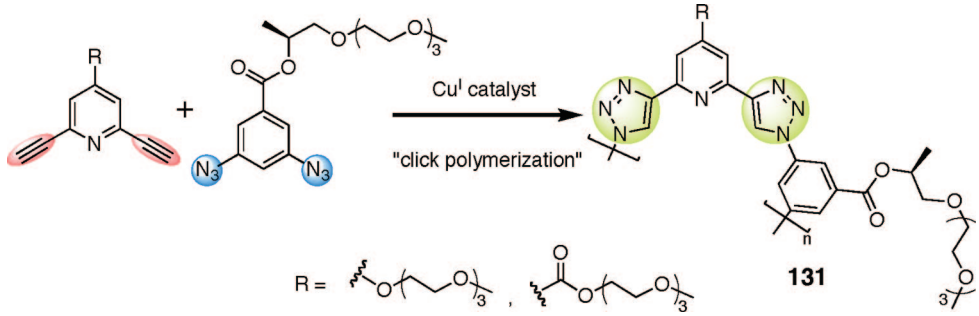

Scheme 17. Polymerization of 132 by the Click Reaction and with a Rhodium Catalyst

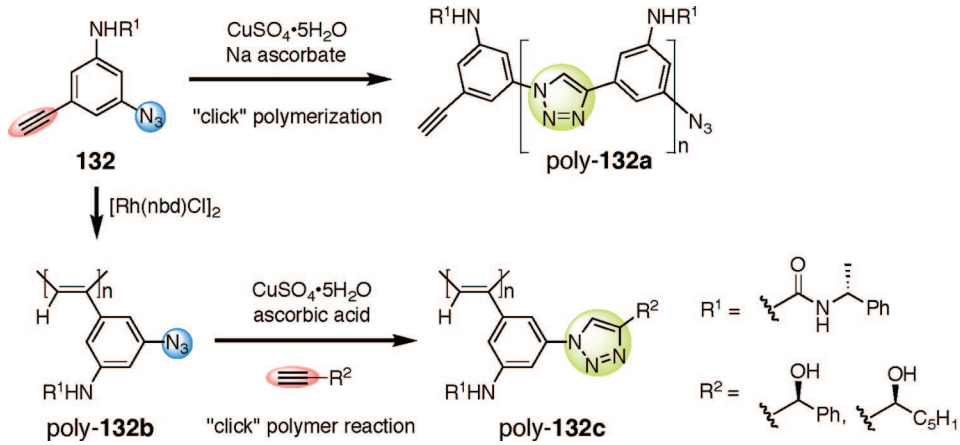

Scheme 18. Synthesis of 134 via the Intramolecular Ring-Closing Reaction with a Controlled Helicity

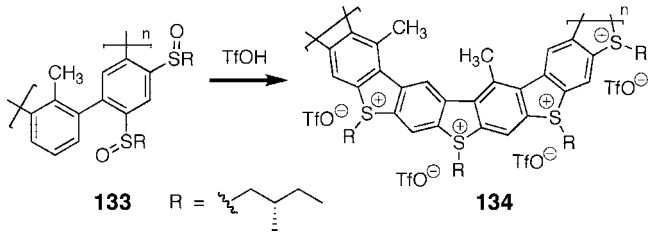

Scheme 19. Synthesis of 136 through the Regioselective Intramolecular Ring-Closing Reaction of the Pendant Chiral Sulfoxide in 135

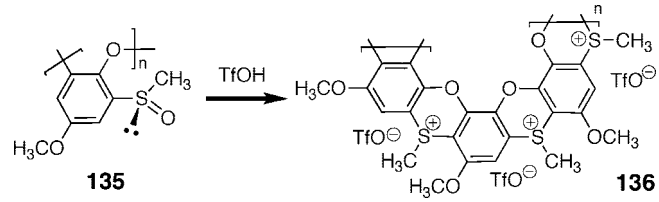

a π-conjugated helical ladder poly(thiaheterohelicene) (**134**), comprised of highly planar fused benzothiophene rings (Scheme 18). In sharp contrast to the prepolymer, the CD intensity and pattern of **134** are independent of temperature as well as the solvent polarities, supporting its stiff helical backbone structure. This unique helical ladder structure may provide the potential for developing a one-dimensional wire in an organic molecular-based electromagnet.

A similar helical ladder polymer (**136**) with no chiral substituents has also been prepared by the regioselective intramolecular ring-closing reaction of the pendant chiral sulfoxide groups in a poly(1,2-phenyleneoxide) (**135**) (Scheme 19).[234] Although the molecular weight was low ($M_n = 1800$ and $M_w/M_n = 1.2$ for **135**), the polymer composed of fused phenoxathiine rings likely has a predominant helical conformation, evidenced by the appearance of a characteristic CD in the $\pi-\pi^*$ transition region of the polymer backbone.

A binaphthyl-derived helical polymer (**138**) has been synthesized by the acid-promoted intramolecular cyclization of the electron-rich aromatic alkynes of the prepolymers (**137**) (Scheme 20).[235] A well-defined helical chain structure is proposed because of the restricted rotation in the repeating units. The magnitude of the CD centered at *ca.* 340 nm tends to increase with an increase in the molecular weight of **138**.

2.4. Other Types of Helical Polymers

2.4.1. π-Conjugated Helical Polymers

Optically active π-conjugated polymers, such as polythiophenes, generally exhibit an optical activity, such as an ICD, in the $\pi-\pi^*$ transition chromophore regions of the polymer backbones when aggregated to form a supramolecular π-stacked, self-assembly with intermolecular interactions in poor solvents or the solid film state, whereas they usually show no CD in good solvents.[236−245] Inganäs et al. have demonstrated that a polythiophene (**139**) bearing L-amino acid functionalized pendants in aqueous solution showed a split-type CD in the main-chain $\pi-\pi^*$ transition region induced from a preferred handedness of the helical *cisoid* conformation (Chart 17).[246−248] The magnitude of the Cotton effect significantly depended on pH, and the highest CD intensity was observed at a pH equal to the isoelectric points of the amino acid in water, at which the polymer backbone adopts a preferred-handed helical conformation stabilized by the hydrophobic interactions within the polymer main-chain, electrostatic interactions, or hydrogen bonding between the zwitterionic side chains, while the aggregation of the polymer took place at a higher pH.[247,248] An optically active polythiophene (**140**) bearing two chiral long alkyl

Scheme 20. Synthesis of 138 via the Acid-Catalyzed Intermolecular Cyclization

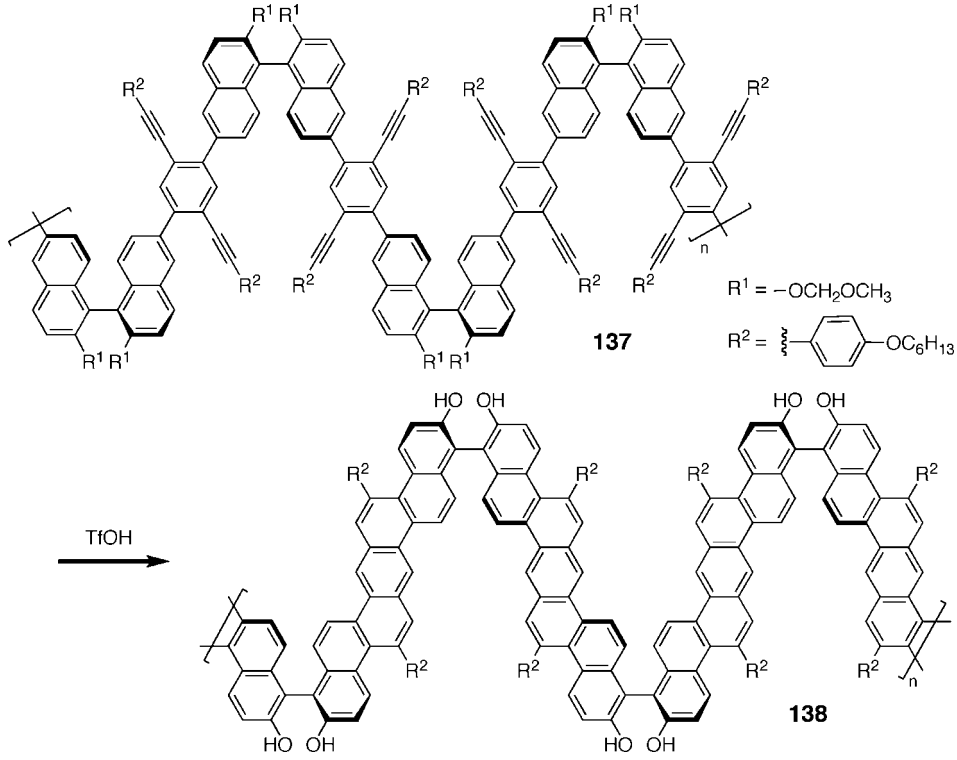

Chart 17. π-Conjugated Polymers Showing Optical Activity in the Molecularly Dispersed State

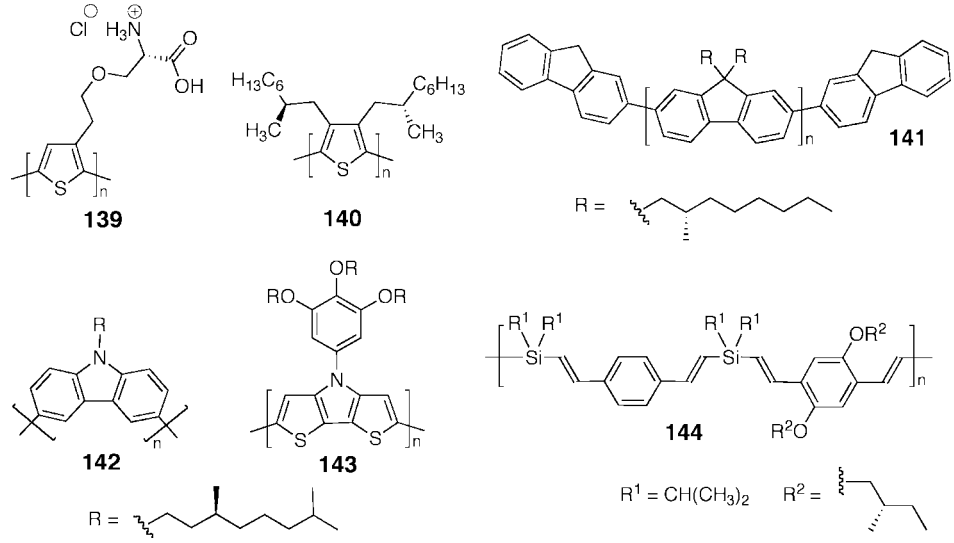

chains at the 3 and 4-positions has also been prepared to show an ICD in the molecularly dispersed state.[249] The sign and intensity of the ICD are dependent on temperature and the solvent polarities but independent of the polymer concentrations, which support the dynamic helical conformation in a single polymer chain.

Other π-conjugated polymers bearing optically active side chains, such as poly(fluorene) (**141**),[250] poly(carbazole) (**142**),[251] poly(dithienopyrrole) (**143**),[252] and a silylene divinylarene copolymer (**144**),[253] are also considered to possess a preference for one particular helical conformation in solution.

2.4.2. Metallosupramolecular Helical Polymers

Metal-directed supramolecular coordination polymerization of bis-functionalized chiral monomers with transition metals can produce infinite metallosupramolecular helical polymers in solids.[254] However, coordination linear polymers with a well-defined helical structure in solution or gel are very rare.

Lee and co-workers reported a bent-shaped bipyridine ligand containing a dendritic aliphatic side chain (**145**) that can complex with Ag^+ ions to form coordination polymers with tunable secondary structures as a function of the counteranions. As the size of the anion increases, the secondary structure changes from a folded helical chain, via a dimeric cycle, to an unfolded zigzag conformation that further self-organized to generate the 2D hexagonal columnar and lamellar structures in the solid state (Figure 16).[255] Interestingly, a dilute solution of the metallosupramolecular helical complex with BF_4^- undergoes spontaneous gelation and the resulting gel displays a significant Cotton effect in the aromatic chromophore region. The further addition of a

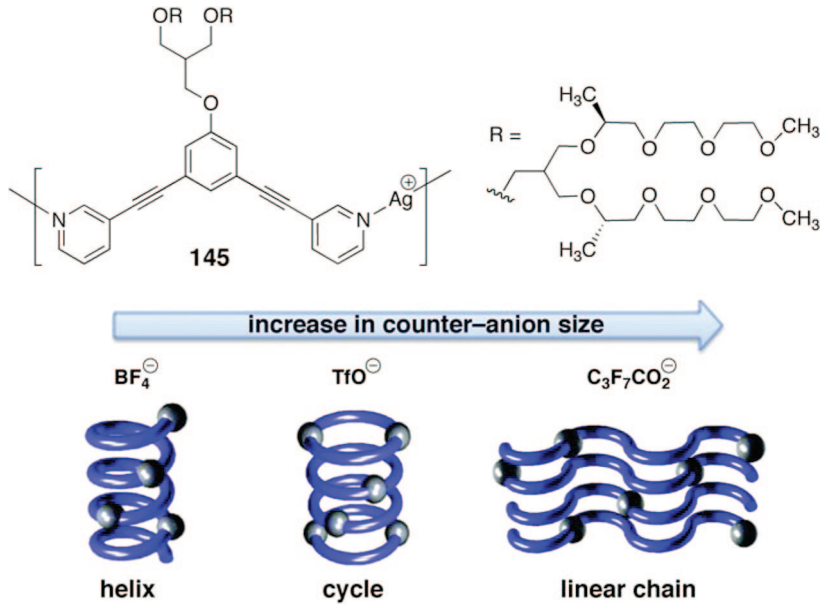

Figure 16. Anion-directed self-assembly of a coordination polymer. (Reproduced with permission from ref 255. Copyright 2004 American Chemical Society.)

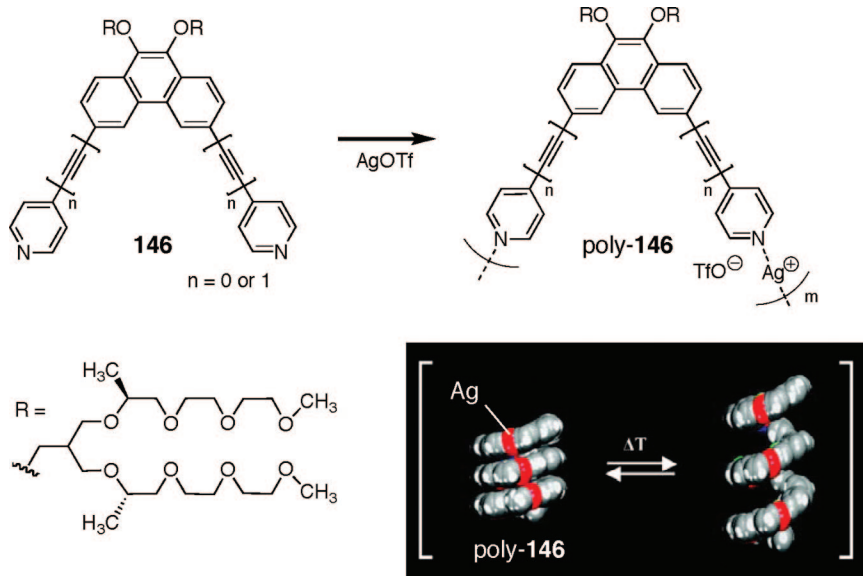

Figure 17. Formation of supramolecular coordination polymers with a switchable helical pitch. (Reproduced with permission from ref 258. Copyright 2007 American Chemical Society.)

larger counteranion, $C_2F_5CO_2^-$, produced transformation into a fluid due to depolymerization or transformation of the folded helical chain into a zigzag chain. This process can be reversible by the alternative addition of BF_4^- and $C_2F_5CO_2^-$.[256]

Helical coordination polymers (poly-**146**) with a switchable pitch ("*helical springs*")[257] have been demonstrated using analogous dipyridyl ligands **146** with Ag^+ ions in aqueous solution (Figure 17).[258] The metallosupramolecular helical springlike structures evidenced by CD, fluorescence, and dynamic light scattering (DLS) measurements as well as transmission electron microscopy (TEM) observations revealed elementary cylindrical fibers with a uniform diameter of about 6.5 ± 0.4 nm and a length of several micrometers. The helical supramolecular springs display reversible extension−contraction motions triggered by temperature. This dynamic conformational change leads to a fluorescence switching, caused by the breakup of the intramolecular $\pi-\pi$ stacking interactions in the polymer backbone. This mechanical springlike motion may offer intriguing potentials for dynamic nanodevices, optical modulators, and fluorescent thermometers.

Moore et al. have extended the foldamer concept to supramolecular folded polymers and rationally designed and synthesized metallosupramolecular helical polymers through the coordination polymerization of oligo(*m*-phenylene ethynylene)s (**147**) containing pyridyl end groups with Pd(II) (Figure 18).[259] Upon the addition of *trans*-dichlorobis(acetonitrile)palladium to a solution of **147**, supramolecular assembly by metal coordination occurred to form the supramolecular folded polymer (poly-**147**) through a nucleation−elongation mechanism.[260] Contrary to the metallosupramolecular polymerization of a tetramer and octamer ($n = 2, 6$), the corresponding hexamer ($n = 4$) formed a shape-persistent macrocycle which further aggregated into a columnar polymer through π-stacking with other macrocycles. As a consequence, the oligomer length, geometry,

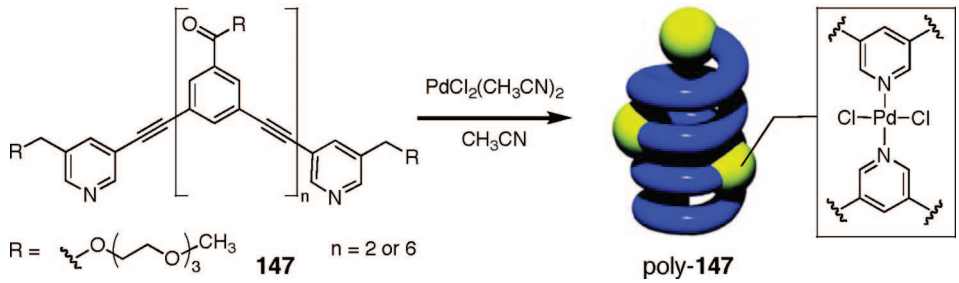

Figure 18. Coordination polymerization of bis-functionalized phenylene ethynylene oligomers. (Reproduced with permission from ref 259. Copyright 2006 American Chemical Society.)

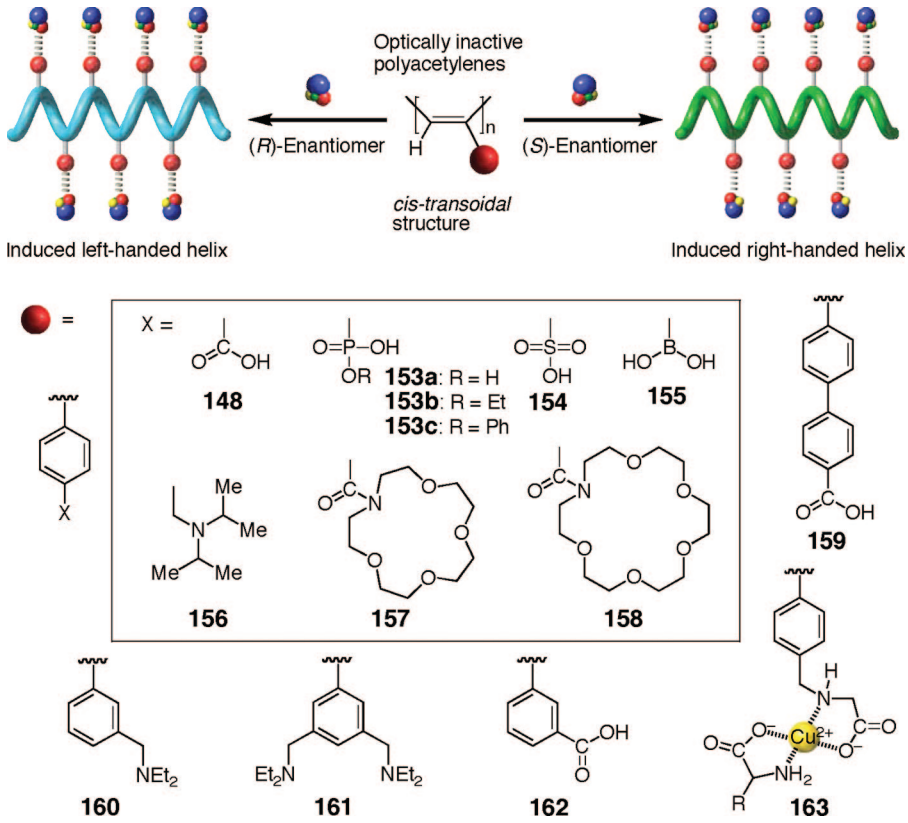

Figure 19. Schematic illustration of a preferred-handed helicity induction in PPAs bearing various functional groups (**148**, **153**−**163**) upon complexation with chiral compounds.

and supramolecular interactions directly influence the polymerization mechanism.

2.5. Induced Helical Polymers

Helix-sense bias can also be induced in optically inactive, dynamically racemic helical polymers through specific noncovalent bonding interactions. This section mainly describes the preferred-handed helicity induction in PPAs through noncovalent chiral interactions[19,20,29,30,261] along with other representative examples.

2.5.1. Induced Helical Polyacetylenes

A *cis*−*transoidal*, stereoregular poly((4-carboxyphenyl)-acetylene) (**148** in Figure 19) is the first dynamic helical polymer with an excess of the one-helical sense biased by noncovalent specific chiral acid−base interactions.[262] Upon complexation with chiral amines in DMSO, a preferred-handed helical conformation is instantaneously induced in the polymer, showing a characteristic ICD in the π-conjugated polymer backbone region. Figure 20 shows the typical CD spectra of **148** in the presence of various optically active amines (**118**, **149**−**152**) in DMSO. The remarkable CD induction is ascribed to a drastic change in the population of the interconvertible right- and left-handed helical domains separated by few helical reversals along the polymer chain. There is a good relation between the Cotton effect signs corresponding to the helical sense of **148** and the absolute configurations of the chiral amines; all primary amines and amino alcohols of the same configuration give the same Cotton effect signs. Therefore, the Cotton effect sign of **148** can be used to sense the chirality of various primary chiral amines.[263,264] The magnitude of the ICD tends to increase with an increase in the bulkiness of the amines, **149** < **150** < **118** ≪ **151** < **152**, indicating that the bulky groups introduced at the *para* position of **148** contribute more efficiently for the polymer to take an excess one handedness.[265] In sharp contrast to the previously mentioned static and dynamic helical polymers with chiral groups connected by covalent bonding, the helical sense can be controlled by the chirality of the small chiral molecules after polymerization. This noncovalent helical sense induction concept has

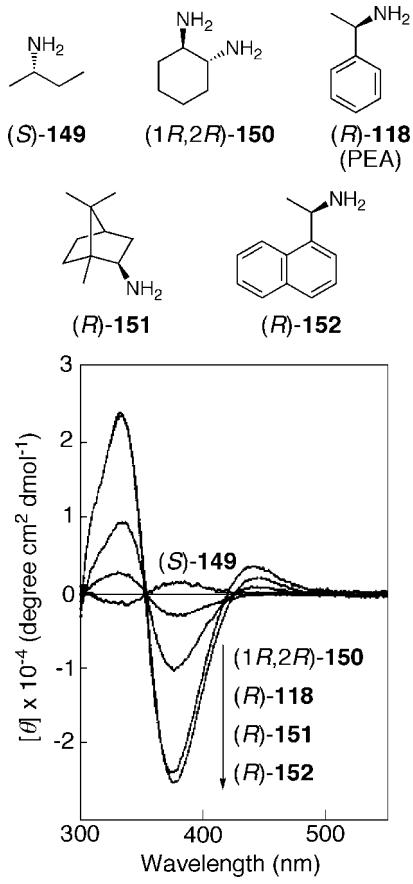

Figure 20. CD spectra of **148** upon complexation with chiral amines (**118**, **149**−**152**) in DMSO. (Reproduced with permission from ref 265. Copyright 1997 American Chemical Society.)

been applied to the design and synthesis of a variety of chirality-responsive PPAs by introducing a specific functional group as the pendant group (**153**−**163** in Figure 19).[266−284] Chiral amplification phenomena of the "sergeants and soldiers" effect and "majority rule", which are characteristic features for dynamic helical polymers as discussed in the preceding sections, are also observed in these functional PPAs through noncovalent bonding chiral interactions (see sections 2.6 and 2.7).

The bulkiness of the chiral guest molecules plays a crucial role in inducing an excess one-handed helix on functional PPAs through noncovalent interactions, as shown in Figure 20. CD experiments with **153b** using a series of chiral glutamate-based dendrons (**164** and **165**) in DMSO have revealed the effect of the bulkiness and chirality of the dendrons on the macromolecular helical sense induction in functional PPAs.[268] The ICD signs depend on the configuration of the terminal glutamate of the dendrons and are independent of the exterior glutamate configuration, so that DLL-**165** shows the same Cotton effect sign as that of DDD-**165** when complexed with **153b** (Figure 21). The magnitude of the ICDs significantly increased with an increase in the dendritic generations, demonstrating that the helix-sense excess of **153b** induced by the optically active dendrons through noncovalent acid−base interactions is highly dependent on the bulkiness (generation) of the dendrons.[268]

2.5.1.1. Helicity Induction in Water. On the other hand, the chiral recognition of charged biomolecules with synthetic receptor molecules in water through polar interactions is quite attractive but still remains very difficult. This is because small electrolytes largely dissociate into free ions in water by hydration, and therefore, attractive polar interactions, such as hydrogen bonding and electrostatic interactions between the receptor and guest molecules, may not effectively occur in water. In sharp contrast, biological macromolecules, such as DNA and proteins, are typical polyelectrolytes and exhibit an elaborate molecular recognition and catalytic activity in aqueous solution, because polyelectrolytes are completely different from small electrolytes; that is, a portion of the counterions are bound to polyelectrolytes with a sufficiently high charge density so that polyelectrolytes can effectively interact with small charged biomolecules even in water. This counterion condensation effect[285] is a characteristic property of polyelectrolytes, thus providing an important clue for the design of charged synthetic receptors for biomolecular recognition in water.

Based on these considerations, the preferred-handed helicity induction in chromophoric dynamic helical polyelectrolytes **148** and **153**−**156** (Figure 19) in water has been explored. These polyelectrolytes have been found to interact with a variety of charged and uncharged biomolecules including amino acids, aminosugars, aromatic and aliphatic carboxylic acids, phosphoric acids, carbohydrates, and peptides due to an ion condensation effect[285] and hydrophobic and hydrogen bonding interactions in water, and the complexes exhibit characteristic ICDs in the main-chain chromophore regions.[266,269,270,278,286] Among the PPA-based polyelectrolytes, **153b** and the hydrochloride of **156** (**156**-HCl) bearing the bulky phosphonate and ammonium groups as pendants, respectively, are the most sensitive to the chirality of amino acids and carboxylic acids in water, respectively. For example, **153b** showed the same Cotton effect sign in response to all 19 of the common free L-amino acids, demonstrating that the polyelectrolyte is indeed a powerful chirality sensor in water.

The positively charged polyelectrolyte **156**-HCl can also respond to the chirality of various acids, including carboxylic, phosphoric, and sulfonic acids in water with an extremely high sensitivity, thus forming a single-handed helical conformation in the presence of a small amount of chiral acids ([chiral acid]/[**156**-HCl] = 0.1) even with a low ee in water (see section 2.6.1). The polyelectrolyte function of the **156**-HCl is indispensable for its remarkable high chiral amplification property in water, because the neutral **156** is not sensitive to the chirality of chiral acids in organic solvents and requires a large excess amount of chiral acids to exhibit the full ICD.[276] This finding, the use of a chromophoric dynamic helical polyelectrolyte, will be promising for the design and synthesis of a more sensitive sensory system in water for a target biomolecule by tuning the functional group of the polyelectrolyte.

2.5.1.2. Helicity Induction in Gel and Solid. A preferred-handed helicity induction is also possible in functional PPA gels and films. PPA-based functional gels **166a** and **166b** have been synthesized either by the copolymerization of (4-carboxyphenyl)acetylene with a bis(phenylacetylene) as the cross-linker using a rhodium catalyst or by the cross-linking of **148** with a diamine, respectively (Figure 22). The gels respond to the chirality of nonracemic amines in DMSO and alkaline water and showed a similar ICD in the main-chain absorption region to that of **148** in solution accompanied by significant swelling in DMSO, thus providing the first chirality-responsive gel.[287]

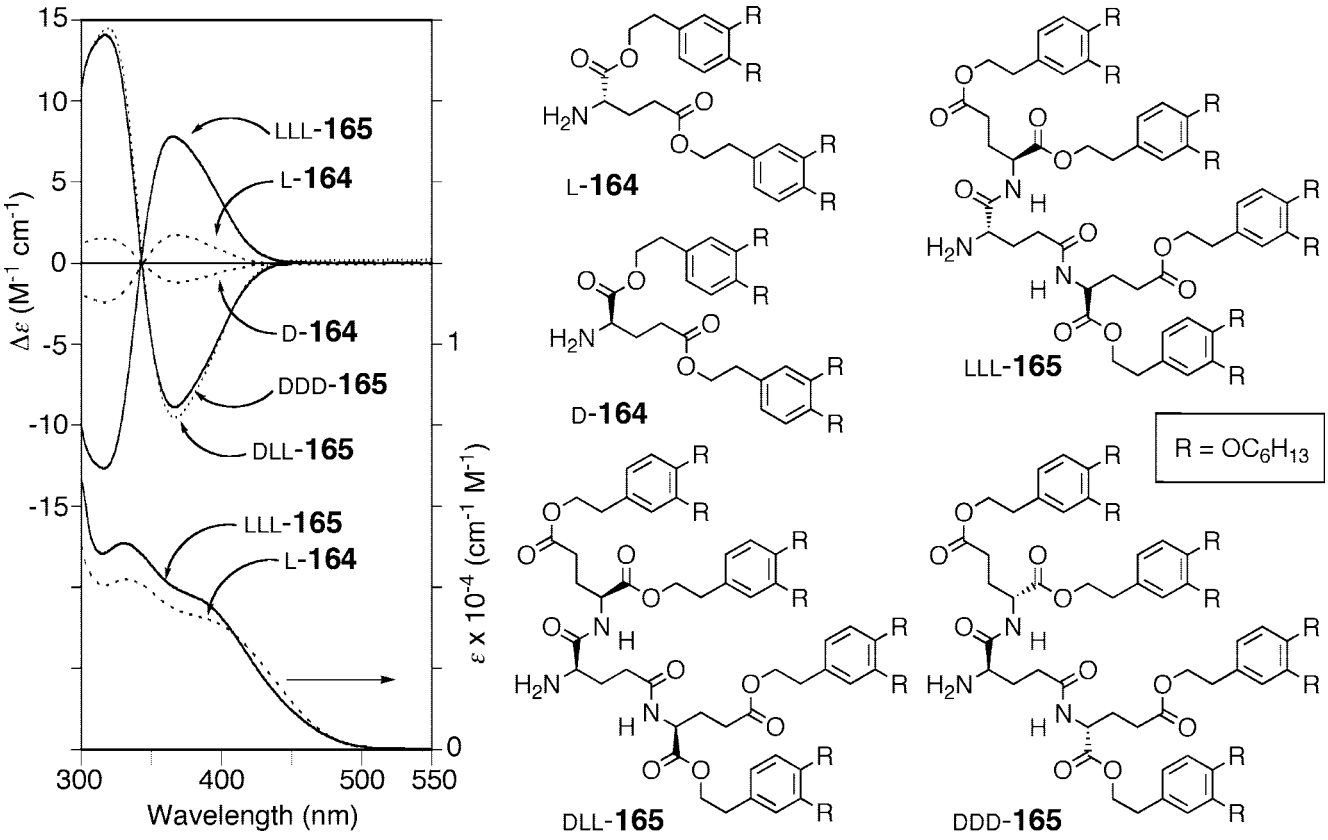

Figure 21. CD spectra of **153b** upon complexation with chiral glutamate-based dendrons (L-**164**, D-**164**, LLL-**165**, DDD-**165**, and DLL-**165**) in DMSO/chloroform (66/34, v/v) at ambient temperature. Absorption spectra of **153b** with L-**164** and LLL-**165** are also shown. (Reproduced with permission from ref 268. Copyright 2004 John Wiley & Sons, Inc.)

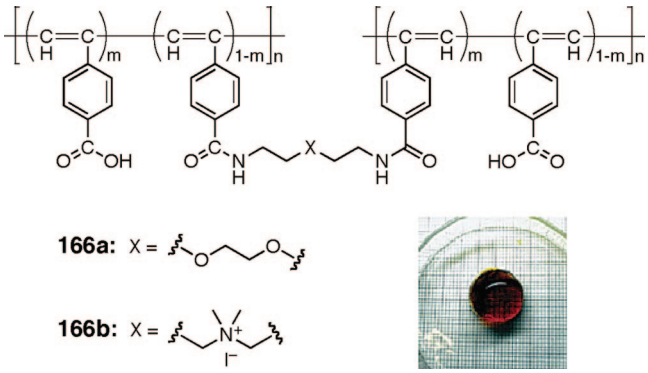

Figure 22. Structure of a chirality-responsive poly(phenylacetylene) gel (**166a**, **166b**) and a photograph of the gel. (Reproduced with permission from ref 287. Copyright 2003 American Chemical Society.)

The aza-18-crown-6 ether-bound PPA (**158**) also forms an optically active gel upon complexation with optically active bis(amino acid)s, such as L-homocystine perchlorate (L-HCys), in acetonitrile, thereby exhibiting an ICD due to an excess of the one-helical sense (Figure 23A).[288] The gelation of **158** is highly sensitive to the structure and chirality of the bisammoniums with respect to the distance between the separated charges. Interestingly, achiral diamines with a structure similar to L-HCys and racemic HCys gave rise to no gelation. However, HCys of more than 60% ee causes gelation with a full ICD as intense as that induced by the 100% ee of HCys (Figure 23B). This is the first chirality-responsive gel induced and assisted by noncovalent interactions in an enantioselective fashion ("sergeants and soldiers" effect).

The cast film of **148** also responds to the chirality of liquid and solid chiral amines, such as **167**, and exhibits an ICD in the polymer backbone region, although it requires a much longer time to reach the maximum ICD value (Figure 24).[289] The observed Cotton effect patterns are similar to those of **148** induced by the chiral amines in solution, indicating that the preference of the helical sense induced in the **148** film is the same as that in solution induced by the same optically active amine.[289] These methods using gels and films composed of dynamic helical polymers are more convenient and practically useful to sense the chirality of chiral amines than the solution method. Recently, Dei and Matsumoto have reported that polydiacetylenes with a 4-carboxyphenyl substituent prepared by the polymerization under UV and γ-irradiation exhibited an ICD in the main-chain visible region in the presence of optically active amines in the dispersion and in the solid state, resulting in a twisted layered structure.[290]

2.5.2. Other Induced Helical Polymers and Oligomers

The preferred-handed helicity induction concept has been further applied to other dynamically racemic chromophoric polymers or oligomers, and a helical conformation with a biased helical sense has been induced through noncovalent interactions with nonracemic guests (Chart 18). Aliphatic polyacetylenes (**168**−**170**),[291−293] polyisocyanates (**62**, **171**−**173**),[119,294−296] poly(phenyl isocyanide) (**174**-H),[297] and polyguanidine (poly-**58**)[106] are typical examples, in which chiral acid−base, host−guest, ionic, and/or hydrogen bonding interactions contribute a great deal to inducing one specific handed helical conformation.

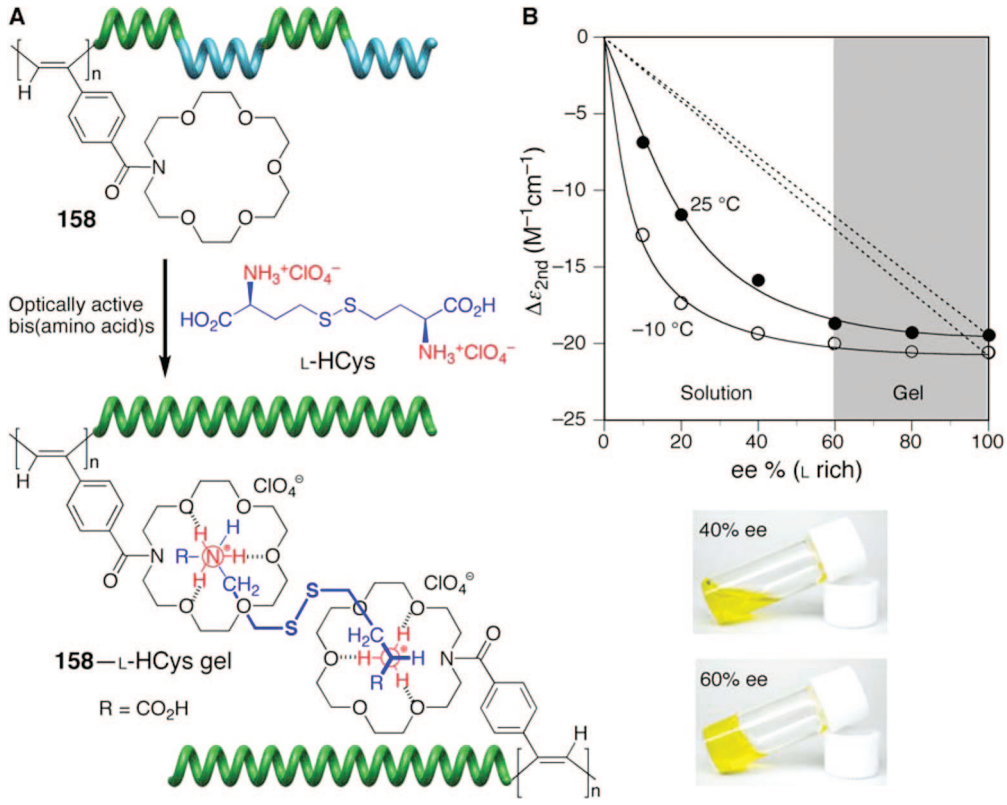

Figure 23. (A) Schematic representation of the macromolecular helicity induction on **158** upon complexation with optically active bis(amino acid)s (L-HCys) and the gelation by noncovalent cross-linking between the crown ether pendants with L-HCys. (B) Nonlinear effects between the second Cotton effect ($\Delta\varepsilon_{second}$) value and percent ee of HCys (L rich) in the complexation with **158** ([HCys]/[**158**] = 2) in acetonitrile containing 0.3 vol % aqueous $HClO_4$ ([$HClO_4$]/[L-HCys] = 2.2 at 25 °C (●) and −10 °C (○)). The ICD intensities of the complexes were measured after the samples had been allowed to stand for 1.5 h at ambient temperature. Photographs of **158** complexed with 40 and 60% ee of HCys are also shown in part B. (Reproduced with permission from ref 288. Copyright 2005 American Chemical Society.)

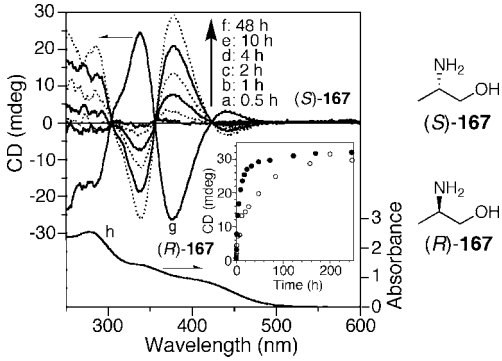

Figure 24. CD spectral changes of **148** film with **167** at ambient temperature (*ca.* 25 °C) with time (a−f). CD and absorption spectra of **148** film with (*R*)-**167** after 49 h are also shown in parts g and h, respectively. The inset shows the plots of ICD intensity (second Cotton effect) of the **148** film with (*S*)-**167** versus time in air (●) and in a drybox under argon atmosphere (○).

A poly(organophosphazene) bearing carboxyl groups (**175**) seems to be an achiral polymer but forms a helical conformation with an excess one-handedness in solution in the presence of the optically active amine (*R*)-**118** (PEA) (Figure 25).[298] Upon heating, the optical rotation of the **175**/(*R*)-**118** complex in DMSO gradually changed from a positive value to a negative one and increased in the negative direction with the increasing temperature. After annealing the solution at 65 °C for *ca.* 2 h, the optical rotation showed a large negative value ($[\alpha]_D^{65}$ −127°), the sign of which is opposite to that of (*R*)-**118** ($[\alpha]_D^{25}$ +33° in DMSO). This annealing process is irreversible, but after the annealing, the complex then exhibits reversible optical rotational changes

Chart 18

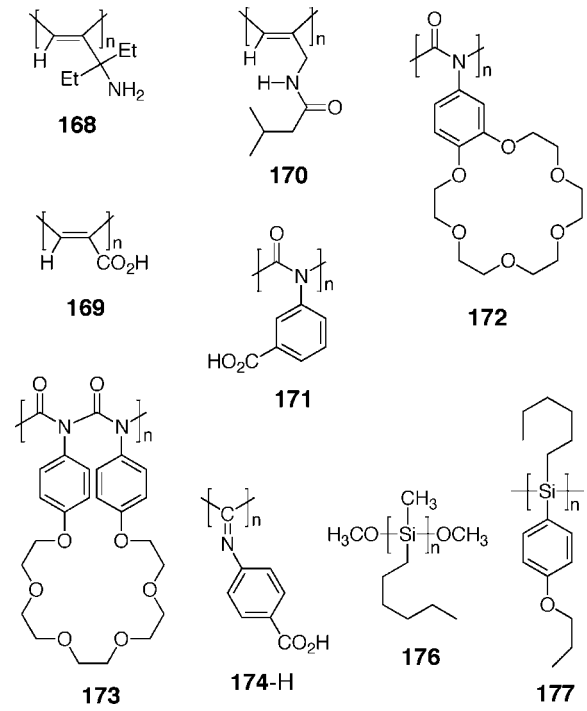

in the temperature range of 20−65 °C and showed a greater optical rotation ($[\alpha]_D^{20}$ −197° in DMSO). In contrast, the optical rotation of the cyclic trimer (**CT**) hardly changed, even after annealing with (*R*)-**118**, and the sign and net specific rotation are the same as those of (*R*)-**118**. Surpris-

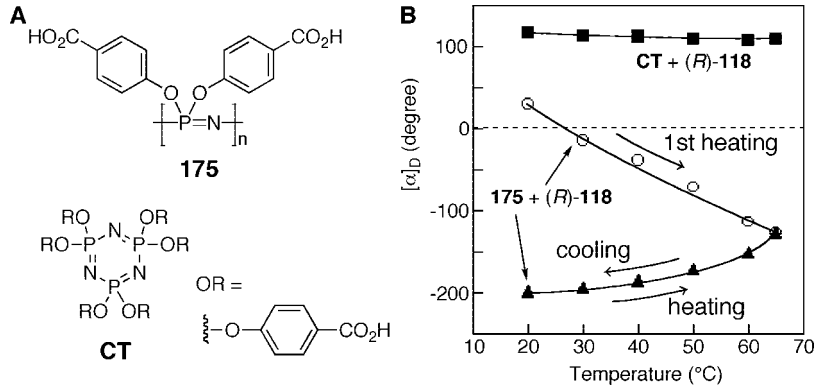

Figure 25. (A) Structures of **175** and cyclic trimer (**CT**) and (B) optical rotation changes in the **175**/(*R*)-**118** (○, ▲) and **CT**/(*R*)-**118** (■) complexes ([(*R*)-**118**]/[COOH of **175** or **CT**] = 5) in DMSO at various temperatures. The rotations were first measured at 20, 30, 40, 50, 60, and 65 °C after annealing the samples at these temperatures for *ca.* 2 h. (Reproduced with permission from ref 298. Copyright 2000 American Chemical Society.)

ingly, the optical activity of the **175**/(*R*)-**118** solution is retained after the addition of an equivalent amount of (*S*)-**118** and further annealing the solution at 65 °C for 3 h. These observations indicate that **175** likely forms a dynamic, preferred-handed helical conformation upon complexation with the chiral amine and the induced helix can be memorized (see section 2.7) even after the (*R*)-**118** complexed with **175** could be randomly replaced by (*S*)-**118** or the helical **175** formed by (*R*)-**118** may act as a chiral filter to exclude one enantiomer for racemic amines.

A helical conformation with an excess one-helical sense can also be induced in a dynamically racemic helical polyisocyanate (**62**)[119] and polysilanes with no functional pendant groups (**176**, **177**)[299,300] when nonracemic solvents are used as a chiral inducer, although the chiral bias seems to be too weak to control the overall handedness of the helical polymers, thus inducing a weak CD. Therefore, this method may not be feasible for general use as a chirality-sensing probe of chiral solvents.

Fujiki et al. have reported that a dynamically racemic helical **177** forms supramolecular helical aggregates in solution containing chiral alcohols as the poor solvent. In contrast to chiral solvation, a small helical sense bias in **177** induced by the chiral alcohols is significantly amplified in the helical aggregates to exhibit an apparent ICD.[300] The Cotton effect signs reflect the absolute configuration of the alcohols together with the position of the hydroxyl group. Therefore, this system has potential to be of general use for the chirality sensing of optically active alcohols.

Holder et al. have found an unexpected chiral solvent effect on the molecular weight distribution during the polymerization of dichloromethylphenylsilane (DCMPS) with sodium metal.[301] The weight-average molecular weight of poly(methylphenylsilane) (PMPS) obtained in either enantiomerically pure (*R*)- or (*S*)-limonene at 90 °C was twice that of PMPS prepared in the racemic limonene. Based on the fact that PMPS forms a preferred-handed helical conformation in (*R*)- or (*S*)-limonene due to chiral solvation, as evidenced by the appearance of the ICD, the differences in the molecular weight and its distribution of PMPS in racemic and nocracemic limonene are ascribed to changes in the balance of the right- and left-handed helical senses of the growing chains; the incidence of the helical reversals is reduced in chiral solvents, which may lead to the reduction of the probability of termination during the polymerization, resulting in generation of the higher molecular weight PMPS.

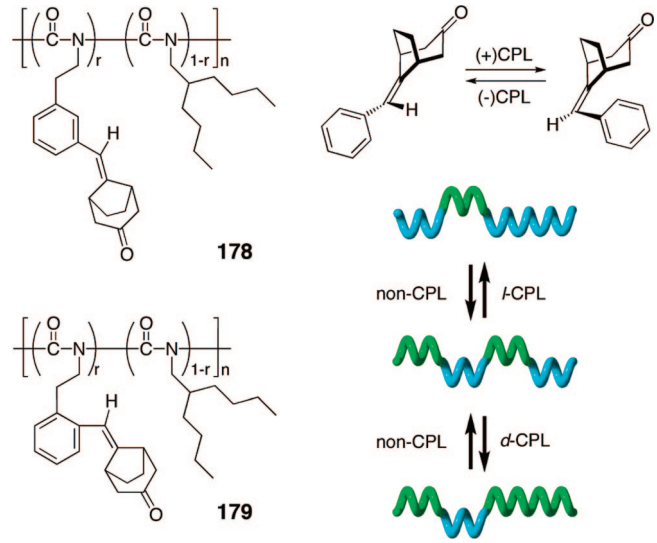

Figure 26. Switching of helical senses of **178** and **179** using CPL as a trigger.

Circularly polarized light (CPL) has been used as a trigger to bias the helical sense of polyisocyanates (Figure 26). Green et al. have prepared a series of polyisocyanate copolymers or terpolymers (**178**, **179**) ($r = 0.02-0.06$) consisting of various proportions of chiral units bearing a photoresolvable axially chiral bicyclo[3.2.1]octan-3-one derivative group and achiral units.[302] A tiny enantiomeric imbalance (ee <1%) in the pendant group is produced by irradiation of **178** and **179** with a right- (*d*) or left- (*l*) handed-CPL in the ketone's chromophore region, showing measurable CD signals in the polymer backbone region. The very small chiral imbalance in the pendant group is transferred to the polymer backbone as an excess of a single-handed helix with a very large amplification of the photoresolution (the majority rule effect (see section 2.6.1)). This remarkable chiral amplification with a high cooperativity observed in the polyisocyanate terpolymer system has been theoretically analyzed based on the quenched random-field Ising model.[302] Irradiation of an opposite handed CPL obviously produced an induction of the mirror-image CD signal. Further irradiation using unpolarized light caused racemization of the ketone unit, resulting in the instant disappearance of the CD signal. As a consequence, the helical sense of the polymer main-chain can be reversibly switched (on−off−on) by alternating irradiation with *d*- or *l*-CPL or returned to the racemic state by irradiation with unpolarized light.

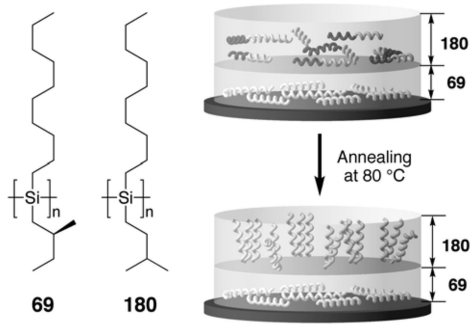

Figure 27. Thermodriven chiroptical transfer and amplification of helical sense excess into dynamically racemic helical **180** from optically active **69**.

Chart 19

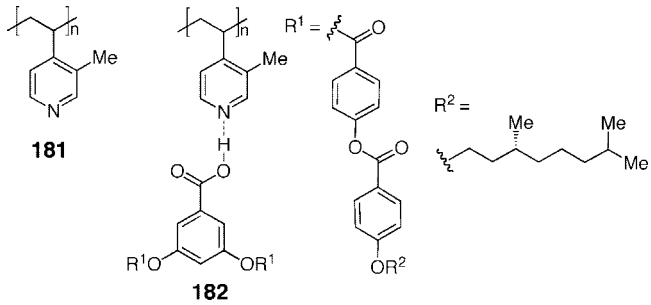

In the film state, it is possible to transfer chiral information of optically active helical polysilanes to optically inactive polysilanes through a weak van der Waals interaction between these two different polymers (Figure 27).[303] An optically active, helical polysilane (**69**) with an almost single-handed helical sense was chemically bonded or spin-coated on the surface of a quartz plate. An optically inactive polysilane (**180**) was further deposited on the film by spin coating, thus producing a binary polysilane film. Upon annealing at 80 °C, the CD intensity of the film dramatically increased, while no significant change in the CD intensity was observed for the single-layer film composed of **69** immobilized on a quartz plate. These results clearly demonstrate that an excess helical sense is induced in the optically inactive **180** as a result of chirality transfer either from the chiral side chain or the one-handed helical backbone of **69** through a weak van der Waals interaction between these two polymers. This phenomenon is a kind of sergeants and soldiers effect and is also called the "command surface".[304]

Khan et al. have reported that poly(3-methyl-4-vinylpyridine) (**181**, Chart 19) prepared by anionic polymerization of the corresponding achiral monomer showed a rather intense CD in the aromatic absorption region in the presence of chiral amino acids, such as L-alanine, in a methanol/water mixture (4/1, v/v), while the polymer prepared via the radical method exhibits only a weaker CD under the same conditions.[305] Presumably, a predominantly one-handed helical conformation is induced in the stereoregular (isotactic) polymer backbone of **181** upon complexation with chiral amino acids. Related to this, a side-chain noncovalent supramolecular polymer (**182**) composed of **181** and an optically active V-shaped acid is also considered to take a helical structure with a preferred-handed helical sense in the film state.[306]

The electrochemically polymerized emeraldine base form of polyaniline (**183a**) (Chart 20) shows an ICD in the long absorption region in solution or in the film when doped with optically active strong acids, such as (*R*)- or (*S*)-CSA.[307] A chirality-responsive polyaniline has been developed by introducing sulfonate residues onto the aniline moieties. A fully sulfonated poly(methoxyaniline) (**183b**) exhibited a similar ICD in solution and in the film upon complexation with chiral amines.[308] The origin of the ICD remains unclear but may be due to either a preferred-handed helical conformation or a supramolecular helical assembly of the polymer main chains induced by the chiral acid−base interactions.[308] Chirality induction of polyaniline derivatives (**183c**) has also been achieved through complexation with the chiral palladium(II) complexes bearing one interchangeable coordination site (**184**). A chiral propeller twist conformation of the π-conjugated backbone has been revealed by the X-ray crystallographic analysis of the model complex prepared from the quinonediimine derivative with **184**.[309]

A partially hydrolyzed polythiophene (PT) (**186**) derived from an optically active PT (**185**) (Scheme 21) is sensitive to the chirality of the (*R*)- and (*S*)-2-amino-1-butanol and exhibited an ICD in the absorption region of the polymer backbone through interactions with the aminoalcohols.[310] Optically inactive π-conjugated copolymers with the C_2-symmetric carboxybiphenol units as the main-chain component (**187**, Chart 21) also showed an ICD in the copolymer backbone regions in the presence of chiral amines.[311] A hierarchical chiral amplification mechanism has been proposed for **187**; the chiral information of the amines first transfers to the carboxybiphenol moieties with a dynamic axial chirality through noncovalent acid−base interactions, and subsequently, the induced twist-sense bias may be further amplified in the π-conjugated copolymer backbone to form an excess one-handed helical conformation.

Chart 20

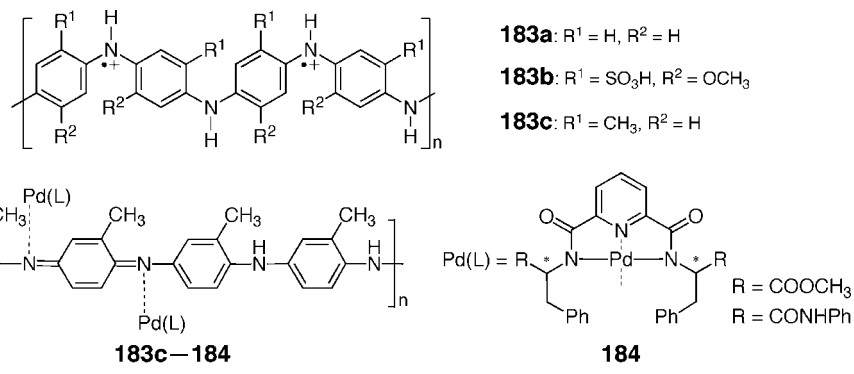

Scheme 21

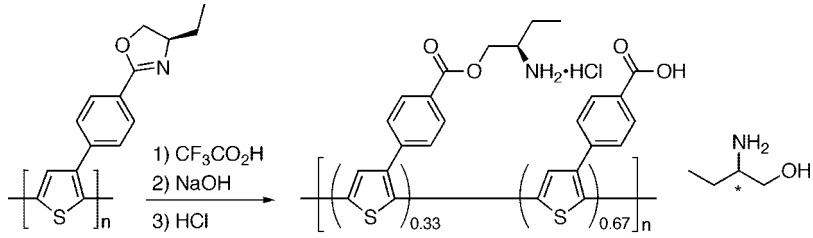

185 186

Chart 21

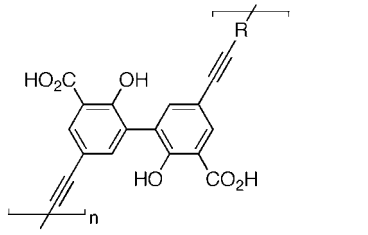

187

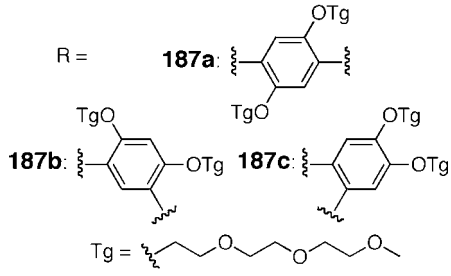

2.5.3. Foldamer-Based Helicity Induction

Several artificial biomimetic oligomers and π-conjugated oligomers fold into a preferred-handed helical conformation (so-called "foldamers"), and a cylindrical cavity suitable for encapsulating specific guest molecules is simultaneously generated under certain conditions (Figure 28).

The induction of such a tubular cavity in a series of oligomers of *m*-phenylene ethynylene (**188**) has been extensively studied by Moore et al. The π-conjugated oligomers are achiral and take a random conformation in chloroform but fold into equimolar amounts of right- and left-handed helices in polar solvents, such as acetonitrile, and in an aqueous solution. However, in the presence of nonracemic hydrophobic and rodlike guests, such as **189**[211] and **190**,[212] respectively, which are favorably encapsulated within the cylindrical cavity of **188**, one of the dynamic helices predominantly forms and the inclusion complexes exhibit an ICD in the *m*-phenylene ethynylene chromophore region.

The analogous poly(*m*-phenylene ethynylene) bearing cationic, polar side chains (**191**) also folds into a helical structure with a one helical sense excess in water/DMSO (9/1, v/v) in the presence of chiral carboxylic acids, such as D-mandelic acid (MA), thus showing an apparent ICD.[312] Poly(*m*-ethynylpyridine) **192** is very sensitive to the chirality of saccharides, such as D-mannose (**193**), and folds into a one-handed helix through intermolecular hydrogen bonding in apolar solvents[313] and even in an aqueous solution,[314] and the complexes showed a similar ICD in the long wavelength main-chain chromophore region. It is well-established that an alternating pyridine/pyrimidine sequence preferentially adopts the *s-trans* conformation.[315] Taking advantage of this unique feature, Lehn et al. have developed a series of foldamers, such as **194**, which can trap hydrophilic guests such as **195** within its helical cavity, thus forming a rotaxane-like inclusion complex with a helical sense bias.[316,317]

A number of aromatic oligoamides, such as **196**,[318,319] **198**,[320] and **200**,[321] have been synthesized in order to mimic biological helices, and their helical handedness has been biased through chiral hydrogen bonding interactions with specific guests, such as a sugar (**197**) and chiral acids (**199**), along the strand and at the terminal units of **196** and **198**, respectively. Chiral solvation has been employed to induce an excess of one particular-handed helical conformation in **200** using L- or D-diethyl tartrate as the chiral solvent. Interestingly, the single helices of **198** self-assemble into a double-stranded helix depending on the concentration of **198** and temperature (see section 4.2).[34] Although the double-helical **198** exists in a mixture of right- and left-handed double helices under equilibrium, a similar preferred-handed helicity induction may be possible for the duplex of **198** in the presence of specific guests.

Moore et al. have extended the solvophobicity-driven foldamer formation to the folding-driven synthesis of oligomers and polymers of *m*-phenylene ethynylene. By taking advantage of the reversible imine metathesis reaction, which is known to have an equilibrium constant close to unity and proceeds at room temperature, it has been revealed that in a helix-promoting solvent, acetonitrile, the helical assembly of oligomers promotes and accelerates the formation of a longer 12mer oligomer (**206**) through heterodimerization between the *N*-terminal imine dimer (**202**) and hexamer (**203**) and the *C*-terminal imine hexamer (**201**) driven solely by the free energy gain due to helix formation of the longer oligomer (12mer of **206**) rather than the shorter one (octamer of **205**), while in a nonhelix forming solvent, chloroform, oligomers formed under equilibrium are largely produced (Figure 29).[322] Higher molecular weight poly(*m*-phenylene ethynylene imine)s have also been synthesized in acetonitrile via a reversible metathesis reaction of bisfunctionalized *m*-phenylene ethynylene imine oligomers.[323]

Hecht et al. have reported an intriguing approach to generate organic nanotubes on the basis of the foldamer concept and subsequent intramolecular cross-linking of the peripheral photoactive residues (Figure 30A).[324] A poly(*m*-phenylene ethynylene) derivative carrying multiple cinnamate moieties (**207**) folds into a tubular secondary structure, which is stabilized by intramolecular cross-linking (**208**) through topochemically controlled [2 + 2] photodimerization reactions (Figure 30B). This approach is promising for generating organic nanotubes with controlled dimensions and a surface functionality that constitutes attractive building blocks for functional nanostructures.

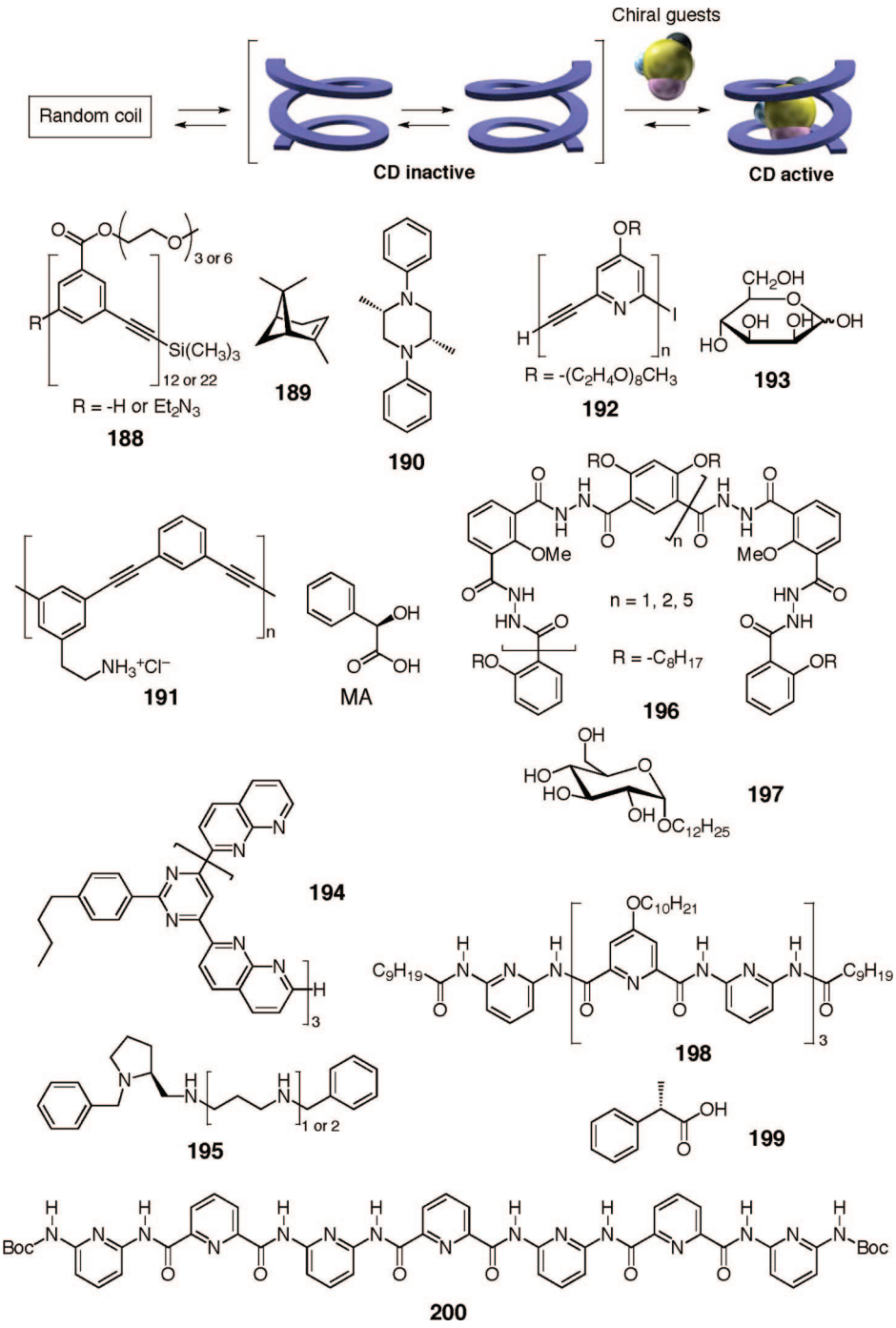

Figure 28. Schematic illustration of a predominantly one-handed helix induction in foldamers by noncovalent chiral interaction with optically active compounds.

2.5.4. Helicity Induction by Inclusion with Optically Active Hosts

An oligosilane (**209**) (Chart 22) takes an induced helical conformation with a helix-sense bias once entrapped in a hydrophobic chiral cavity created by helical polysaccharides, such as right-handed triple-stranded helical schizophyllan and left-handed helical amylose in water, thereby showing ICDs with Cotton effect signs opposite to each other, which reflect the helical sense of the oligosilane.[325,326] A similar helicity induction also takes places in a water-soluble polythiophene (**210**) or an oligothiophene (**211**) when it is confined within the schizophyllan interior in water.[327,328]

2.6. Chiral Amplification

Chiral amplification is a unique process from which a small chiral bias is significantly enhanced through covalent and/or noncovalent bonding interactions, and this intriguing phenomenon is significantly associated with the origin of homochirality in biological systems.[40,111,329−331] As discussed in section 2.2, chiral amplification in polymeric systems has been for the first time investigated by Green and coworkers using a typical stiff, rodlike helical polymer, i.e., polyisocyanates, and the substantial nature of the dynamic macromolecular helicity of polyisocyanates, that are

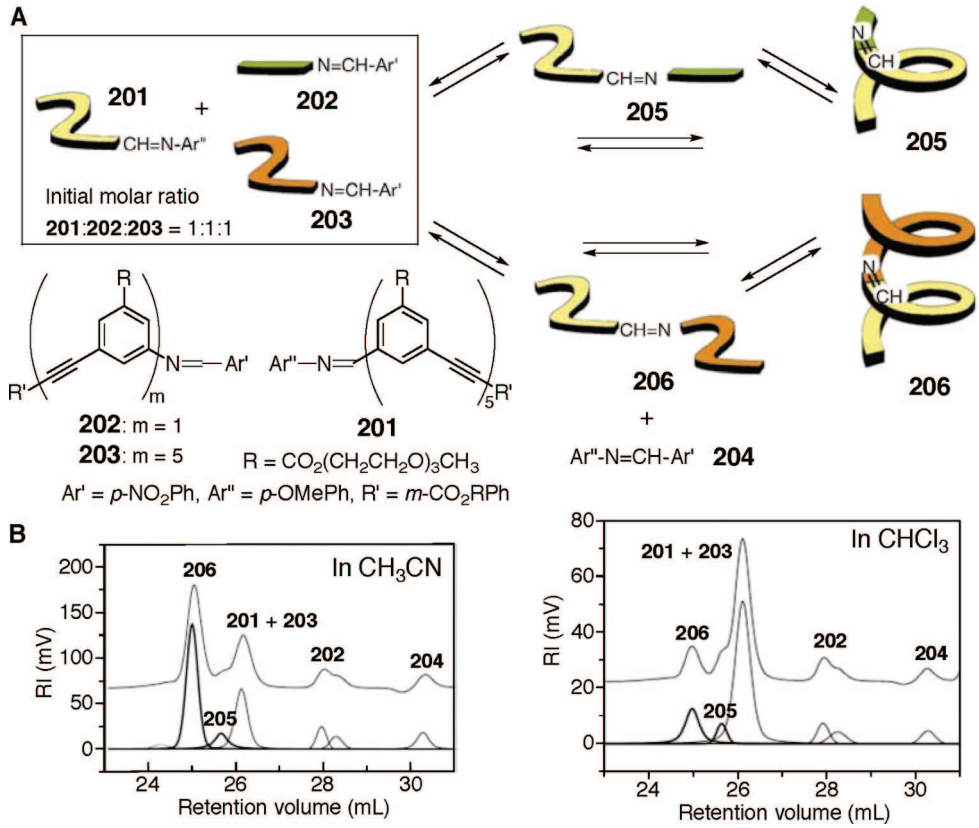

Figure 29. (A) Schematic illustration of imine methathesis between oligo(*m*-phenylene ethynylene) imines (*N*-terminal dimer **202**, *N*-terminal hexamer **203**, and *C*-terminal hexamer **201**). (B) SEC of the reaction mixture from imine methathesis between equimolar amounts of **201**, **202**, and **203** performed in acetonitrile (left) and chloroform (right). (Reproduced with permission from ref 322. Copyright 2001 Nature Publishing Group.)

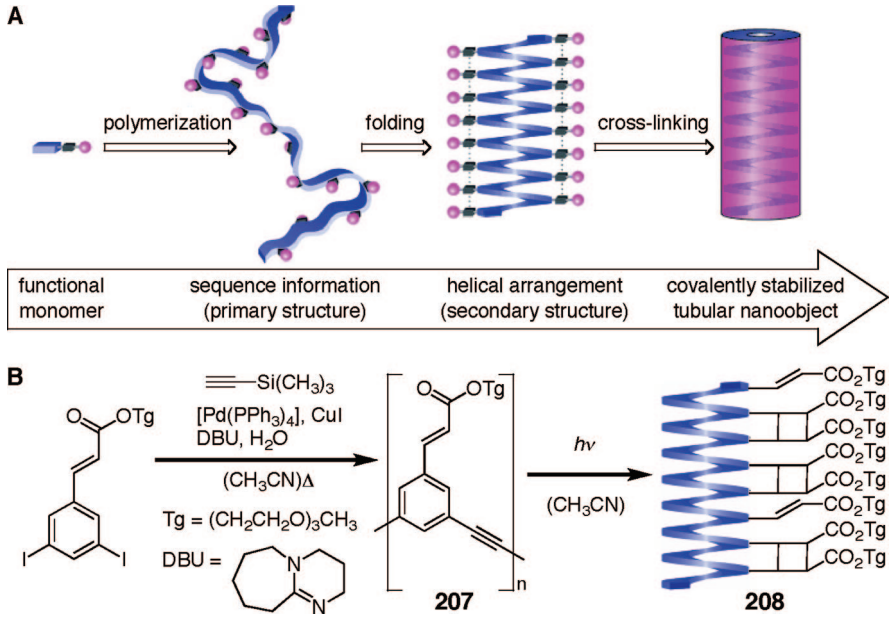

Figure 30. (A) Schematic illustration of formation of organic tubes by the intramolecular cross-linking of folded helical polymer backbones: Polymerization of a functional monomer carrying both solvophilic (magenta) and cross-linking groups (gray) generates a polymer strand that folds (solvophobically driven) into a helical conformation that is subsequently stabilized by covalent cross-linking using adjacent reactive groups. (B) Synthesis of amphiphilic poly(*m*-phenylene ethynylene) (**207**) and subsequent photoirradiation to stabilize the folded helical conformation. (Reproduced with permission from ref 324. Copyright 2003 Wiley-VCH.)

composed of right- and left-handed helical segments separated by energetically unfavorable, rarely occurring helical reversals, has been experimentally and theoretically elucidated.[17,111] The "sergeants and soldiers" effect[112] and the "majority rule"[120] introduced by Green et al. are representative chiral amplification phenomena discovered for the first time in covalent polymeric systems and have been now proved to be universal and observed in other varieties of covalent and noncovalent polymeric and supramolecular helical systems that involve noncovalent helical assemblies composed of chiral−achiral or chiral−chiral (*R*/*S*) small molecular components.[19,40,331−334]

Chart 22

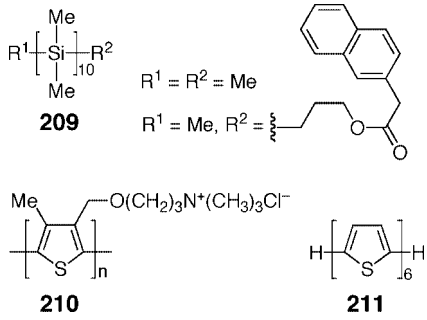

2.6.1. Sergeants and Soldiers Effect and Majority Rule

The "sergeants and soldiers" and "majority rule" effects have been observed in a variety of dynamic and static helical polymers, such as polysilanes,[18] polyacetylenes,[157,161,174,190,335−337] poly(phenyl isocyanate)s,[338] polyisocyanides,[339,340] polymethacrylates,[341] and foldamers,[342] and typical examples are shown in parts A and B, respectively, of Figure 31, where the copolymers consist of achiral and chiral monomer units (A) or a mixture of (*R*)- and (*S*)-enantiomeric monomer units (B), respectively; the *r* represents the molar fraction of chiral units (A) and one of enantiomer units (B) of copolymers at which the copolymers show the full CD or optical rotation values, suggesting a complete one-handed helix formation. Like polyisocyanates, polysilanes and polyacetylenes tend to form an almost one-handed helical conformation with a smaller amount of chiral units (A) and a lower ee of the monomer units (B) during the copolymerization, while polyisocyanides and polymethacrylates bearing high helix inversion barriers require a rather higher amount of chiral units (A) and a greater optical purity (B) for the copolymers with a single-handed helix.

The "sergeants and soldiers" and "majority rule" effects have also been observed for dynamic helical polyacetylenes through noncovalent chiral interactions. Typically, in the presence of **167** of 50% ee, the PPA **148** showed an intense ICD as high as that of 100% ee in DMSO.[265] Moreover, **148** exhibits a very weak ICD in the presence of a small amount of (*R*)-**152** due to the lack of a single-handed helical conformation. However, the coaddition of the excess bulky, achiral 1-naphthylmethylamine (**212**) with a small amount of (*R*)-**152** gave rise to a dramatic increase in the ICD magnitude, being comparable to the full ICD, as observed for the addition of an excess of (*R*)-**152** (Figure 32).[343] Thus, an almost one-handed helical conformation can be induced on **148** upon complexation with a small amount of (*R*)-**152** assisted by the achiral **212**.

A PPA (**158**) bearing the bulky aza-18-crown-6-ether, a typical host molecule in host−guest chemistry, as the functional pendant group is the most sensitive to the chirality of chiral molecules, such as amino acids, among the functional PPAs prepared so far, and an almost one-handed helix is induced in **158** in the presence of 0.1 equiv of L-Ala in acetonitrile (Figure 33B).[279] This extremely high sensitivity may be ascribed to the main-chain stiffness by the bulky pendant group, which may reduce the helical reversals and then increase the helical segments. In addition, **158** showed an apparent ICD even with 0.01 equiv of L-Ala, indicating a remarkable chiral amplification with cooperative interaction in the pendant groups through noncovalent interactions. A tiny chiral bias in the pendant crown units complexed with L-Ala is significantly amplified and induces the same helix on the major free crown ether units. Moreover, **158** showed the same Cotton effect signs upon complexation with all the common 19 L-amino acids, which indicated that **158** is one of the most sensitive and practically useful synthetic receptors for detecting the amino acid chirality. More interestingly, even a 5% ee of Ala gave rise to the full ICD in **158**, as induced by the optically pure Ala (Figure 33C). With this remarkable majority rule effect, **158** can detect an extremely small enantiomeric imbalance in the amino acids, for instance, Ala of less than 0.005% ee (L/D = 50.0025/49.9975), showing an apparent ICD without derivatization. Therefore, this method has the potential to detect a very small imbalance in amino acids and related chiral molecules from meteorites[344] and also those produced by CPL.[345]

This unique chiral amplification observed in the rigid rod helical PPAs can provide a useful scaffold or template for arranging chromophoric and functional pendant groups in a one-handed helical array along the polymer backbone through covalent or noncovalent bonding. For example, the copolymerization of achiral phenylacetylenes bearing a fullerene pendant with a small amount of optically active phenylacetylenes (**213** and **214**) using a rhodium catalyst produces the C_{60}-containing helical PPAs with an excess one-handedness, in which the pendant C_{60} groups are arranged in a preferred-handed helical array along the polymer backbone (Figure 34A), and hence, the copolymer exhibited an ICD both in the main chain and in the fullerene chromophoric regions.[346−348] Taking advantage of the noncovalent "helicity induction" concept, a preferred-handed helicity can be induced in an optically inactive C_{60}-bound PPA (**215**) bearing the bulky aza-18-crown-6 ether pendants upon complexation with L- or D-amino acids, such as alanine, and the complex showed a similar ICD due to the helical arrangement of the pendant C_{60} along the predominantly twisted helical backbone (Figure 34B).[349] In a complementary approach, an enantiomerically pure cationic C_{60}-bisadduct (**216**) can induce a preferred-handed helix in a dynamically racemic PPA (**153b**) with the opposite negative charges in DMSO/water mixtures through noncovalent bonding interactions, which further gives rise to the formation of a helical array of the C_{60}-bisadducts with an excess of one-handedness along the polymer chain (Figure 34C).[350]

2.6.2. Domino Effect

Helicity induction of one particular handedness in helical polymers and oligomers is also possible by covalently or noncovalently incorporating chiral residues at the chain ends, which generates a preferred-handed helix. Synthetic peptides consisting of achiral α-aminoisobutyric acid (Aib) and *Z*-α,β-dehydrophenyalanine (Δ^ZPhe) residues possess a dynamically racemic helical structure,[351] and covalent insertion of chiral α-amino acid residues into a specific position of the racemic peptides can induce a preferred-handed helix.[352]

Inai and co-workers took advantage of such a dynamic helical feature of peptides and have achieved a preferred-handed helicity induction of optically inactive oligopeptides composed of achiral Aib and Δ^ZPhe sequences bearing the *N*-terminal amino group (**217**, **218**) upon noncovalent interactions with chiral carboxylic acids (Figure 35).[353,354] The peptides showed an ICD arising from an excess of one particular helical conformation of the entire peptide chain through acid−base interactions with chiral carboxylic acids. This phenomenon is called the "*noncovalent domino effect*".[355,356] Here, the chiral information of the carboxylic

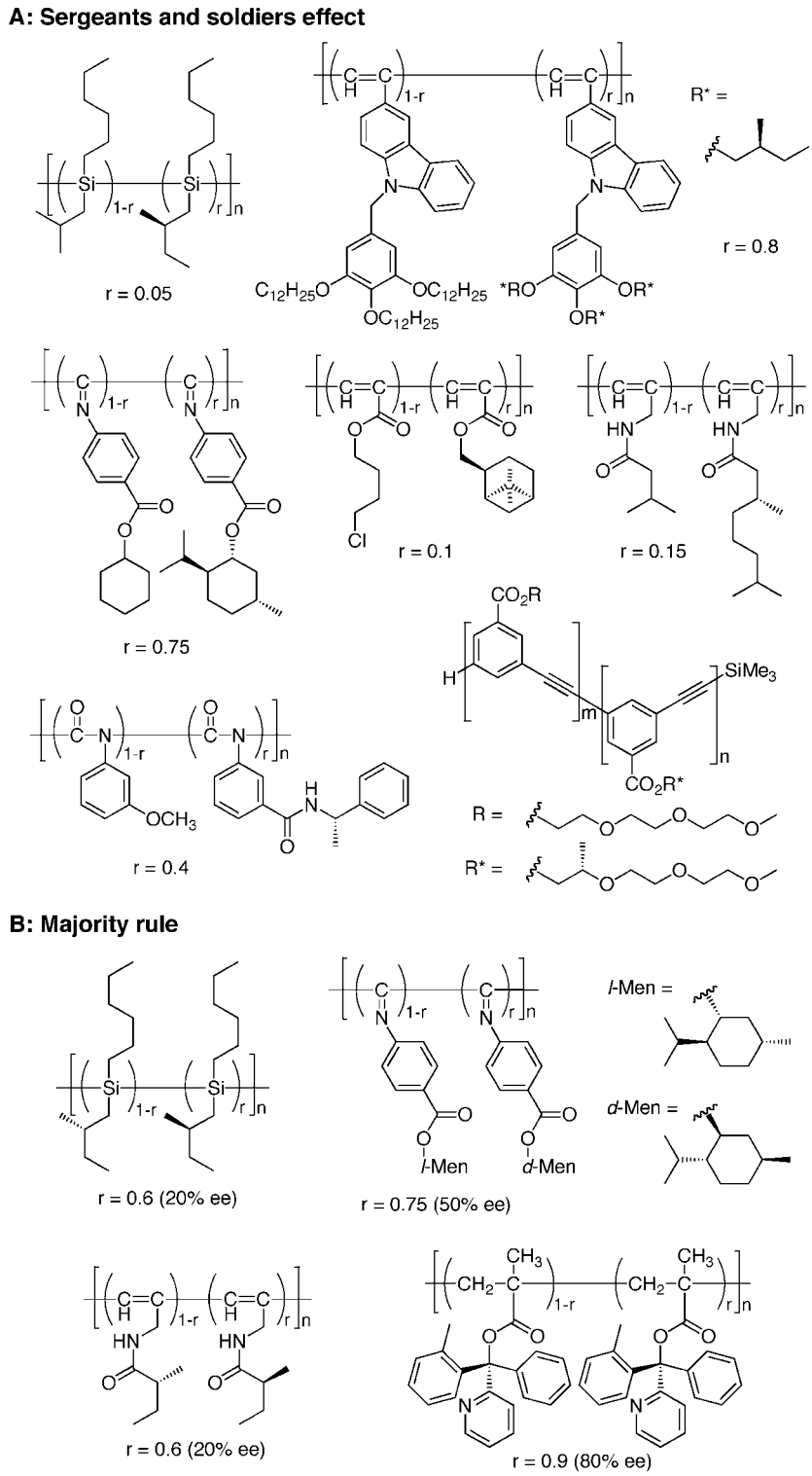

Figure 31. Representative examples of helical polymers showing the "sergeants and soldiers" effect (A) and "majority rule" (B). The *r* values represent the molar fraction of chiral units (A) and one of enantiomers (B) where the magnitude of CD or optical rotation of the copolymers almost saturates.

acids is transferred to the whole peptide chain via noncovalent interactions at the *N*-terminal amino group with a significantly large amplification. Analogous covalent terminus-triggered preferred-handed helicity induction ("*covalent domino effect*") has been investigated and well established in dynamic helical polymers and oligomers, such as polyisocyanates (**219**−**221**),[357−359] oligosilanes (**222**),[360] and polysilanes (**223**−**225**) (Chart 23).[361−364] These polymers and oligomers were prepared by the anionic polymerization of achiral monomers with optically active initiators (**219**−**221**), by helix-sense-selective block copolymerization (**224**), or by incorporation of chiral residues at the ends of the polymer chains (**222**, **223**, and **225**).

As described in section 2.5.3, biomimetic and π-conjugated foldamers fold into one particular helical conformation in the presence of chiral guests through noncovalent chiral interactions. Quite obviously, the covalent domino effect can be applied to foldamers, leading to the formation of an excess

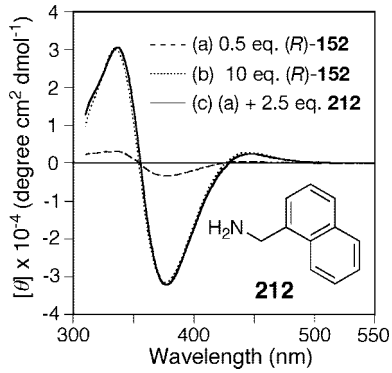

Figure 32. CD spectra of **148**—(*R*)-**152** complexes in the absence ([(*R*)-**152**]/[**148**] = 0.5 (a) and 10 (b)) and presence of **212** ([(*R*)-**152**]/[**212**]/[**148**] = 0.5/2.5/1) in DMSO. (Reproduced with permission from ref 343. Copyright 2004 Wiley-VCH.)

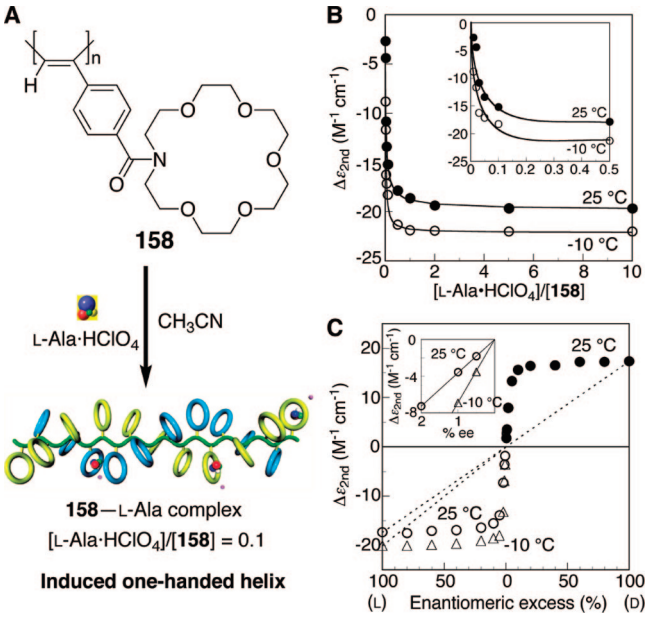

Figure 33. (A) Schematic illustration of helicity induction on **158** with a small amount of L-Ala·$HClO_4$. (B) Titration curves of **158** with L-Ala·$HClO_4$ in acetonitrile at 25 and −10 °C. (C) Changes in ICD intensity ($\Delta\varepsilon_{second}$) of **158** vs the % ee of L-Ala·$HClO_4$ during the complexation with **158** in acetonitrile at 25 and −10 °C. (Reproduced with permission from ref 279. Copyright 2003 American Chemical Society.)

one-handed helix (Figure 36). Saccharide-linked oligomeric *m*-ethynylpyridines (**226**) fold into a predominantly one-handed helical structure biased by the terminal saccharide units encapsulated within the cylindrical cavity of **226** through intramolecular hydrogen bonds.[365] An oligoindole comprising a tetraindole backbone bearing (1*S*)- or (1*R*)-phenylethylamide units at both ends (**227**) forms a helical conformation with an excess helical sense upon binding an anion, such as chloride, by multiple hydrogen bonds.[366] Although the **227** alone exhibits almost no CD, the addition of a chloride anion induced a strong Cotton effect, which implies the preferential formation of one helical isomer over another. Theoretical calculations suggest that the *P*-helix of the **227**/Cl^- complex with the termini having the (*S,S*)-configuration is more energetically stable than the corresponding (*M*)-helix. Phenanthroline-derived oligoamides bearing an optically active terminal group (**228**) also form a preferred-handed helix in solution stabilized by intramolecular hydrogen bonds between the phenanthroline dicarboxamide units biased by the terminal chiral unit.[367] The protonation of one of the two nitrogen atoms of the phenanthroline groups upon the addition of 1 equiv of trifluoromethanesulfonic acid triggered a transition from the helical conformation to the unfolded one. Subsequent neutralization with base can regenerate the original helical conformation; thus, switching (on and off) of the folding and unfolding can be controllable in this system.

Helical oligomers composed of alternating pyridine-2,6-dicarboxamides and *m*-(phenylazo)azobenzenes (**229**) have been reported to fold into a preferred-handed helix when optically active units derived from L-Ala are attached at the terminal positions.[368] Irradiating **229** with 350-nm light induced *E*−*Z* photoisomerization of the terminal azo linkages, which displaces the chiral terminal units from the helical backbone and suppresses chiral induction, resulting in the significantly diminished CD intensity of **229** (Figure 37).

Clayden et al. have proposed the "apparent diastereotopicity" (anisochronicity) that provides a general empirical method for identifying the ordered chiral secondary structure in solution (Figure 38).[369] Attaching a chiral controlling element (X*) to the terminus of the foldamer generates a diastereomeric pair of structures. If X* is able to induce a helical sense bias under equilibrium, the H_a and H_b protons remain in diastereomeric environments due to the unequally populated interconvertible right- and left-handed helical conformations; they remain anisochronous and will still appear as an AB system, in principle, regardless of the distance from X* and irrespective of the helix inversion rate. However, as the helix lengthens, the conformation becomes disordered in such a way that X* no longer has control over the local chiral environment of H_a and H_b via the helix; then, the signal arising from the diastereotopic pair of protons will collapse into a 2H singlet. The chemical shift difference ($\Delta\nu$) between H_a and H_b may thus be useful as a chain-length dependent empirical measure of the distance over which the helicity of an oligomer persists in solution. This idea has been applied to the oligoureas derived from *m*-phenylenediamine bearing a chiral sulfinyl group at one end and an *N*-benzyl group at the other end to act as a diastereotopic probe (**230**).[369] The ^1H NMR signals arising from the CH_2 group of the diastereotopic probe (H_a and H_b) remained anisochronous even when separated from the chiral sulfur atom by up to 24 bonds ($n = 3$), indicating that the short oligoureas adopt a defined helical conformation in solution, but in longer oligomers, the helicity breaks down and the transfer of chiral information along the backbone in these systems is limited to about 24 bond lengths.

It has been pointed out that the perfluoroalkyl chains adopt a helical conformation in solution.[370] Monde et al. have succeeded in controlling the helicity of perfluoroalkyl chains by introducing an optically active group at the chain end (**231**, **232**, Chart 24).[371] The helicity of the perfluoroalkyl chain in solution has been revealed by VCD together with the density functional theory (DFT) calculations, being also supported by an X-ray crystallographic study.

2.7. Memory of Helical Chirality

2.7.1. Macromolecular Helicity Memory in Solution

The preferred-handed macromolecular helicity induced in PPAs (**148**, **153**, **154**) (Figure 19) upon complexation with nonracemic amines is not static but possesses a dynamic feature; therefore, the ICD generated due to the helical sense

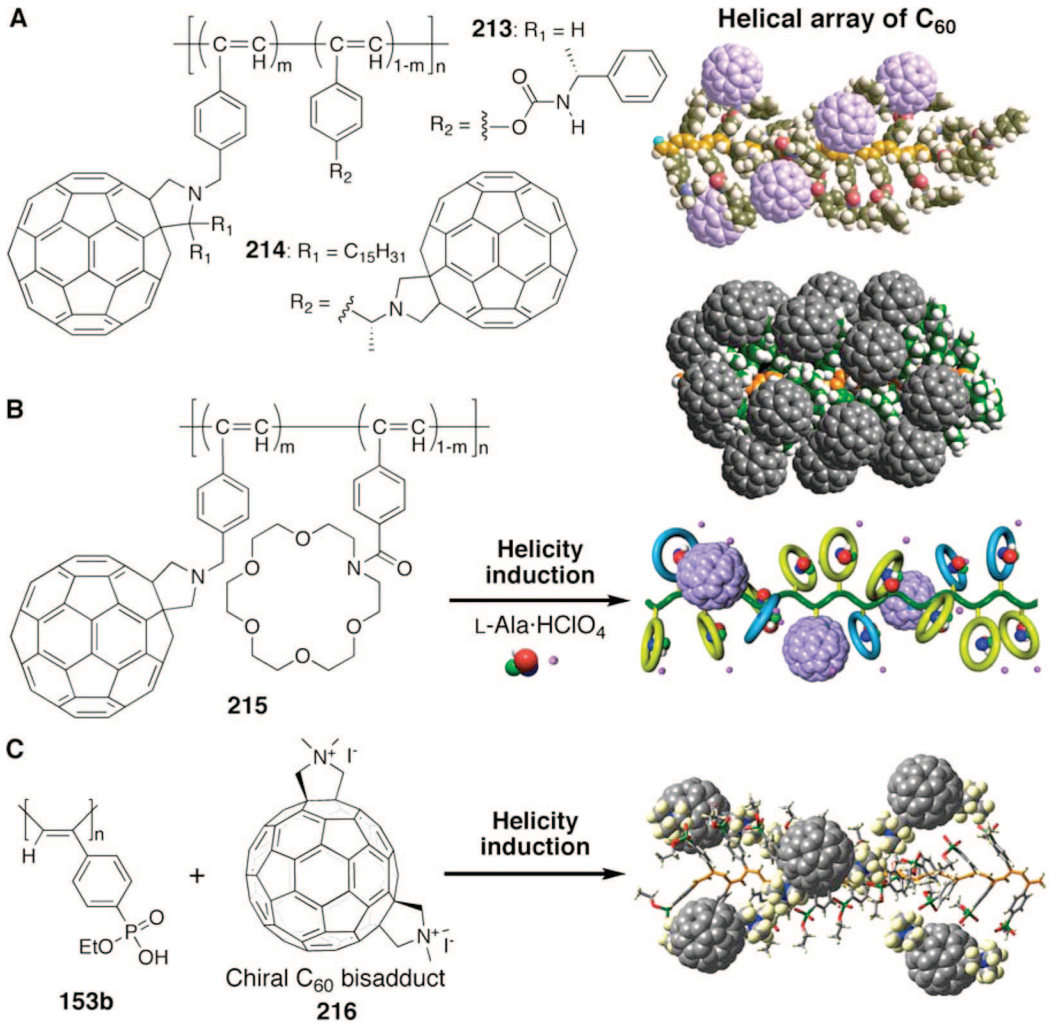

Figure 34. Schematic illustration of preferred-handed helical arrays of fullerenes along the helical PPA backbones.

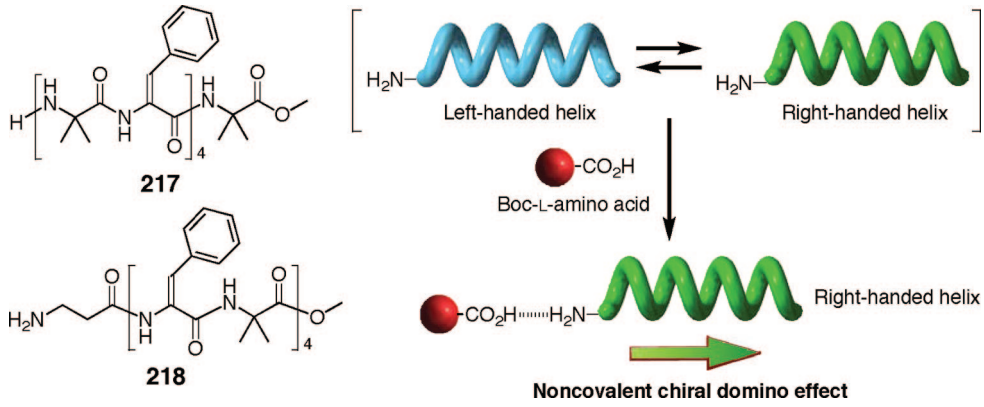

Figure 35. Schematic illustration of a preferred-handed helix induction in optically inactive oligopeptides through acid−base interaction with chiral carboxylic acids at the *N*-terminal (domino effect).

bias immediately disappears when the amines are removed by exposure to a stronger acid, such as TFA. However, the helical conformations of **148**, **153**, and **154** induced by nonracemic amines, such as (*R*)-**152**, are retained, namely "*memorized*", after the chiral amines are completely removed and replaced by achiral amines, e.g., **233** and **234** for **148** and diamines, such as ethylenediamine (**235**), for **153** and **154** in DMSO (Figure 39A).[267,272,372,373] This unprecedented macromolecular helicity memory is not transient but lasts for an extremely long time with a half-life time of over two years for **148**. This means that the thermodynamically controlled, dynamic helical conformations assisted by nonracemic amines are locked, transforming into kinetically controlled static ones after replacement with the achiral amines. For example, **148** complexed with (*R*)-**152** shows an intense ICD in the polymer backbone region, which is almost retained after isolation by SEC fractionation using DMSO containing an achiral amino alcohol **233** (0.8 M) as the mobile phase. On the basis of the ratio of the ICD intensity of the second Cotton effect ($[\theta]_{second}$) just after the SEC fractionation to the original ICD intensity of the **148**/(*R*)-**152** complex, the memory efficiency with the achiral **233** was estimated to be 87% (Figure 39B). The memory efficiency is influenced by small structural changes in the achiral amines.

Chart 23

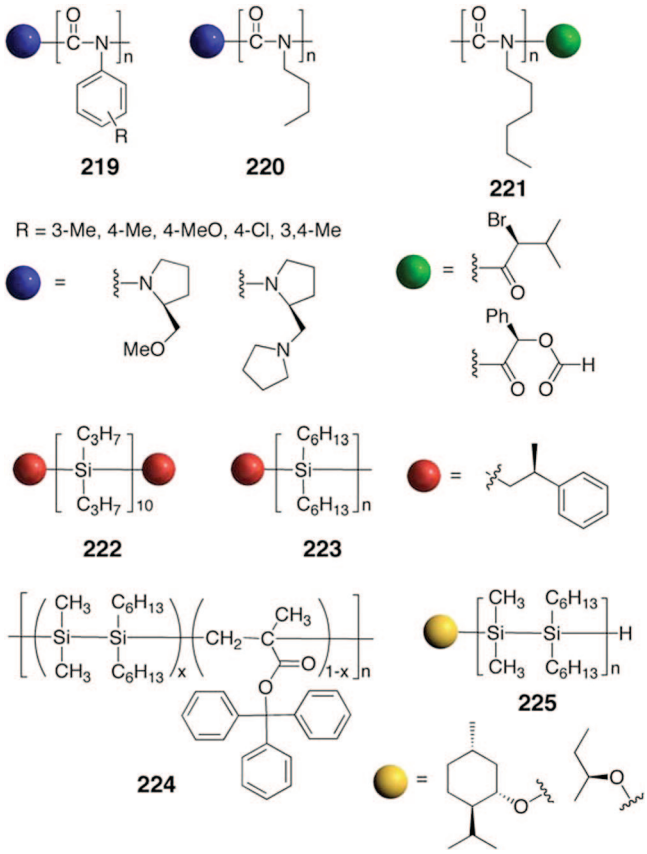

Fully detailed studies on the mechanism of the helix-sense bias induction and subsequent memory of the helical chirality of **148** by means of UV−visible, CD, and IR spectroscopies reveal that a one-handed helical sense is cooperatively induced on **148** upon the ion pair formation of the carboxy groups of **148** with optically active amines and that the bulkiness of the chiral amines plays an important role for inducing an excess of a single-handed helix, as already described in section 2.5.1.[373] In addition, the free ion formation has been found to be essential for the helicity memory of **148** after the replacement of the chiral amine by achiral amines, because the intramolecular electrostatic repulsion between the neighboring negatively charged carboxylate ions of **148** significantly contributes to reducing the atropisomerization process of **148**, in other words, the helix inversion of the polymer.[373]

The preferred-handed helicity induction in **148** with a small amount of (*R*)-**152** can be further amplified by an achiral amine **212** as shown in Figure 32 (section 2.6.1).[343] The chirally amplified helical **148** has also been memorized in the same manner by the replacement of (*R*)-**152** and **212** with achiral amines,[343] indicating that the chiral amplification combined with the macromolecular helicity memory provides a highly sensitive, chirality sensing method for specific chiral molecules when their optical activities are too low to be detected by conventional spectroscopic means.

For the macromolecular helicity memory, the use of achiral amines is indispensable. That is, in the absence of the achiral amines, the memory will be instantly lost. However, such a dynamic helicity memory in **153b** bearing a phosphonic acid monoethyl ester as the pendant group can be "*stored*" after the pendant group is converted to its methyl ester using diazomethane, resulting in the generation of a phosphorus stereogenic center with optical activity (Figure 40).[374] The esterification enantioselectively proceeds when **153b** has a biased helical conformation induced by (*R*)- or (*S*)-**152** or a macromolecular helicity memory assisted by **235**. Although the enantioselectivity was low (4−11% ee), the pendant chirality is transferred to the main-chain helicity with a significant amplification at low temperatures, leading to a higher helix-sense excess than that expected from the ee of the pendant groups; the helix-sense excess of the polymer reached 62% ee at −95 °C.

Combination of the noncovalent helicity induction with the helicity memory provides a versatile method to produce either a right- or left-handed helix with an excess helical handedness. However, the helical sense is predetermined by the chirality of the employed enantiomeric amines. Accordingly, the opposite handed helicity memory requires the opposite enantiomeric amine before the replacement with achiral amines. Interestingly, both enantiomeric helices with the mirror image to each other have been produced with a high memory efficiency from a helical PPA (**153c**) induced by a single enantiomer (Figure 41).[271] This so-called "*dual memory*" of enantiomeric helices takes advantage of the temperature-dependent inversion of the macromolecular helicity (see section 2.8). The PPA **153c** folds into a preferred-handed helical conformation biased by (*R*)-**152** at 25 °C in DMSO. Upon heating, the helix-sense inverts at 65 °C, as evidenced by the Cotton effect inversion. These diastereomeric right- and left-handed helices of **153c** obtained at 25 and 65 °C can be further memorized using an achiral diamine, such as **236**, at these temperatures, and accordingly, the resulting enantiomeric helices of the **153c/236** complexes showed the perfect mirror image Cotton effects and identical absorption spectra. The chiral amplification concept has also been applied to this system; a 35% ee of **152** induced as intense an ICD as that with the 100% ee of **152** at 25 °C and also 65 °C after helicity inversion. Subsequent replacement of the nonracemic **152** with the achiral **236** gave the enantiomeric helices of **153c** with an excess single-handedness.[271]

Although the chiral memory effect has also been observed in other dynamic supramolecular systems,[332,375−379] the use of achiral guests is essential for the memory effect in most cases. Otherwise, the chiral memory cannot be retained with the exception of the "storage of helicity memory" shown in Figure 40. However, the sodium salt of the helical **174** (**174**-Na) with an excess single-handed helix induced by (*S*)-**237** has been found to memorize its helicity after complete removal of the (*S*)-**237** in water (Figure 42A).[380] In sharp contrast to the conformational memory of the induced helical sense of the PPAs, the helix formation of **174**-Na is accompanied by a configurational isomerization around the C═N double bonds (*syn*−*anti* isomerization) (Figure 42B) into one single configuration upon complexation with the chiral amine, which forces the polymer backbone to take an excess helical sense. This is an unprecedented example showing an optically active static helical polymer that can be helix-sense selectively synthesized after polymerization through specific noncovalent chiral interactions. This helicity memory observed in the polyisocyanide is significantly advantageous over that of the helical PPAs, since the chaperoning achiral amines are no longer required in order to retain the helicity in the polyisocyanide. Therefore, further modifications of the side groups are possible by maintaining the macromolecular helicity memory,

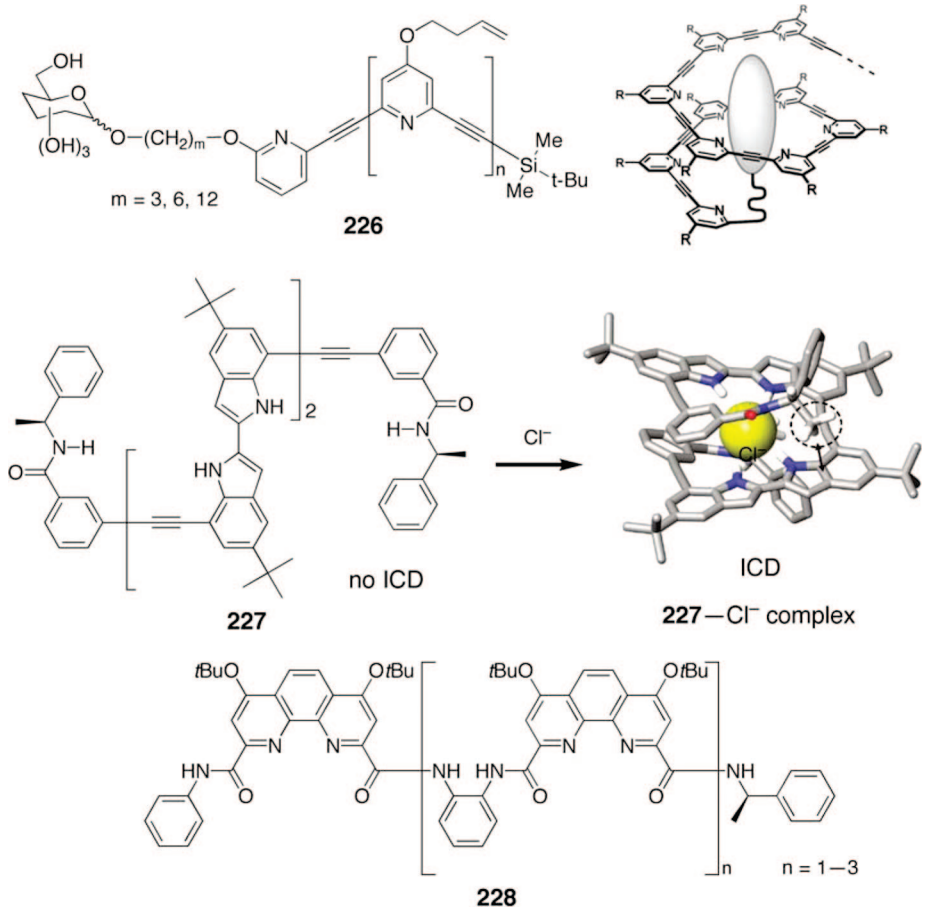

Figure 36. Typical covalent domino effects observed in foldamers. (Reproduced with permission from refs 365 and 366. Copyright 2008 American Chemical Society.)

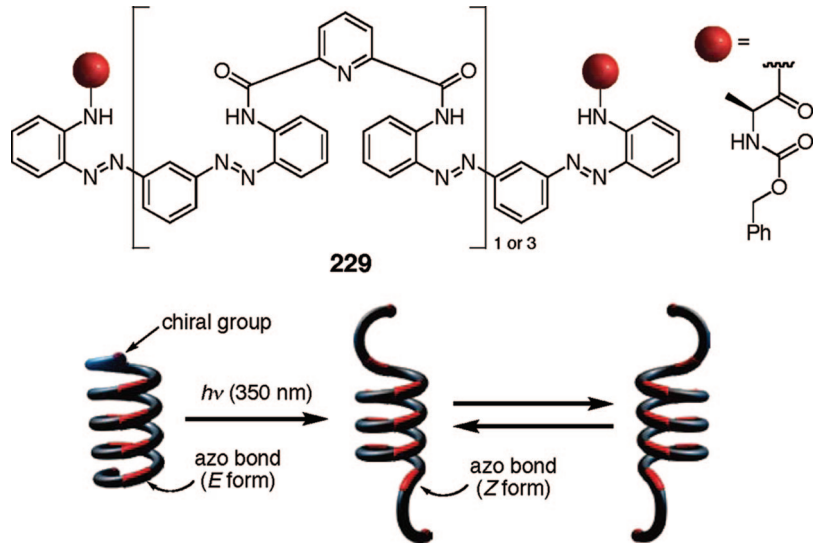

Figure 37. Schematic illustration of photomodulated chiral induction in helical azobenzene oligomers with chiral terminal groups. (Reproduced with permission from ref 368. Copyright 2008 American Chemical Society.)

thus affording a variety of helical arrays of functional pendants, such as alcohols (**238**, **239**), ether (**240**), crown ethers (**241**−**243**), oligoglycines (**244**), and pyridyl groups (**245**, **246**), along the helical polymer backbone (Figure 42C).[381,382] As described in section 2.1.2, polyisocyanides belong to static helical polymers when they have a bulky side group. However, the present results unambiguously reveal that poly(phenyl isocyanide)s with less bulky side groups have a dynamic helical feature as well as a static one; this behavior is distinct from that of the other static and dynamic helical polymers. A similar dynamic helical model has also been proposed by Nolte and co-workers for helical poly(isocyanopeptide)s derived from β-amino acids (**27**, **28**) (Chart 4 in section 2.1.2).[76]

The **174**-Na with a macromolecular helicity memory is an optically active polyelectrolyte with negative charges, which can serve as the template for further induction of a preferred-handed helicity in a different, dynamically racemic helical polyelectrolyte with opposite charges in water ("*helicity-replication*"), forming biomimetic interpolymer helix

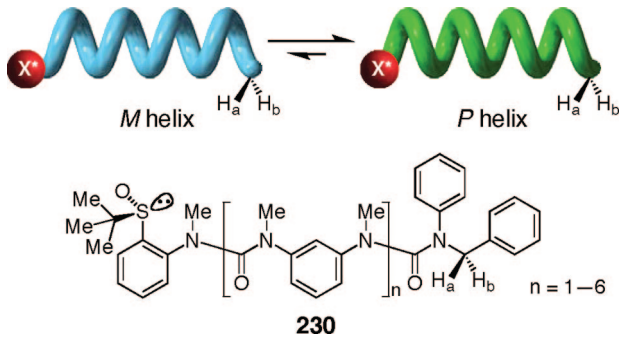

230

Figure 38. Schematic illustration of interconversion of diastereomeric helices of oligoureas derived from *m*-phenylenediamine bearing a terminal chiral sulfinyl group and an *N*-benzyl group to act as a diastereotopic probe (**230**).

Chart 24

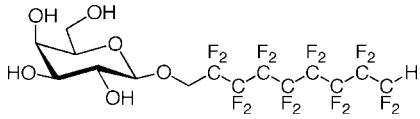

231

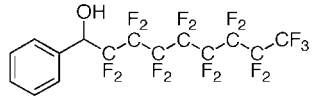

232

bundles and helical assemblies with a controlled helicity in water (Figure 42D).[383] Although the helical **174**-Na no longer has any chiral components and stereogenic centers, the helical chirality of the polyisocyanide is efficiently transformed into the dynamically racemic, cationic polyelectrolyte **156**-HCl through electrostatic interaction to show an ICD in the **156**-HCl chromophore region due to an excess of the preferred-handed helical sense.

The noncovalent *domino effect* and subsequent chiral memory effect have been applied to a dynamically racemic helical oligopeptide composed of achiral amino acids with a single intramolecular side-chain cross-link (**247**) (Figure 43).[384] In this system, a helix-sense bias is induced in the oligopeptide through noncovalent chiral interactions at the *N*-terminal amino group with a chiral carboxylic acid (L-**248**) and is stored in the peptide backbone with the aid of the side-chain cross-linking at *i* and *i* + 3 in a 3/10-helix. The peptide showed a split CD pattern around 286 nm due to the Δ^ZPhe chromophore region, suggesting a right-handed helix formation. Upon complete removal of L-**248** by the addition of a large excess of achiral acid **249**, the induced CD signal slowly reduced its intensity and reached an undetectable level after *ca.* 20 min at 20 °C. The thermodynamic parameters ($\Delta G^{\neq}_{20} = 86.6$ kJ mol^{-1}; $\Delta H^{\neq} = 95.4$ kJ mol^{-1}; $\Delta S^{\neq} = 30.0$ J mol^{-1} K^{-1}; see Table 1) have been estimated on the basis of the racemization kinetics of the **247**/**249** complex.

Wan et al. have reported that the free radical polymerization of a bulky vinyl monomer bearing optically active groups, 2,5-bis[(4′-alkoxycarbonyl)phenyl]styrene (**250**), produces a chiral, likely helical, secondary structure of the polymer backbone (poly-**250a**). After the chemical removal of the optically active alkyl chains (poly-**250b**) and a further methylation with dimethyl sulfate (poly-**250c**), the optical activity of the polymers remained (Scheme 22).[385]

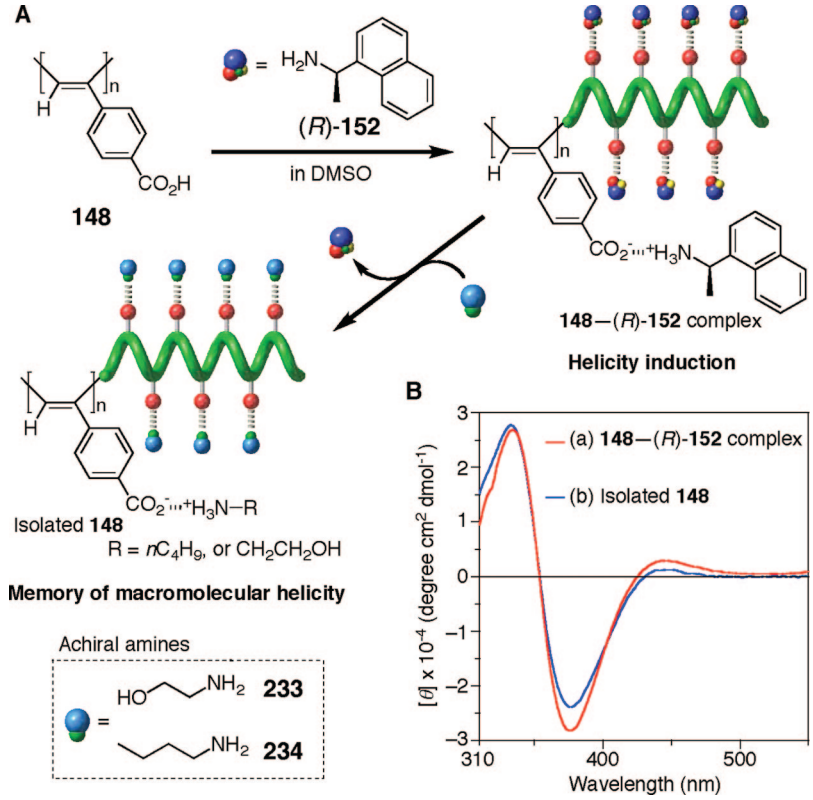

Figure 39. (A) Schematic illustration of a preferred-handed helicity induction in **148** upon complexation with (*R*)-**152** and subsequent memory of the helicity after replacement by achiral amines (**233**, **234**). (B) CD spectra of the **148**—(*R*)-**152** complex (red line) and the isolated **148** by SEC fractionation using a DMSO solution containing an achiral amine **233** as the mobile phase (blue line) in DMSO.

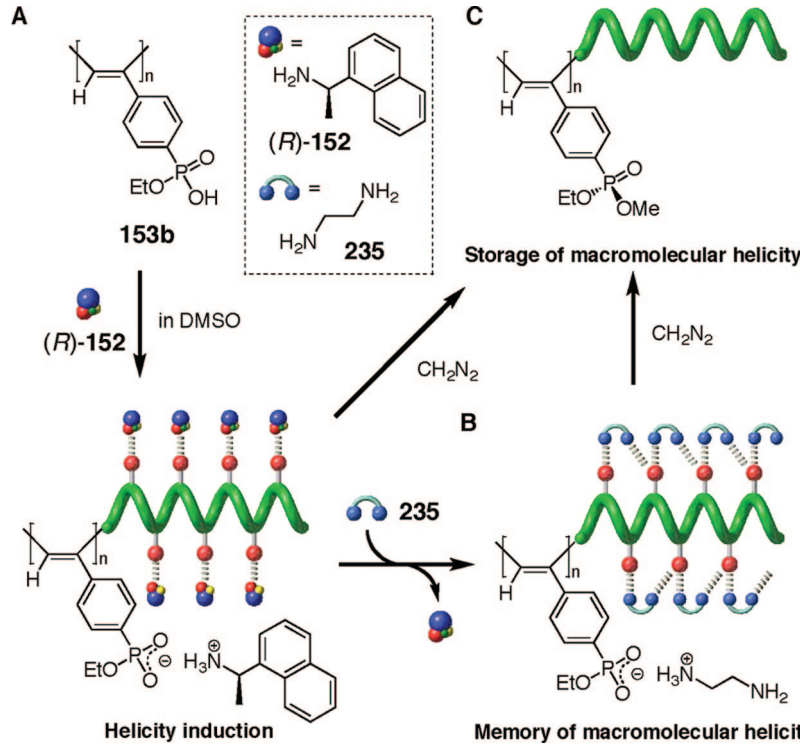

Figure 40. (A) Schematic illustration of an excess one-helical sense induction in **153b** upon complexation with (*R*)-**152**, (B) memory of the induced macromolecular helicity after replacement by achiral **235**, and (C) storage of the induced helicity or helicity memory by asymmetric esterification with diazomethane.

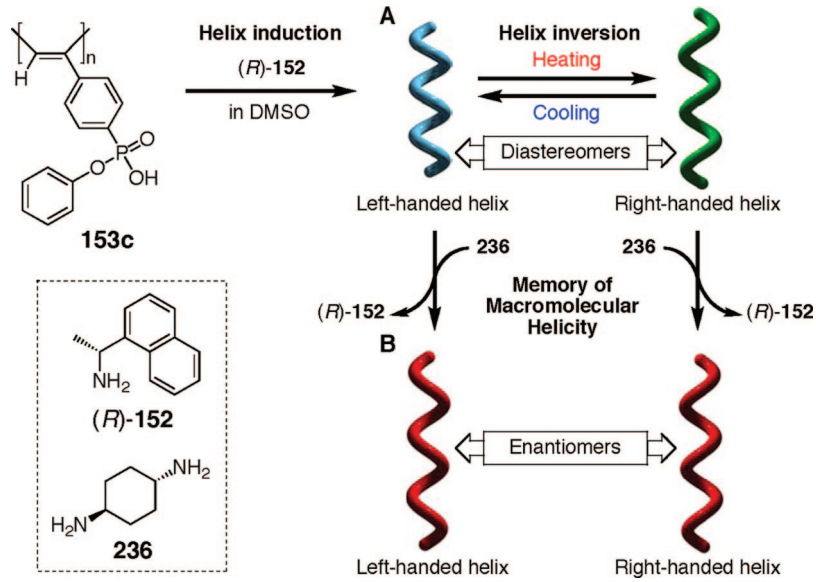

Figure 41. Schematic illustration of an induced one-handed helicity in optically inactive **153c**, helix inversion with temperature, and subsequent memory of the diastereomeric macromolecular helicity at different temperatures. The left-handed helical conformation of **153c** induced by (*R*)-**152** at low temperature reversibly changes into the opposite right-handed helix at high temperature (A), and these diastereomeric helices of **153c** are memorized at different temperatures by replacement of the (*R*)-**152** with achiral **236**, resulting in the formation of the enantiomeric mirror image helices of **153c** (B). (Reproduced with permission from ref 271. Copyright 2005 American Chemical Society.)

2.7.2. Macromolecular Helicity Memory in a Solid

As discussed in the preceding section, the macromolecular helicity memory of functional PPAs has been achieved in organic solvents but was difficult to realize in water, because dynamic helical PPAs memorize their helicity only when the acidic pendant groups of the induced helical PPAs complexed with achiral molecules dissociate into free ions to prevent the atropisomerization process of the polymers in organic solvents. However, in water, the pendant charged groups of the induced helical PPAs appear to be highly solvated with water molecules, and therefore, the helix inversion readily takes place, resulting in the loss of the induced helical sense bias in water.

Using the recently developed layer-by-layer (LbL) assembly technique,[386] the macromolecular helicity memory in water has been realized (Figure 44).[387] A negatively charged helical PPA **153b** induced by a chiral amine ((*S*)-**237**) in water showing a full ICD was first deposited on a

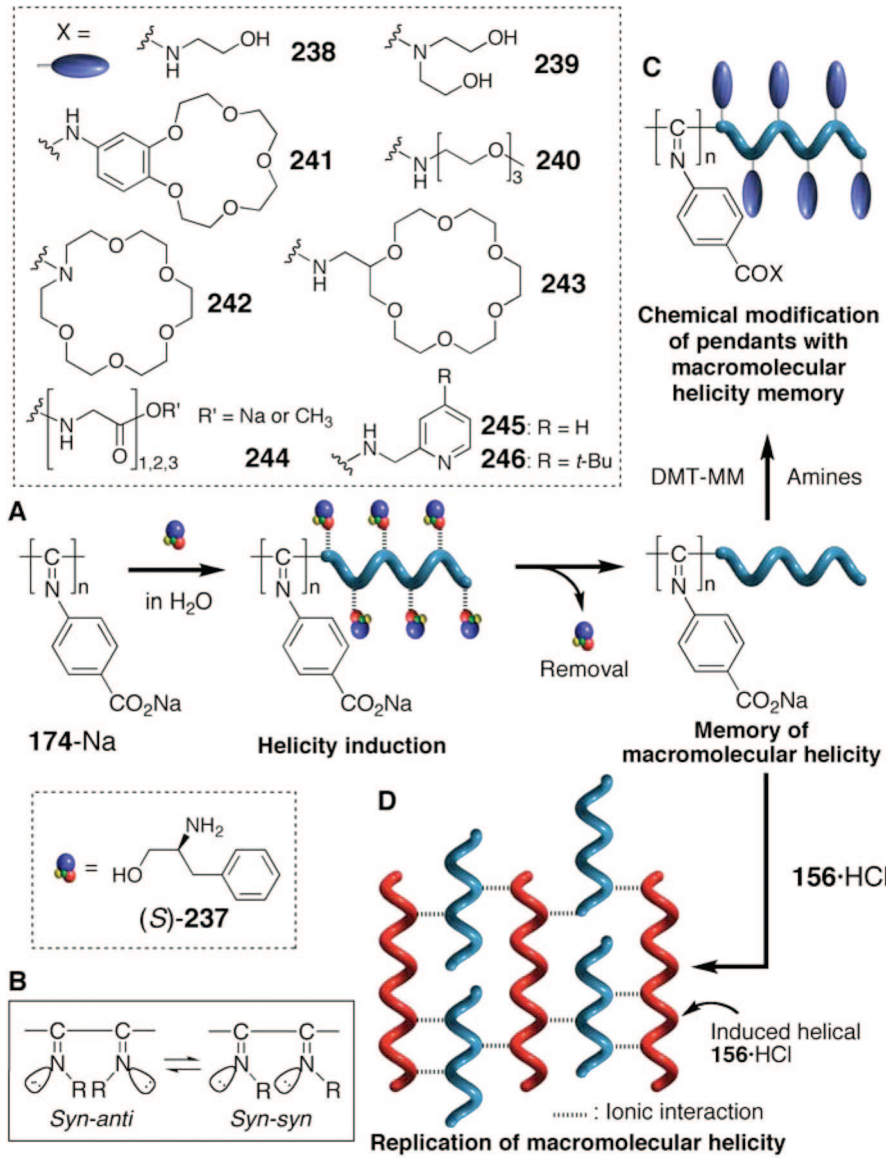

Figure 42. Schematic illustrations of a helicity induction in **174**-Na upon complexation with (*S*)-**237** and memory of the induced macromolecular helicity after complete removal of (*S*)-**237** (A) through *syn*−*anti* isomerization of the C═N bond (B), modification of the pendants with macromolecular helicity memory (C), and the replication of the macromolecular helicity (D).

quartz substrate. Subsequently, an achiral positively charged vinylpolymer, such as the hydrochloride of poly(allylamine) (PAH), was LbL assembled. The (*S*)-**237** molecules used for the helical sense bias in **153b** were automatically removed during the LbL assembly process, and optically active multilayer thin films with a macromolecular helicity memory were thus formed after repeating the alternative deposition cycle. When a positively charged, induced helical **156**-HCl was used instead, the alternative deposition of an achiral vinylpolymer with opposite charges produced a similar thin film with a macromolecular helicity memory.[387] These multilayer thin films with optical activity will be applicable as novel chiral materials for enantioseparation and catalysis after the deposition of specific metals.

An optically active poly(diphenylacetylene) having chiral *p*-(dimethylpinanylsilyl) pendant groups (**251**) exhibits a large optical rotation and intense CD signals in the range of 350−450 nm, corresponding to the backbone $\pi-\pi^*$ transition region, which indicates the formation of a helical conformation with a preferred handedness. After complete removal of the optically active pinanylsilyl groups of the membrane of **251** by desilylation, the resultant polymer membrane *de*-**251** still showed a specific rotation and intense CD signals comparable to those of the original **251** in the 350−450 nm region (Scheme 23).[388] Presumably, the *de*-**251** retains the same handed helical conformation in the main-chain as in the original **251** in the solid state after the chemical reaction. In other words, the main-chain likely exists in a sufficiently stable helical conformation in the solid state in spite of the absence of chiral pendant groups. This method has been applied to PPAs, such as **252**. The depinanylsilylated membranes (*de*-**252**) also exhibited CD signals similar to those of the original **252**s after removal of the chiral substituents, suggesting that the *de*-**252** retains its macromolecular helicity in the absence of the chiral pendant groups.[389] These pinanylsilyl-group-free membranes with the macromolecular helicity memory have been used as enantioselective permeable membranes for separating some racemates (see section 5.1).

δ-Form syndiotactic polystyrene (st-PS) films have been reported to show an intense ICD in the aromatic region of the polymer after a few minutes of exposure to nonracemic

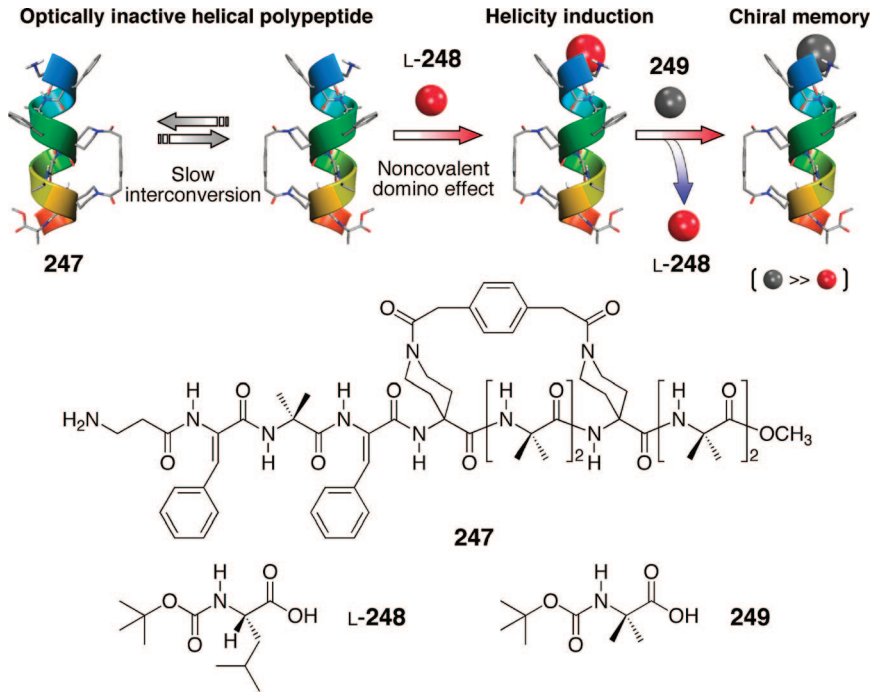

Figure 43. Schematic illustration of a preferred-handed helicity induction in optically inactive 3/10-helical **247** with L-**248** and memory of the macromolecular helicity in the presence of an excess achiral **249**. (Reproduced with permission from ref 384. Copyright 2008 American Chemical Society.)

Scheme 22. Synthesis of Optically Active Vinyl Polymers by Free Radical Polymerization and Memory of Chirality after Removal of the Optically Active Pendants

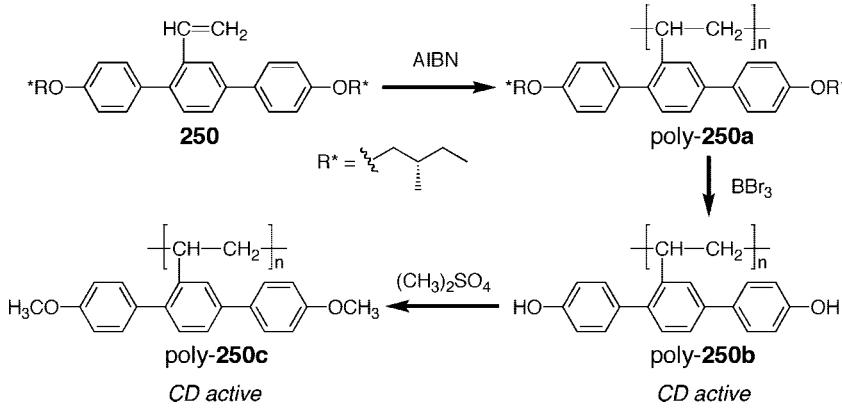

volatile molecules, such as (*R*)- and (*S*)-limonene (**253**) and carvone, at ambient temperature (Figure 45).[390,391] Unexpectedly, the ICD remains essentially unaltered after complete removal of the guests by extraction with supercritical carbon dioxide as well as after successive absorption of other racemic or nonracemic guests. This chiral memory imprinted by nonracemic guests in the nanoporous st-PS films is quite stable and remains after heat treatments up to 240 °C, which is below the melting temperature of st-PS (270 °C), at which the memory is erased. Amorphous or dense crystalline (α, *β*, or *γ*) st-PS films showed no ICD after exposure to the same nonracemic guests, suggesting the nanoporous crystalline phase is necessary for appearance of the ICD,[390] although the ICD remains after the thermal transition toward the *trans*-planar α crystalline phase, suggesting that the chiral memory may not be associated with the molecular structure of the st-PS but derived from the formation of nonracemic supramolecular crystalline structures, although the morphology associated with the origin of the chiral memory effect of the st-PS remains unclear. The ICD intensity of st-PS also significantly depends on the experimental conditions, such as the spin rate of the spin-coating of a polymer solution and its solvent.[391]

As described in section 2.5.2, the (*R*)-CSA doped polyaniline thin films exhibit an ICD due to either the preferred-handed helix or the supramolecular helical assembly of the polymer chains. The film retained its optical activity after removal of the dopants.[392] The (*R*)-CSA dedoped polyaniline thin films with a chiral memory showed chiral recognition toward a pair of phenylalanine enantiomers (see section 5.3).[393]

2.7.3. Macromolecular Helicity Memory in Poly(methyl methacrylate)

The preferred-handed helical sense induction and subsequent memory of the helicity can also be applicable to a commodity plastic, such as syndiotactic poly(methyl methacrylate) (st-PMMA). st-PMMA is known to form a thermoreversible physical gel in aromatic solvents such as toluene, in which the st-PMMA adopts a helical structure with a sufficiently large cavity of about 1 nm, in which

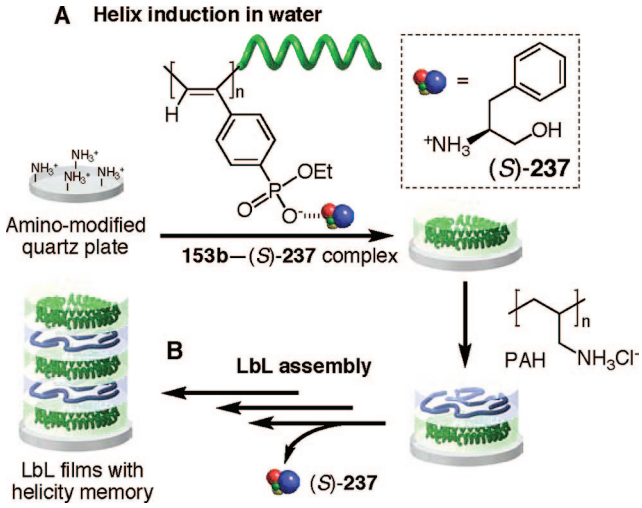

Figure 44. Schematic illustration of the LbL self-assembly of a charged PPA with induced macromolecular helicity. (A) An excess of the one-handed helical sense is induced in **153b** with the optically active (*S*)-**237** in water. (B) An induced helical **153b** can be LbL assembled with an achiral polyelectrolyte having opposite charges (PAH), resulting in multilayer thin films with an induced macromolecular helicity memory on a substrate. (Reproduced with permission from ref 387. Copyright 2005 The Royal Society of Chemistry.)

Scheme 23

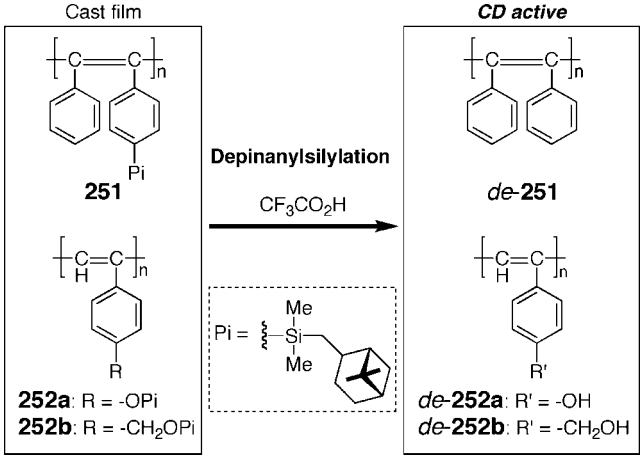

solvents are encapsulated.[394] In the presence of an optically active alcohol, such as (*S*)- or (*R*)-1-phenylethanol (**254**) in toluene, st-PMMA folds into a preferred-handed helix accompanied by gelation, and at the same time, fullerenes, such as C_{60}, C_{70}, and C_{84}, are encapsulated within its helical cavity to form a robust, processable peapod-like complex (Figure 46), as revealed by DSC and XRD profiles of the st-PMMA/C_{60} films and also by AFM and TEM images of a st-PMMA/C_{60} Langmuir−Blodgett (LB) film.[395] After removal of **254**, the st-PMMA gel complexed with C_{60} exhibited apparent VCD and ICD signals in the PMMA IR regions and in the encapsulated C_{60} chromophore regions, respectively, although C_{60} itself is achiral.

The optically active, fullerene-encapsulated st-PMMA with a macromolecular helicity memory serves as a novel template for the further helix-sense-controlled supramolecular inclusion of the complementary isotactic PMMA (it-PMMA) through replacement of the encapsulated C_{60} molecules, resulting in a practically versatile PMMA stereocomplex[396−398] with optical activity (Figure 46).[399] The it-PMMA replaced the encapsulated C_{60} molecules to form a double-stranded helix with the same handedness as that of the st-PMMA single helix through the formation of a topological triple-stranded helix,[400] as revealed by the good coincidence of the calculated VCD spectra with the observed ones. These results provide the first molecular basis of the structure and the mechanism for the PMMA stereocomplex formation, which have been a long-standing question in polymer chemistry; that is, a double-stranded helix of it-PMMA is likely included in a preformed single helix of st-PMMA, resulting in a supramolecular inclusion complex with a triple-stranded helical structure.

2.7.4. Supramolecular Helicity Memory

Saddle-shaped porphyrins, such as **255** (Figure 47), adopt a nonplanar conformation due to the steric repulsion among the neighboring meso and pyrrole-β substituents on the periphery. The porphyrins **255** bearing two different substituents at the neighboring meso positions have D_2 symmetry and are thus chiral as a result of this nonplanar structure. However, the enantiomers of the D_2-symmetric **255** are not separable from one another at ambient temperature because of a rapid saddle-to-saddle macrocyclic inversion (racemization). However, such a thermodynamic equilibrium can be shifted to either of the two enantiomeric forms by converting them to a diastereomeric pair with chiral acids, such as mandelic acid (MA), through a 1:2 hydrogen-bonding

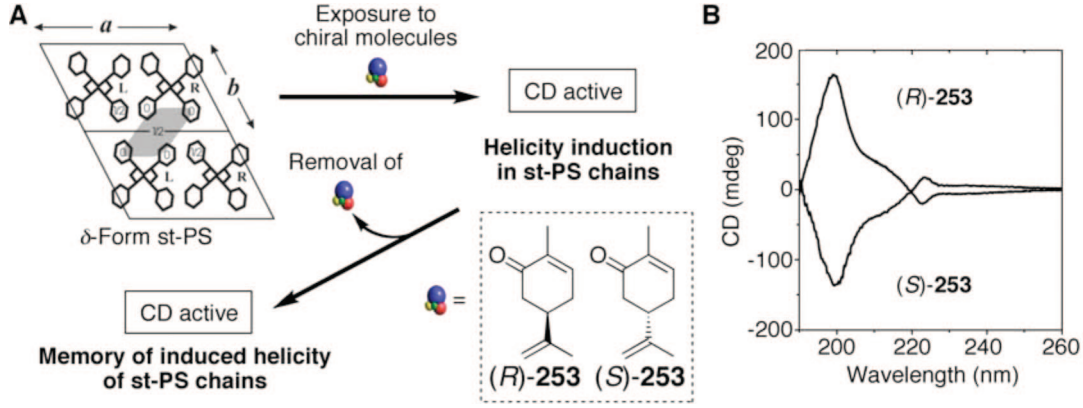

Figure 45. (A) Schematic illustration of a helicity induction in achiral st-PS chains upon exposure to chiral molecules ((*R*)- or (*S*)-**253**) and subsequent memory of the helicity after removal of **253** by extraction with supercritical CO_2 in a δ-form st-PS film. (B) CD spectra of a δ-form st-PS film after exposure to a vapor of (*R*)- or (*S*)-**253**. (Reprinted with permission from refs 390 and 391. Copyright 2007 American Chemical Society and 2008 The Royal Society of Chemistry.)

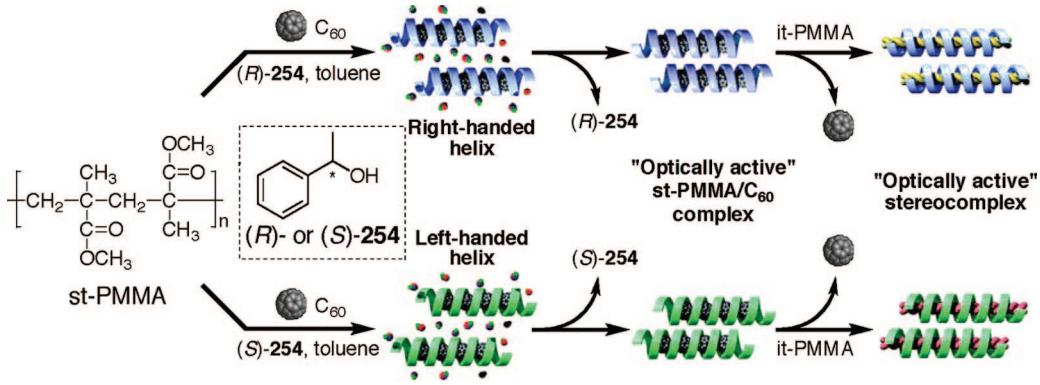

Figure 46. Schematic illustration of a preferred-handed helicity induction in achiral st-PMMA in the presence of C_{60} with (*S*)- or (*R*)-**254**, memory of the induced helicity after removal of **254**, and subsequent "optically active" stereocomplex formation after the addition of it-PMMA, resulting from replacement of the encapsulated C_{60} molecules by it-PMMA strands. (Reproduced with permission from ref 395. Copyright 2008 American Chemical Society.)

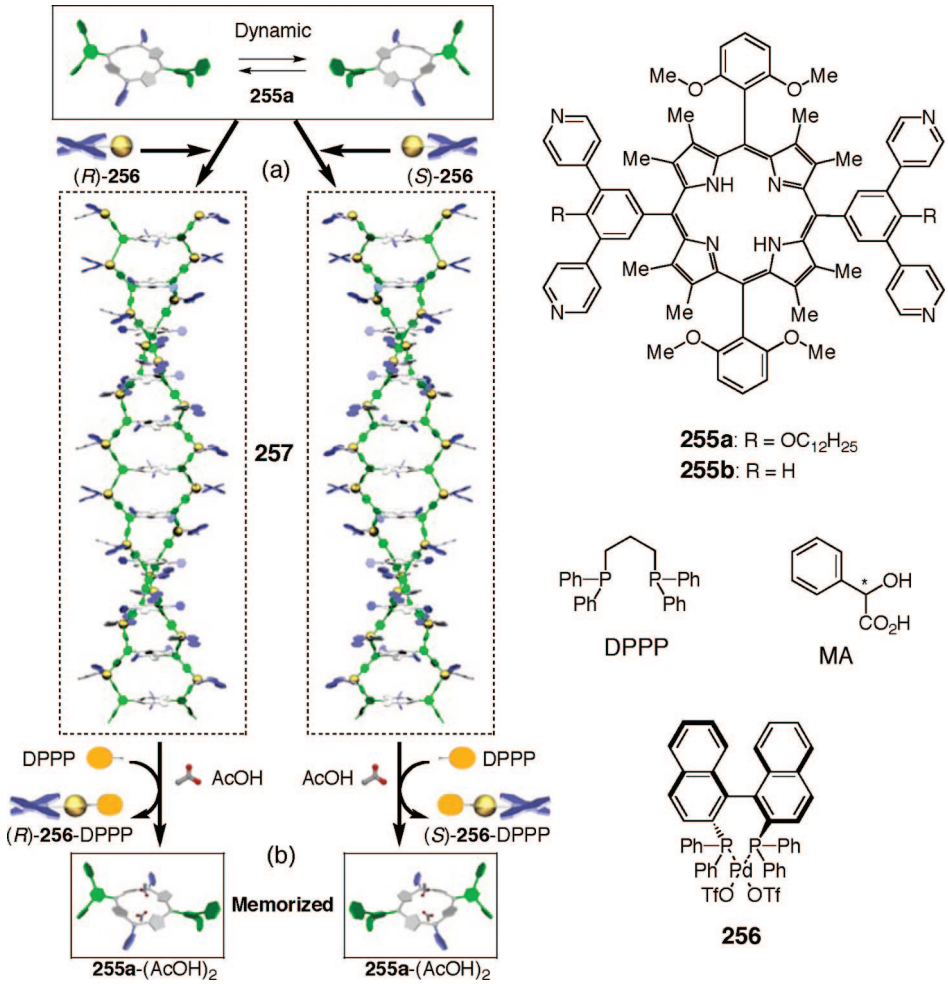

Figure 47. Schematic representation of (a) induction of a helical chirality by supramolecular polymerization of chirality-memorizing **255a** with chiral Pd(II) (BINAP) (**256**) and (b) its translation into the chirality of monomer **255a** (hydrogen-bonded with acetic acid (AcOH)) by stereochemically retentive depolymerization in AcOH containing 1,3-bis(diphenylphosphino)propane (DPPP) as a decomplexing agent. (Reproduced with permission from ref 402. Copyright 2008 Elsevier.)

interaction. In addition, the induced enantiomeric bias can be fixed by the addition of an excess of achiral acids such as acetic acid.[375] In this system, the hydrogen-bonded MA molecules on **255** are readily replaced with acetic acid, but the inversion of the porphyrin macrocycle, which leads to the racemization of **255**, can be suppressed by regenerated hydrogen bonds with acetic acid. This saddle-shaped porphyrin is called a chirality-memory molecule after discovery of this unique feature.[375,401]

Taking advantage of this unique feature of the chirality-memory molecule as a building block, Aida et al. have succeeded in constructing a supramolecular ladder-shaped polymer with an excess helix-sense bias, and the helical chirality is translated into the saddle-shaped chirality of the monomer porphyrin, which is further memorized upon depolymerization of the ladder polymer in the presence of acetic acid (Figure 47).[402,403] A saddle-shaped porphyrin having 3,5-dipyridylphenyl side arms at the opposite meso

Scheme 24

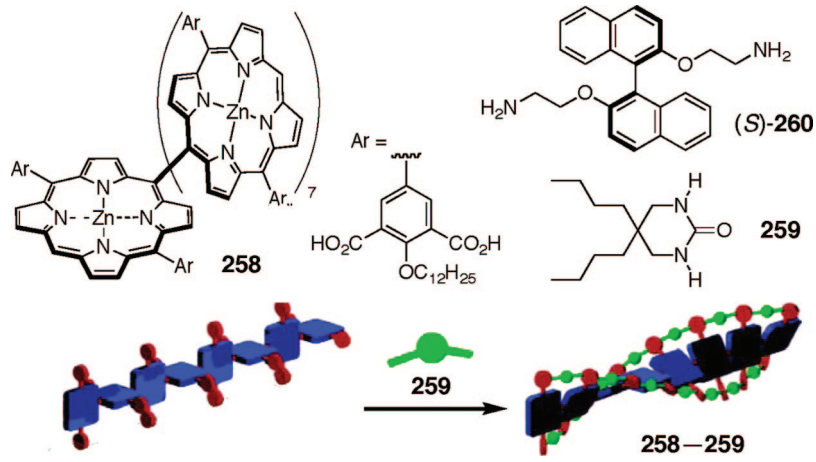

positions (**255a**) undergoes supramolecular polymerization through coordination with a chiral Pd(II) complex of BINAP (**256**), thus forming a one-handed helical ladder-shaped polymer (**257**), of which the helix-sense bias along the main-chain is induced by the optically pure Pd(II)/BINAP complex moieties. When the helical ladder polymer was poured into acetic acid containing 1,3-bis(diphenylphosphino)propane (DPPP) as a decomplexing agent, **257** was depolymerized in a stereochemically retentive way to give the optically active **255a**, hydrogen-bonded with acetic acid.[402] A ladder-shaped polymer consisting of **255b** has also been constructed by employing an achiral Pt(II) complex of DPPP as the linkages. (*R*)- or (*S*)-MA causes a helix-sense bias in the ladder polymer along the main-chain upon complexation with the saddle-shaped porphyrin units of **255b** through hydrogen-bonding interactions. Interestingly, helix induction experiments changing the optical purity of MA have shown a distinct chiral amplification, which originates from the "majority rule" operative in the ladder polymer consisting of **255b**.[403]

A zinc(II) meso−meso linked porphyrin oligomer (**258**) exists in a nonhelical conformation in solution but changes its structure to a dynamic helical conformation upon complexation with an achiral urea (**259**) through complementary hydrogen-bonding interactions.[404] A predominantly one-handed helical conformation can be biased in the porphyrin oligomer complexed with **259** in the presence of the chiral diamine ((*S*)-**260**) (Scheme 24). The ternary complex showed a characteristic ICD in the visible absorption region of the porphyrin chromophore. A chiral memory effect has been observed for this system.[404] Upon the addition of an equimolar amount of the opposite (*R*)-**260** to a solution of **258**−**259** and (*S*)-**260**, the Cotton effect around 320 nm due to the binaphthyl moiety was exactly canceled out because **260** exists as a racemic mixture in the solution. However, the ICD at 429 nm due to the porphyrin array was still observed along with a slight decrease in its intensity even after the further addition of (*R*)-**260**, indicating that an induced helical conformation of the porphyrin oligomer can be locked, although a chiral filter effect (section 2.5.2) in which the helical **258** formed by (*S*)-**260** selectively excludes one enantiomer for racemic **260** was not negligible. Such a chiral memory effect is not observed for shorter porphyrin oligomers (trimer and tetramer), probably arising from the insufficient kinetic stability of the helical conformation.

Trialkyl-1,3,5-benzenetricarboxamides, such as **261** and **262**, self-assemble to form a helically twisted columnar structure through a 3-fold intermolecular hydrogen bonding in apolar solvents, and the "sergeants and soldiers" effect has been observed in this supramolecular helical assembly system (Figure 48).[405,406] A small amount (0.1 equiv) of chiral **262** induces a one-handed helical columnar assembly composed of the major achiral **261** bearing a sorbyl residue, as evidenced by the appearance of a CD signal, thus indicating the strong chiral amplification. The 1,4-polymerization of the sorbyl residue of each achiral **261** unit with UV light preferentially took place within the columnar assembly and produced an optically active linear polymer while maintaining its supramolecular helical columnar structure after removal of the chiral template **262** in specific solvents.[407] In the presence of a polar solvent, the CD effect completely disappeared, but it was regenerated when the solvent was changed to the original one. This process can be repeated via a reversible unfolding/refolding cycle of the polymer. The chiral information seems to be encoded in the stereochemistry of the sorbyl main-chain, although the polysorbate

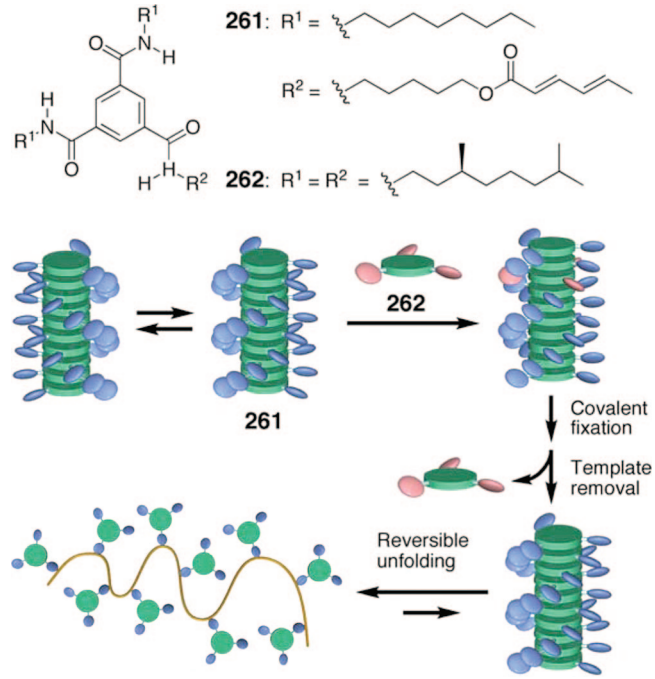

Figure 48. Schematic illustration of supramolecular helicity induction in columnar self-assemblies of **261** with chiral **262** and locking and memory of the supramolecular helicity after photoirradiation and subsequent removal of the chiral **262**.

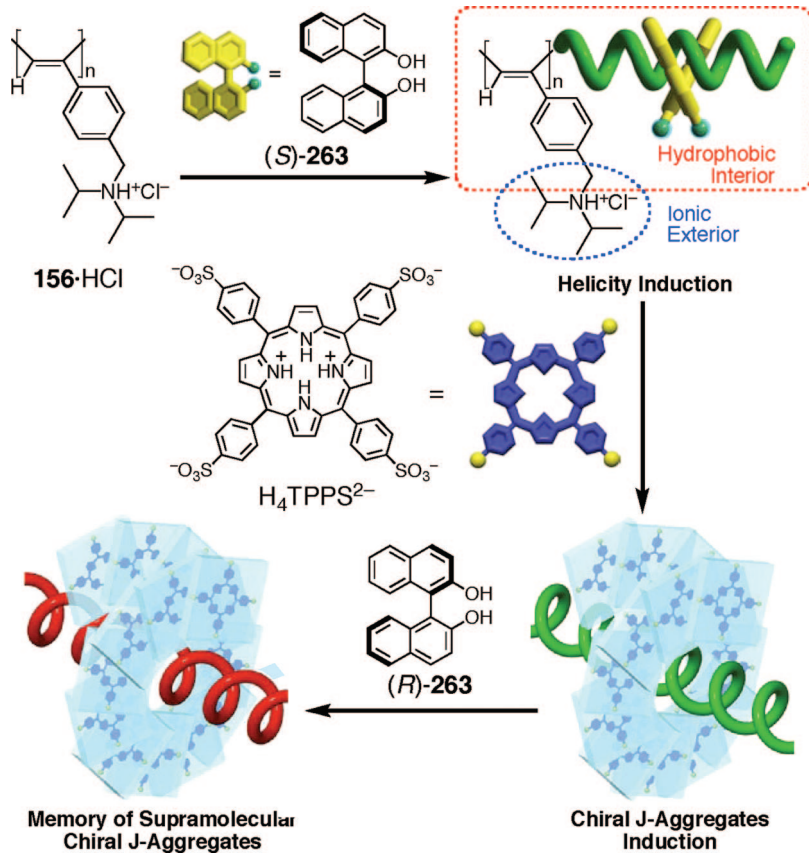

Figure 49. Schematic illustration of the induction of a preferred-handed helicity in **156**-HCl upon complexation with (*S*)-**263**, subsequent formation of supramolecular helical J-aggregates of achiral H_4TPPS^{2-}, and memory of the supramolecular chirality after inversion of the helicity of the **156**-HCl by addition of excess (*R*)-**263** in acidic water. (Reproduced with permission from ref 408. Copyright 2006 Wiley-VCH.)

backbone is not completely stereoregular, leading to a kind of chiral memory effect.

The induced helical polyelectrolytes derived from the PPAs with a helical sense bias can serve as a novel template for the formation of supramolecular helical aggregates of achiral porphyrin and cyanine dyes in water. A hydrophobic chiral guest, (*S*)-1,1′-bi-2-naphthol ((*S*)-**263**), can be trapped within the hydrophobic helical cavity of the charged PPA (**156**-HCl) in water and induces an excess one-handed helix in the PPA. The induced helical PPA serves as a template for the further induction of supramolecular chirality in achiral porphyrin aggregates with opposite charges (H_4TPPS^{2-}) driven by electrostatic interactions (Figure 49). This ionic complexation promotes the formation of J-homoaggregates in a preferred-handed helical array, as demonstrated by the appearance of an intense ICD in the J-aggregated porphyrin chromophore region that has a remarkable stability to temperature and organic solvents.[408] For example, the J-aggregated porphyrins hardly dissociate into the solvent under the conditions in which H_4TPPS^{2-} favorably exists in the monomeric form. The supramolecular chirality of the J-aggregates, once formed, remained unchanged after the template helical polymer loses its optical activity or even takes the opposite helical sense by the addition of excess (*R*)-**263**.[408] Therefore, the supramolecular chirality of the H_4TPPS^{2-} homoaggregates has been memorized.

A water-soluble neutral PPA bearing the bulky amphiphilic aza-18-crown-6 ether pendants (**158**) can also trap an achiral cyanine dye, 3,3-diethyloxadicarbocyanine iodide (**264**), within its hydrophobic cavity in acidic water, and the cyanine dye forms supramolecular J-aggregates (Figure 50).[409] In the presence of chiral amino acids, such as L- or D-tryptophan (Trp), which interacts with the exterior crown ether pendants through specific host−guest complexations, the host polymer **158** forms an excess single-handed helical conformation[279] and further encapsulates the cyanine dye within its helical cavity. The cyanine dye aggregates in an excess one-handed helical array along the helical backbone of the PPA after annealing, thus exhibiting an ICD in the achiral cyanine chromophore region. Furthermore, the supramolecular chirality induced in the cyanine aggregates can be "memorized" even after inversion of the macromolecular helicity of the template **158** by the addition of excess Trp with the opposite configuration.[409] Thereafter, thermal racemization of the helical aggregates slowly takes place. Although a number of cyanine aggregates with optical activity arising from supramolecular chirality have been reported, most of them are formed on the exterior surfaces of charged biopolymers as a template, except for DNA.[410] Thus, for the first time, helical cyanine dye aggregates with a chiral memory formed within a helical cavity of artificial helical polymers have been achieved.

2.8. Helix Inversion

2.8.1. Macromolecular Helix Inversion

Another interesting and unique feature of dynamic helical polymers is the reversible inversion of macromolecular helicity (helix−helix or PM transition) between right- and left-handed helical conformations regulated by external stimuli, such as a change in temperature or solvent polarity,

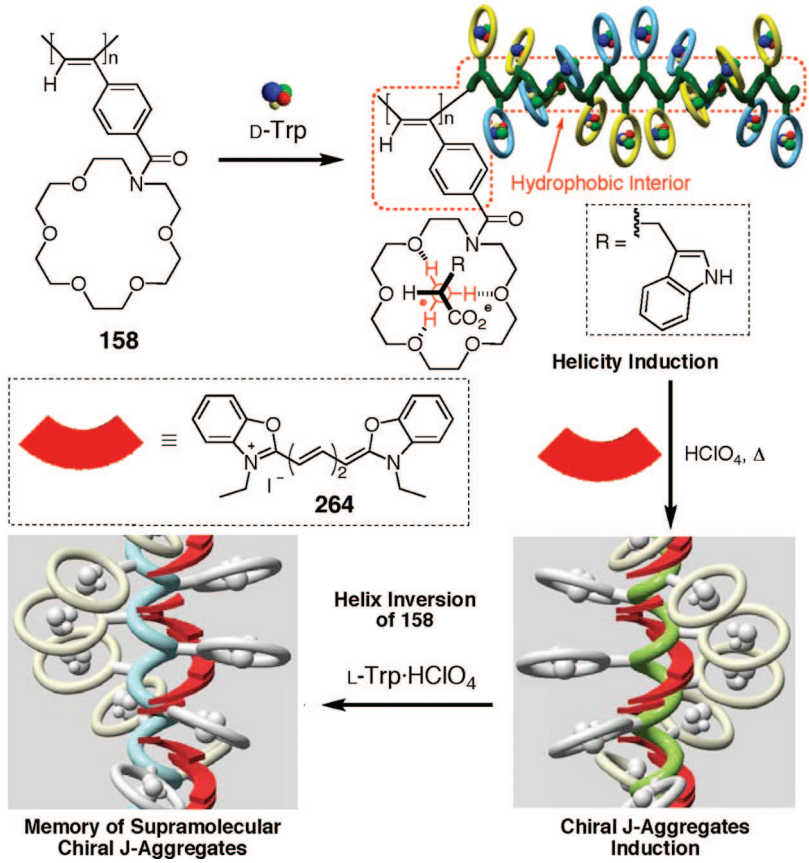

Figure 50. Schematic illustration of a preferred-handed helicity induction in **158** upon complexation with D-Trp, subsequent supramolecular helical aggregate formation of achiral **264** within the helical cavity of **158** in acidic water, and memory of the supramolecular chirality after helix inversion of the **158** by excess L-Trp. (Reproduced with permission from ref 409. Copyright 2007 American Chemical Society.)

Chart 25

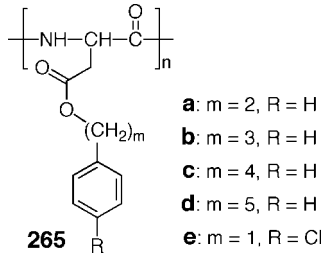

or by irradiation with light. Because dynamic helical conformations separated by helical reversals are extremely sensitive to a chiral environment arising from a high cooperativity, the formation of an excess of the preferred handed helix can be altered, resulting in the helix inversion. Biopolymers, such as DNA[411] and polypeptides[412−419] with specific sequences, are known to undergo inversion of their helicity regulated by a change in the salt concentration and temperature, respectively. The structure of a junction between the right-handed B-DNA and the left-handed Z-DNA has been revealed by X-ray crystallography at a 2.6 Å resolution.[420] Among the polypeptides, the helix-sense inversion behaviors of poly(aspartic acid ester)s (polyaspartates), such as **265a−e** (Chart 25), have been extensively studied.[415−419] The reversible helix inversion of **265a** takes place in the anisotropic LC state as well as in a dilute isotropic solution, and the inversion of the helix-sense of **265a** in the lyotropic LC simultaneously triggers an inversion of the macroscopic helix of the cholesteric LC.[415,416] More interestingly, **265b−d** show the reversible and first order transition from the right-handed α-helix to the left-handed *ω*-helix even in the solid state.[418] Some static helical polymers (poly-**9**)[63] and chloral oligomers[27,421] also exhibit a transition in their helical senses, but their inversion processes are not reversible, and racemization occurs. Several synthetic, dynamic helical polymers exhibit a reversible helix−helix transition by changing the external conditions, such as temperature (**70**, **93a**, **93b**, **108a**, **113**, **266−277**),[130,175,422−431] solvent polarity (**84**, **88**, **90d**, **93a**, **93b**, **95b**, **278**, **279**),[144,150,153,158,424,432−434] or both (**95a**, **280**, **281**)[435,436] (Figure 51).

Fujiki et al. have synthesized a series of optically active homopolymers and copolymers of helical polysilanes to develop chiral switchable materials based on the helix inversion.[130] A typical rodlike helical polysilane **266** undergoes a temperature-dependent helix−helix transition through a transition temperature (T_c) at −20 °C in isooctane, and the polysilane exhibited opposite Cotton effect signs to each other above and below the T_c (Figure 52).[431] The helix inversion of helical polysilanes is sensitive to the structure of the pendants, and a polysilane (**282**) bearing a slightly different *β*-branched achiral side chain showed no inversion of the Cotton effect signs from −90 to +80 °C. Although the origin of the helix−helix transition is still unclear, molecular mechanics (MM) calculations for the polylsilanes revealed that **266** has a clear double-well ("W") shaped potential energy curve of the main-chain torsion angle, which may be responsible for the temperature-dependent helix−helix transition, whereas **282**, showing no helix−helix transition, has an unclear double-well potential curve. The helix−helix transition temperature has been controlled by the copolymerization with appropriate achiral monomers (**270−272**)[429−431]

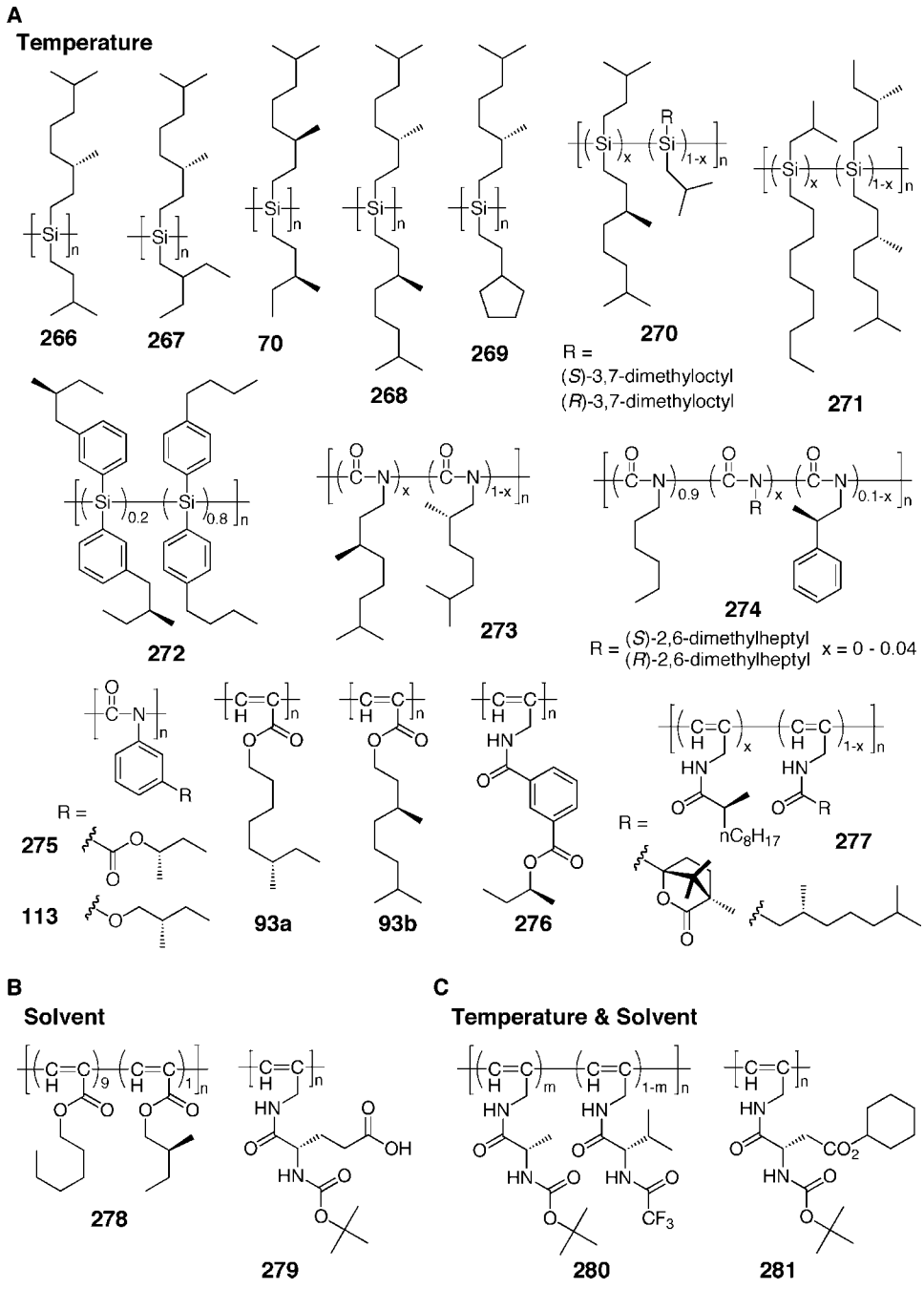

Figure 51. Representative examples of dynamic helical polymers that exhibit helix inversion generated by changing temperature (A, C) and/or solvent polarity (B, C).

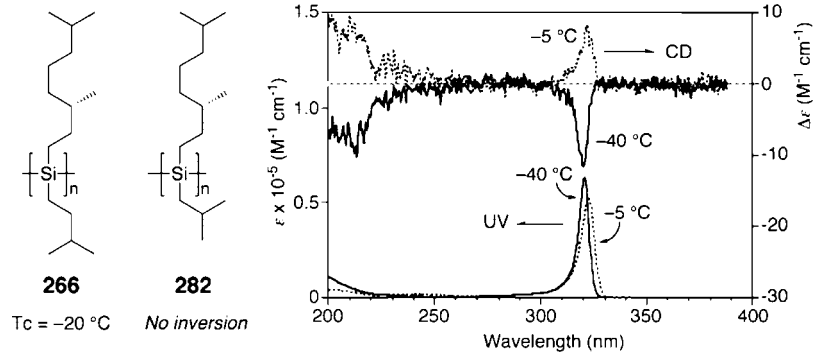

Figure 52. CD and UV absorption spectra of **266** at −40 °C (solid line) and −5 °C (dotted line) in isooctane. (Reproduced with permission from ref 431. Copyright 2000 American Chemical Society.)

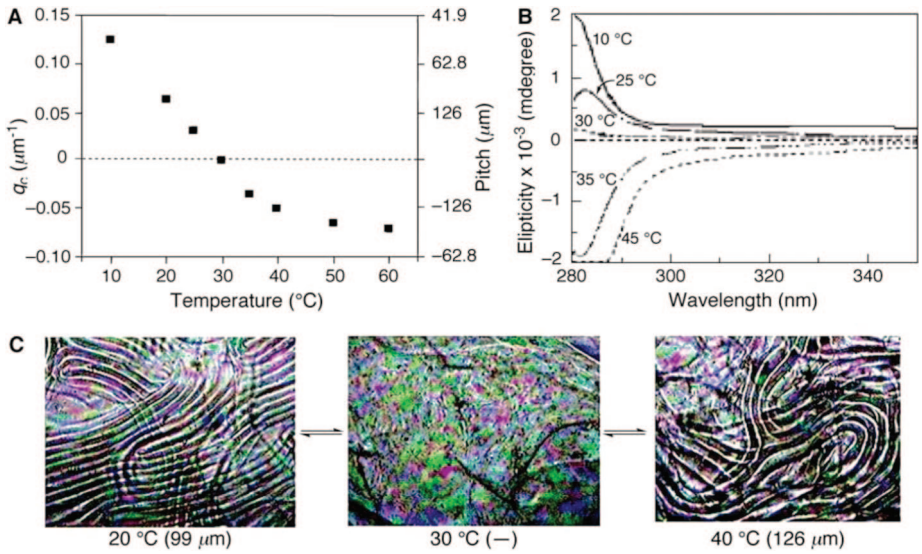

Figure 53. (A) Temperature dependence of the pitch and pitch wavenumber, q_c, of 2 wt % of **274** ($x = 0.0008$, R = (*R*)-2,6-dimethylheptyl) used as a dopant in the LC formed from a 40% solution of **62** in toluene. (B) CD spectra of the planar texture of the corresponding LC. (C) Temperature dependence of the fingerprint texture of the corresponding LC. (Reproduced with permission from ref 427. Copyright Copyright 2003 American Chemical Society.)

or by changing the molecular shape of the hydrocarbon solvents.[130,437]

Green et al. have also prepared designer polyisocyanates (**273**, **274**, Figure 51) that show an inversion of the helicity with a desired T_c in dilute solution by the copolymerization of paired enantiomers with different structures, which are in competition in helical sense preferences of each other.[427,428] This concept has further been applied to the lyotropic LC system of poly(*n*-hexyl isocyanate) (**62**) using the thermo-driven switchable helical polyisocyanates as chiral dopants. The addition of **274** showing a T_c near 30 °C to a nematic solution of **62** gave rise to a typical finger texture above and below the T_c due to a cholesteric LC phase (Figure 53).[427] The mesoscopic cholesteric states of an opposite twist sense can thus be controlled by changing the temperature.

Helical polyacetylenes bearing amino acids as the pendants also show inversion of the helicity (**84**, **88**, **95b**, **279**−**281**) by responding to the temperature and/or solvent polarity, which mainly results from the presence or absence of the intramolecular hydrogen bonding between the pendant amide groups in nonpolar and polar solvents, respectively.[144,150,158,432,434−436] The direct evidence for the macromolecular helicity inversion of a helical **88** triggered by solvent polarity has been directly observed by high-resolution AFM measurements of the diastereomeric helical structures deposited on graphite (see Figure 75 in section 3.2.2.1).[434]

The macromolecular helicity inversion can also be regulated by the change in the ordered structure of the peptides that occur at the remote side chain (Figure 54).[438] The optically active PPAs bearing poly(γ-benzyl-L-glutamate) as a polypeptide side chain (**283**) form an excess of a one-handed helical conformation, in which the helical polypeptide pendants are arranged in a helical array with a preferred handedness along the helical PPA backbone. The Cotton effect of **283** in the PPA backbone region is inverted when the α-helix content of the pendant poly(γ-benzyl-L-glutamate) chains changes in response to the change in the solvent composition. Thus, **283** undergoes a helix-sense inversion of the polymer backbone stimulated by the solvent-driven conformational change of the peptide side chains remote from the main-chain.

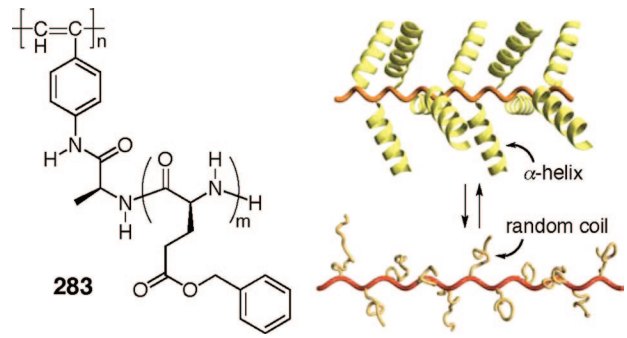

Figure 54. Schematic illustration of interconvertible right- and left-handed helices of **283** stimulated by the helix−coil transition of the pendant peptide chains. (Reproduced with permission from ref 438. Copyright 2004 Wiley-VCH.)

Chart 26

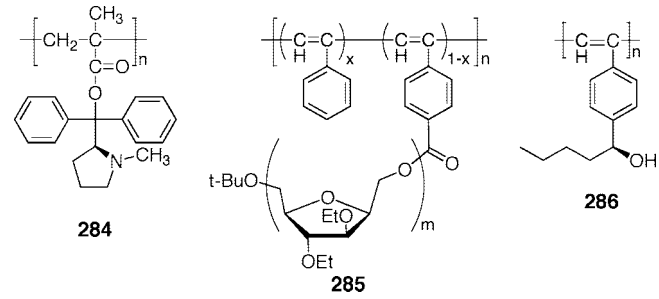

An optically active isotactic polymethacrylate (**284**, Chart 26) with an excess of a single-handed helical conformation prepared by the anionic polymerization of the corresponding chiral monomer derived from L-proline also exhibits a helix−helix transition by changing the acidity of the solution.[439] The polymer showed a positive optical rotation ($[\alpha]_{365}^{25}$ +780°) once dissolved in methanol containing 0.01 vol % trifluoromethanesulfonic acid, which slowly changed to a negative value ($[\alpha]_{365}^{25}$ −410°) with time. Interestingly, the further addition of the acid (13%) induced the returning of the optical activity to the initial value ($[\alpha]_{365}^{25}$ +779°). The protonation of the amino groups of **284** with a small amount of the acid has probably been considered to induce

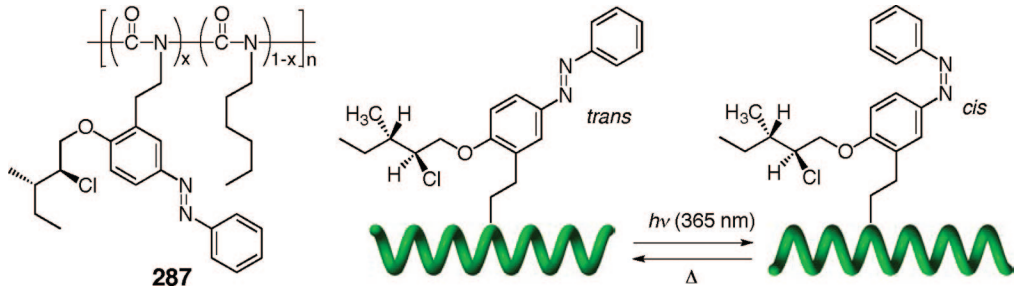

Figure 55. Schematic illustration of helix inversion of **287** by a photochemical *trans*−*cis* isomerization of the azobenzene moieties in the side chains.

the first stereomutation due to the repulsion of the charges at the pendant groups, while the further addition of the acid may weaken the repulsion of the charges by solvation or by decreasing the degree of dissociation of the ion pair on the pendants, which likely forces the helical conformation to return to the original one.

A helical PPA bearing a polycarbohydrate ionophore as a graft chain prepared by the copolymerization of an end-functionalized (1−6)-2,5-anhydro-3,4-di-*O*-ethyl-D-glucitol having a 4-ethynylbenzoyl group with phenylacetylene (**285**) undergoes a helix inversion through the host−guest complexation between the grafted ionophore units and the selected metal cations whose cationic radii were greater than 1.16 Å, such as Ba^{2+}, Pb^{2+}, and Sr^{2+}.[440,441]

Tsuchihara et al. have found an interesting reversible and repeatable inversion of the helicity of an optically active PPA having a simple chiral alcohol pendant (**286**) in the film state, as revealed by inversion of the Cotton effect signs, when exposed to appropriate polar or nonpolar organic solvent vapors only for several minutes.[442] The polymer adopts an either right- or left-handed helical conformation with an excess one-handedness in organic solvents, such as chloroform and Et_2NH, because the solutions exhibited intense split-type Cotton effects in the polymer backbone regions at 20 °C, which are mirror images to each other, indicating the opposite helical sense in each solvent. The helical conformation and its handedness of **286** in solution appear to be similar to those in the film made by spin-casting from the same solution because of their basically identical CD spectral patterns. When a film prepared from a Et_2NH solution of **286** was exposed to chloroform vapors, the Cotton effect signs inverted within 30 s of contact. Further exposure of the film to polar solvent vapors, such as methanol, Et_3N, or Et_2NH, for 1 min, brought about a full inversion of the Cotton effects again, thus recovering to the original CD. This switching of the helicity process can be repeated using an appropriate set of solvent vapors in an alternate manner. Thermodriven, irreversible inversion of the helix-sense of **286** in the film prepared from polar solvents has also been achieved by heating at 110 °C for 5 min.[442]

2.8.1.1. Photoinduced Helix Inversion. Photoresponsive conformational changes in the polypeptides are a very active research area endowed with a large number of reports. However, photoresponsive polypeptides exhibiting a helix−helix transition upon photoirradiation, most of which are composed of L-aspartates as the amino acid component, remain rare.[443,444] Comprehensive reviews of photoresponsive polypeptides including an inversion of the helicity with a historical background are available elsewhere.[445] This section discusses and deals with the photoinduced inversion of synthetic helical polymers.

A remarkable helix inversion in the helical conformation of synthetic polymers upon photoirradiation has been achieved for the azobenzene-modified polyisocyanates. Zentel et al. have synthesized a series of photoresponsive, optically active polyisocyanates to investigate the effect of photoirradiation on the helical conformation of the polyisocyanates (Figure 55).[446] They discovered that the helix-sense of an optically active polyisocyanate copolymer of a chiral isocyanate bearing a photosensitive azobenzene side group containing two stereogenic centers with an achiral isocyanate (**287**) can be switched by the photoisomerization of the azobenzene moiety from the *trans* to *cis* state.[447] Photoirradiation results in the complete inversion of the CD spectral pattern.

As described in section 2.5.2, alternating irradiation with *d*- or *l*-CPL combined with irradiation by unpolarized light to extremely chirality-sensitive polyisocyanate terpolymers (**178**, **179**, Figure 26) also gave rise to the inversion of helicity in a controllable manner.[302]

Feringa et al. have demonstrated an effective and remarkable helical sense induction and switch by a single chiral photochromic unit covalently attached at the α-chain-end of a dynamically racemic helical poly(*n*-hexyl isocyanate) (**288**), which allows the fully reversible control over the preferred helical sense of the polymer backbone through the powerful *domino effect* (Figure 56).[448] In this system, both light and heat were used as control elements to achieve the helical sense bias and switch toward the polymer. The light-driven molecular motor unit developed by Feringa et al.[449] acts as a chiral trigger to undergo unidirectional rotation in a four-step cycle by a combination of two photochemically induced *cis*−*trans* isomerizations, each followed by an irreversible thermal isomerization. Irradiation of a sample of (*M*)-*trans*-**288** in ether at −20 °C (365 nm) provided (*P*)-*cis*-**288** (step 1), which showed CD signals typical of poly(*n*-hexyl isocyanate) with an excess left-handed helical structure. When (*P*)-*cis*-**288** was kept in the dark for 30 min at 20 °C, it thermally converted into (*M*)-*cis*-**288** (step 2), resulting in a change of the Cotton effect signs due to the polymer backbone, thereby indicating inversion of the helicity from a predominant left-handed to the opposite right-handed helical sense. Further photochemical *cis*-to-*trans* isomerization (step 3) by irradiation (365 nm) and subsequent thermal isomerization at 20 °C (step 4) gave rise to the original (*M*)-*trans*-**288** with a random helical sense. As a consequence, a fully reversible induction and inversion of the preferred helical sense of the dynamically racemic helical polymer has been realized.

An analogous α-chain-end functionalized poly(*n*-hexyl isocyanate) (**289**) bearing a structurally similar but photochemically bistable molecular motor unit has also been developed.[450] In this system, the preferred helical sense of

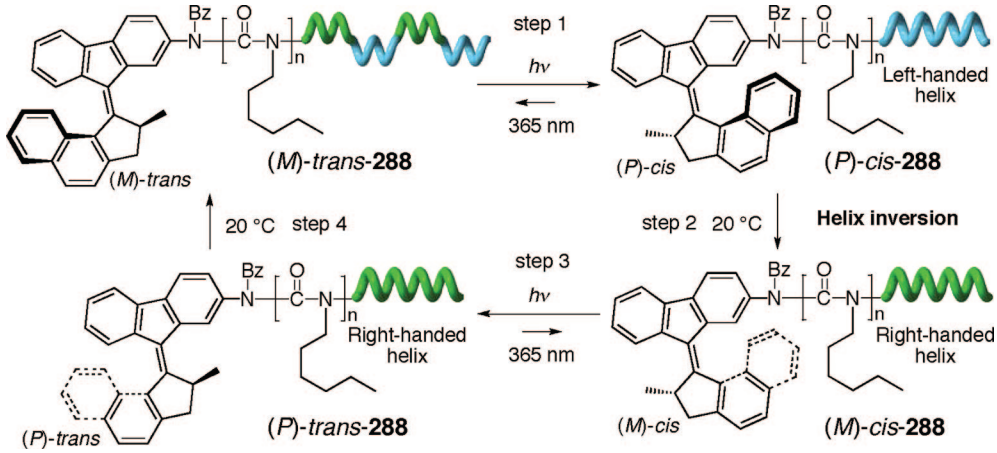

Figure 56. Schematic illustration of the reversible induction and inversion of the helicity of **288** by a single light-driven molecular motor attached at the chain-end. A thermal isomerization of the rotor unit inverts the preferred-handed helicity of the polymer chain. Subsequent photochemical and thermal isomerizations produce the original situation with a random helicity of the polymer backbone of **288**.

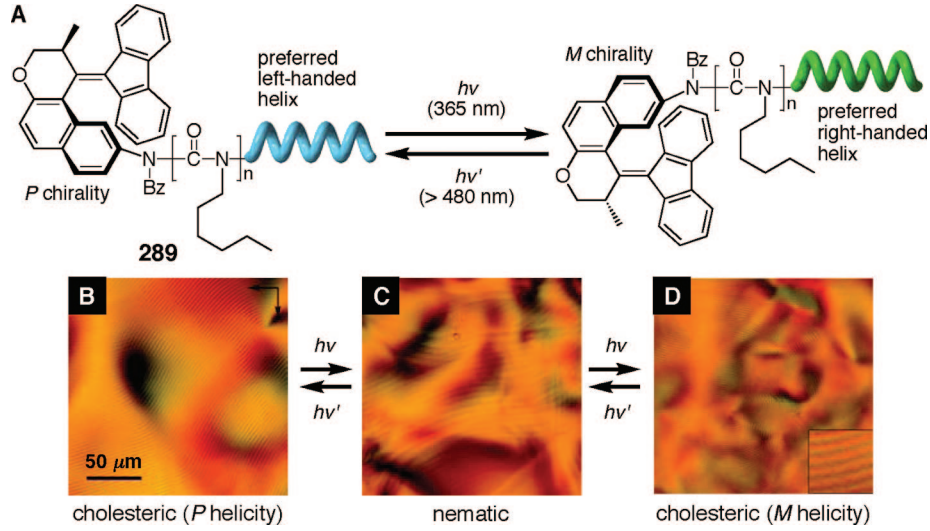

Figure 57. (A) Schematic illustration of the reversible inversion of the preferred helical twist sense of a polymer backbone of the chain-end molecular motor functionalized poly(*n*-hexyl isocyanate) (**289**) induced by a chiroptical molecular switch at its terminus. (B) Optical micrographs of a 30 wt % solution of **289** in toluene showing a cholesteric LC phase before irradiation (B) and after 150 min UV (365 nm) irradiation followed by leaving it in the dark overnight (D), and a nematic LC phase after 45 min UV (365 nm) irradiation (C). (Reproduced with permission from ref 450. Copyright 2008 American Chemical Society.)

the polyisocyanate can be fully controlled by a single photochemically bistable chiroptical molecular switch covalently attached to the polymer's terminus, of which the two thermally stable states can be readily controlled by light using two different wavelengths (Figure 57A). The hierarchical transmission of chiral information from the molecular level of the chiroptical switch, via the macromolecular level of the helical polymer to the macroscopic supramolecular level of a cholesteric LC phase formed by these helically switchable polymers, allows for the full control of the magnitude and sign of the supramolecular helical pitch of the LC phase using two different wavelengths of light (Figures 57B−D).

2.8.1.2. Chirality-Induced Helix Inversion. In contrast to various helical polymers that undergo inversion of the helicity regulated by achiral stimuli, the macromolecular helicity inversion by chiral stimuli still remains rare, but a current challenging issue. The first example of such a helix inversion induced by external chiral stimuli through diastereomeric, noncovalent acid−base interactions has been reported for a PPA bearing an optically active (1*R*,2*S*)-norephedrin residue (**290**, Chart 27).[451] The addition of an

Chart 27

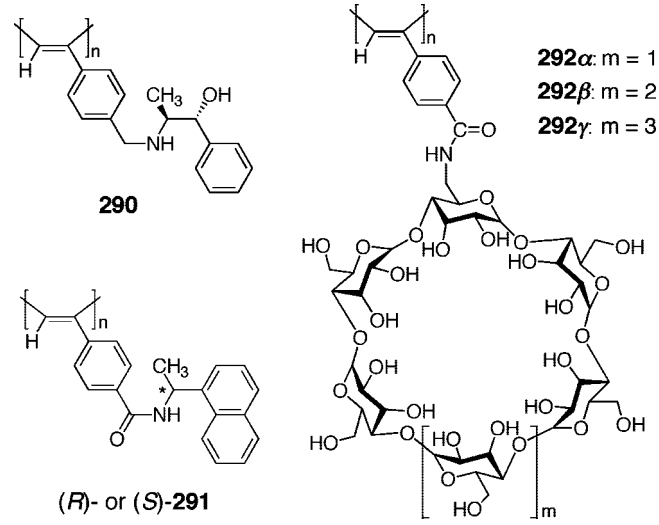

excess (*R*)-mandelic acid ((*R*)-MA) induced inversion of the Cotton effect signs of **290**, while the ICD of **290** hardly

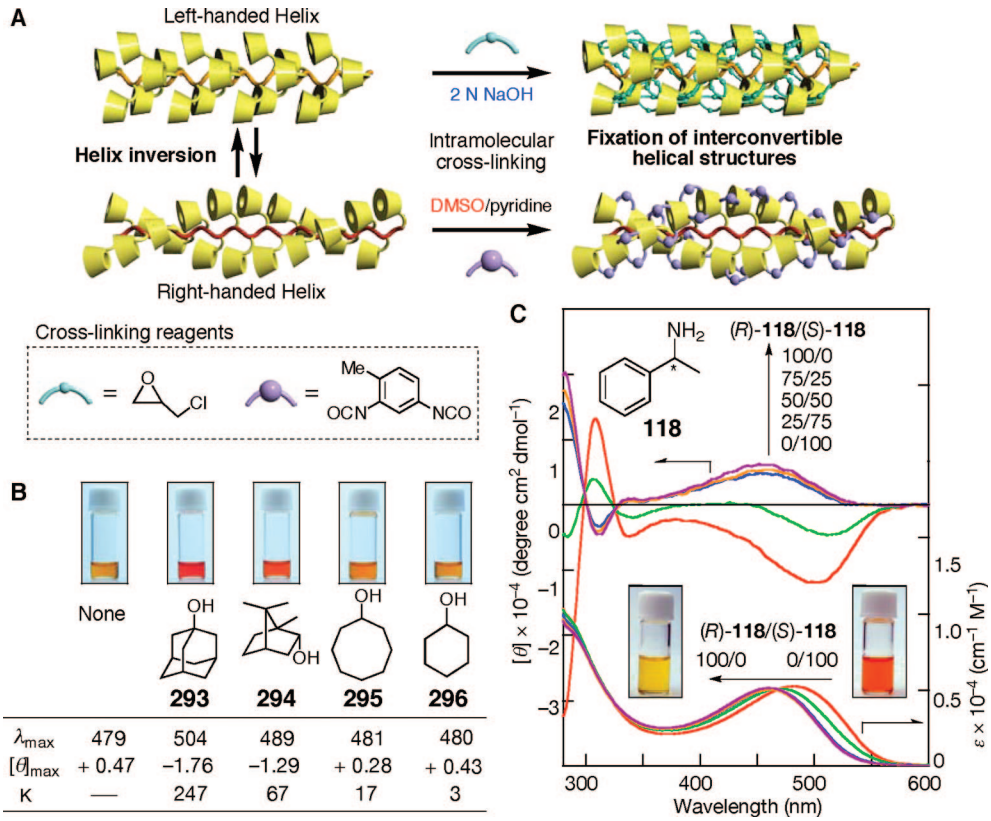

Figure 58. (A) Schematic illustrations of helix inversion of **292*β*** and subsequent intramolecular cross-linking of the *β*-CyD pendants which suppresses the inversion of the helicity of **292*β***. (B) Visible color changes in **292*β*** in DMSO/water (8/2, v/v) by the addition of **293**−**296**. (C) CD and absorption spectral changes of **292*β*** in alkaline water (pH 11.7)/DMSO (7/3, v/v) in the presence of 0−100% ee of **118** at 25 °C. (Reproduced with permission from ref 454. Copyright 2006 American Chemical Society.)

changed with an excess (*S*)-MA. These results suggest that **290** undergoes a helix inversion in response to the chirality of (*R*)-MA, and therefore, this change in the CD spectra of **290** can be used for sensing the chirality of specific chiral guests. Macromolecular helicity inversion by external chiral stimuli has also been observed for (*R*)- or (*S*)-**291** bearing an optically active (1-(1-naphthyl)ethyl)carbamoyl group by interacting with optically active small molecules, such as (*R*)- and (*S*)-**152**.[452] The ICD of (*R*)- or (*S*)-**291** in DMF changed to an almost mirror image in the presence of an excess of (*R*)- or (*S*)-**152**, respectively.

Introducing optically active cyclic host molecules, such as α-, *β*-, and *γ*-cyclodextrin (CyD) residues to a dynamic helical PPA backbone as the side groups (**292**, Chart 27) provides a unique and conceptually new colorimetric detection system for neutral chemical species including enantiomers as well as solvent and temperature based on the inversion of the macromolecular helicity (Figure 58A). The helical sense inversion is accompanied by a visible color change due to a structural change in the twist angle of the conjugated double bonds (tunable helical pitch) that is readily visible with the naked eye and can be quantified by absorption and CD spectroscopies. For instance, **292*β*** bearing *β*-CyD residues exhibits a helical sense inversion stimulated by an inclusion of guest molecules inside the chiral *β*-CyD cavity.[453] When 1-adamantanol (**293**) or (−)-borneol (**294**) was added to the **292*β*** solution, the solution showed an immediate color change from yellow-orange to red due to a large red-shift of λ_{max}, which is accompanied by the inversion of the Cotton effect signs (Figure 58B). On the other hand, cyclooctanol (**295**) and cyclohexanol (**296**) produced no such dramatic color change in solution nor a Cotton effect inversion. **292*γ*** also exhibited a similar CD inversion as well as a color change by responding to the specific guest molecules capable of interacting with *γ*-CyD. Moreover, the addition of racemic **118** and (*R*)-rich **118** of 50% ee induced a negligible conformational change in **292*β***, resulting in almost no change in their absorption and CD spectra. However, **292*β*** is sensitive to the chirality of (*S*)-**118**, and **118** of 50% ee ((*S*)-rich) as well as the 100% ee of (*S*)-**118** produced a dramatic color change along with significant CD and absorption spectral changes (Figure 58C).[454] **292*β*** has a dynamic helical conformation and shows opposite Cotton effect signs in different solvents, such as DMSO and alkaline water, probably due to inversion of the macromolecular helicity in these solvents. To obtain direct evidence for inversion of the helicity, **292*β***, showing opposite Cotton effect signs, was further fixed by intramolecular cross-linking between the hydroxy groups of the neighboring *β*-CyD units in each solvent (Figure 58A). The cross-link between the pendant CyD units likely suppresses the inversion of the helicity, and therefore, the cross-linked **292*β***s showed no further Cotton effect inversion, which reveals that switchable dynamic helical conformations can be fixed in each handedness as a result of the intramolecular cross-linking.[454]

The covalent and noncovalent chiral domino effects have also been applied to the chirality sensing of chiral acids by helix inversion of optically active peptides bearing the *N*-terminal amino group and *C*-terminal chiral residue upon noncovalent interactions with chiral carboxylic acids, such as Boc-L-amino acids (Boc = *tert*-butoxycarbonyl) (Figure 59).[455] The peptide **297** consists of an achiral Aib and Δ^ZPhe sequence with *C*-terminal L-leucine and the *N*-terminal amino group that favorably adopts a left-handed screw-sense in

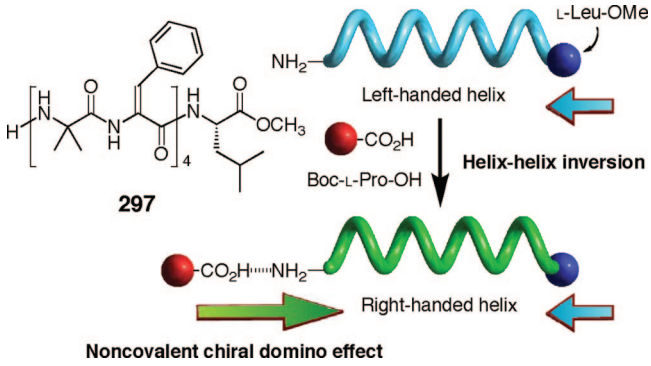

Figure 59. Schematic illustration of helix inversion of a peptide possessing a chiral residue at the C-terminus of **297** by the noncovalent chiral domino effect with a chiral carboxylic acid.

chloroform induced by the chiral *C*-terminal covalent domino effect, whereas, upon the addition of Boc-D-Pro-OH (Pro = proline), the split Cotton effect sign remained, but its intensity reflecting a helical sense excess of the left-handedness remarkably increased. On the contrary, the addition of its enantiomeric counterpart, Boc-L-Pro-OH, gave rise to a helix inversion from the left- to right-handed screw-sense generated by the noncovalent domino effect, as revealed by inversion of the Cotton effect signs.

2.8.2. Supramolecular Helix Inversion

Helix inversion phenomena have also been observed for foldamers. Meijer et al. have reported a solvent-driven helicity inversion of a chiral water-soluble poly(ureidophthalimide) decorated with hydrophilic side chains (**128**; see Figure 15 in section 2.3) in THF/water mixtures.[220] Inouye et al. have found that helix inversion occurs in the poly(*m*-ethynylpyridine) foldamer **192** (see Figure 28 in section 2.5.3) as a result of anomerization of D-glucose between the α- and *β*-forms (Figure 60).[456] In other words, each anomer of D-glucose caused a helix-sense bias in **192** in the opposite sense. Just after crystalline α-D-glucose was added, an aqueous solution of **192** showed a rather strong ICD, of which the CD signs were inverted with time and the changes reached a steady state within 24 h. These results indicate that the α-anomer first induced an excess one-handed helix and then gradually converted to the *β*-anomer through a mutarotation process, which biased the opposite helical sense. This finding means that real-time information concerning the mutarotation of glucose is translated into ICD signals of the dynamic helical polymer through an inclusion-induced chirality transfer from the small molecules to the supramolecular architectures.

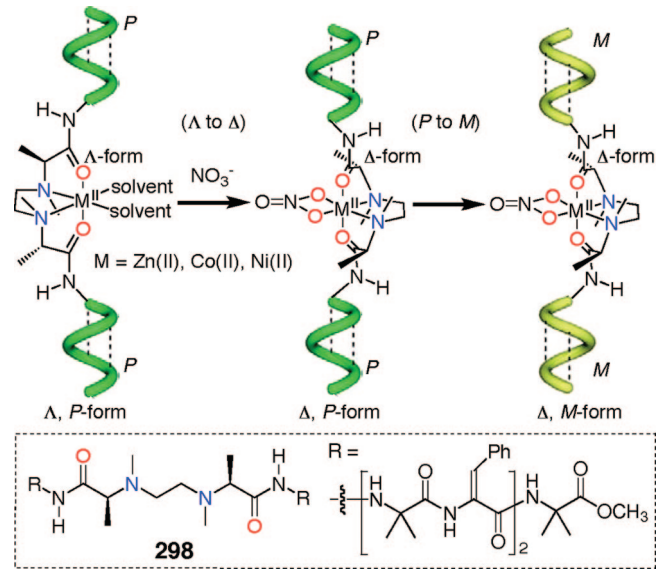

Figure 61. Schematic illustration of helicity inversion around a metal center and sequential chirality transfer to peptide helices. Green and yellow colored tubes indicate right-handed (*P* form) and left-handed (*M* form) 3/10 helical structures of the pentapeptide moiety of **298**, respectively. (Reproduced with permission from ref 457. Copyright 2008 American Chemical Society.)

Tsukube et al. have demonstrated that the metal complex composed of two achiral pentapeptide chains consisting of Aib and Δ^{Z}Phe residues linked by an optically active hexacoordinated metal center (**298**) shows a dynamic and efficient inversion of peptide helices induced by an achiral NO_3^- anion, of which the time scale can be fine-tuned by changing the substitution lability of the metal center (Figure 61).[457] A chirality-switchable Co(II) complex (**298**) undergoes a helix inversion upon addition of the NO_3^- anion.[458] When the NO_3^- anion was added to **298**, the metal complex center changed its left-handed Λ *cis*-α structure to a right-handed Δ *cis*-α one, which inverts the helical sense of the peptide side chains. In addition to the Co(II) complex, the Zn(II) and Ni(II) complexes of **298** showed a similar inversion of their peptide helices upon addition of the NO_3^- anion but provided different time scales for the helix inversion from milliseconds to hours.[457]

A novel family of responsive foldamers, so-called clickamers (see also section 2.3.1), have been synthesized to display a helix inversion in response to achiral halide ions.[459] A clickamer **299** (Chart 28) adopts a helical conformation with a helical sense bias as a result of chirality transfer from the chiral side chains to the polymer backbone in water/

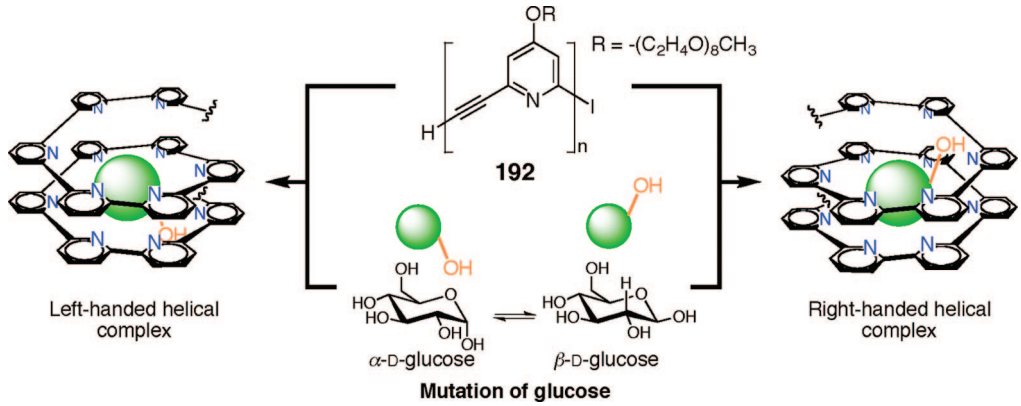

Figure 60. Schematic illustration of helix inversion of the complex formed between **192** and D-glucose induced by mutation of D-glucose.

Chart 28

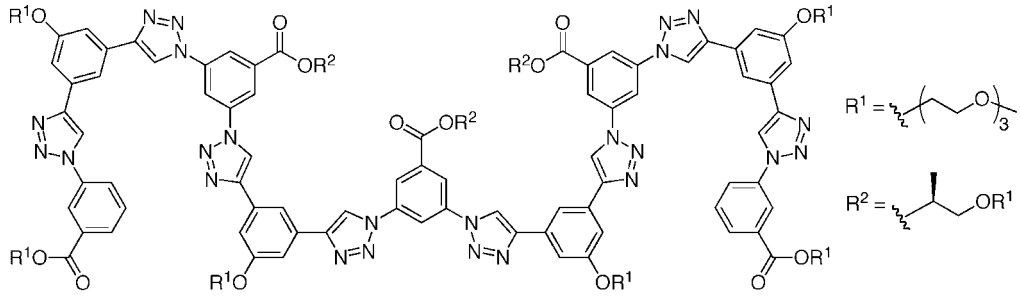

299

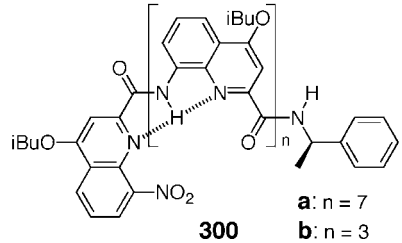

300 **a**: n = 7 **b**: n = 3

acetonitrile mixtures. However, the addition of fluoride ions leads to a slight increase in the CD intensity, the presence of chloride ions caused an inverted signature of small CD intensity, and finally, the addition of bromide ions resulted in an inverted CD spectrum of higher intensity. These results indicate an inversion of the helical twist of **299** stimulated by the addition of achiral halide ions.

Huc et al. have found an equilibrium between the solution and solid states that provides an original means to control helical handedness in aromatic oligoamides of 8-amino-2-quinolinecarboxylic acid bearing a chiral end group at the *C*-terminus (**300a**).[460] An excess one-handed helicity induced in **300a** was demonstrated by CD spectroscopy, and **300a** exhibited an intense CD in the absorption region of the quinoline rings between 250 and 450 nm in solution. The diastereomeric excess of the left- and right-handed helical **300a** in $CDCl_3$ was evaluated by ^1H NMR to be about 82%. The same tendency was observed in other solvents, such as DMSO-d_6 and toluene-d_8, showing that neither the helix stability nor chiral induction itself is affected by the polarity of the environment. However, the chiral induction observed in solutions of **300a** was reversibly switched off upon crystallization from toluene and was enhanced up to 100% upon crystallization from benzene. The crystals obtained from toluene were an equal mixture of the left- and right-handed **300a**, while those from benzene exclusively contained one diastereomer.

3. Structures of Helical Polymers

Although numerous synthetic helical polymers have been prepared in the past three decades, their exact helical structures including helical pitch and handedness (right- or left-handed helix) remain unsolved. The detailed structural determinations of helical polymers are essential to significantly understand the mechanism of helix formation and the relationships between their helical structures and functions, and also to develop new helical polymers with sophisticated functions. Figure 62 shows the general methods for the structural analyses of helical polymers.

Evidence for a helix formation with a preferable helical sense of synthetic helical polymers is usually obtained by CD or optical rotation. VCD is now recognized as a facile method to investigate the chiroptical properties of certain small molecules and biological polymers.[461,462] NMR, absorption, and IR can also provide structural information including the conformation, configuration, and/or molecular ordering of helical polymers, particularly in solution. XRD, neutron diffraction, and electron diffraction methods are also useful to obtain information about ordered polymer structures, particularly in the solid state. Among them, XRD is the most convenient and widely used technique for elucidating the structures of helical polymers, as demonstrated for polypeptides[463] and DNA.[2] In fact, based on the XRD measurements of oriented films or fibers derived from a few

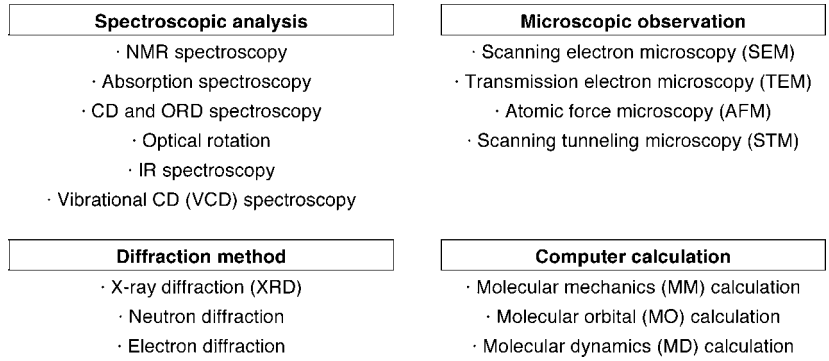

Figure 62. General methods for structural analyses of helical polymers.

Chart 29. Synthetic Helical Polymers Whose Helical Structures Were Determined by XRD Measurements of Their Oriented Films

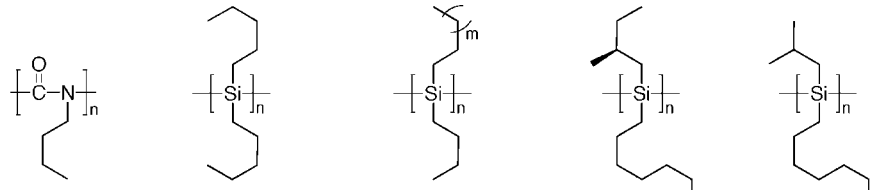

301 8/3 helix (1969) | **302** 7/3 helix (1987) | **303a**: m = 1, **303b**: m = 2, **303c**: m = 3 7/3 helix (1989, 1993) | **69** 7/3 helix (2001) | **76** 7/3 helix (2008)

synthetic helical polymers, their helical structures have been elucidated. However, due to the limited number of diffractions and difficulty in obtaining crystalline samples from synthetic helical polymers, the XRD method may not provide unambiguous helical structural information.

Microscopic observations of the helical structures of helical polymers using scanning electron microscopy (SEM) and TEM are potentially attractive but still remain very difficult due to poor resolution, except for self-assembled supramolecular helical aggregates generated from small molecules and oligomers.[19,36−43] The direct observation of helical structures by scanning probe microscopy (SPM), such as scanning tunneling microscopy (STM) and AFM, is one of the most promising methods to determine the helical structures and has been extensively studied.[464,465]

The recent striking progress in computer performance has made it possible to predict the structures and dynamic behaviors of helical polymers by means of MM, molecular orbital (MO), and MD calculations. However, these computer methods are not straightforward and may not provide unambiguous helical structural information. In this section, we describe a brief overview of the helical structures of synthetic helical polymers determined by various methods.

As mentioned above, the helical structures of biomacromolecules, such as polypeptides (18/5 helix)[463] and DNA (10/1 helix),[2] were determined using the fiber XRD technique. In the same way, the helical structures of poly(*n*-butyl isocyanate) (**301**)[466] and poly(di-*n*-pentylsilane) (**302**)[467] have been determined to be an 8/3 helix and 7/3 helix, respectively, by XRD measurements of their oriented films (Chart 29). The 7/3 helical structure of polysilanes has been further supported by XRD measurements of analogous helical poly(*n*-alkylsilane)s (**303**),[468−470] poly(*n*-decyl-(*S*)-2-methylbutylsilane) (**69**),[471,472] and poly(*n*-decyl-2-methylpropylsilane) (**76**).[473]

3.1. Helical Structure Determination

3.1.1. Single-Crystal X-ray Analysis of Uniform Oligomers

The structural elucidation of helical polymers by XRD on a molecular level is, in general, a laborious task, particularly for helical polymers bearing a complex repeating unit and those being insoluble in common solvents after polymerization. However, when the corresponding uniform oligomers are isolated and crystallized for the single-crystal X-ray analysis, convincing evidence of their helical structures can be obtained (Figure 63).

Isotactic polychloral (**3**) prepared by the helix-sense-selective polymerization of chloral with optically active initiators was believed to possess a 4/1 helical conformation and showed a high optical activity in films ($[\alpha]_D$ +4000°).[25,474] Because the polymer is totally insoluble in solvents, further structural investigations in solutions were hampered. Ute et al. have prepared and isolated isotactic enantiomerically pure uniform oligomers bearing different end groups (**304**) by SEC from the oligomerization products and subsequent optical resolution into enantiomers by chiral HPLC. They found that the (−)-pentamer with the (*R*,*R*,*R*,*R*,*R*) main-chain configuration adopts a right-handed 4/1 helical conformation by an X-ray crystallographic analysis.[27] Analogous isotactic and enantiomerically pure uniform oligomers bearing the identical end groups (**305**) have also been isolated, and their activation energies for the helix-sense inversion ($\Delta G^{\neq}$) for **305a−d** were estimated to be 34.3−82.0 (kJ mol^{-1}) on the basis of the dynamic NMR technique (Table 1).[26,27] The helical structure of the dodecamer of *n*-butyl isocyanate (**306**) has also been determined to be approximately an 8/3 helix.[475] This helical structure resembles the corresponding helical structure of a polyisocyanate **301** determined by the fiber XRD method.[466]

Poly(2,3-quinoxaline)s are considered to possess a one-handed helical conformation, as supported by their intense Cotton effects.[102] The helical structure and handedness have been determined by the X-ray crystallographic analysis of an optically and catalytic active pentamer of a diastereomerically pure oligo(2,3-quinoxaline) (**307**) to be a right-handed 5/2 helix in the solid state.[476] A helical structure of an analogous uniform oligomer, a hexamer of oligo(quinoline) (**55**), has also been determined to be a 5/2 helix.[105] Yokozawa et al. have prepared a series of uniform *N*-methyl substituted oligo(*p*-benzamide)s (**308**) by a step-growth oligomerization technique and determined their helical structure by a single X-ray crystallographic analysis to be a 3/1 helix;[224] this helical structure is consistent with that proposed for the corresponding optically active *N*-alkyl substituted poly(*p*-benzamide)s (**129a**, Chart 16) based on their observed and calculated CD spectra (see section 3.2.1).[224]

3.1.2. X-ray Diffraction of Liquid Crystalline Helical Polymers

As described in section 3.1, very few helical structures of synthetic helical polymers (**69**, **76**, **301**−**303**) have been elucidated by an XRD analysis. This may be due to the difficulty in obtaining oriented films suitable for the XRD measurements. As anticipated, when helical polymers are rigid rods that form a lyotropic or thermotropic LC phase based on their main-chain stiffness, uniaxially oriented films with a regular helical structure over a long distance can be prepared by physical shearing or under electric- and magnetic-fields, thus providing useful structural information available

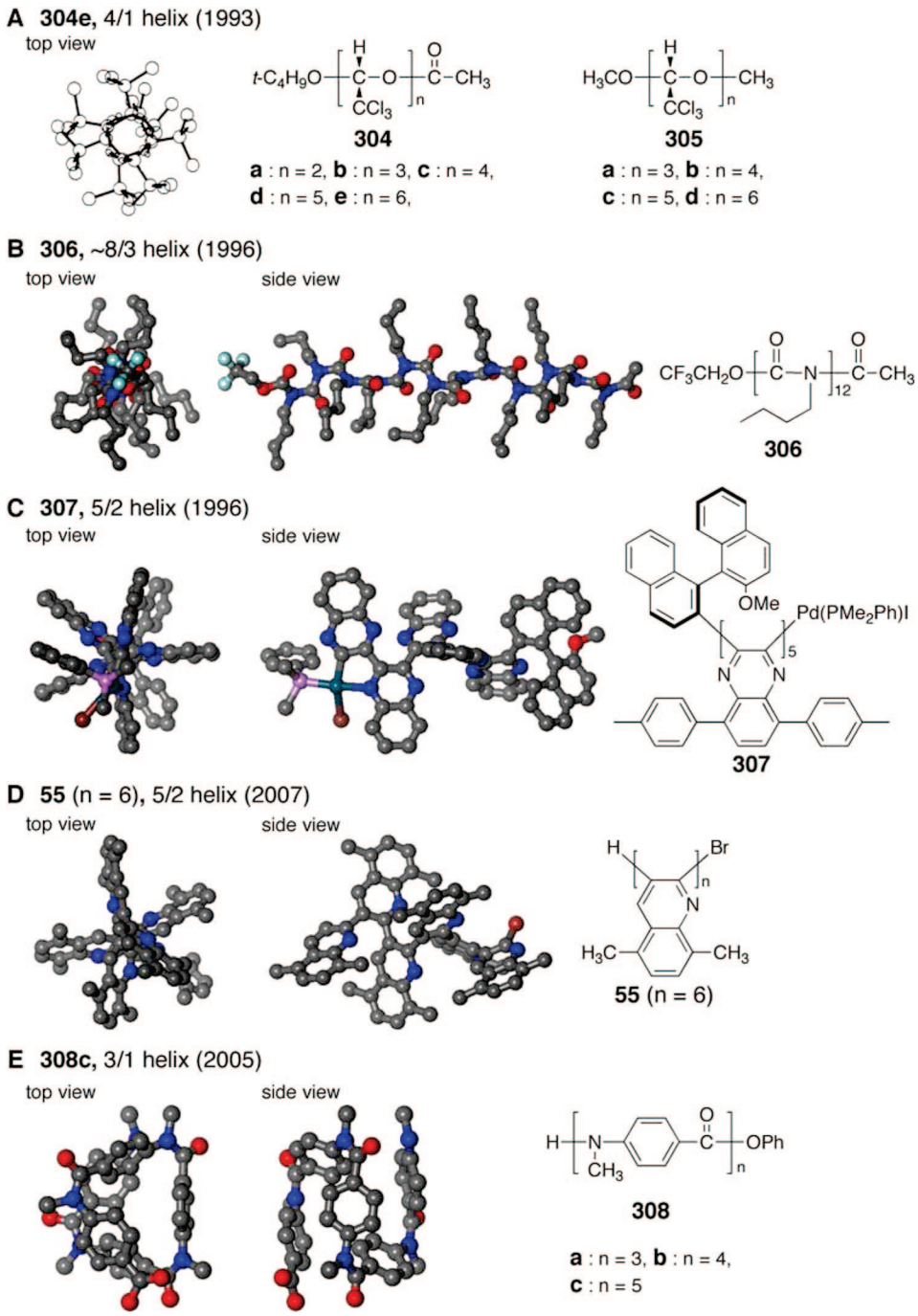

Figure 63. Synthetic uniform helical oligomers whose helical structures were determined by the single-crystal X-ray crystallographic analyses. Hydrogen atoms of all structures are omitted for clarity. (A) 4/1 helical structure of **304e**. (Reproduced with permission from ref 27. Copyright 1993 The Society of Polymer Science, Japan) (B) ~8/3 helical structure of **306**. (C) 5/2 helical structure of **307**. Tolyl groups are omitted for clarity. (D) 5/2 helical structure of **55** ($n = 6$). (E) 3/1 helical structure of **308c**. Terminal *O*-phenyl group is omitted for clarity. Crystallographic data (C−E) were obtained from Cambridge Crystallographic Data Centre.

to define the main-chain helical structures by XRD. In fact, the helical structures of **69**[471,472] and **76**[473] (Chart 29) have been determined by the XRD analysis of the oriented films prepared from their thermotropic LC states in the melt to be a 7/3 helix.

Since the pioneering research by Aharoni and Millich et al. in the late 1970s on the LC formations of polyisocyanates[477] and polyisocyanides,[66,478] various liquid crystalline helical polymers based on their main-chain stiffness, such as polyisocyanides (poly-**25**,[72,74,479] **27**,[76] poly-L-**32**,[85,89,480] **240**−**242**,[381] **245**,[382] **246**,[382] **309**,[481] **310**,[478,481] **311**,[66] **312**,[66] **313**,[482] **314**−**316**,[480] **317**[483]), polyguanidines (poly-**58**,[484] **318**,[485] **319**,[486] **320**[485]), poly(quinoxaline)s (poly-**51**, **321**),[487] poly(methacrylamide) (poly-**17**[488]), polysilanes (**69**,[471,472,489−491] **75**,[492] **76**,[473] **302**,[493] **303**,[468,494] **322**,[493] **323**,[468] **324**[470,495]), polyisocyanates (**62**,[427,450,477,496−498] **112**,[497] **301**,[496] **325**,[477,496] **326**,[477] **327**[499,500]), and polyacetylenes (**156**·HCl,[501,502] L-**88**,[151,434,503,504] **111**[193]), have been synthesized, as summarized in Figure 64.

Interestingly, these LC polymers belong to either static (poly-**17**, poly-**25**, **27**, poly-**32**, poly-**51**, poly-**58**, **240**−**242**, **245**, **246**, **309**−**321**) or dynamic (**62**, **69**, **75**, **76**, L-**88**, **111**, **112**, **156**·HCl, **301**−**303**, **322**−**327**) helical polymers. The LC formation of polymers requires main-chain stiffness in

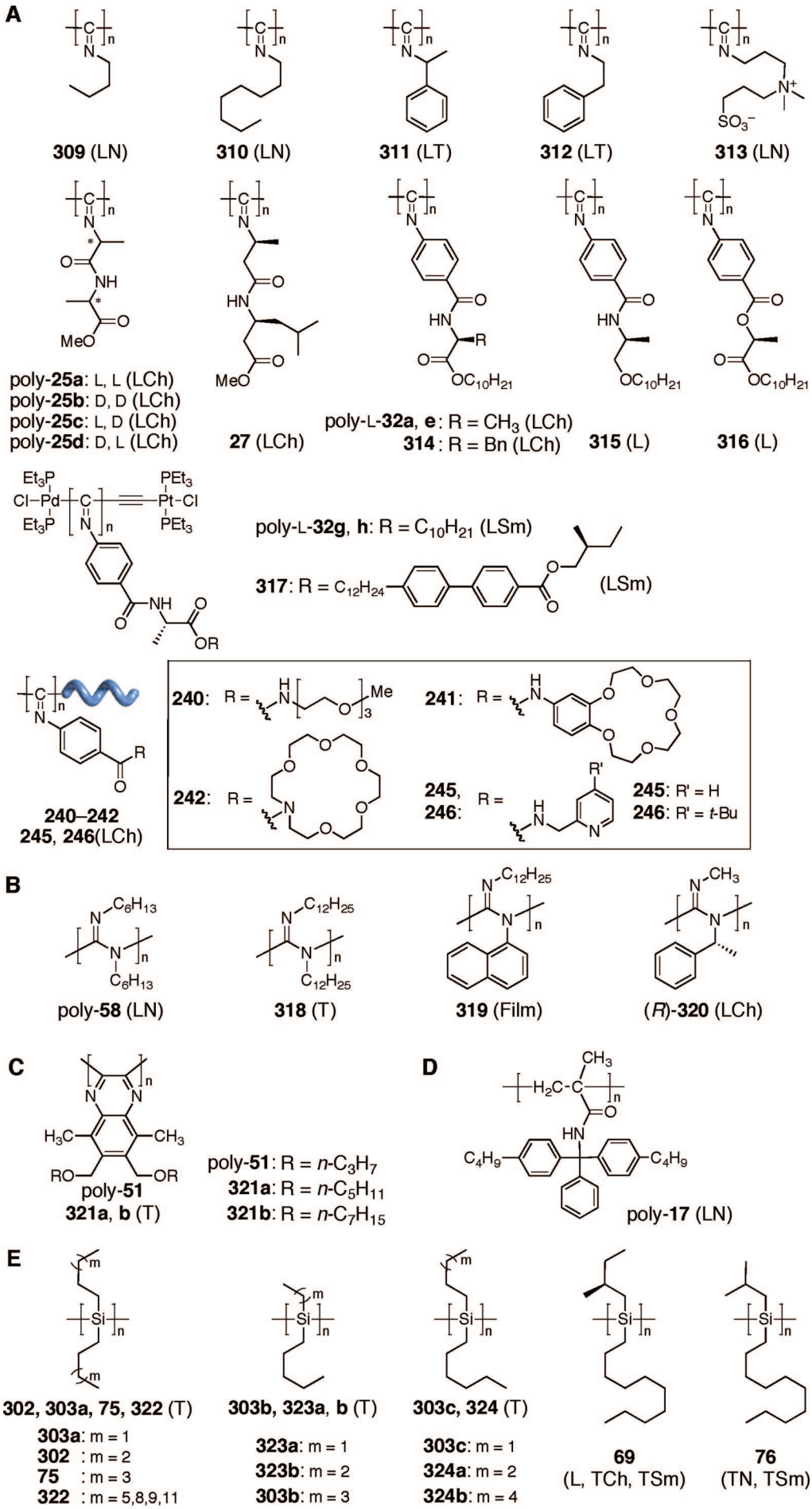
A
309 (LN)
310 (LN)
311 (LT)
312 (LT)
313 (LN)
poly-25a: L, L (LCh)
poly-25b: D, D (LCh)
poly-25c: L, D (LCh)
poly-25d: D, L (LCh)
27 (LCh)
poly-L-32a, e: R = CH3 (LCh)
314: R = Bn (LCh)
315 (L)
316 (L)
poly-L-32g, h: R = C10H21 (LSm)
317: R = C12H24 (LSm)
240–242
245, 246(LCh)
240:
241:
242:
245, 246:
245: R' = H
246: R' = t-Bu
B
poly-58 (LN)
318 (T)
319 (Film)
(R)-320 (LCh)
C
poly-51
321a, b (T)
poly-51: R = n-C3H7
321a: R = n-C5H11
321b: R = n-C7H15
D
poly-17 (LN)
E
302, 303a, 75, 322 (T)
303a: m = 1
302 : m = 2
75 : m = 3
322 : m = 5,8,9,11
303b, 323a, b (T)
323a: m = 1
323b: m = 2
303b: m = 3
303c, 324 (T)
303c: m = 1
324a: m = 2
324b: m = 4
69
(L, TCh, TSm)
76
(TN, TSm)

Figure 64.

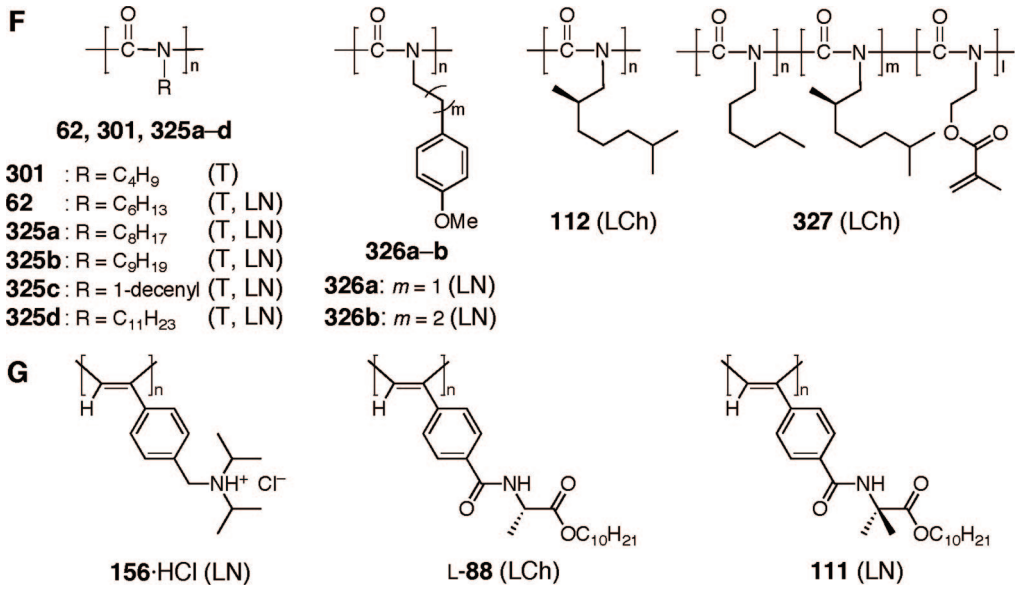

Figure 64. Structures of LC helical polymers due to the main-chain stiffness in concentrated solution or in a melt: (A) polyisocyanides, (B) polyguanidines, (C) poly(quinoxaline)s, (D) poly(methacrylamide), (E) polysilanes, (F) polyisocyanates, and (G) polyacetylenes. Reported LC phases are shown in the parentheses: T = thermotropic, L = lyotropic, N = nematic, Ch = cholesteric, and Sm = smectic.

order to self-assemble in a close parallel packing of the polymer chains in a concentrated solution or in a melt. The persistence length (q) is a useful measure to evaluate the stiffness of the LC polymers and can be estimated on the basis of the wormlike chain model[505,506] when the molecular-weight dependent changes in the radius of gyration, intrinsic viscosity, or sedimentation coefficient are available.[507] The q values can also be obtained by measuring the isotropic-LC phase boundary concentrations of particular LC polymers in solution in conjunction with the scaled particle theory.[508,509] The minimum q value required for lyotropic LC formation is considered between 1 and 6 nm.[507] It should be noted that a number of LC helical polymers have been prepared as shown in Figure 64, but only a limited number of q values have been determined for helical polymers. Table 3 summarizes the reported q values for already prepared synthetic helical polymers, and most of them show lyotropic and/or thermotropic LC phases.[160,191,193,196,198,480,482,502,503,510−523]

An optically active helical PPA bearing an L-alanine residue with a long *n*-decyl chain as the pendant (L-**88**) has an exceptionally long q value of *ca.* 130 nm in nonpolar solvents, such as CCl_4 and toluene. Interestingly, L-**88** showed a dramatic decrease in its q value to 19−43 nm in polar solvents, such as THF and chloroform. This significant change in the main-chain stiffness is accompanied by inversion of the helix-sense of the polymer main-chain, resulting from the "on and off" fashion of the intramolecular hydrogen bonding networks between the pendant amide residues in nonpolar and polar solvents, respectively (see section 2.2.3). Additional strong evidence for the change in the main-chain stiffness of the polymer depending on the solvent polarity has also been obtained from AFM measurements as well as the rheological property. Moreover, cholesteric LC phases of L-**88** with an opposite twist sense to each other are also produced due to inversion of the macromolecular helicity of the polymer chain using nonpolar and polar solvents (Figure 65).[503] The macromolecular helicity inversion process can be directly followed by AFM (see section 3.2.2.1). The cholesteric LC L-**88** in benzene self-assembles to form a highly uniaxially oriented film in an electric field due to the large electric dipole moment along the main-chain helical axis.[504] The POM, polarized IR spectroscopy, and XRD as well as the molecular modeling suggest that two sets of extended intramolecular hydrogen-bonded arrays of the pendant amide groups are helically arranged in a parallel fashion so as to generate the large dipole moment along the helical axis, as demonstrated in the α-helical polypeptides.[524]

A poly(phenyl isocyanide) (poly-L-**32e**) bearing the same L-alanine pendant groups such as L-**88** possesses an unprecedented long persistence length of 220 nm.[480] This value is, to the best of our knowledge, the highest among all the synthetic helical polymers and is comparable to those of biological, multistranded helical polymers, such as the triple-stranded helical collagen (160−180 nm)[525] and schizophyllan (150−200 nm),[526,527] and even stiffer than the double-stranded helical DNA (<60 nm)[528] and xanthan (120 nm).[529]

The optically inactive poly(*n*-hexyl isocyanate) (**62**) is one of the most extensively studied dynamic helical polymers and forms a lyotropic nematic LC phase, which further converts to the cholesteric counterpart by doping with small chiral molecules or optically active polyisocyanates in organic solvents.[497] Green et al. found the amplification of the helix-sense excess of **62** in the LC state doped with two different optically active polyisocyanates in their helical characteristics, one of which has a single-handed helix and the other, unequal interconverting right- and left-handed helical senses. A nonlinear relationship between their dilute solution optical activities and cholesteric LC properties in the latter system gives rise to a higher helical sense excess than the former system. The amplification is considered to occur by reduction in population of the mobile kinked helical reversals in **62**, and this phenomenon is called the "bad neighbors" rule.[498]

A similar amplification of the macromolecular helical sense excess in a lyotropic cholesteric LC state has also been observed in a dynamically racemic helical PPA derivative. A water-soluble **156**·HCl forms a lyotropic, nematic LC phase in concentrated water (>8 wt %), and the LC phase changed into a cholesteric one by the addition of a tiny amount of optically active acids such as (*S*)-**331**.[501] This LC formation is proved due to its main-chain stiffness in water,

Table 3. Persistence Length (q) Values of Synthetic Helical Polymers

polymer[a]		solvent	q (nm)	method[b]	temp	LC phase[c]	ref
polyisocyanides	poly-**25c**		76	AFM	*d*	LCh	510
	poly-L-**32e**	0.1 wt % TBAB/THF	220	SEC-LS	25 °C	LCh	480
	174-Me	$CHCl_3$	59	SEC-LS	25 °C	LN	531
	174a-Me	$CHCl_3$	43	SEC-LS	25 °C		531
	h-**174b-Me**	$CHCl_3$	88	SEC-LS	25 °C	LCh	531
	(*R*)-**311**	THF	3.2	LS	*d*	LT	511
	313	0.05 M $LiClO_4$ aq	5.7	Vis	25 °C	LN	482
	314	0.1 wt % TBAB/THF	103	SEC-LS	25 °C	LCh	480
	315	0.1 wt % TBAB/THF	81.8	SEC-LS	25 °C	L	480
	316	0.1 wt % TBAB/THF	30.8	SEC-LS	25 °C	L	480
	328	0.05 M LiCl/DMF	6.3	Vis	25 °C		482
polyguanidine	*rac*-**320**	THF	42	SEC-LS	25 °C	LN	512
polysilanes	**67**	isooctane	6.1	LS, Vis, Sed	25 °C		513
	68	isooctane	85	LS, Vis	20 °C		514
	69	isooctane	70	LS, Vis, SPT	25 °C	TCh, TSm, L	515
	70	isooctane	103	LS, Vis, Sed	25 °C		198
	75	THF	3−4	LS, Vis, SEC-LS	25 °C	T	516, 517
	329	THF	8−10	SEC-LS	*d*		516
polyisocyanates	**62**	toluene	37−38	Vis, SPT	25 °C	T, LN	518, 519
		CH_2Cl_2	19−21	Vis, SPT	20 °C	T, LN	518, 519
		hexane	42	LS, Vis, Sed	25 °C	T, LN	520
		1-chlorobutane	35	Vis	25 °C	T, LN	521
	112	hexane	56	LS, Vis	25 °C	LCh	522
		$CHCl_3$	34	LS, Vis	25 °C	LCh	522
	113	THF	3	Vis	25 °C		196
	301	$CHCl_3$	30	LS	*d*	T	523
	(*S*)-**330**	$CHCl_3$	60	LS	*d*		523
	rac-**330**	$CHCl_3$	25	LS	*d*		523
polyacetylenes	L-**88**	CCl_4	134.5	SEC-LS	25 °C	LCh	503
		toluene	126.3	SEC-LS	25 °C	*d*	503
		$CHCl_3$	42.9	SEC-LS	25 °C	LCh	503
		THF	19.2	SEC-LS	25 °C	*d*	503
	95c	$CHCl_3$	13.5	Vis	25 °C		160
	111	toluene	89.6	SEC-LS	25 °C	LN	193
	148	DMSO	4.2	Vis	25 °C		191
	148 + (*R*)-**152**	DMSO	8.6	Vis	25 °C		191
	156·HCl	H_2O	26	SPT	rt	LN	502

[a] See also Chart 30 for the structures. [b] Method for estimating the q values: LS = light scattering, Vis = viscosity, AFM = atomic force microscopy, SEC-LS = size exclusion chromatography equipped with a light scattering detector, SPT = scaled particle theory, Sed = sedimentation equilibrium. [c] Liquid crystalline (LC) phase: N = nematic, Ch = cholesteric, L = lyotropic, T = thermotropic, Sm = smectic. [d] Not available.

Chart 30

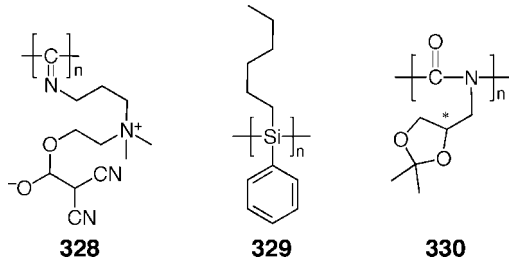

328 **329** **330**

as evidenced by its long persistence length before (26.2 nm) and after the one-handed helicity induction (28.0 nm) in the polymer. The preferred-handed helical conformation induced in **156**·HCl by (*S*)-**331** in dilute solution was further amplified in the LC state (Figure 66A), as revealed by direct comparison of the excess of the one helical sense of the polymer in dilute solution with that in the cholesteric LC state (Figure 66B). In the LC state, the population of the helical reversals between the interconverting right- and left-handed helical segments of the polymer may be reduced when compared to that in dilute solution, because the kinked helical polymer chain likely interferes with the close parallel packing of helical polymer chains in the LC state as observed in the LC system of **62** (Figure 66A). On the basis of the X-ray analysis of the LC samples, the most plausible helical structure of **156**·HCl is proposed to be a 23 unit/10 turn (23/10) helix (Figure 66C).[502]

As described in sections 2.5.2 and 2.7, the optically inactive **174-H** changes its structure into the prevailing, one-handed helical structure upon complexation with optically active amines in DMSO[297] and water,[380] and the macromolecular helicity induced in water can be "*memorized*" after complete removal of the chiral amines (***h*-174b-H**), while that induced in DMSO cannot be retained after removing the chiral amines (**174a-H**).[530] To investigate the helicity induction mechanisms of **174-H** in DMSO and water with chiral amines and to address the question why the helical structure induced in DMSO cannot be memorized after removal of the chiral amines, a series of isotopically labeled **174-H**'s and their methyl esters (**174-Me**'s) with deuterium, ^{13}C, and ^{15}N and nonlabeled polyisocyanides were prepared, and their structures before and after the helicity induction with chiral amines in water and DMSO and subsequent memory were studied in detail by absorption, CD, IR, VCD, and NMR spectroscopies together with XRD of the oriented films prepared from the nematic and cholesteric LC **174-Me**'s, persistence length measurements, and theoretical calculations.[531] The spectroscopic measurement results revealed that the specific configurational isomerization around the C=N double bonds (*syn*−*anti* isomerism) takes place during the helicity induction processes in each solvent. XRD of the uniaxially oriented films of the corresponding methyl esters (**174-Me**, **174a-Me**, and ***h*-174b-Me**) prepared from their LC polymer solutions suggests that the most plausible

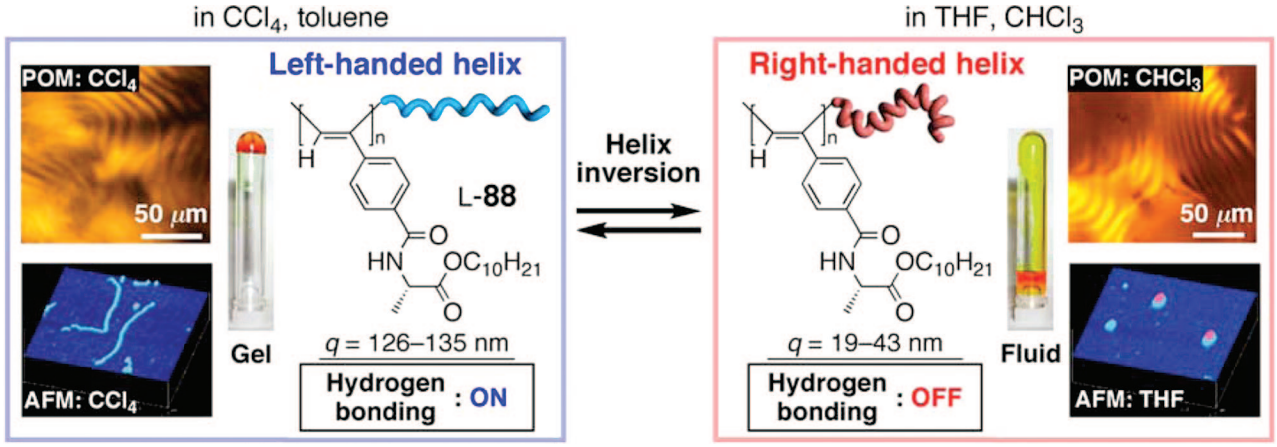

Figure 65. Schematic illustration of the helix inversion of L-**88** regulated by solvents with different polarities, leading to diastereomeric helical L-**88**'s with extremely different main-chain stiffness. POMs, AFM height images, and the visible differences of L-**88** in different solvents are also shown. The helical senses of the diastereomeric L-**88**'s were determined by direct observation of each helical structure on graphite using AFM (see section 3.2.2). (Reproduced with permission from ref 503. Copyright 2006 Wiley-VCH.)

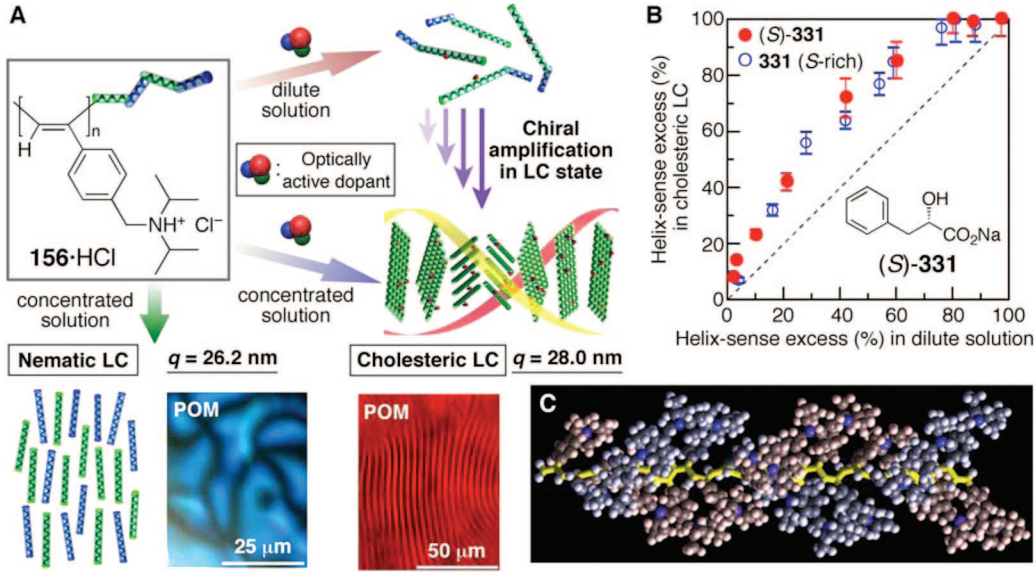

Figure 66. (A) Schematic illustration of hierarchical chiral amplification in the macromolecular helicity of **156**·HCl in dilute solution and the LC state and POMs of cholesteric and nematic LC phases of **156**·HCl. (B) Plots of the calculated % ee of helix-sense excess values of **156**·HCl with a chiral dopant ((*S*)-**331** (red) and **331** (*S*-rich) (blue)) in the cholesteric LC state versus those in dilute water solution. (C) A 23/10 helical structure of **156** postulated by XRD analysis. (Reproduced with permission from ref 502. Copyright 2006 American Chemical Society.)

helical structure of **174a-Me** is a 9/5 helix with two monomer units as a repeating unit, while that of ***h*-174b-Me** is a 10/3 helix consisting of one repeating monomer unit (Figure 67). The DFT calculations of poly(phenyl isocyanide) (PPI), a model polymer of the ***h*-174b-Me**, give a 7/2 helix as the most possible structure; this calculated helical structure can explain the XRD results. In addition, the persistence length (q) of ***h*-174b-Me** remarkably increases from 59 nm (**174-Me**) to 88 nm once an excess one-handed helicity is induced and memorized in ***h*-174b-Me**. In contrast, the q value of **174a-Me**, which lost its optically activity after helicity induction, dramatically decreases to 43 nm, resulting in a rather semirigid polymer.

The variable-temperature NMR and CD spectra unambiguously show that the polyisocyanides with different main-chain structures, **174-H**, **174a-H**, and ***h*-174b-H**, can interconvert to each other in solution. The ***h*-174b-H** and **174a-H** with and without memory of the macromolecular helicity, respectively, preferentially changed their helical structures to the original **174-H** upon heating in solution through configurational isomerization of the main-chain. Furthermore, the as-prepared **174-H** and ***h*-174b-H** also changed their structures into a structure analogous to that of **174a-H** after standing in solution for a very long time with no heat treatment. After subsequent complexation with chiral amines, a preferred-handed helix with a helicity memory can also be induced in **174a-H** in water (Figure 67).[531]

On the basis of these data together with the significant changes in the main-chain stiffness and the difference in the helical structures of **174a-Me** and ***h*-174b-Me**, the mechanism of helix induction in **174-H** with chiral amines in DMSO and water and the subsequent memory of the macromolecular helicity in water have been proposed as follows. The original optically inactive **174-H** folds into a rigid preferred-handed 10/3 helix upon complexation with chiral amines in water, accompanied by transformation of an imino configurational mixture of *syn* and *anti* **174-H** to one of a single configuration, and this selective configurational isomerization assisted by hydrophobic and chiral ionic interactions in water assists the helical conformation on the

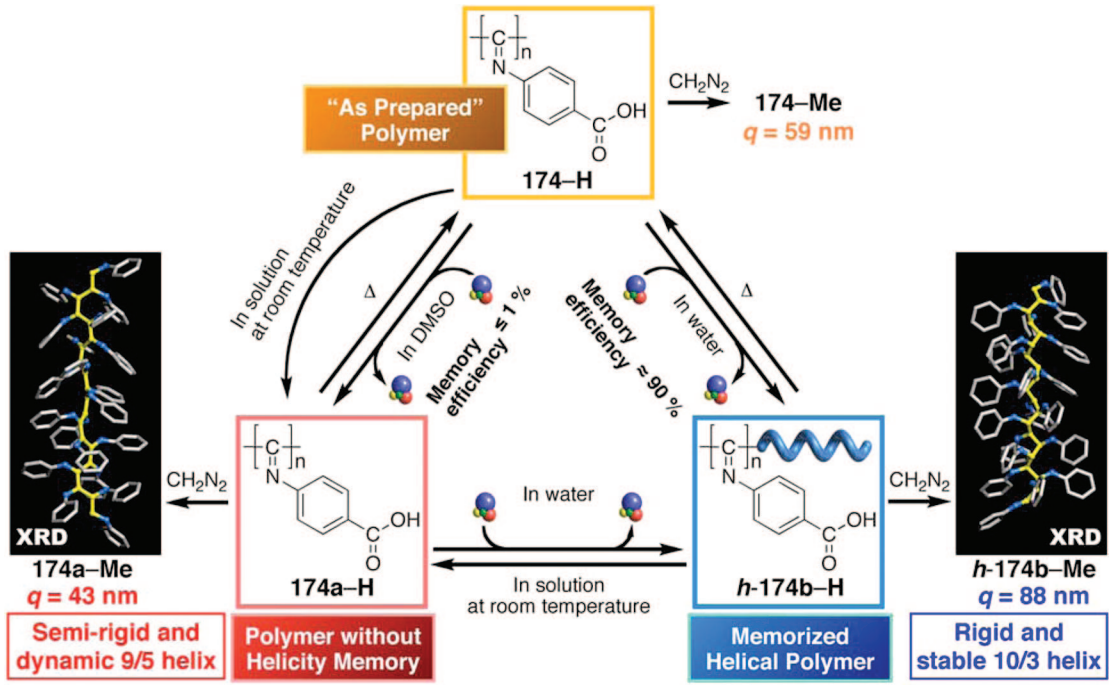

Figure 67. Schematic illustration of helicity induction in **174-H** in DMSO and water with chiral amines. The macromolecular helicity induced in water is memorized after complete removal of the chiral amines (***h*-174b-H**), whereas that induced in DMSO (**174a-H**) cannot be memorized. The persistence length (q) values of the corresponding methyl esters, **174-Me**, **174a-Me**, and ***h*-174b-Me**, and the helical structures of **174a-Me** and ***h*-174b-Me** postulated by XRD measurements are also shown. Hydrogen atoms and the methyl ester groups are omitted for clarity. Reproduced with permission from ref 531. Copyright 2009 American Chemical Society.

polymer backbone to possess an excess helical sense. Therefore, the induced helical conformation appears to be kinetically controlled and is maintained after removal of the chiral amines at ambient temperature. At high temperature, however, the helical conformation is not stable and unfolds to the analogous structure of **174-H** through the *syn*−*anti* configurational isomerization of the C═N double bonds.

The **174-H** also folds into a preferred-handed, semirigid 9/5 helix with an excess helical sense upon complexation with chiral amines in DMSO, arising from the similar *syn*−*anti* configurational isomerization. In sharp contrast to ***h*-174b-H**, the resulting 9/5 helical conformation is most likely dynamic and spontaneously racemizes once the chiral amines are removed, as observed for dynamically racemic helical polyacetylenes (section 2.5.1). Therefore, the induced helix in **174a-H** is controlled by thermodynamics in DMSO and may be the thermodynamically most stable structure because the original **174-H** and ***h*-174b-H** finally transform into the **174a-H** at the end after standing in solution for an extremely long time. As a consequence, optically inactive poly(4-carboxyphenyl isocyanide) can adopt either a static or dynamic helical conformation upon complexation with chiral amines in water or organic solvents, respectively, accompanied by selective configurational isomerization around the C═N double bonds, and these different helical conformations can interconvert to each other (Figure 67).[531]

Percec et al. have thoroughly investigated cooperative helical ordering within the columns in a series of *cis*-PPAs bearing bulky self-assembling dendron units (Chart 14 in section 2.2.3) based on structural and retrostructural analyses using the XRD data of oriented fibers.[180,182,183] Helical PPAs having the first generation (G1) dendrons or minidendrons (**108**) self-assemble into cylindrical macromolecules with an intracolumnar helical order in bulk. The cylindrical macromolecules reversibly interconvert between a 3D centered rectangular lattice with a long-range helical order at lower temperatures and a 2D hexagonal columnar lattice with short-range helical order at higher temperatures. The peripheral nonracemic alkyl tails in dendronized **108a** are able to impose a conformational change that stretches the polymer backbone, leading to an ∼10% increase in the average column stratum thickness (l) (Figure 68A), as revealed by the XRD pattern of an oriented fiber of **108a** as compared to those of **108b** and **108c** with achiral side chains, through which a preference for a single-handed helical sense of **108a** is efficiently communicated in bulk. A molecular modeling study reveals that a small change in the dihedral angle (θ) (Figure 68B) (*ca.* 3−5°) can account for the observed ∼10% increase in the l for **108a**.[179]

The dendronized helical *cis*-**100**s also self-organize into hexagonal columnar lattices with intracolumnar order (Φ_h^{io}) at lower temperatures, which change into hexagonal columnar lattices without intracolumnar order (Φ_h) at high temperature, as revealed by the DSC and XRD results of the oriented films. This thermoreversible transition is generated by an unprecedented conformational change in the *cis*-PPA backbones from the *cisoidal* conformation in the Φ_h^{io} phase to the *transoidal* conformation in the Φ_h phase. This conformational change is accompanied by a decrease in the external column diameter induced by stretching of the polymer backbone along the axis of the cylinder (Figure 69).[176] Taking advantage of this thermoreversible *cisoid-to-transoid* conformational isomerization of **100**, the molecular nanomachines capable of expressing their motions at macroscopic length scales have been constructed (see section 5.3).[532] In the same way, structural and retrostructural analyses of other *cis*-PPAs with first- or second-generation dendrons (**98**−**108** in Chart 14) have also been conducted.[174,177,178,180−183]

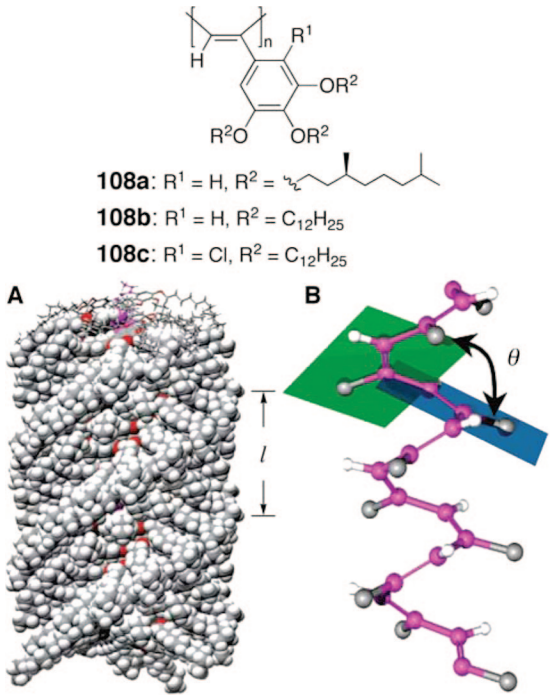

Figure 68. Structure of the cylindrical **108b**. (A) Side view of **108b** using the space filling model and (B) detail of the polymer backbone. An increase of the indicated dihedral angle (θ) of approximately 3−5° is enough to modify the average column stratum thickness (l) from 4.1 Å observed in the 3D centered rectangular lattice phase to 4.4 Å in the 2D hexagonal columnar lattice phase. (Reproduced with permission from ref 179. Copyright 2006 American Chemical Society.)

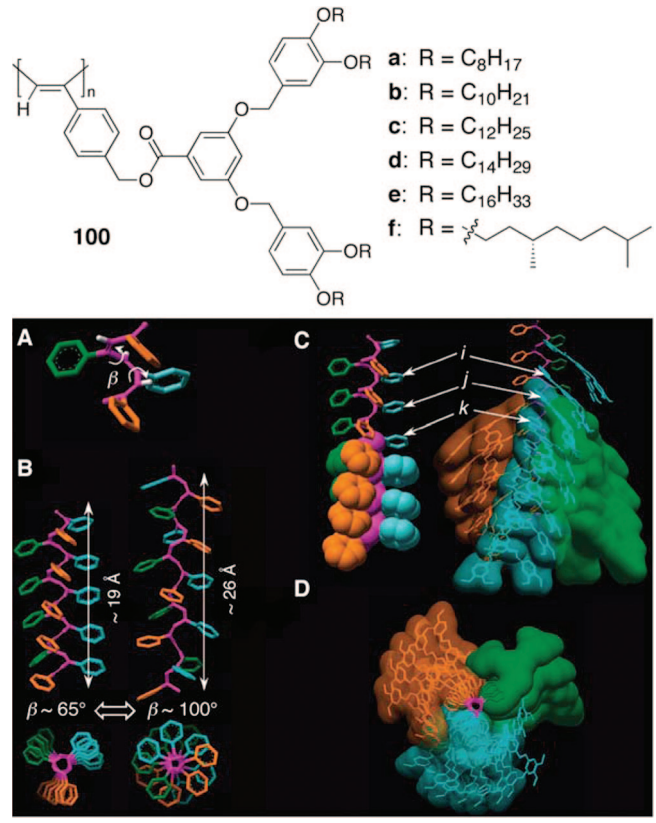

Figure 69. Models illustrating the thermoreversible *cisoid*-to-*transoid* conformational isomerism and porous columnar structure of **100**. (A) The dihedral angle (β) about the single bond in the polyene backbone; (B) side and top views of PPA oligomers with $\beta \sim 65°$ (*cis*−*cisoidal*) and 100° (*cis*−*transoidal*) and the corresponding change in length along the helix axis; (C) side views of space-filling models of PPA and **100** showing the helical registry of aromatic rings that explains the 6.6 (i−j) and 13.5 Å (i−k) helical features in the Φ_h^{io} phase; and (D) a top view of a space filling model of **100** with a low-electron-density core. (Reproduced with permission from ref 176. Copyright 2005 American Chemical Society.)

3.2. Helical Sense Determination

3.2.1. Exciton Chirality Method

As described in section 3.1.1, the X-ray crystallographic analysis of uniform oligomers as a model of the corresponding helical polymers is certainly a powerful method to unambiguously determine the helical structures including the helical pitch and handedness as well, if single crystals of uniform oligomers with an optical activity like those of **304** and **307** are available.

The nonempirical exciton-coupled CD method developed by Nakanishi and Harada, that is a practically useful method for determining the absolute configuration of a variety of chiral small molecules,[533,534] is often used for predicting the predominant helical sense of synthetic helical polymers, although the method, when applied to helical polymers, may involve a more or less uncertainty (Figure 70). Achiral chromophores, such as porphyrin and diazo dye residues, have been covalently introduced as the pendant groups in the optically active polyisocyanide **332**[88] and poly(*N*-propargylamide) **333**[535] and polyisocyanide **334**,[536] respectively, and their helical senses have been proposed on the basis of the signs of the split exciton-coupled Cotton effects.

Theoretical calculations of the electric CD and subsequent comparison with the observed CD may suggest a possible helical sense of certain helical polymers, although calculating the electric CD involves difficulty in resolving the contributions from individual electronic transitions from the main-chain and side-chain chromophores. Nevertheless, the preferred-handed helical sense of the optically active **1** isolated by chromatographic resolution was predicted by calculating the CD in the imino chromophore region.[537] Yokozawa and Kobayashi et al. have performed an exciton model analysis of the absorption and CD spectra of the *N*-alkylated optically active poly(*p*-benzamide) (**129**, Chart 16) based on the crystal structure of the corresponding uniform oligomers (**308**) and proposed a right-handed helical structure (*P*-helix) for **129a** in solution.[224] The helical senses of a series of poly(*N*-butynylamide)s having various optically active side chains (**335a**−**d**),[538] a phenylpropyl ether dendronized PPA (**106**),[178] and an optically active PPA bearing achiral galvinoxyl pendants (**119**) prepared by the helix-sense-selective polymerization[539] have also been postulated by comparison of the observed CD spectra with the simulated ones.

In sharp contrast to the electric CD, VCD has significant advantages not only for its sensitivity to chiral nonchromophoric molecules but also for the reliable theoretical calculations of its spectrum using the DFT available in the Gaussian program. Taking advantage of the available DFT calculation method, the helical structure of a model polymer of the optically active polyguanidine (poly-**61**) prepared by the helix-sense-selective polymerization of the corresponding achiral carbodiimide with a chiral titanium complex was calculated to simulate its VCD spectrum, which has been further used to determine the

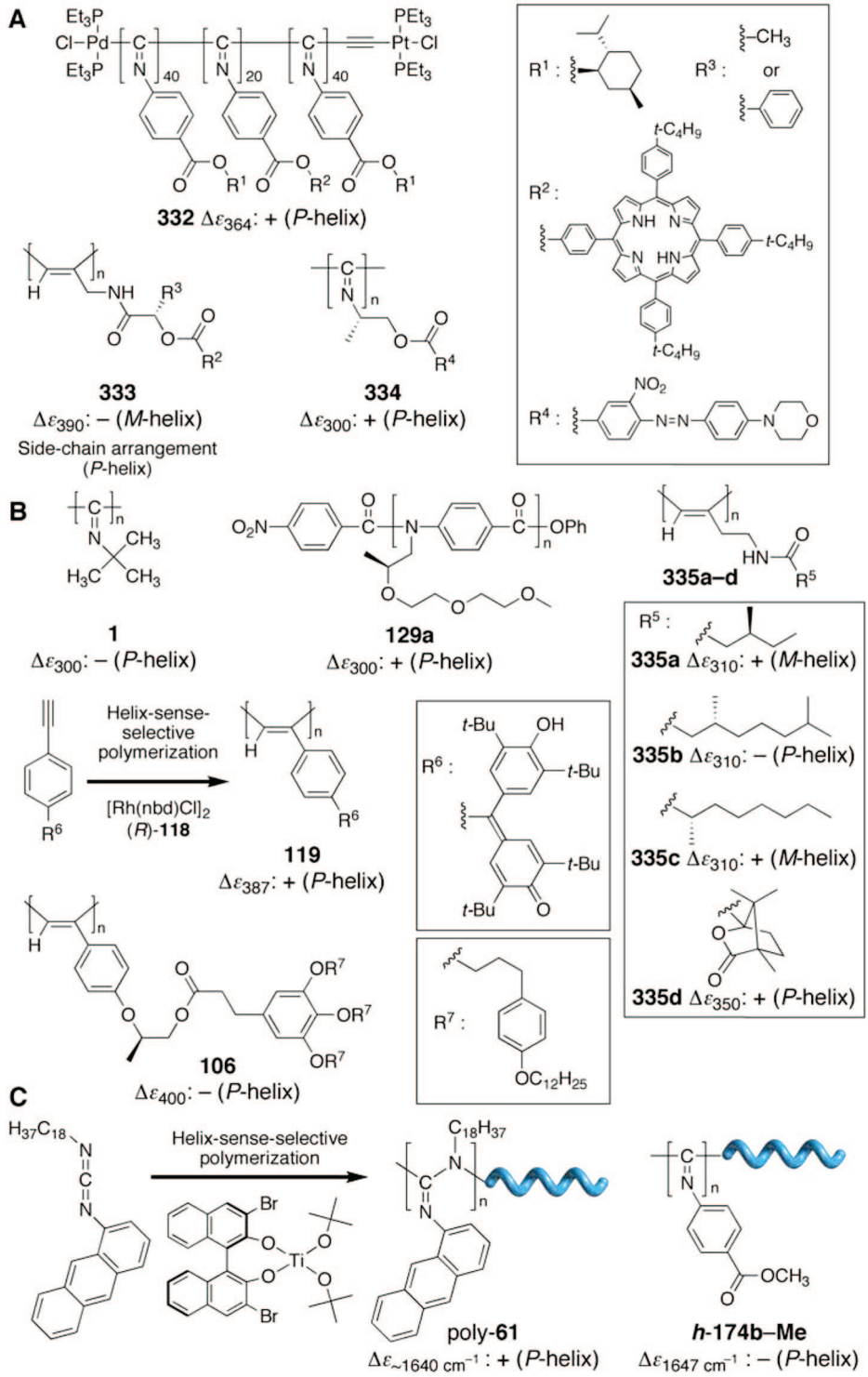

Figure 70. Synthetic helical polymers whose helical senses were determined by the exciton-coupled CD method (A), theoretical calculation of the CD spectra (B), and DFT calculations coupled with VCD measurements (C). The signs of the observed CD and VCD spectra and the determined helical senses are also shown. *P*-helix and *M*-helix represent the right- and left-handed helical main-chain structures, respectively.

helical sense of poly-**61** by comparison with the experimental VCD spectrum.[109] In a similar way using VCD combined with DFT calculations, preferred-handed helical structures and their helical senses of the polyisocyanide with a macromolecular helicity memory (***h*-174b-Me**, Figure 67),[531] an aromatic oligoamide of 8-amino-2-quinolinecarboxylic acid bearing a chiral end group at the *C*-terminus (**300b**, Chart 28),[540] and optically active st-PMMA (Figure 46)[395] have been determined.

3.2.2. Microscopic Observations

As discussed in the preceding section, the CD and XRD methods are convenient and useful for investigating helical structures in solution and bulk, respectively, but may not provide unambiguous helical structural information of synthetic helical polymers and, in particular, the helical sense. The recently developed SPM techniques offer a great opportunity to visualize the real shapes of polymers on

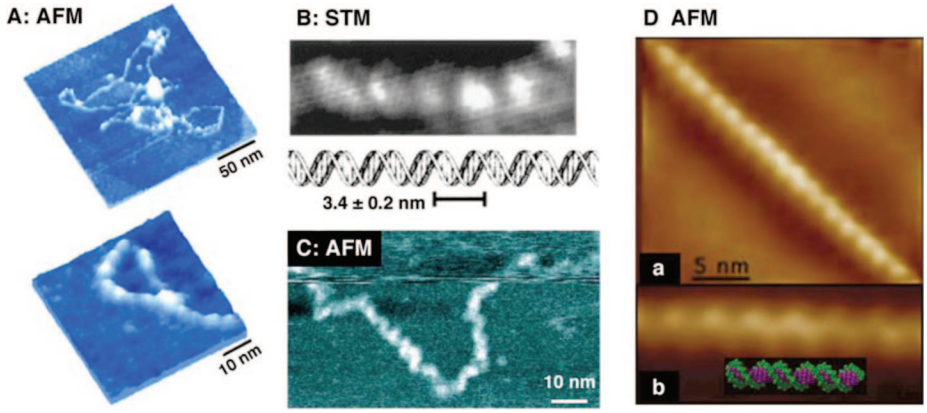

Figure 71. (A) High-resolution noncontact AFM images of DNA taken in the constant-amplitude mode. (Reproduced with permission from ref 544. Copyright 1999 Institute of Pure and Applied Physics) (B) High-resolution STM image of a 2739 base-paired double-stranded plasmid DNA observed at ~95 K. An internal structure with periodicity of 2.6−3.6 nm along the strand was observed. (Reproduced with permission from ref 545. Copyright 1999 Elsevier) (C) Tapping mode AFM image of DNA in propanol. (Reproduced with permission from ref 543. Copyright 1995 Elsevier) (D) High-resolution AFM image of a right-handed double-helical DNA (a) and standard model of the B-DNA double helix (b). (Reproduced with permission from ref 542. Copyright 2003 Springer.)

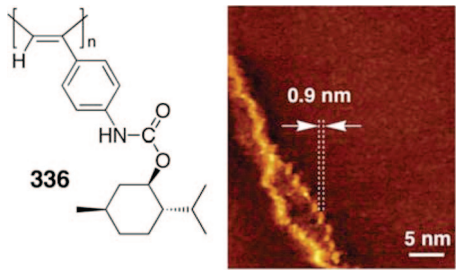

Figure 72. STM height image of **336** on HOPG. (Reproduced with permission from ref 546. Copyright 2001 American Chemical Society.)

surfaces and even in solutions,[541] although the SPM observations of synthetic helical polymers remain rare but challenging even for a large biopolymer, the right-handed double-helix DNA (Figure 71); few high-resolution AFM[542−544] and STM[545] images of DNA revealed the helical pitch (3.4 nm) and right handedness, indicating that it is likely more difficult to directly observe the helical structures of synthetic helical polymers with a smaller helical pitch than that of DNA, although an STM image of the helical structure of an optically active PPA **336** measured on a highly oriented pyrolytic graphite (HOPG) substrate was reported (Figure 72).[546]

3.2.2.1. Atomic Force Microscopy Observations of Helical Polymers. Nowadays, AFM has been frequently used for the visualization of polymer materials,[464,465] but those of helical polymer chains with an either right- and/or left-handed helical structure are quite rare. Figure 73A shows the AFM images of helical PPAs bearing a chiral ruthenium (Ru) complex with opposite chirality (Δ and Λ forms) as bulky pendant groups (**337**). The polymers are considered to have a predominantly one-handed helical conformation biased by the chiral Ru pendants, but their absolute helical senses of each polymer were not determined by conventional methods. However, the helical polymers adsorbed on mica have been easily discerned as an isolated strand and the visualization and discrimination of the right- and left-handed helical structures of **337** induced by the pendant's chirality (Δ and Λ forms) is possible by high-resolution AFM imaging, although the observed helical pitch in the AFM images (10−18 nm) is one order longer than that expected from the computer-generated models (1.6 nm).[547]

Similar right- and/or left-handed twisted polymer chains with a long helical pitch are also observed for the PPA homopolymers such as (*R*)-**291**[548] and copolymers with optically active pendant groups,[346,347] and PPA with achiral bulky aza-18-crown-6 ether pendant groups (**158**) (Figure 73B and C).[549] In the dynamically racemic helical **158** molecules, both the right- and left-handed helices are equally observed on mica. However, in the presence of the optically pure L- or D-Ala, the helical **158** chain changed its structure to a right- or left-handed helical conformation, respectively. The observed helical pitch of **158** estimated from the AFM images is *ca.* 12 nm, which is again much higher than those of the computer-generated helical pitch (1.5 nm) of the helical **158**. The difference in the helical pitch has been considered to be due to the coiled-coil, superhelix formation of **158** on the mica substrate (Figure 73C). These results indicate that the helical sense and its one-handed excess of certain helical polymers induced by chiral molecules covalently or noncovalently attached to the pendants can be differentiated by observing isolated single molecules by AFM, but this method may not provide a real structure of the helical polymers because of the broadening effect of the tip and unfavorable interactions with substrates.

In order to overcome this difficulty, a facile and reliable method for visualizing synthetic helical polymers using a conventional AFM instrument in the tapping mode has been developed. The helical structures including the helical pitch and handedness of some helical polymer chains have been observed at a resolution close to or slightly better than 1 nm when the polymers self-assemble to form regular 2D crystals on substrates after annealing under organic solvent vapors.[30,550] The 2D crystals of the polymer chains have advantages that they are sufficiently robust to resist damaged by the tip during high-resolution AFM observations and the flat surface of the 2D crystals allows optimizing the AFM settings for high-resolution imaging, and therefore, the self-assembled helical chains in the 2D crystals may be more recognizable as regular structures than amorphous polymers composed of irregular single chains.

cis-transoidal-PPAs bearing L- or D-Ala residues with a long *n*-decyl chain as the pendants (L-**88** and L-**88**) showed the typical ICD spectra in the polymer backbone regions that are mirror images of each other, indicating that these polymers possess a preferred-handed helical conformation

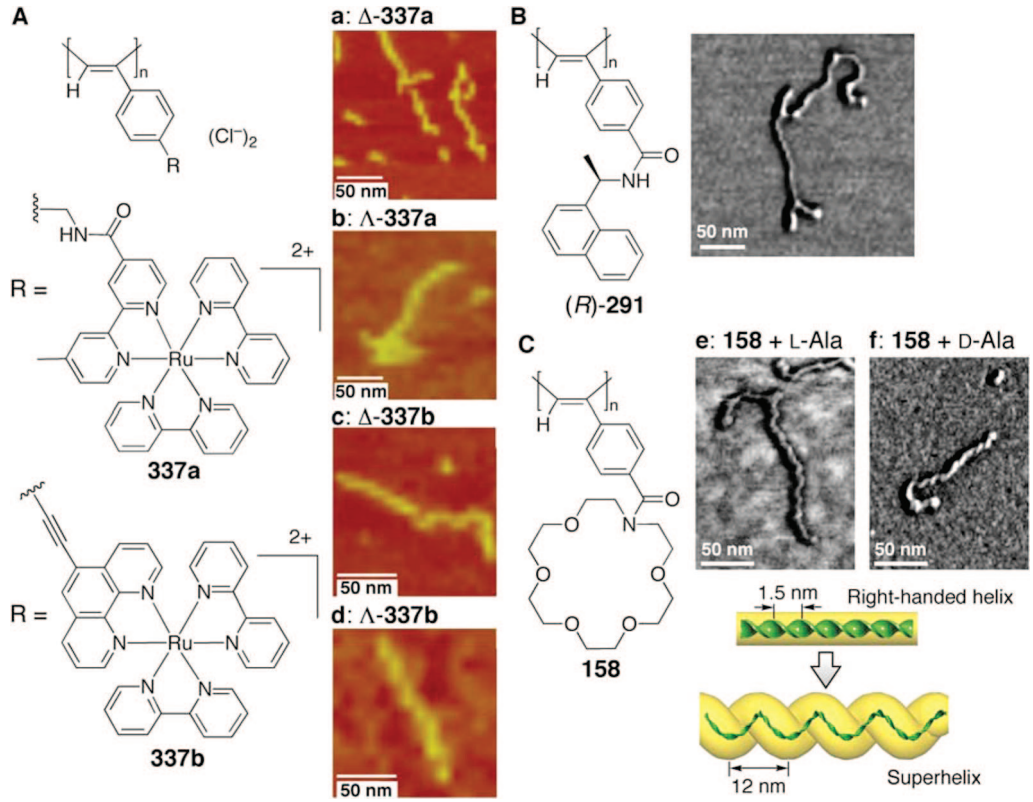

Figure 73. (A) AFM images of **Δ-337a** (a), **Λ-337a** (b), **Δ-337b** (c), and **Λ-337b** (d) deposited on mica from aqueous solutions. (Reproduced with permission from ref 547. Copyright 2004 John Wiley & Sons, Inc.) (B) AFM phase image of single strands of (*R*)-**291** prepared by spin-casting a dilute dimethylformamide (DMF) solution on mica. (Reproduced with permission from ref 548. Copyright 2003 American Chemical Society.) (C) AFM images of **158** in the presence of L-Ala (e) and D-Ala (f) on mica. A schematic representation of a possible helical structure (top) and superhelix of **158** (bottom) visualized by AFM on the mica surface is also shown. (Reproduced with permission from ref 549. Copyright 2004 Wiley-VCH.)

with exactly the same structure except for the helical sense (Figure 74A). However, the absolute helical sense of each polymer is unknown.

The helical **88**s are found to hierarchically self-assemble on HOPG upon exposure to benzene vapors. First, highly ordered flat PPA monolayers spontaneously and epitaxially formed on the basal plane of the graphite due to the strong and epitaxial adsorption of the pendant's alkyl chains on the graphite lattice (first layer in Figures 74B and C), on which amorphous-like polymers with no specific conformation were deposited on this 2D ordered monolayer (second layer). However, once exposed to benzene vapors, the second-layered amorphous polymers further self-assembled into well-defined 2D helix-bundles with a relatively constant height (Figure 74D).[551] A high resolution AFM image of L-**88** revealed that the 2D bundle structures can be clearly resolved into individual left-handed helical polymer chains packed parallel to each other (Figure 74D, left). When D-**88** bearing the opposite D-Ala residues as the pendants is used instead, the opposite right-handed 2D bundle helical chains have been observed on the HOPG after benzene vapor exposure (Figure 74D, right). These remarkable 2D mirror-image relationships ambiguously assign their helical sense, helical pitch, and chain arrangement. L-**88** and D-**88** have enantiomeric left- and right-handed helical structures with respect to the pendant arrangements, respectively, as indicated by the periodic oblique stripes (blue and green lines in the AFM images in Figure 74D) with an almost identical helical pitch (2.34 ± 0.21 nm for L-**88** and 2.47 ± 0.18 nm for D-**88**) and chain−chain spacing (2.13 ± 0.11 nm for L-**88** and 2.18 ± 0.10 nm for D-**88**).[551]

As described in section 3.1.2, L-**88** and D-**88** are stiff, rigid-rod helical polymers and exhibit cholesteric LC phases in concentrated benzene solutions. Taking advantage of the liquid crystallinity of **88**, uniaxially oriented films suitable for XRD analysis have been prepared, and based on the XRD data, a plausible helical structure for **88**, that is, an 11/5 helix with a half pitch of the pendant helical arrangement of 2.33 nm, is proposed. This structure is in good agreement with the helical pitch observed in the high-resolution AFM (Figure 74D). Thus, the AFM and XRD results clearly reveal that the helical structures observed by AFM certainly reflect the helical structures of the polymers, and L-**88** and D-**88** possess an 11/5 helix with a helical pitch of 2.3 nm, and L-**88** showing the negative first Cotton effect in benzene has a left-handed helical array with respect to the pendant arrangements, while the main-chain has the opposite, right-handed helical structure.[551]

As described in section 2.8, **88** shows an unprecedented change in the main-chain stiffness accompanied by inversion of the Cotton effect signs, resulting from the "on and off" fashion of the intramolecular hydrogen-bonding networks in nonpolar solvents, such as benzene and toluene, and polar solvents, such as THF and chloroform. This suggests inversion of the helicity of **88** that takes place by changing the solvent polarity. In order to obtain convincing evidence for inversion of the macromolecular helicity, the AFM image of D-**88** deposited on HOPG from a dilute THF solution after THF vapor exposure was measured (Figure 75A). In contrast to the helical structure obtained from a benzene solution of D-**88**, D-**88** cast from a THF solution self-assembled into regular 2D helix bundles with the opposite left-handed helical structure. These AFM results are consistent with the CD

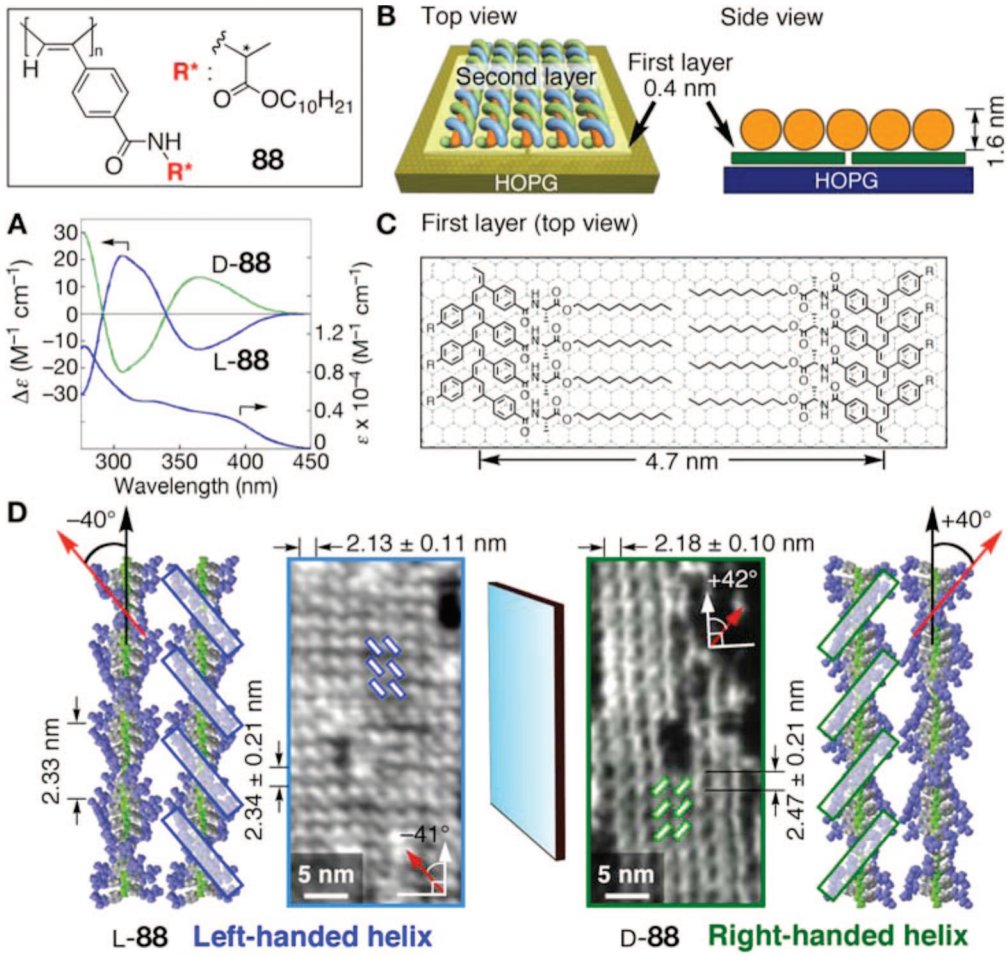

Figure 74. (A) CD and absorption spectra of L- and D-**88** in benzene. (B, C) Schematic drawings of the hierarchical structure of the self-assembled L-**88** on HOPG. (D) High resolution AFM phase images of L- and D-**88** with antipodal oblique pendant arrangements (blue and green lines, respectively). Scale = 20 × 40 nm. Possible models (left and right) were constructed on the basis of the X-ray structural analysis. Decyl side groups are replaced by methyl groups for clarity. (Reproduced with permission from ref 551. Copyright 2006 Wiley-VCH.)

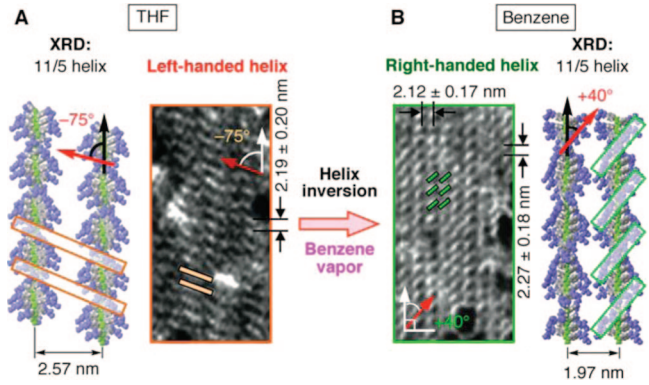

Figure 75. (A) AFM phase image of self-assembled left-handed helical D-**88** spin-cast on HOPG from a dilute THF solution. Scale = 20 nm × 40 nm. The white arrow indicates the direction of the polymer main-chain axis. (B) AFM phase image of right-handed helical D-**88** 2D crystals after helicity inversion by benzene vapor. Scale = 20 nm × 40 nm. Schematic drawings of left- (A) and right-handed (B) helical D-**88** 2D crystals with antipodal oblique pendant arrangements are also shown. The models were constructed based on the X-ray structural analysis results. (Reproduced with permission from ref 434. Copyright 2006 American Chemical Society.)

results. The average helical pitch of 2.19 ± 0.20 nm obtained from the AFM image is in good agreement with the half pitch of the helical arrangements of the pendants as determined by the XRD analysis of a uniaxially oriented polymer film (2.11 nm) prepared from a cholesteric LC THF solution of D-**88**. Interestingly, the macromolecular helicity of D-**88** deposited on HOPG from THF was further inverted into the opposite handedness by exposure to a benzene vapor atmosphere, and these switchable changes in the surface chirality based on the inversion of the macromolecular helicity of a dynamic helical PPA have been visualized for the first time by AFM with molecular resolution (Figure 75B).[434]

Given the success in visualizing the helical structure of **88** by AFM, this procedure has been applied to other helical polymers. Specific solvent vapor exposure to helical polymers deposited on HOPG is the key process, through which helical polymers self-assemble into 2D crystals on graphite with well-defined helix-bundle structures. An analogous PPA bearing achiral α-aminoisobutyric acid (Aib) residues with the same *n*-decyl chain as the pendants (**111**) is totally optically inactive but believed to be chiral because **111** likely exists as an equal mixture of interconvertible right- and left-handed helical segments separated by helical reversals in solution, although there is no direct evidence because of the extreme difficulty in detecting such dynamic interconvertible helical segments and rarely occurring helical reversals by conventional spectroscopic methods.

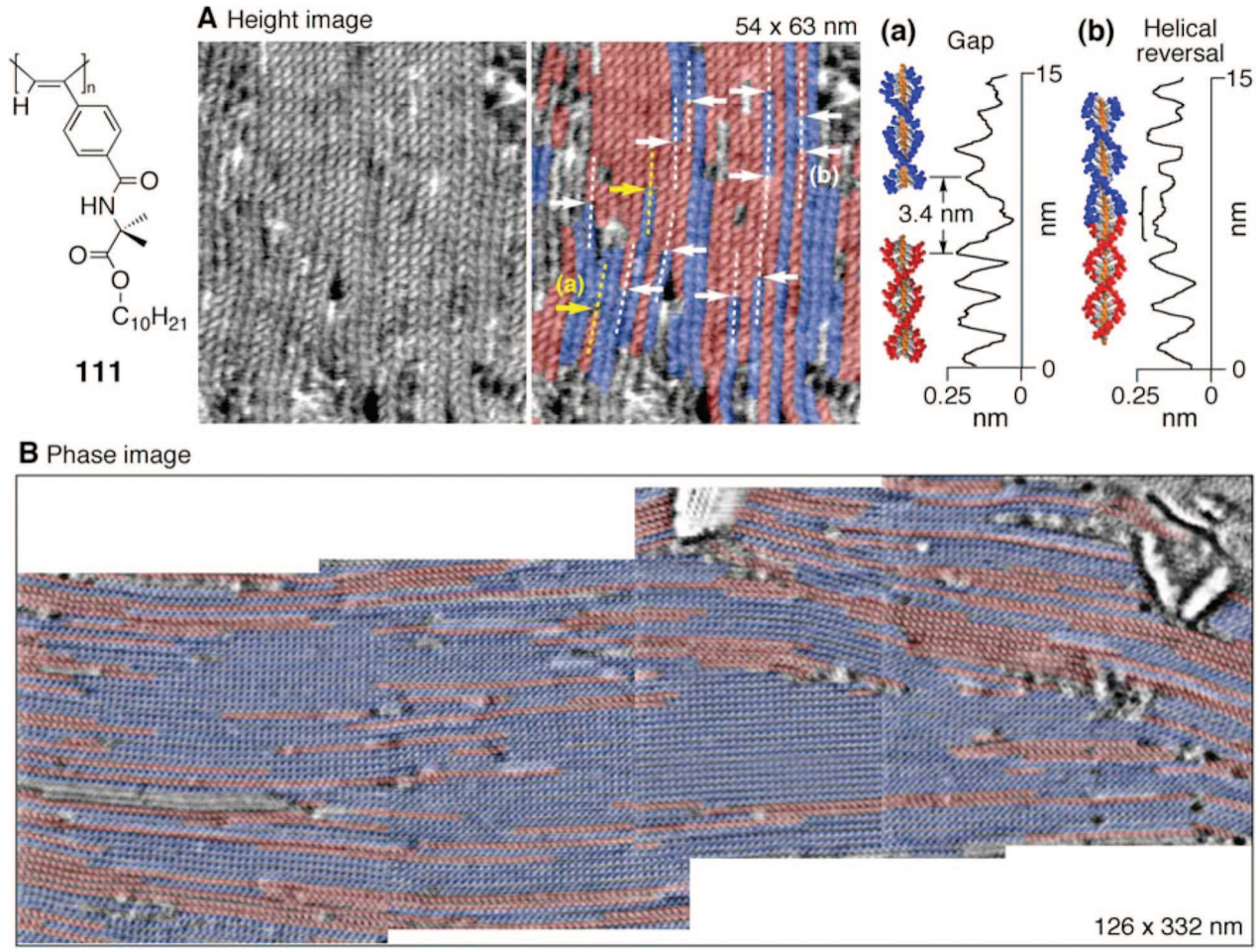

Figure 76. (A) AFM height images of 2D self-assembled **111** cast on HOPG from a dilute benzene solution. Scale = 54 nm × 63 nm. The cross-section height profile denoted by yellow and white dashed lines, which represent a right- and left-handed helical blocks separated by a gap (a) and a helical reversal (b), along with helical blocks of opposite handedness are also shown. Polymer models (a and b) are constructed by molecular modeling and MM calculations on the basis of the X-ray analysis. (B) Wide-view AFM phase images of 2D self-assembled **111** cast on HOPG. The wide-view high-resolution AFM images were obtained by the sequential high-resolution AFM measurements (scale = 100 nm × 100 nm). The obtained four sequential high-resolution AFM images were then overlapped to reconstruct the whole image, covering a wider area with maintaining the high-resolution. The polymer strands with clearly identifiable right- and left-handed helical blocks are shown in red and blue colors, respectively (A, B). Unidentifiable strands are uncolored. (Reproduced with permission from ref 193. Copyright 2007 Wiley-VCH.)

The high-resolution AFM images of **111** on HOPG clearly display enantiomeric right- and left-handed helical block segments packed parallel to each other (red and blue colors, respectively, in Figure 76A) separated by rarely occurring helical reversals in individual polymer chains (red and blue colors and white arrows, respectively, in Figure 76A).[193] By carefully evaluating the height profiles, there is a gap along with helical blocks of opposite handedness (yellow arrows), which are different from the helical reversal (white arrows); for example, two **111** chains align with a distance of 3.4 nm (a in Figure 76A). The helical pitch determined from the AFM image (2.0 nm) agrees well with that determined by the XRD analysis of a one-directionally oriented **111** film obtained from a concentrated nematic LC benzene solution in an electric field. A further statistical analysis of a series of high-resolution AFM images of **111** covering a wider area (Figure 76B) reveals that helical reversals appear only once in every 287 monomer units on average, corresponding to a 60 nm length in the dynamic helical **111**. Using the average length, the free energy difference between the helical reversal states (ΔG_r) of **111**, one of the most important thermodynamic stability parameters for dynamic helical polymers, has been calculated to be *ca.* 14 kJ mol^{-1} (see Table 2).[193]

The helical structures of some polyisocyanides have been postulated to be a 4/1 (**1**, poly-**25**),[22,67,72,552−554] 10/3 (***h*-174b-Me**),[531] and 15/4 (poly-L-**32h** and poly-L-**32g**)[89] helix based on XRD analyses, but the absolute helical sense of the helical polyisocyanides remains obscure. Diastereomeric right- and left-handed helical polyisocyanides (poly-L-**32**) were found to form by an unprecedented helix-sense-controlled polymerization of an enantiomerically pure phenyl isocyanide bearing the same L-Ala residue with a long *n*-decyl chain as the pendant using an achiral nickel catalyst ($NiCl_2$) in different solvents, such as CCl_4 and toluene, at different temperatures (see Figure 4 in section 2.1.2). High-resolution AFM reveals their helical conformations and enables the determination of the helical senses (Figure 77).[85] Poly-L-**32a** obtained in CCl_4 showed a positive first Cotton effect sign ($\Delta\varepsilon_{first} = +8.1$) and self-assembled on HOPG to form slightly irregular 2D helix bundles consisting of major right-handed helical segments with a helical pitch of 1.25 nm, together with minor but distinctly left-handed helical segments, suggesting that poly-L-**32a** has a predominantly right-handed helical structure, but the helical structure is imperfect (Figure 77A). In contrast, poly-L-**32e** prepared in toluene exhibited a negative first Cotton effect sign ($\Delta\varepsilon_{first} = -11$)

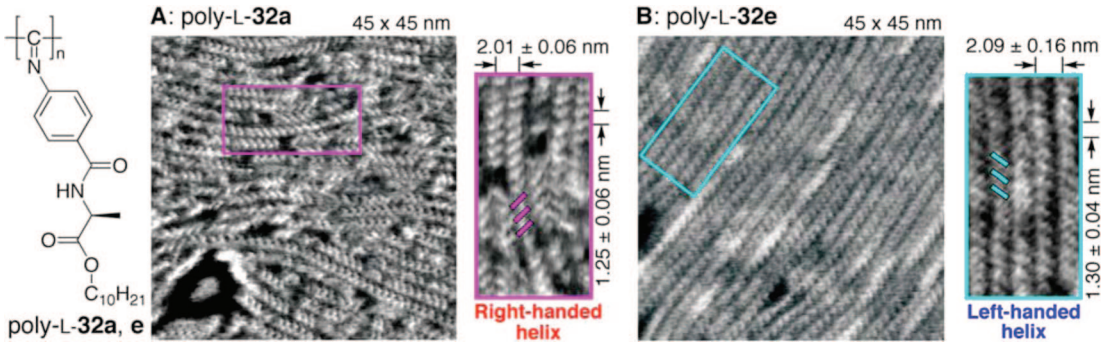

Figure 77. AFM phase images of self-assembled diastereomeric helical poly-L-**32a** (A) and poly-L-**32e** (B) obtained in CCl_4 and toluene at 100 °C followed by annealing in toluene at 100 °C for 6 days, respectively, on HOPG. Scale = 45 nm × 45 nm. The magnified images correspond to the areas indicated by the red and blue squares, respectively. (Reproduced with permission from ref 85. Copyright 2006 American Chemical Society.)

after further annealing in toluene at 100 °C for 6 days and the AFM image of the self-assembled 2D helix bundles showed a predominantly left-handed helical structure (Figure 77B). As a consequence, poly(phenyl isocyanide)s with a positive first Cotton effect sign are assigned to a right-handed helix. This assignment agrees with that proposed by the exciton-coupled CD method.[88]

When the same L-Ala-bound isocyanide monomer is polymerized with the living Pt−Pd catalyst (**33**), almost completely right-handed (poly-L-**32h**) and left-handed (poly-L-**32g**) helical polyisocyanides with different molecular weights and narrow molecular weight distributions have simultaneously been produced (Figure 5 in section 2.1.2). Quite interestingly, each single-handed, rodlike helical polyisocyanide with a controlled length and handedness can be separated by solvent fractionation with acetone and exhibits a smectic LC phase in concentrated solution (Figure 5) and also forms 2D smectic layer-like helix-bundle structures on HOPG, which can be directly observed by AFM (Figure 78A).[89] Based on the high-resolution AFM combined with the XRD analysis, it is concluded that both right- and left-handed helical poly-L-**32h** and poly-L-**32g** possess a stiff 15/4 helix with a helical pitch of *ca.* 1.3 nm assisted by four sets of intramolecular hydrogen bondings. In addition, the helical sense excesses of the poly-L-**32h** and poly-L-**32g** have been directly determined to be 97 and 99%, respectively, by counting the number of helical senses using high-resolution AFM (Figures 78B and C). Binary mixtures of smectic LC polysilanes (**69**) with different molecular weights and narrow molecular weight distributions also form characteristic smectic layers (smectic A1−A3) reflecting the molecular weight ratio and the mixing ratio as revealed by AFM observations of the film surface.[491]

The poly-L-**32g** and poly-L-**32h** maintain the polymerization activity and further block copolymerize the corresponding enantiomers of L-**32** and D-**32** in a highly enantiomer-selective manner while maintaining narrow molecular weight distributions. The poly-L-**32g** preferentially copolymerized L-**32** over the antipode by a factor of 6.4−7.7, whereas the D-**32** was preferentially copolymerized with poly-L-**32h**, composed of the same L-**32** units, but possessing the opposite helicity by a factor of 4.0.[555] Interestingly, the enantiomer-selective block copolymerizations proceed in an extremely high helix-sense-selective fashion, as revealed by high-resolution AFM (Figure 79) and supported by CD spectra of the block copolymers, indicating that the helical handedness of the poly-L-**32g** and poly-L-**32h** used as the initiators determines the overall helical sense of the block polyisocyanides irrespective of the configuration of the monomer units of the initiators during the block copolymerizations. The block copolymers maintain rigid-rod characteristics with a narrow molecular weight distribution and showed lyotropic smectic LC phases.

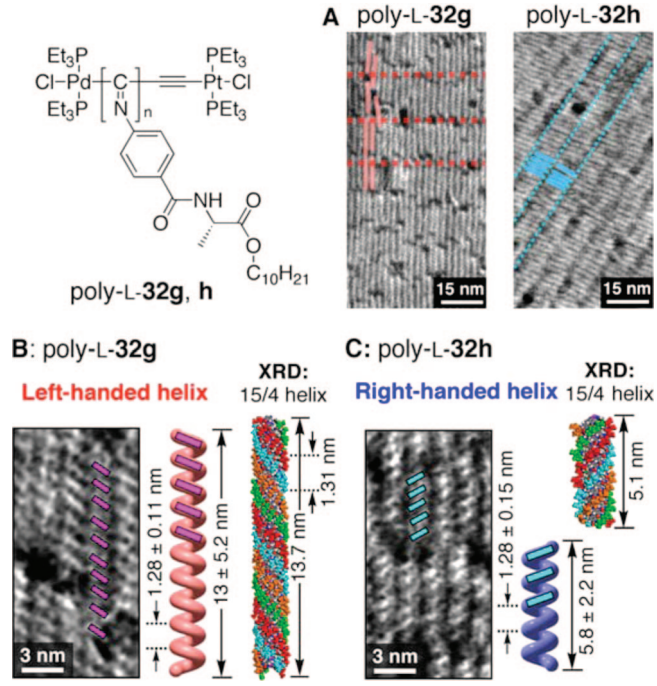

Figure 78. (A) AFM phase images of 2D self-assembled poly-L-**32g** and poly-L-**32h**. Scale = 50 nm × 100 nm. The bars and dotted lines indicate the individual polymer chains and 2D smectic layer lines, respectively. (B and C) AFM phase images of poly-L-**32g** (B) and poly-L-**32h** (C) on HOPG. Scale = 10 nm × 20 nm. Schematic representations of the left-handed helical poly-L-**32g** and right-handed helical poly-L-**32h** with periodic oblique stripes (pink and blue lines, respectively), which denote a one-handed helical array of the pendants and optimized 15/4 helical structures of poly-L-**32g** and poly-L-**32h** on the basis of X-ray structural analysis results, are also shown (B and C). (Reproduced with permission from ref 89. Copyright 2008 American Chemical Society.)

This newly developed method utilizing the supramolecular self-assembly into well-defined 2D crystals on substrates has been applied to other helical polymers, since the helical conformations are maintained in the 2D lattice, and therefore, helical structures can be observed by high-resolution AFM with molecular resolution.

3.2.2.2. Atomic Force Microscopy Observations of Poly(methyl methacrylate)s. As described in section 2.7.3,

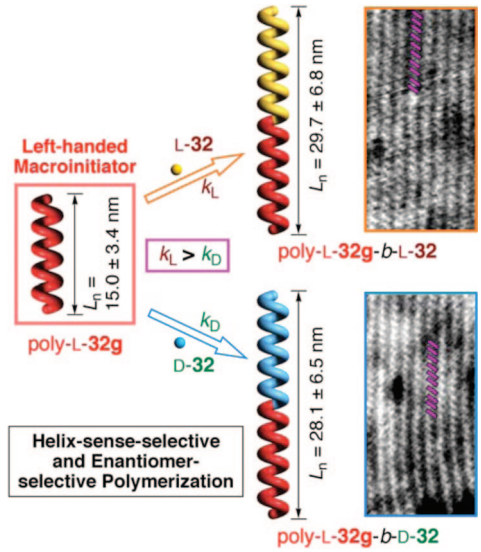

Figure 79. Schematic illustration of the enantiomer-selective and helix-sense-selective block copolymerization of L-**32** and D-**32** with the left-handed helical poly-L-**32g** as the macroinitiator, resulting in almost perfect single-handed helical block copolymers with different polymerization rate constants (k_L and k_D). AFM phase images of poly-L-**32g**-*b*-L-**32** and poly-L-**32g**-*b*-D-**32** on HOPG with periodic oblique stripes (pink lines), which denote a left-handed helical array of the pendants, are also shown (right). Scale = 20 nm × 40 nm. (Reproduced with permission from ref 555. Copyright 2009 American Chemical Society.)

it has been reported that stereoregular it- and st-PMMAs form the double-stranded helix in crystals[556,557] and a single-stranded helix in specific organic solvents, such as toluene,[394,558] by X-ray analyses, respectively. Mixing it- and st-PMMAs in a 1/2 stoichiometry, a stereocomplex, a class of unique polymer-based crystalline supramolecules, is formed in specific solvents. Although the history of the stereocomplex extends back to the 1950s, the molecular basis of the structure and the complex formation mechanism have not been elucidated, in spite of its practical importance as hollow fiber dialyzers.[559] In 1989, Schomaker and Challa proposed a double-stranded helix model for the stereocomplex based on the XRD analysis of the stretched fiber; the model is composed of a 9/1 it-PMMA helix surrounded by an 18/1 st-PMMA helix with a monomer ratio of 1:2, resulting in a complementary double-stranded helix with a helical pitch of 1.84 nm (Figure 80A).[560] Since then, the double-stranded helix model has been commonly accepted.

Taking advantage of the fact that a mixed monolayer of it- and st-PMMA chains spread on a water surface forms a stereocomplex upon compression based on the surface pressure−area isotherms,[561] the molecular structure of a 2D stereocomplex monolayer has been investigated by high-resolution AFM.[400] The AFM phase image (Figure 80C) shows helix-bundle-like structures, which can be further resolved into individual stripe-patterned chains with a chain−chain lateral spacing of *ca.* 2.4 nm. The high-resolution zoomed image (Figure 80D) indicates a number of periodic oblique stripes (green arrows) having a pitch of 0.92 nm which are tilted either counterclockwise or clockwise along the stereocomplex main-chain (pink lines) (Figure 80D). These results are convincing evidence that the stereocomplex is indeed a helical polymer-based supramolecule. Most importantly, the observed helical pitch (0.92 nm) is equal to half the helical pitch of the proposed double-helix model (1.84 nm), suggesting that the double-helix model for the PMMA stereocomplex requires a revision.

On the basis of the ratio (it/st = 1/2) combined with the helical pitch (0.92 nm) of the stereocomplex observed by AFM, a more plausible model for the helical structure of the stereocomplex has been proposed, that is, a triple-stranded helix model (Figure 80B), where a double-stranded helix composed of two 9/1 *it*-PMMA helices with a 1.84 nm helical pitch is surrounded by a 18/1 *st*-PMMA helix with the observed 0.92 nm helical pitch. The model satisfies the AFM results, the stoichiometry, and the reported helical structures of each component, it-[556,557] and st-PMMAs,[394,558] and also leads to the conclusion that the stereocomplex may not be an intertwined double helix but may be a supramolecular-assembled inclusion complex composed of an outer st-PMMA helix and an inner it-PMMA double helix. This speculation is supported by the fact that st-PMMA can encapsulate fullerenes within its helical cavity to form a robust and peapod-like complex[395] and further supported by "molecular sorting" experiment results using uniform it- and st-PMMAs with different molecular weights.[562] As described in section 2.7.3, a preferred-handed helical st-PMMA can be induced in toluene in the presence of optically active alcohols. Taking advantage of the helicity induction in st-PMMA and its inclusion complexation functionality, an

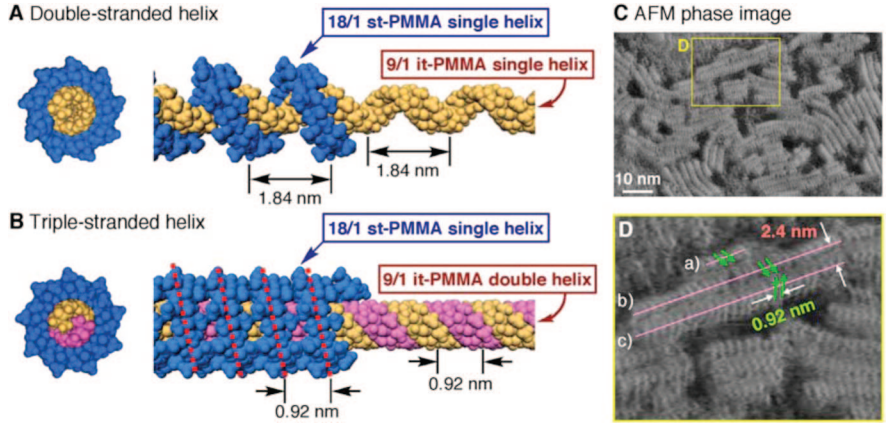

Figure 80. Space-filling models of double-stranded helix (A) and triple-stranded helix models (B) for an it- and st-PMMA stereocomplex (it/st = 1/2). (left, through-view; right, side-view). The right part of the st-PMMA helices is omitted for clarity. (C) AFM phase image of a monolayer of an it- and st-PMMA mixture (it/st = 1/2) deposited on mica at 10 mN/m. (D) Magnified image of the area indicated by the yellow square in part C. The pink lines represent the main-chain axes of the stereocomplex; the green arrows indicate the antipodal oblique pendant helical arrangements with respect to the main-chain axes. (Reproduced with permission from ref 400. Copyright 2006 Wiley-VCH.)

optically active stereocomplex has been prepared through the supramolecular inclusion of it-PMMA within the helical cavity of an optically active st-PMMA (Figure 46),[399] which also supports a triple-stranded helical structure of the stereocomplex.[400]

3.2.2.3. Microscopic Observations of Helical Aggregates Composed of Synthetic Polymers. A significantly high number of helical assemblies have been constructed from small molecules and oligomers through noncovalent bonding interactions, and their helical structures have been observed by various microscopic means.[19,36−43,563,564] However, a limited number of studies has reported supramolecular helical assemblies based on synthetic polymers, in particular, helical polymers except for biological polypeptides.[565−568]

Linear amorphous triblock copolymers consisting of immiscible achiral components with specific compositions, for example, polystyrene-*b*-polybutadiene-*b*-PMMA[569] and polystyrene-*b*-poly(2-vinylpyridine)-*b*-poly(*tert*-butyl methacrylate),[570] have been reported to form a helical supramolecular mesophase (helices wound around a cylindrical core) in which the chirality is not defined on a molecular level but on a meso- or nanoscopic level. In the latter case, the poly(2-vinylpyridine) middle block forms helical strands surrounding the polystyrene cylinders, which are embedded in a poly(*tert*-butyl methacrylate) matrix, resulting in an equal mixture of right- and left-handed nanohelical phases (Figure 81A).

When a chiral diblock copolymer system containing both achiral and chiral blocks, polystyrene-*b*-poly(L-lactide) (**338**) (Figure 81B), was used, hexagonally packed left-handed nanohelices of poly(L-lactide) (PLLA) in the polystyrene matrix have been formed in the bulk (Figure 81c and d).[571] The helical morphology of **338** is dynamic and can be tuned in a reversible way by applying stimuli; the amorphous nanohelices in the bulk transformed into crystalline cylinders via crystallization of the PLLA by heating and reverted to the original nanohelices upon remelting and annealing.[572,573] Taking advantage of the degradability of the nanohelical PLLA amorphous domains by hydrolysis, nanoporous polystyrene with helical nanochannels has been obtained by removal of the PLLA blocks after hydrolysis. A further sol−gel reaction within the nanochannels followed by degeneration of the polystyrene template produces the silica nanohelices that preserve the nanohelical texture during the replication process (Figure 81e).[574]

An amphiphilic block copolymer **339** composed of a hydrophobic tail of flexible polystyrene and a hydrophilic headgroup of a charged, rigid-rod helical polyisocyanopeptide self-assembles in a hierarchical fashion in water to form superhelices with a controlled helix-sense. Interestingly, the chirality of the right-handed helical polyisocyanopeptide results in the formation of helical superstructures that have an opposite left-handed superhelix, as clearly revealed in a TEM image (Figure 82A).[575] This behavior resembles that of natural systems, for instance, with helix bundle proteins, which contain right-handed α-helices that can pack in an opposite twist fashion to generate left-handed superstructures.[576] Related to this, but a totally achiral poly(2-(acetoacetoxy)ethyl methacrylate) (**340**) with neither a high stereoregularity, chirality, nor amphiphilicity was found to form a kind of self-assembled double-stranded helical tubes of either screw-sense. The formation of such twisted superhelices is considered due to hydrogen-bridging interactions between adjacent acetoacetoxy groups.[577]

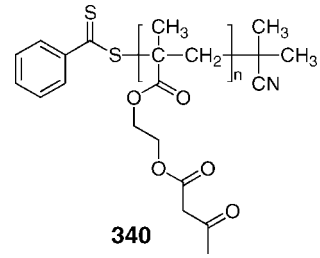

340

Another interesting class of supramolecular helical assemblies has been explored by Cheng and co-workers using optically active but nonhelical main-chain LC polyesters (**341**) (Figure 82B), which crystallize to form flat-elongated and left-handed helical lamellar single crystals (b in Figure 82B) when grown from the melt at 160 and 145 °C for 1 day, respectively (n = 9, **341**). Dark and bright field images and selected area electron diffraction experiments using TEM provide a convincing double-twisted molecular orientation model; that is, the chain

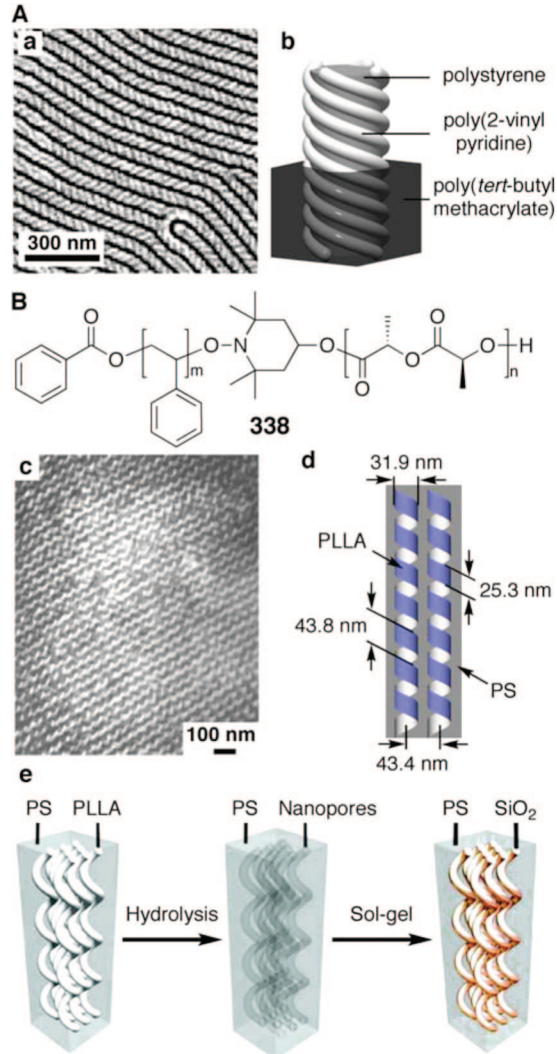

Figure 81. (A) SEM image (a) and illustration (b) of the first layer of a thin film of polystyrene-*b*-poly(2-vinylpyridine)-*b*-poly(*tert*-butyl methacrylate) triblock copolymer after staining with OsO_4. (Reproduced with permission from ref 570. Copyright 2002 American Chemical Society.) (B) TEM micrograph (c) and schematic representation (d) of **338** (f_{PLLA}^{v} = 0.35). (Reproduced with permission from ref 571. Copyright 2004 American Chemical Society.) (e) Schematic illustration of the templation for generating well-defined helical nanocomposites. (Reproduced with permission from ref 574. Copyright 2009 American Chemical Society.)

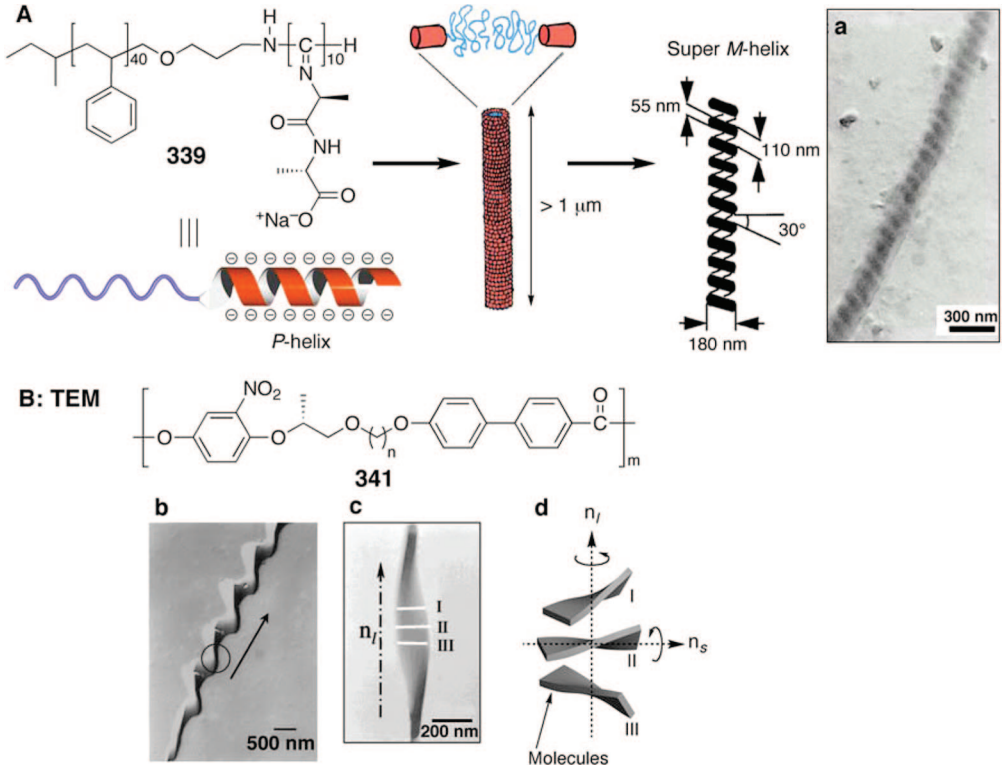

Figure 82. Microscopic observations of helically assembled optically active polymers. (A) Schematic illustration of the formation of a superhelix by hierarchical self-assembly of a poly(styrene)-*b*-poly(isocyanodipeptide) **339**. (a) TEM image of a left-handed superhelix from **339**. (Reproduced with permission from ref 575. Copyright 1998 American Association for the Advancement of Science.) (B) (b, c) TEM images of a double-twisted helical lamellar crystal of **341** ($n = 9$) grown from the melt at 145 °C for 24 h. (Reproduced with permission from ref 579. Copyright 1999 American Chemical Society.) (d) Schematic drawings of a twist model of the helical lamellar crystal. (Reproduced with permission from ref 578. Copyright 2000 American Chemical Society.)

orientation in the helical lamellar crystal is double twisted along both the long and short helical axes (n_l and n_s), respectively (c and d in Figure 82B).[578−580] Surprisingly, **341** ($n = 10$) was found to crystallize to form an opposite handed helical lamellar crystal when grown from the melt at 130 °C for 1 day.[581]

Helical morphologies of a series of L-amino acid-bound *cis*−*transoidal*-PPAs with either a right- or left-handed helical conformation on substrates have been investigated by Tang et al. using AFM. Natural evaporation of a methanol solution of **84c** bearing free carboxy acids as the pendants on mica gives rise to long, bundled nanofibers with a predominant handedness through self-assemblies of the **84c** helices assisted by the lateral interstrand hydrogen bonds (Figure 83A).[582] A PPA bearing L-Ala methyl ester residues (**84b**) also spontaneously and instantly assembles in a cooperative manner into a well-organized variety of helical morphologies including spiral and superhelical nanoribbons with right-handed and left-handed twist senses upon natural evaporation of its methanol and THF solution, respectively (Figure 83B and C, respectively).[144]

Similar helical nanofibers have also been prepared by the polymerization of aniline with ammonium persulfate in water in the presence of D- and L-CSAs as the dopant, resulting in right- and left-handed twisted polyaniline nanofibers (Figure 84A and B). The polyanilines doped with D- and L-CSAs showed mirror-image ICDs in solution (Figure 84C and see also section 2.5.2), suggesting that indeed helical polyanilines self-assemble to form superhelices with a helical bias originated from the polyaniline helicity induced by the dopants.[583] Interestingly, copolymerization of aniline with *m*-toluidine using D-CSA as the dopant under the same conditions produces opposite, left-handed helical nanofibers. Thus, the helical sense of polyaniline nanofibers can be adjusted by copolymerization with aniline derivatives as in solution.[584]

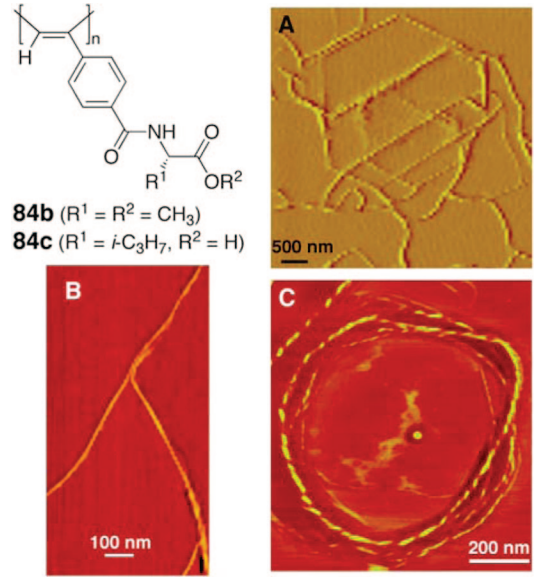

Figure 83. AFM images of helical aggregates based on helical polymers. (A) Helical nanofibers formed by **84c** upon natural evaporation of its methanol solution (7 μg/mL) on mica at room temperature. (Reproduced with permission from ref 582. Copyright 2001 American Chemical Society.) (B) Right-handed helical nanoribbons formed upon natural evaporation of a methanol solution of **84b** (~2.5 μg/mL) on mica. (C) Left-handed superhelical ribbons formed upon natural evaporation of a THF solution of **84b** (Reproduced with permission from ref 144. Copyright 2008 American Chemical Society.)

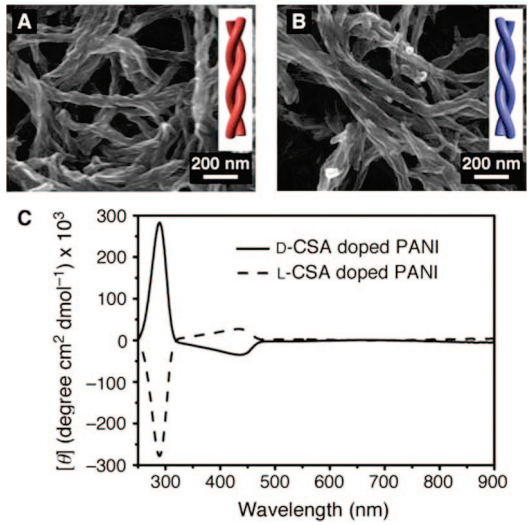

Figure 84. SEM images of left- (A) and right-handed (B) twisted polyaniline (PANI) nanofibers obtained using (A) D-CSA and (B) L-CSA as the dopant. The corresponding CD spectra are shown in part C. (Reproduced with permission from ref 583. Copyright 2007 Wiley-VCH.)

4. Double-Helical Polymers and Oligomers

As discussed in the preceding sections, a significant number of synthetic helical polymers and oligomers with a single-helical conformation have been prepared. In contrast, only a limited number of structural motifs for double-helical oligomers have been reported,[30,585−589] and synthetic double-helical polymers are hitherto unknown except for supramolecular double-helical polymers in the solid state.[254] In this section, we describe the recent advances in the synthesis, structures, and functions of double-helical polymers and oligomers along with a brief historical overview of synthetic double- and triple-stranded helices and knots.

4.1. Double- and Triple-Stranded Helicates and Trefoil Knots

In 1987, J.-M. Lehn reported the seminal work on double-stranded helicates that marked the beginning of intelligent self-assembly, introducing the term "helicate" to describe helical metal complexes that contain organic strands intertwining around the metal centers (Figure 85).[590] Lehn's group discovered the ether-linked 6,6′-methyl-2,2′-bipyridine oligomers (**342**) that instantly self-assemble to form double-stranded helical metal complexes with Cu^+ ions. The helical structures were determined by the geometrical preferences of the metal centers as well as the structures of the organic ligand strands, so that a rational design of a double-helical structure is possible, thereby enabling the introduction of some properties into helicates by functionalization. A few years later, the Strasbourg group synthesized thymidine-substituted ligands, which assembled into deoxyribo-nucleohelicates (**343**).[591] A structural analogy with DNA was pointed out, although, in contrast to the DNA, the thymidine residues are attached to the periphery of the double helix. The chiral thymidine substituents have the potential to induce a bias in the helix-sense, which, however, was not reported.

Induction of helix-sense bias in double-stranded helicates has been achieved by using optically active ligands (**344**) that have three- and five bipyridine units connected through ether linkages bearing methyl groups in the central benzylic positions with an (*S*)-configuration (Chart 31).[592] Upon complexation with Cu^+ and Ag^+ ions, the C_2-symmntric ligands self-assembled to form helicates with an excess one-handedness. ^{1}H NMR spectroscopy has revealed only one of the diastereomers in either case, of which the helical sense was assumed to be right-handed by CD along with CPK model inspection.

Siegel et al. have demonstrated that a helix-sense in the double-stranded helicates (**345**) can be biased using a chiral scaffold or template, such as an (*R*)- or (*S*)-biphenyl or binaphthyl group, which dictates the twist sense (*P* or *M*) of the double-stranded helicates with an almost one handedness, as evidenced by NMR.[593,594] Thus, the chiral terminal group controls the overall handedness of the helicates throughout a span of 20 Å. Interestingly, after removal of the biphenyl group of the tris(bipyridine)-based helicate, **345a**, by treatment with sodium methoxide followed by chromatography purification, the resulting double-stranded helicate without any chiral director maintained its optical activity, although it is a 66:34 mixture of enantiomers.[594] Thus, the twist-sense bias in the helicate is retained or "*memorized*" during the removal process of the template. Otera and co-workers have taken advantage of this chiral template strategy to construct a preferred-handed double-stranded helicate from pyridine-containing arylene ethynylene strands connected by an enantiomerically pure binaphthyl moiety.[595]

An Fe^{2+} helicate bearing tris(terpyridine) ligands with ethylene linkages (**346**) has also been prepared.[596] The obtained trinuclear helicates are kinetically inert toward racemization arising from the nature of the terpyridine ligand, and the resolution into enantiomers has been, for the first time for double-stranded helicates, achieved by chromatography using an eluent containing an optically pure salt.

Another interesting feature of oligobipyridine-based helicates is self-recognition, or "the recognition of self from non-self", in the helicate forming process (Scheme 25). A mixture of 2mer to 5mer strands (**347a**−**d**) complexed with Cu^+ ions and produced selectively the double-stranded helicates (**348a**−**d**) with no trace of cross-hybrid species according to 1D ^{1}H NMR and diffusion-ordered spectroscopy (DOSY) data.[597,598] Besides the structural factors such as ligand structures and the coordination geometries of the metal ions, this self-recognition process is governed by the energy-related principle of "maximum site occupancy" and the entropic factors.

Sequence information reminiscent of the genetic information of DNA can also be incorporated into molecular strands of helicates when two different binding units are employed (Chart 32). Two molecular strands with a different sequence of bipyridine and terpyridine units are "complementary" to each other and complexed with Cu^{2+} ions to selectively and exclusively form the corresponding heteroleptic double-stranded helicates (**349** and **350**), since the Cu^{2+} ion has a tendency to adopt a penta- or hexacoordinate geometry in contrast to the Cu^+ ion's preference over tetracoordination.[599−601] The complementary double-helical structures were confirmed by electron-splay ionization (ESI)-mass spectrometry and X-ray crystallographic analysis. The sequence information of the molecular strands was thus successfully read out and processed through the metal ion complexation.

In general, helicates embrace transition metal ions as templates for the oligopyridine-based molecular strands, whereas typical metal ions were rarely employed. In particular, group I metal ions exhibit a nondirectional and

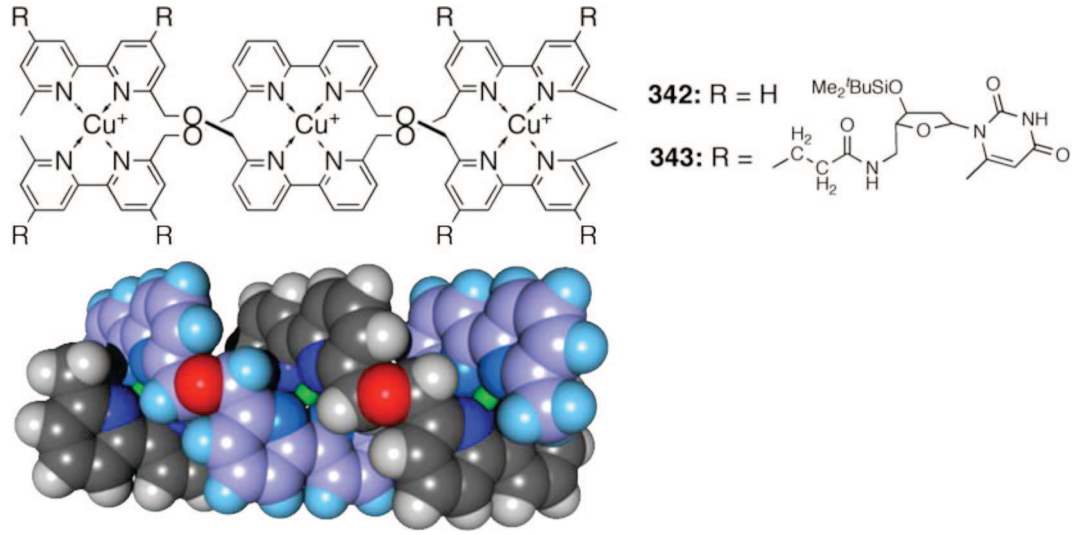

Figure 85. Structural formulas of the Cu(I) helicates (**342**, **343**, top) and a space-filling drawing of an energy-minimized structure of **342** (bottom).

inherently weak bonding, so that they will not readily form helicates with oligopyridine ligands. Nevertheless, the first helicate consisting of a typical metal ion, Na^+ wrapped by two ring-shaped rigid strands (**351**) in a double-helical arrangement, has been developed by Bell and Jousselin (Chart 33).[602] A compartmental bridging ligand (**352**) containing two chelating tridentate *N*-donor arms connected by an anionic -BH_2- bridge forms a dinuclear double-stranded helicate with two K^+ ions.[603] The double-helical structure was revealed by an X-ray crystallographic study for the first time as a typical metal helicate. Sauvage and Dietrich-Buchecker have reported that a phenanthroline-based rigid ligand is versatile for the synthesis of a double-stranded helicate containing three Li^+ ions (**353a**), which is surprisingly stable and further converted into a [2]catenane (**353b**) by the ring-closing metathesis reaction.[604]

It was not until 2006 that boron was used as a typical metal to construct double-stranded helicates. A mixture of sodium borohydride and *ortho*-linked hexaphenol, a class of oligo(*m*-phenylene)s, in 1,2-dichloroethane/ethanol (1/1, vol/vol) at 80 °C gives rise to the formation of a spiroborate-containing helicate.[605] The X-ray single-crystal analysis revealed the double-stranded helical structure of the complex (**354**), in which the two strands are bridged by spiroborates formed from the terminal biphenol units and the boron atoms. Interestingly, an octacoordinated sodium cation is found at

Chart 31. Optically-Active Helicates with a Twist-Sense Bias Caused by Chiral Induction or Resolved by Chromatography

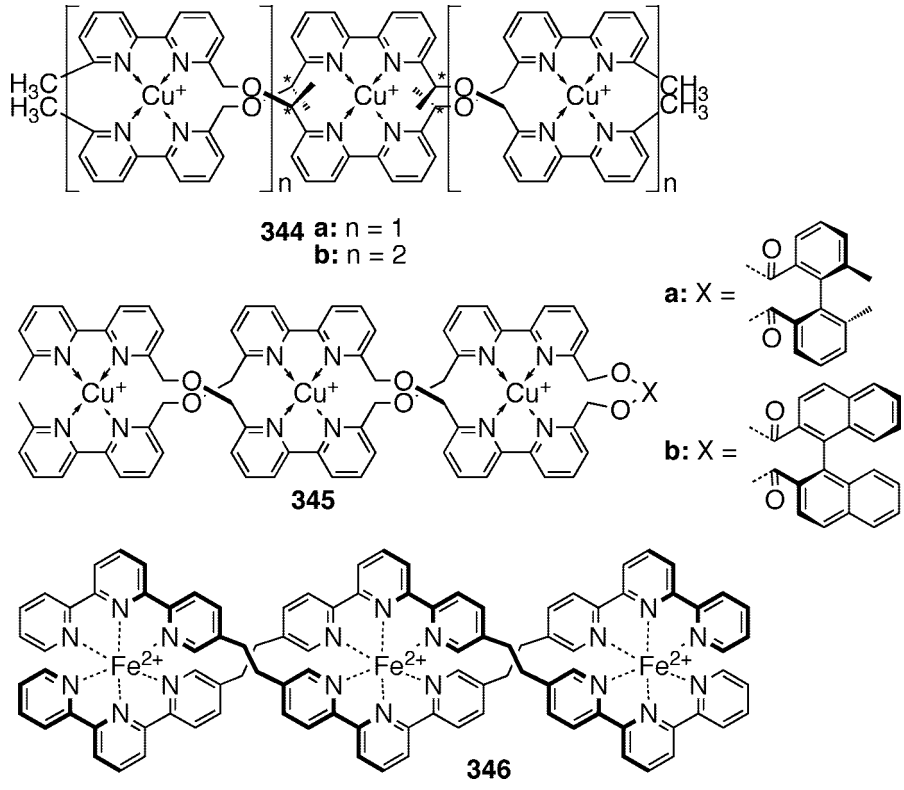

Scheme 25. Self-recognition in the Self-assembly of the Double Helicates (348a−d) from a Mixture of the Oligobipyridine Strands (347a−d) and Cu(I) Ions[a]

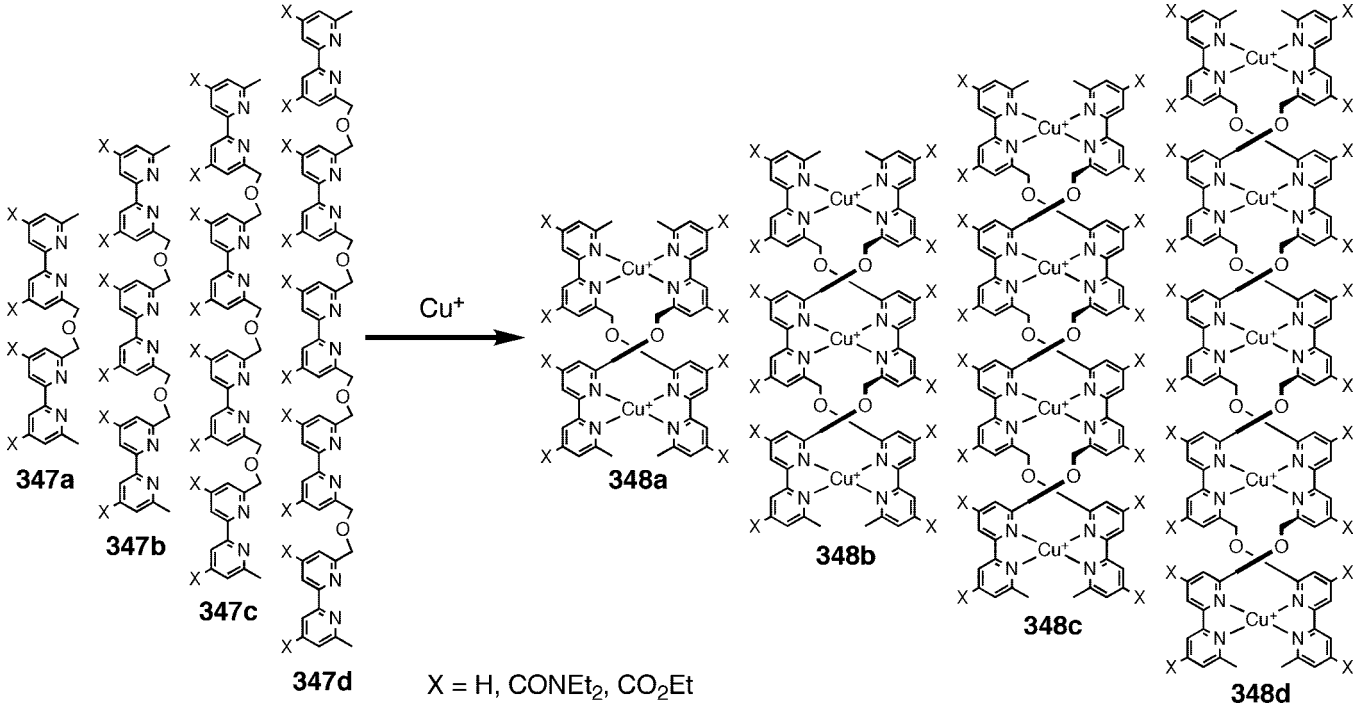

[a] Counteranions are omitted for clarity.

Chart 32. Heterotopic Helicates Composed of Molecular Strands Complementary to Each Other (349 and 350)

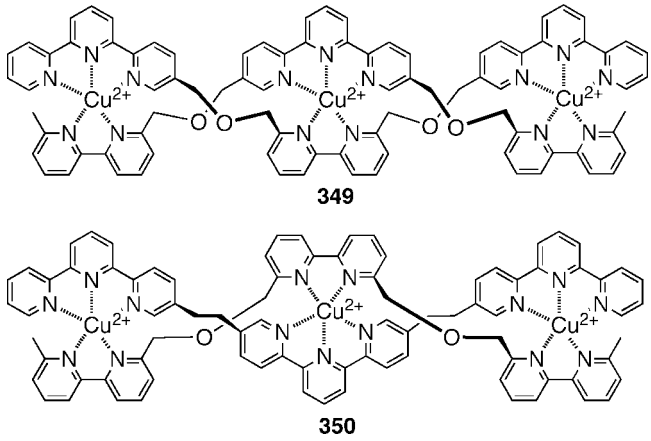

the center of the complex. Both enantiomers of (±)-**354** can be resolved by the diastereomeric salt formation through a cation exchange using a chiral ammonium salt as the resolving agent, followed by further cation exchange with an achiral ammonium salt. The spiroborate groups are chemically so stable that neither the racemization nor decomposition of the helicate took place after heating in acetonitrile and methanol.

Although some examples of triple-stranded helicates were already known for those with natural or synthetic ligands before the term helicate was introduced, Williams and co-workers reported for the first time a fully characterized, triple-stranded helicate with the X-ray crystal structure ($[Co(II)_2(\mathbf{355})_3]^{4+}$), being aware of the concept of helicate (Figure 86).[606] Later on, they transformed the labile cobalt(II) triple-stranded helicate ($[Co(II)_2(\mathbf{356})_3]^{4+}$) into the kinetically stable cobalt(III) helicate ($[Co(III)_2(\mathbf{356})_3]^{6+}$) and achieved optical resolution by chromatography using an optically active aqueous eluent.[607]

Oligobipyridines connected at the 6 positions are suitable for producing double-stranded helicates upon complexation with metal ions that undergo tetrahedral coordination, whereas they fail to give self-assembled triple-stranded helicates as a result of steric crowding around the metal ions. Lehn and co-workers designed new oligobipyridine strands by shifting the linkages from the 6- to 5-positions, and they have synthesized a triple-stranded helicate using hexacoordinate nickel(II) ions ($[Ni(II)_3(\mathbf{357})_3](ClO_4)_6$).[608] X-ray crystallography unambiguously determined the triple-stranded helical structure of $[Ni(II)_3(\mathbf{357})_3](ClO_4)_6$, in which the three nickel(II) ions are wrapped around by the three intertwined oligobipyridine strands. Interestingly, the single crystals contain only one of the two triple-helical enantiomers, either right-handed or left-handed, and their solutions showed Cotton effects that are mirror images of each other. Thus, the spontaneous resolution of $[Ni(II)_3(\mathbf{357})_3](ClO_4)_6$ was achieved.

Taking full advantage of a phenanthroline-based rigid ligand for the synthesis of a double-stranded helicate, a topologically nontrivial trefoil knot (**359**, Figure 87) has been prepared.[609] The copper(II)-bound double-stranded helicates (**358a** and **358b**) used as precursors were allowed to react with hexaethyleneglycol diiodide in the presence of cesium carbonate, giving the desired knots (**359a** and **359b**) in 3 and 29% yields, respectively.[610,611] In addition, both enantiomers of **359b** can be separated by diastereomer salt formation through the counteranion exchange from the triflate to an optically pure binaphthyl cyclic phosphate.[612,613] By further anion exchange to achiral hexafluorophosphate anions, both enantiomers were obtained with an excellent enantiomeric excess of higher than 98% ee. The left-handed configuration has been assigned to the dextrorotatory knot on the basis of an X-ray crystal analysis.

Chart 33. Typical Metal Helicates (353 for Li and 354 for B) and Molecular Strands That Form the Typical Metal Helicates (351 for Na and 352 for K)

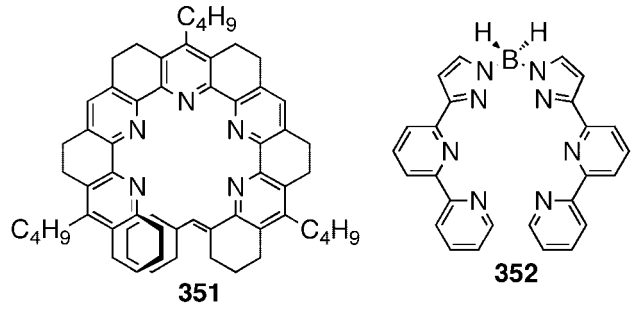

351 352

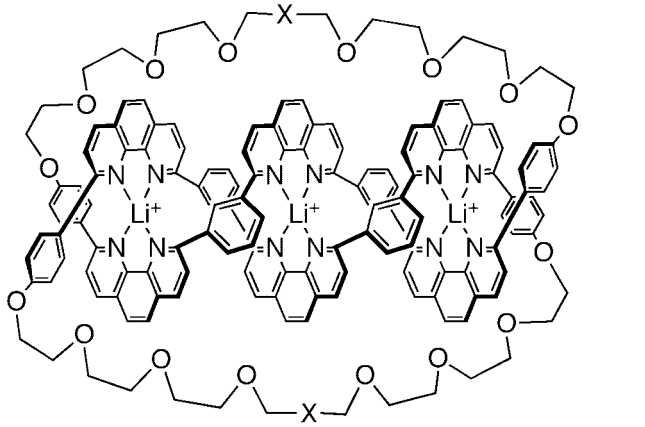

353 **a:** X = CH=CH$_2$ CH=CH$_2$
b: X = CH=CH

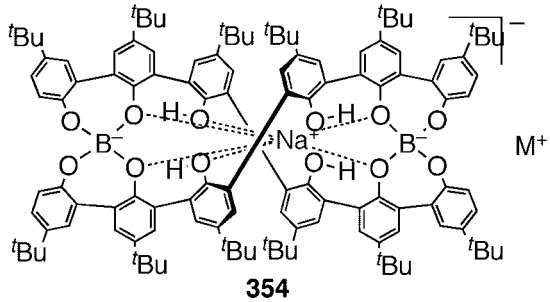

354

4.2. Aromatic Oligoamides

A very interesting class of metal-free double-stranded helices has been prepared by Lehn, Huc, and co-workers using aromatic oligoamides consisting of alternating 2,6-diaminopyridines and 2,6-pyridinedicarboxylic acids (**360**) (Figure 88).[34,614] An intramolecular interaction between the amide NH protons and the pyridine nitrogen atoms is responsible for the curved conformation of the molecular strands, which further dimerize into stable double helices in solution, primarily driven by aromatic interactions between the pyridine rings located on top of each other. The oligomeric strands are in a dynamic exchange equilibrium between single and double helices, and the equilibrium shifts to double helices at low temperatures, whereas the double helices dissociate into single strands at high temperatures, thus showing a distinct temperature-dependent, dynamic double-helical property. Both the single- and double-helical structures were fully characterized by NMR and X-ray crystallography. Interestingly, the hybridization of the aromatic oligoamide strands of this kind is limited to a certain chain length.[615] Huc and co-workers showed that the double-helix formation increased with the strand length to reach a maximum value and that, "somewhat counterintuitively", it decreased for longer strands. The chain-length dependence of the stability of the double helices is considered due to the consequence of two competing factors; i.e., the enthalpic gain of dimerization decreases as the strand length increases, whereas the entropic loss also decreases. The significant contribution of interstrand interactions between the side chains to the stability of the double helices has been pointed out by careful investigation of the solid as well as solution structures of the oligoamide double helices with different side chains.[616,617]

Huc et al. found an intriguing reactivity change driven through the double-helix formation of analogous oligoamide strands. Folding into double helices is anticipated to reduce the specific reactivity of the central units of the strands (Figure 89).[618] In fact, self-assembly of the oligopyridine-dicarboxamide strands (**361**) into double helices inhibited the *N*-oxidation of the central pyridine rings in the sequence. Surprisingly, the double-helix formation of the aromatic oligoamide strands significantly enhanced the *N*-oxidation of the pyridine rings peripheral in the sequence. X-ray crystallography and ^{1}H NMR studies showed that the *N*-oxidized strands (**362**) can still self-assemble into homostranded double helices (Figure 89B). The resultant oligoamide strands with *N*-oxide functionalities at both ends (**362**) cross-hybridize with the non-*N*-oxide strands (**361**) into heterostranded double helices, of which the stability relies on electrostatic interactions between the amide, pyridine, and pyridine *N*-oxide moieties, as suggested by an X-ray crystallographic analysis (Figure 89C).[619]

The replacement of a pyridine ring in **360b** with a 1,8-diazaanthracene unit enlarges the helix diameter by 4.7 Å parallel to the long anthracene axis in **363**, resulting in a spectacular stabilization of the double helices derived from these strands with the K_{dim} of *ca.* 10^7 M^{-1} (Figure 90).[620] Based on the van't Hoff study along with an X-ray crystallographic analysis and MM calculations, the duplex stabilization has been assigned to enthalpic effects, which were attributed to an enhanced surface area of the aromatic rings as well as a decrease in a tilt angle with respect to the helix axis. The latter results in a smaller dihedral angle at the aryl−amide linkages, thus significantly lowering the enthalpic cost of the springlike extension of the molecular strands during the dimerization process.

Analogous oligomers of 7-amino-8-fluoro-2-quinolinecarboxamide (**364**) also give rise to stable double helices in solution (Figure 91).[621] Unexpectedly, a tetrameric oligoamide (**364a**) has been found to adopt a double-helical conformation with a large helical pitch, which further self-assembled into a quadruple helix both in solution and in the solid state. In contrast, the octameric oligoamide (**364b**) formed only the double helix, and no further self-assembly into quadruple helix could be attained.

Some water-soluble helical foldamers bearing ammonium side chains (**365**, **366**) have recently been successfully employed for biological applications (Chart 34). A water-soluble quinoline-based helical tetramide (**365**) stabilized the human telomeric G-quadruplex as strongly as the potent ligand, telomestatin.[622] Upon complexation, a CD band was induced at *ca.* 400 nm in the absorption region of the quinoline chromophore, suggesting that a preferred-handed helical conformation is induced on **365**. These observations imply that a more selective binding is possible by imposing a right- or left-handedness by introducing chiral residues.

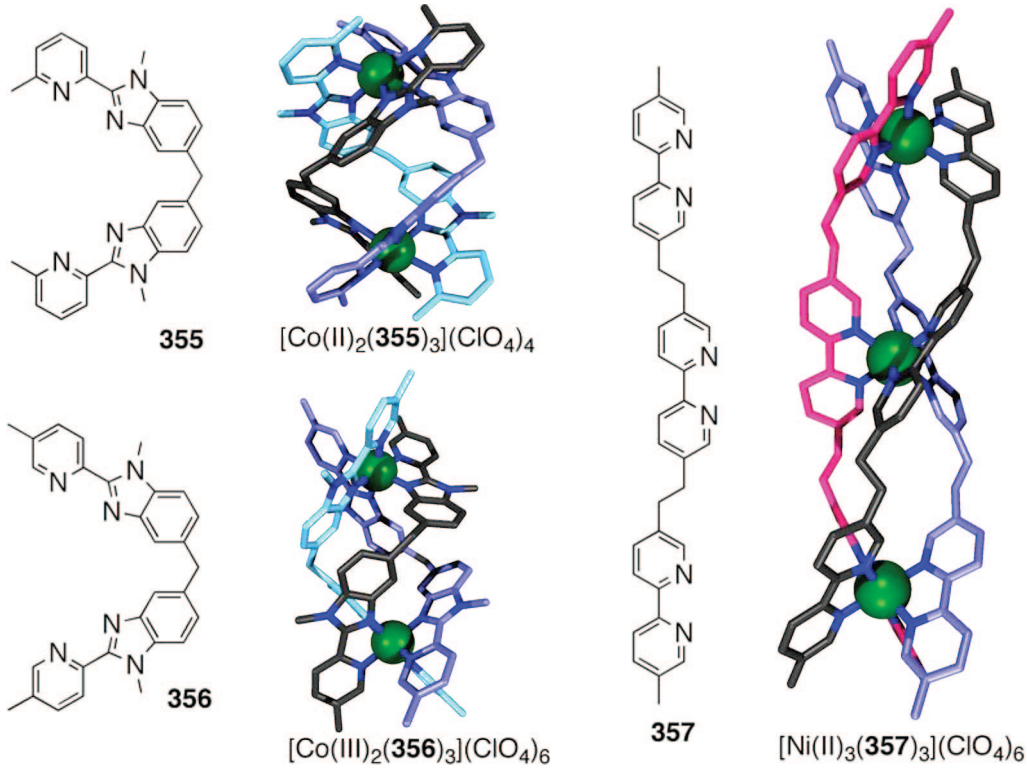

Figure 86. Structural formulas of the molecular ligands that form the triple-stranded helicates and capped-stick representations of the single-crystal structures of the triple-stranded helicates.

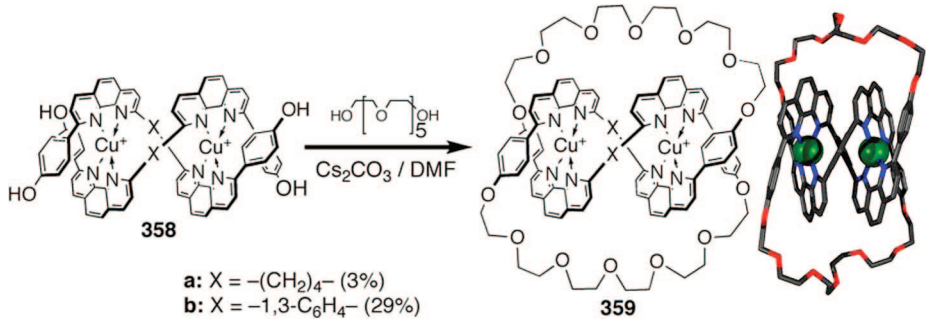

Figure 87. Synthesis of the trefoil knot (**359**) from the double-stranded helicate (**358**) and a capped-stick representation of the single-crystal structure of **359b**.

Huc and co-workers also investigated the toxicity of the water-soluble helical oligoamides by a DNA transfection assay using HeLa cells.[623] The fluorescein-functionalized octamide (**366**) was found to localize within the cytoplasm and in nucleoli, and the uptake was comparable to that of the well-known transporter HIV Tat peptides.

4.3. Complementary Double Helices Based on an Amidinium-Carboxylate Salt Bridge

The hydrogen-bonding interaction is a readily available versatile tool for constructing supramolecular assemblies.[624] However, it is still a difficult and challenging task to design double helices of which the formation is predictable, since most duplexes assembled by hydrogen-bonding interactions result in zipper or ladder structures.[625] Recently, rationally designed artificial complementary double helices bound together through amidinium-carboxylate salt bridges have been synthesized (**367·368**) (Figure 92).[626] Amidinium-carboxylate salt bridges have been widely used as a joint for constructing various supramolecular assemblies, since they have a well-defined geometry by their nature of double hydrogen bonding and high association constants even in polar media arising from the partially charged structure. The key to the success is the *m*-terphenyl-based, rigid π-conjugated backbones, which prevent the duplexes from taking any conformations other than double helices. The bisamidine and dicarboxylic acid strands (**367** and **368**) immediately form a duplex (**367·368**) in chloroform, which is evidenced by its ^{1}H NMR and mass spectra. An X-ray crystallographic study unambiguously has revealed the right-handed double-helical structure of **367·368**, which is retained in solution, as indicated by its strong Cotton effects in the absorption region of the diacetylene linkages. The double helices are synthetic compounds of a new class consisting of two complementary molecular strands that are entwined through a hydrogen bonding interaction, similar to DNA.

Related to this, Wisner and co-workers synthesized an alternate pentamer (ADADA, **369**), employing pyridine and 1,4-thiazine-1,1-dioxide as a hydrogen acceptor (A) and donor (D), respectively (Scheme 26).[627] The pentamer

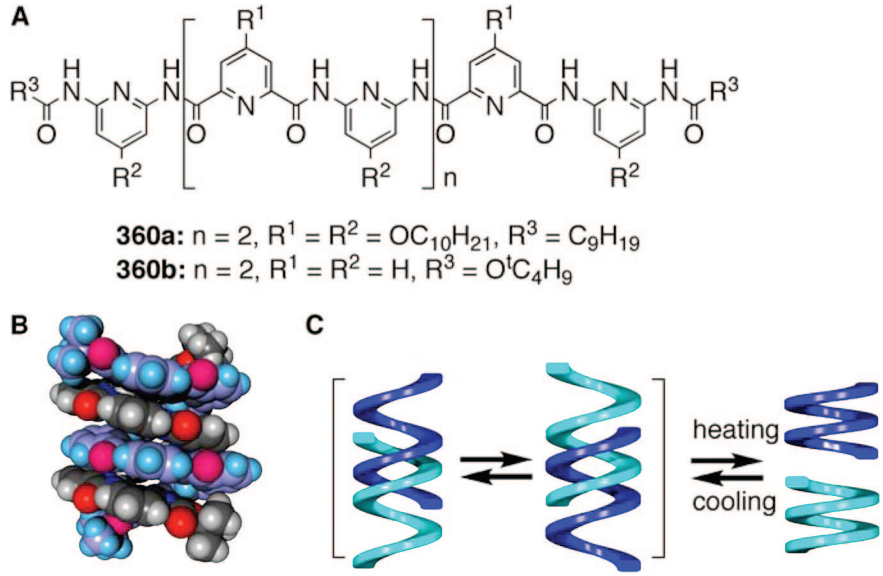

360a: n = 2, $R^1 = R^2 = OC_{10}H_{21}$, $R^3 = C_9H_{19}$
360b: n = 2, $R^1 = R^2 = H$, $R^3 = O^tC_4H_9$

Figure 88. (A) Structural formulas of the oligopyridinecarboxamides (**360**), (B) the X-ray single-crystal structure of **360b**, and (C) schematic representation of the interconversion between two identical forms of dissymmetrical double helices by a sliding motion, and their dissociation into two single helices. (Reproduced with permission from ref 34. Copyright 2000 Nature Publishing Group.)

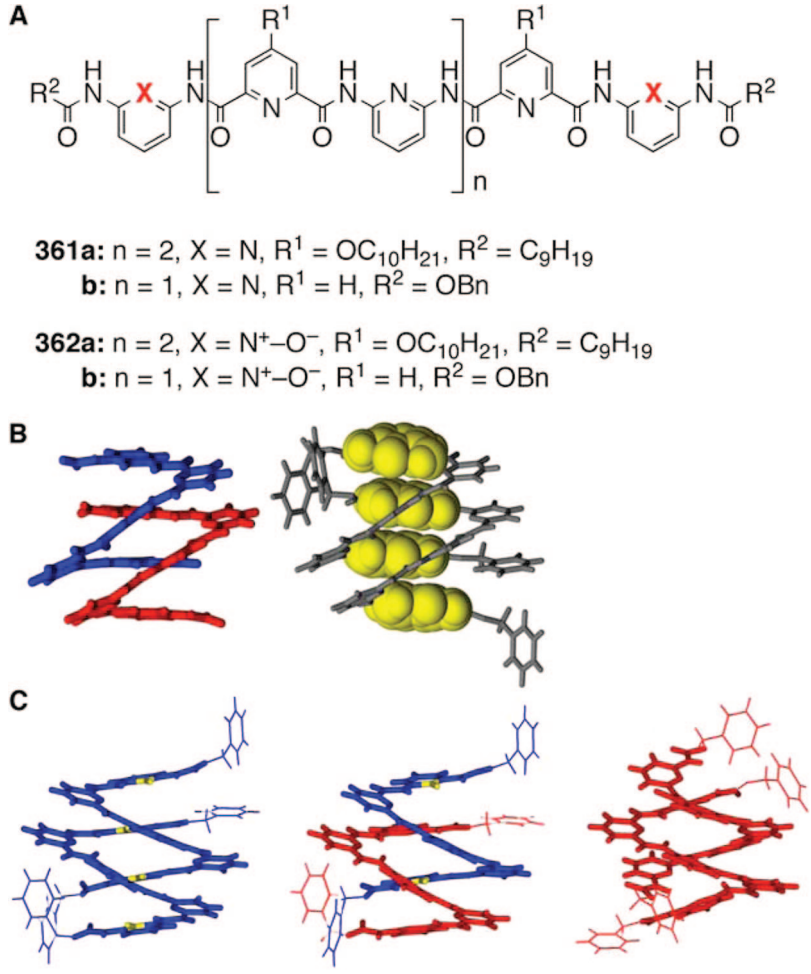

361a: n = 2, X = N, $R^1 = OC_{10}H_{21}$, $R^2 = C_9H_{19}$
b: n = 1, X = N, $R^1 = H$, $R^2 = OBn$

362a: n = 2, X = N^+–O^-, $R^1 = OC_{10}H_{21}$, $R^2 = C_9H_{19}$
b: n = 1, X = N^+–O^-, $R^1 = H$, $R^2 = OBn$

Figure 89. (A) Structural formulas of the oligopyridinecarboxamides with (**362**) and without *N*-oxide functionalities (**361**). (B) Capped stick representation of the crystal structure of the double helix of $(\mathbf{362b})_2$. The benzyl side chains in the left model are omitted for clarity. The stack of four pyridine *N*-oxide rings is represented in CPK (right). (C) Capped stick representation of the crystal structures of $(\mathbf{362b})_2$ (left), **361b·362b** (center), and $(\mathbf{361b})_2$ (right). The *N*-oxide functions are shown in yellow. (Reproduced with permission from ref 619. Copyright 2006 Wiley-VCH.)

self-assembled to form a self-complementary double helix in a staggered fashion through hydrogen bonding interactions, which has been confirmed by the 2D ^{1}H NMR spectra as well as an X-ray single-crystal analysis.

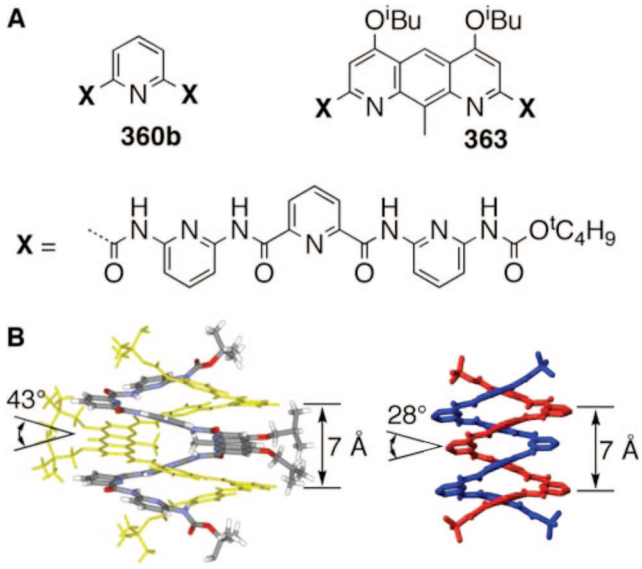

Figure 90. (A) Structural formulas of the oligopyridinecarboxamides (**360b** and **363**). (B) Side views of the crystal structures of **363** (left) and **360b** (right) at the same scale. Isobutyl side chains, hydrogen atoms, and included solvent molecules are omitted for clarity. (Reproduced with permission from ref 620. Copyright 2007 Wiley-VCH.)

One of the advantages of the complementary amidine/carboxylic acid system is that the double-helical structures and its helical sense are determined by the crescent-shaped *m*-terphenyl ligands and the chiral amidine substituents, respectively, so that various functional groups can be further introduced to the linker sites without breaking the double-helical structures.

In fact, complementary double helices bearing phenylene (**370**)[628] or azobenzene units (**371**)[629] as the linkers of the *m*-terphenyl units have been prepared (Scheme 27). Both of them also adopt a double-helical structure with a twist-sense bias. The duplex **371** is photoresponsive and undergoes a reversible double helix-to-double helix transformation through the *trans*/*cis* photoisomerization of the azobenzene linkers upon sequential UV and visible light irradiation in an alternating manner.[629] The detailed kinetics analysis and MM calculations suggest that the isomerization of the azobenzene residues of (*R*)-**371** synchronously proceeds at once in the form of a duplex without dissociation into each single strand accompanied by a change in its molecular length by *ca.* 15% through the *trans*/*cis* photoisomerization. Therefore, this double helix can be considered as a photoresponsive helical spring.

In a similar fashion, the complementary double helix bearing *trans*-Pt(II) complex moieties with pendant triphenylphosphine ligands as the linkers of the *m*-terphenyl units has been prepared (**372**).[630] The ^{1}H NMR and ESI-mass spectra support a double-helical structure in chloroform assisted by the salt bridge formation, of which a helical sense is biased by the chiral amidine residues, as evidenced by the distinct induced Cotton effects in the metal to ligand charge transfer (MLCT) band region of the achiral *trans*-Pt(II)−PPh_3 complex moieties. When treated with *cis*-1,2-bis(diphenylphosphino)ethylene (dppee) in chloroform for 1 h at ambient temperature, (*R*)-*trans*-**372** is quantitatively converted to the corresponding double helix (*R*)-*cis*-**373**, which also takes a preferred one-handed double helix. Furthermore, the treatment of (*R*)-*cis*-**373** with iodine in chloroform leads to the oxidatively induced reductive elimination of the (*R*)-*cis*-Pt(II)-dppee linkers, giving the original fully organic double helix with diacetylene linkers ((*R*)-**367**·**368**). Thus, the *in situ* double helix-to-double helix transformation has been achieved for the first time for synthetic double helices, driven by the chemical reactions.

The rational design of complementary dimeric double helices has been successfully extended to a supramolecular double-stranded helical polymer, (*R*)- or (*S*)-poly-**375**, in combination of the salt bridges with metal−ligand coordina-

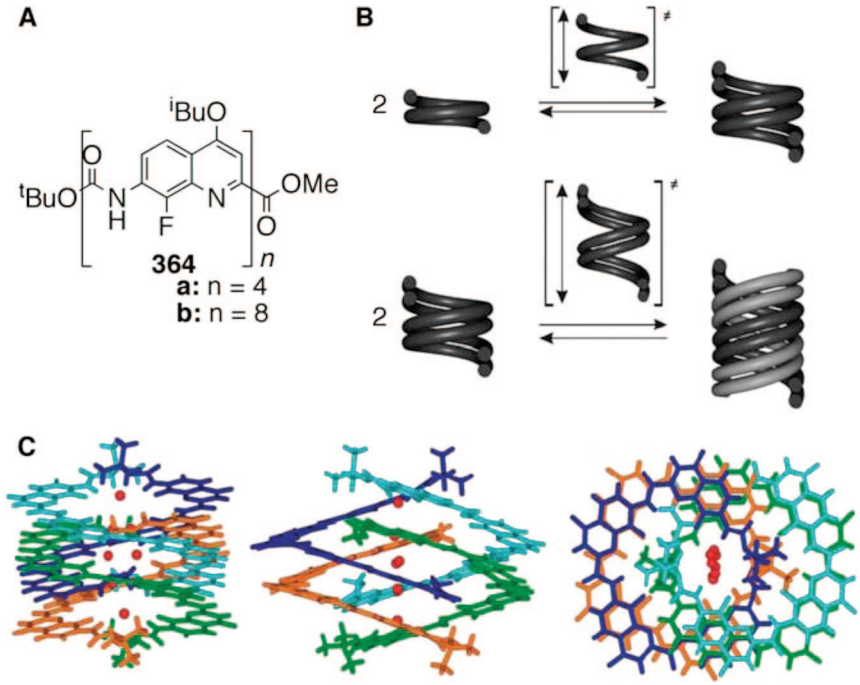

Figure 91. (A) Structures of the quinoxalinecarboxamides (**364**, left). (B) Schematic representation of the hybridization of a single helix to a double helix (top), and of a double helix to a quadruple helix (bottom), both through springlike extension. (C) Side views and top views of the crystal structures of **364a** as a quadruple helix. (Reproduced with permission from ref 621. Copyright 2008 Wiley-VCH.)

Chart 34. Structures of the Water-Soluble Quinolinecarboxamides (365, 366)

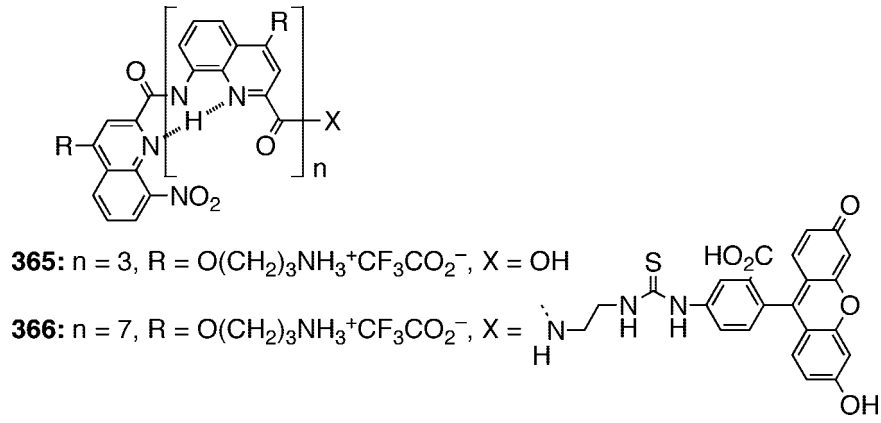

tion (Figure 93).[631] Upon mixing (*R*)-**374** with 2 equiv of *cis*-diphenylbis(dimethyl sulfoxide)platinum(II) (*cis*-$Ph_2Pt(DMSO)_2$) in 1,2-dichloroethane, the supramolecular polymerization readily proceeded at ambient temperature to yield (*R*)-poly-**375**, of which the formation was confirmed by ^{1}H NMR and DLS measurements along with the direct AFM observation. The polymers exhibit distinct Cotton effects in the MLCT region of the Pt(II) linkages, indicative of an excess one-handed double-helical structure in solution.

Lee et al. recently reported an interesting supramolecular double-helical polymer formation (Chart 35).[632] A bent-shaped bispyridine ligand bearing a dendron and Cu^{2+} ion formed the corresponding metallopolymer (**376**-Cu), which further self-assembles into a double helix, and the double-helix formation was confirmed by XRD and TEM measurements with the aid of the DFT calculations. In contrast, a similar metallopolymer prepared from the same bispyridine ligand with a Pd^{2+} ion (**376**-Pd) self-assembles into a lamellar structure. Chen and co-workers have also described a similar supramolecular double-helical polymer.[633] A self-complementary aromatic oligohydrazide (**377**) assembles into a zipper with a staggered fashion, leaving free hydrogen-bonding sites at the termini, with which the zipper further assembles to form a supramolecular zipper. Interestingly, an STM observation has revealed a polymeric double-helical structure for the 2D crystals prepared on HOPG.

The rational design of double helices has also been used for the synthesis of fully organic double-helical polymers

Scheme 26. Structure of ADADA Pentamer (369)

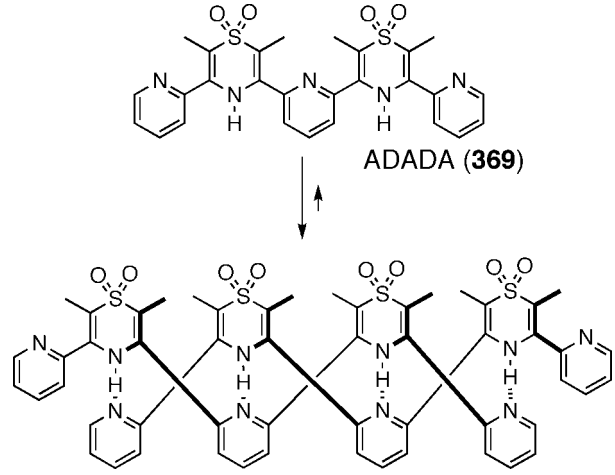

in another fashion by employing complementary homopolymers composed of amidine and carboxylic acid units, respectively (poly-(*R*)-**378** and poly-**379**), which are prepared by the Sonogashira polycondensation of the corresponding monomers (Figure 94A).[628] When mixed in THF, poly-(*R*)-**378** and poly-**379** assembled into a double-helical polymer that has a twist-sense bias, as evidenced from the absorption and CD spectra. The double-helical structure of poly-(*R*)-**378**·poly-**379** was revealed by XRD analysis of the uniaxially oriented films and further directly elucidated by high-resolution AFM measurements of the 2D crystals

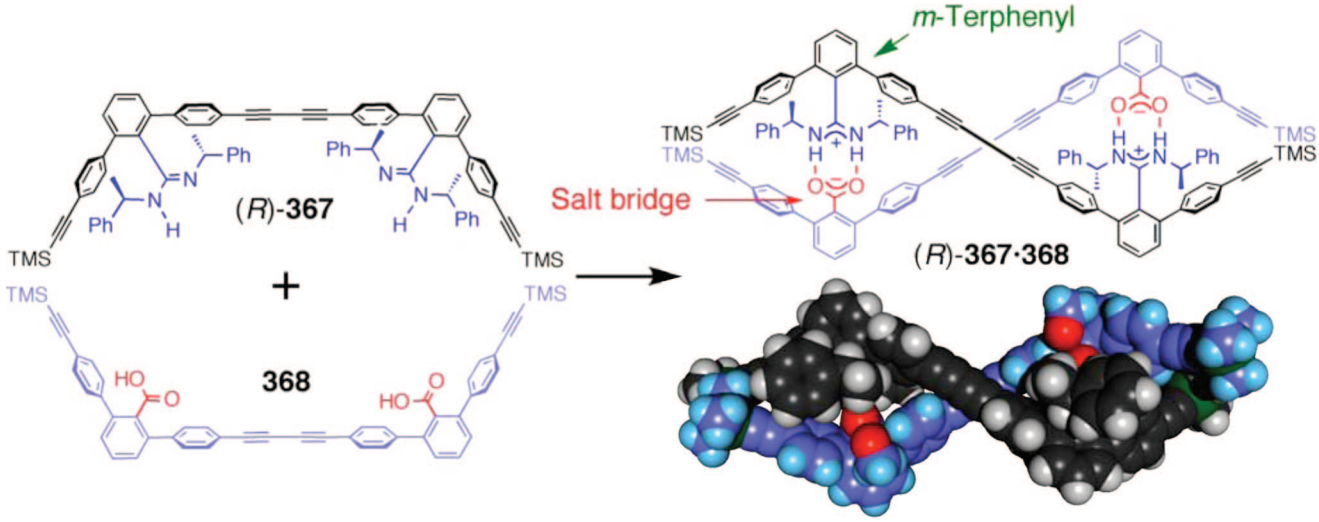

Figure 92. Complementary double-stranded helix formation and crystal structure of (*R*)-**367**·**368**.

Scheme 27. (A) Structure of the Double Helix Bearing *p*-phenylene Linkers (370). (B) Photoisomerization of (*R*)-*trans*-371 and (*R*)-*cis*-371. (C) Synthesis and *in-situ* Transformations of the Double Helices (372, 373, and 367·368)

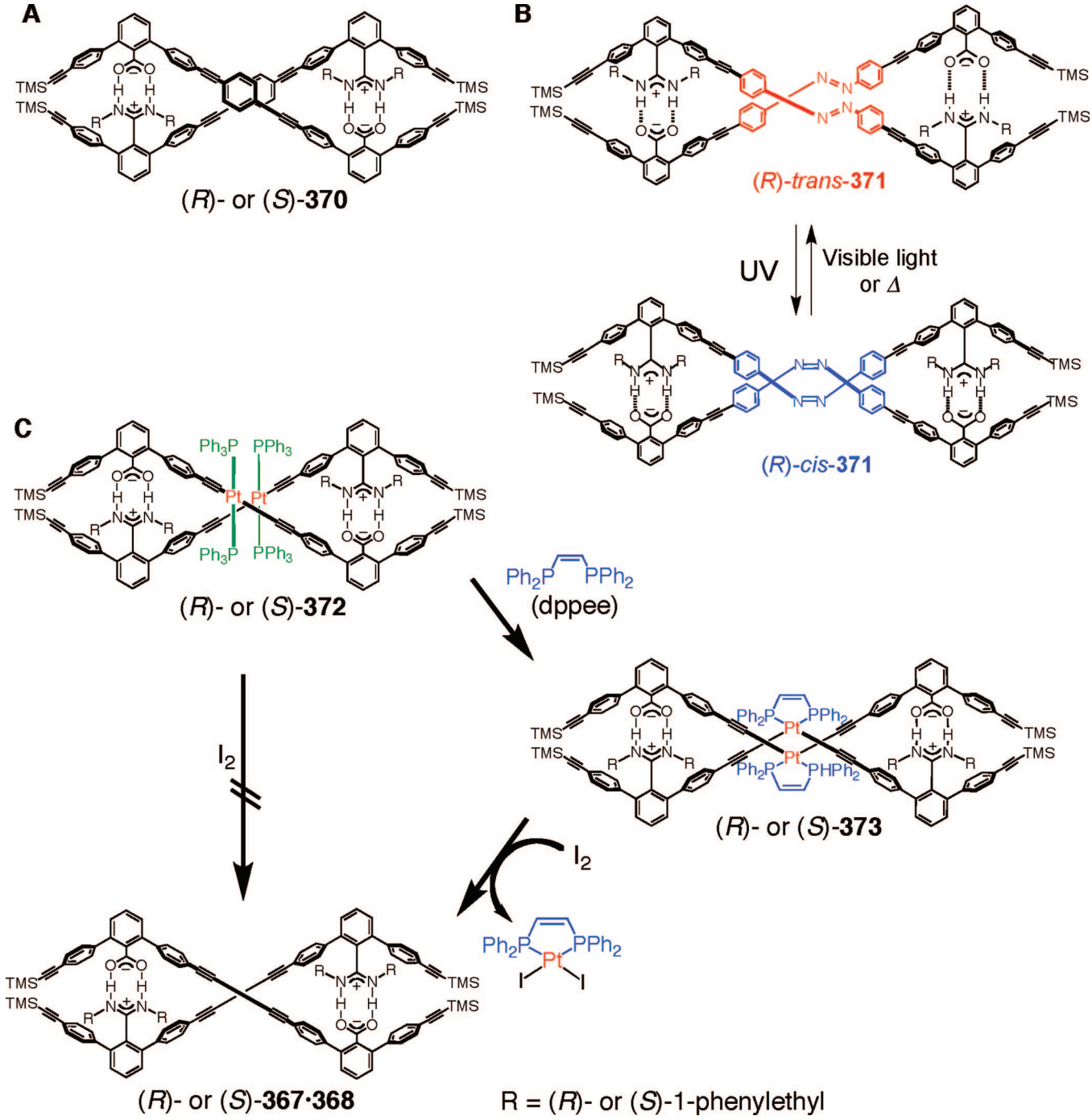

of the polymer complex adsorbed on HOPG followed by toluene vapor exposure for 12 h, which disclosed the helical pitch and its handedness (Figure 94B) (see section 3.2.2.1). In contrast, when mixed in less polar solvents, such as chloroform, the complementary strands kinetically form an imperfect double-helical polymer that contains a randomly hybridized cross-linked structure. This primary interpolymer complex is rearranged into the thermodynamically stable, fully double-helical polymer by untangling with an excess of TFA followed by neutralization with diisopropylamine (Figure 94C).

The sequence-specific double-helix formation is the most important feature of DNA and is an essential process for the self-replication and protein synthesis. The first step to crack the monopoly of nature is construction of synthetic double helices consisting of complementary molecular strands with sequence information. Six trimeric molecular strands with sequential information of the amidine and carboxylic acid (AAA, CCC, AAC, CCA, ACA, and CAC) have been synthesized in a stepwise manner (Figure 95A).[634] Upon mixing the six trimeric strands in chloroform, the complementary strands sequence-specifically and exclusively hybridize to form one-handed double-helical trimers (AAA·CCC, AAC·CCA, and ACA·CAC) through complementary amidinium-carboxylate salt bridges (Figure 95B). When CCA is added to an equimolar solution of AAA, AAC, and ACA, CCA binds the complementary AAC and selectively forms the double-helical AAC·CCA, which is isolated from the

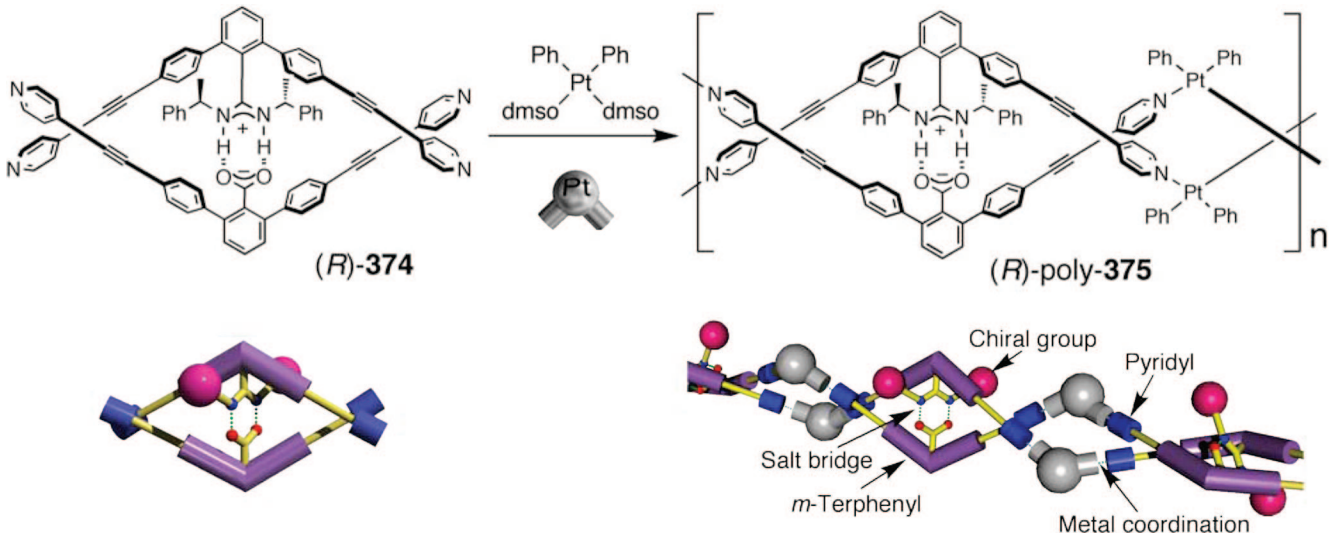

Figure 93. Synthesis of the double-stranded metallosupramolecular polymer with complementary strands (poly-**375**).

Chart 35. Structures of the Coordination Foldamer (376-M) and the Double-Helical Organogel (377)

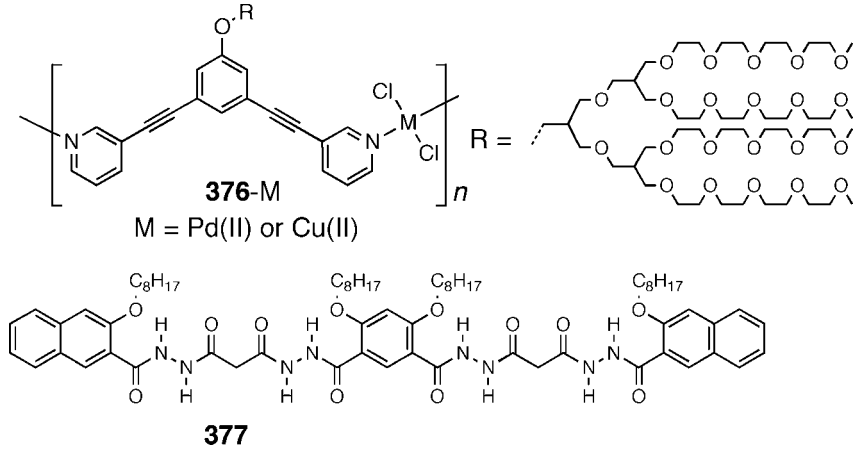

mixture by HPLC (Figure 95C). Moreover, the homo-oligomers of the amidine or carboxylic acid from monomers to tetramers (A, AA, AAAA, C, CC, and CCCC) assemble with a perfect chain-length recognition to form the complementary duplexes (A·C, AA·CC, and AAAA·CCCC), which can be separated by chromatography. As a consequence, the synthetic double-helical oligomers are capable of discriminating the structural information on the molecular strands, such as chain lengths and sequences, through the double-helix formation driven by the complementary amidinium-carboxylate salt bridge that is reminiscent of the complementary nucleic acid base pairs in DNA.

A platinum containing double helix composed of achiral amidine and carboxylic acid strands bridged by achiral diphosphine ligands (**382**) has been enantioselectively prepared by using the strategy of "helicity induction and memory" (Figure 96).[635] The double helices bearing achiral isopropyl groups on the amidine groups and chiral phosphine ligands (*R*)- or (*S*)-2-diphenylphosphino-2′-methoxy-1,1′-binaphthyl ((*R*)- or (*S*)-MOP) on the Pt(II)-acetylide linkers (*R*)- or (*S*)-**380·381** adopt a dynamic double-helical structure with a helix-sense bias, as suggested by an enhancement of the Cotton effects in the MLCT region of the Pt(II) complex linkers at low temperatures. Thus, the chiral phosphine ligands can induce a helix-sense bias of the double helices as in the case of chiral amidine groups. Interestingly, the bias in the helical sense in chloroform is inverted in toluene, as indicated by the inverted Cotton effect signs around the MLCT region. When treated with an excess of an achiral diphosphine with one methylene spacer, bis(diphenylphosphinomethane) (dppm), the dynamic double helix ((*R*)-**380·381**) readily undergoes the interstrand ligand exchange reaction and is quantitatively converted into the bridged double helix (+)-**382**, of which the bridged double-helical structure was unambiguously revealed by an X-ray crystallographic study. The bias in the helix-sense is maintained during the course of the ligand exchange reaction, as evidenced by the distinct and slightly shifted CD bands exhibited by (+)-**382**. The bridged double helices are quite stable toward racemization, as demonstrated by no change in the CD intensity observed after 100 days at 25 °C and 13 days at 50 °C in the dark. As expected, (−)-**382** prepared from the idential double helix (*R*)-**380·381** in toluene shows a complete mirror-image CD pattern except for the intensities due to the enantiomeric double-helical structures. Thus, both enantiomers of the bridged double helix can be synthesized with a single enantiomer of MOP by simply changing the solvents. The optically active bridged double helices when complexed with Cu(I) have been successfully applied to the asymmetric cyclopropanation of styrene with ethyl diazoac-

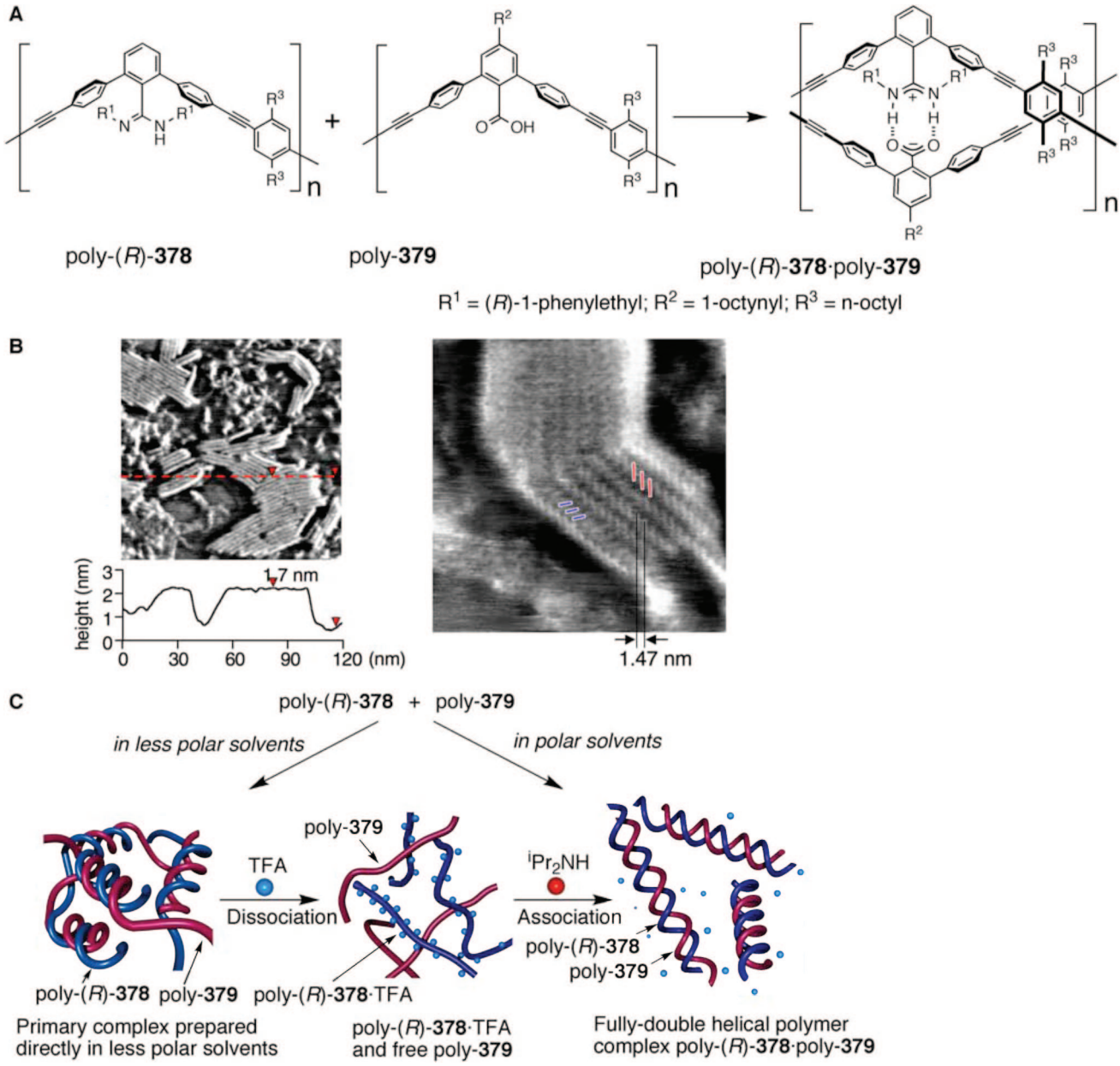

Figure 94. (A) Synthesis of the complementary double-helical polymer, (B) AFM phase images of (*R*)-**378·379** on HOPG with the height profile measured along the dashed line in the image (left) and its magnified AFM image (right), and (C) schematic illustrations of the possible mechanism for double-helix formation in $CDCl_3$/THF (99/1, v/v) through rearrangement of the primary complex by unraveling with TFA and neutralization with *i*-Pr_2NH. (Reproduced with permission from ref 628. Copyright 2008 American Chemical Society.)

etate, and a good asymmetric yield up to 85% ee has been achieved (section 5.2).

The preparation of discrete, well-defined 3D supramolecular assemblies still remains a synthetic challenge, although a variety of supramolecular arrays have been constructed on the basis of metal−ligand coordination or hydrogen-bonding interactions. In particular, multicomponent cylindrical complexes are limited to a few examples, mainly owing to the difficulty in controlling the heteroleptic complexation over the self-assembly process. The amidinium-carboxylate salt bridge system with *m*-terphenyl ligands generates a type of orthogonal complex and has a substantial compatibility with a wide range of functional groups, thereby enabling construction of multicomponent self-assemblies. When the chiral bisamidine ((*R*)-**383**) is mixed with 1,3,5-benzenetricarboxylic acid in organic solvents at the molar ratio of 3:2, the self-assembly process readily proceeds at ambient temperature to quantitatively yield the [3 + 2] cylindrical complex ((*R*)-**384**), of which the formation has been evidenced by the ^{1}H NMR and ESI-mass spectra along with an X-ray crystallographic analysis (Figure 97).[636] The cylinder is tilted in one direction by the chiral amidine substituents to form a one-handed triple helical structure, which is retained in solution, as indicated by the distinct Cotton effects in the absorption region of the diacetylene linkers. Furthermore, the multicomponent self-assembly of (*R*)-**383** and zinc 5,10,15,20-tetrakis(carboxyphenyl)porphyrin affords the corresponding [4 + 2] cylindrical complex ((*R*)-**385**) through specific salt bridges, which adopts an untwisted cylindrical shape, as suggested by the weak CD spectra and MM calculations. However, the cylindrical complex becomes

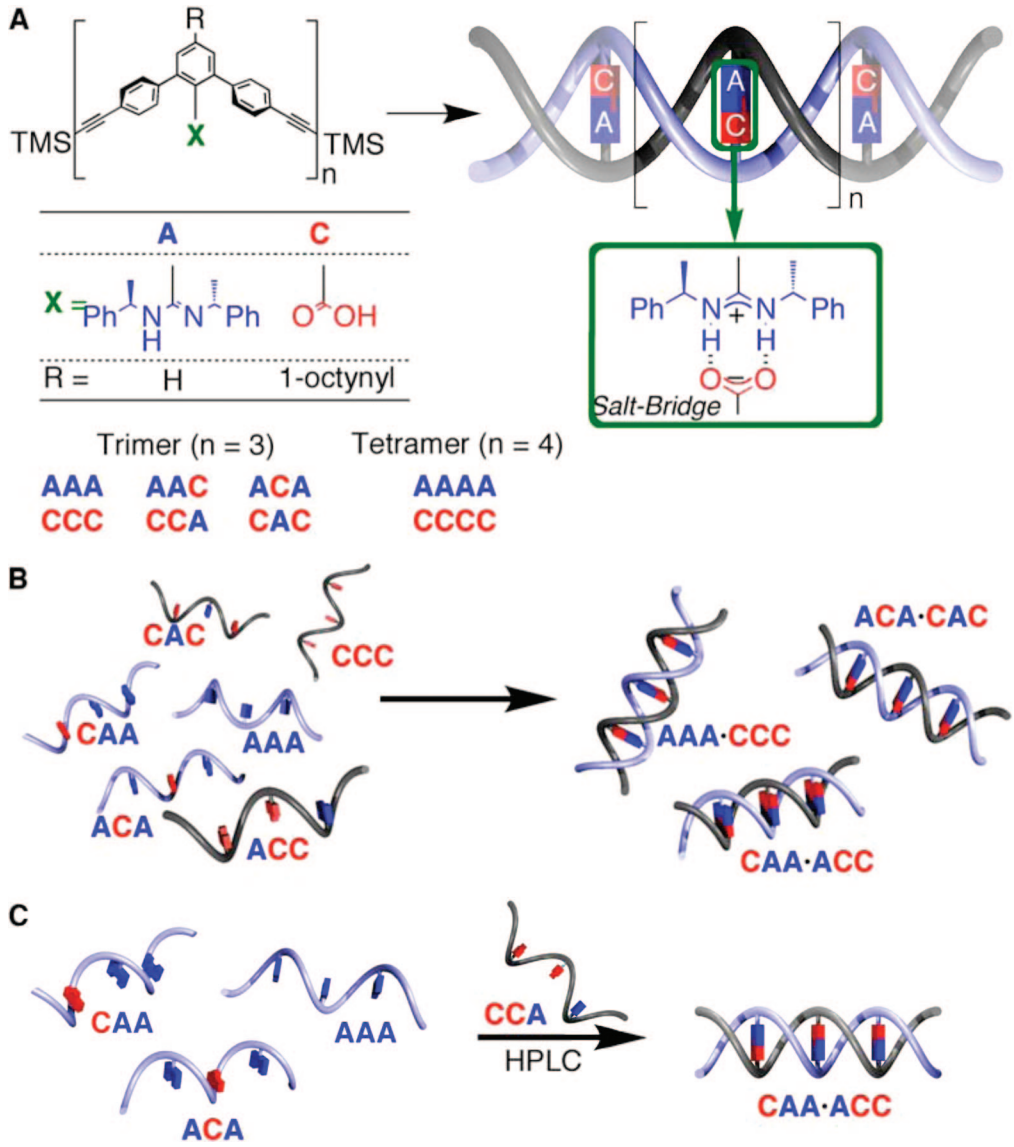

Figure 95. (A) Structures of *m*-terphenyl-based molecular strands bearing amidine and/or carboxyl groups and an illustration of double-helical oligomers consisting of complementary molecular strands stabilized by amidinium-carboxylate salt bridges. "A" and "C" denote the monomer units bearing the chiral amidine and achiral carboxyl groups, respectively. Schematic illustration of (B) the sequence-specific sorting of the six trimeric oligomers bearing amidine and/or carboxyl groups through double-helix formation, and (C) the sequence-specific binding and extraction of AAC with CCA from a mixture of AAA, ACA, and AAC.

twisted in one direction to take a one-handed quadruple helical conformation, upon sandwiching the 4,4′-bipyridine between the two porphyrin rings through a metal coordination, as evidenced by the absorption, CD, and ^{1}H NMR spectroscopies. Thus, these results demonstrate that the amidinium-carboxylate salt bridges bearing *m*-terphenyl ligands provide a means to construct various 3D supramolecular helical assemblies.

4.4. Poly- and Oligo(*m*-phenylene)s

Water-soluble helical polymers and oligomers are of particular interest, because most important biological events occur in water, where biomacromolecules adopt helical conformations. However, despite a number of synthetic helical polymers and oligomers that are soluble in organic solvents, water-soluble counterparts are quite rare and remain a synthetically challenging target in spite of the recent development in supramolecular chemistry.

Single-stranded helical foldamers based on the oligo- and poly(*m*-phenylene)s are known to form a 5/1 helical conformation in the solid state.[637,638] Surprisingly, the oligoresorcinols (**386**) with specific chain lengths have been found to self-assemble into well-defined double-stranded helical structures in water through interstrand aromatic interactions, as evidenced by a remarkable hypochromic effect in absorption spectroscopy, upfield shifts in ^{1}H NMR spectra, and vapor pressure osmometry (VPO) measurements, while they adopt a random-coil conformation in organic solvents, such as methanol (Figure 98).[639] An X-ray crystallographic study revealed that **386** ($n = 5$) forms single and double helices when crystallized from a chloroform/acetonitrile mixture and from water, respectively. Obviously, the single-helical structure immediately unravels once dissolved in organic solvents. In the solid state, the double-helical structure is stabilized by several $\pi-\pi$ and CH$-\pi$ interactions being in good agreement with the absorption and NMR results in water. The oligoresorcinols double helices formed in water exist as equimolar mixtures of the right- and left-handed forms. The introduction of an optically active group at both ends of the strand **387** induces an excess one-handed screw-

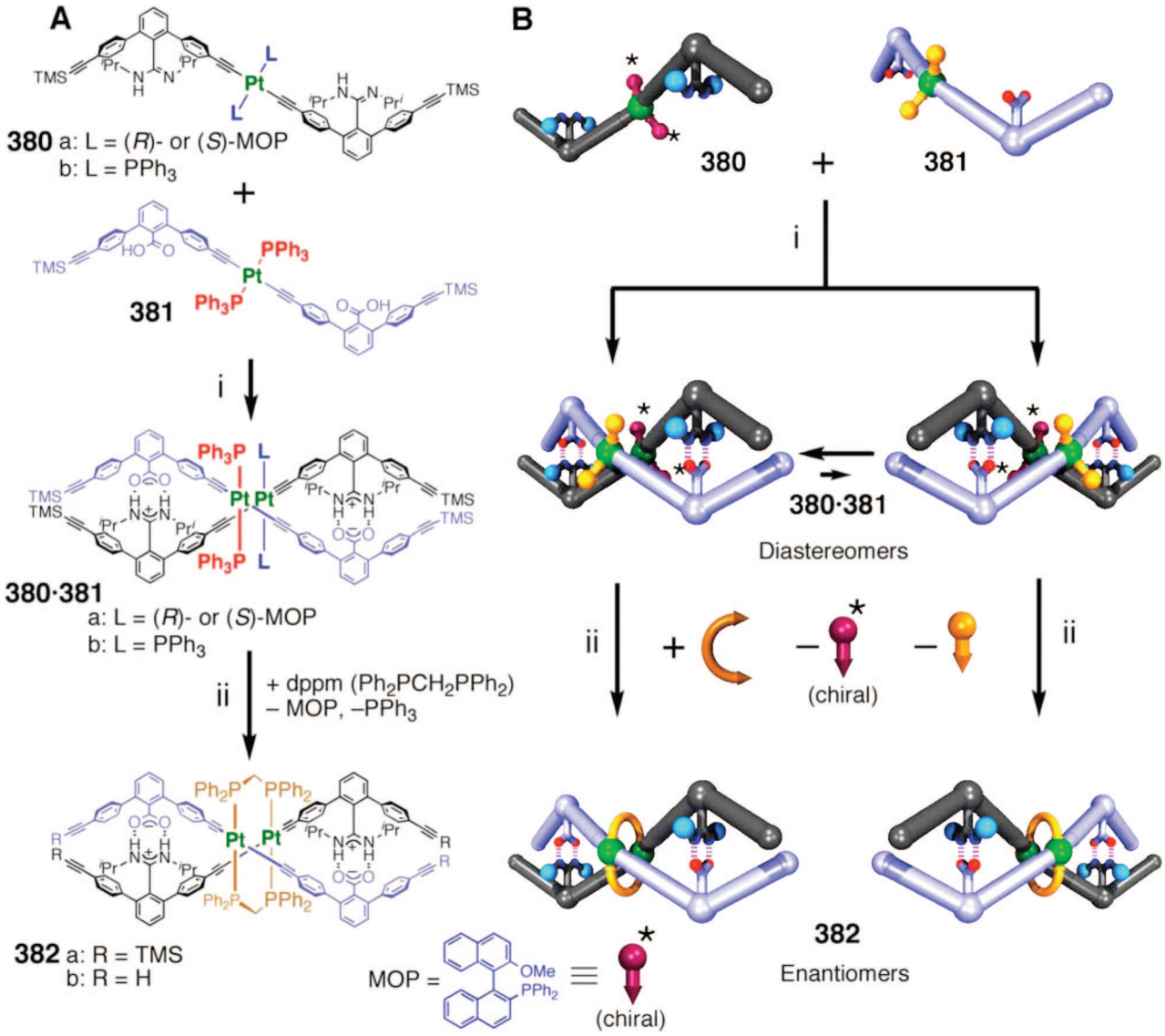

Figure 96. Enantioselective synthesis of complementary double-helical molecules. Schematic representation (A) and illustration (B) of the diastereomeric double-helix formation from complementary molecular strands (**380** and **381**) containing Pt(II) acetylide complex moieties through amidinium carboxylate salt-bridge formation (step i); the chiral phosphine ligand (MOP) induces diastereomeric double helices. Removal of the chiral ligands by ligand exchange on the Pt(II) with achiral diphosphine ligands (dppm) generates the enantiomeric double helices **382** with controlled helicity (step ii); the right- and left-handed double helices can be controlled by the type of solvent used. (Reproduced with permission from ref 635. Copyright 2007 Wiley-VCH.)

sense, thus showing an apparent Cotton effect in the main-chain chromophore region. In methanol, however, the oligoresorcinol shows no CD, as expected from the fact that it takes a random-coil conformation in methanol.

The thorough investigation of a series of chiral and achiral oligomers from 2mer to 15mer[640] has revealed that the double-helix formation of the oligoresorcinols in water is significantly affected by the external conditions, such as the solvent, pH, salt, and temperature, and has also a remarkable chain-length dependence, similarly to Huc's aromatic oligoamides;[615] the stability of the double helices increased with an increase in the chain length up to 11mer, while it remains the same for oligomers longer than 11mer. The detailed kinetic analysis of the chain exchange reaction between the double helices of the optically active and optically inactive 11mers discloses the double-helix formation mechanism; the chain exchange reaction is a very fast process with a small $\Delta S^{\ddagger}$ value, and proceeds not via a dissociation-exchange pathway, but via a direct exchange one.

The double-helix formation of the oligoresorcinols is significantly affected by pH, since they have the two acidic hydroxyl groups on each benzene ring.[1]H NMR, absorption, and CD spectroscopic investigations using optically active and inactive oligoresorcinols suggest that the double-stranded helices are unwound into the single strands through intramolecular hydrogen bonds in alkaline water as a result of the electrostatic repulsion between the two negatively charged strands by the deprotonation of the hydroxyl groups.[640] A preferred-handed helical sense can be induced in achiral **386** ($n = 9$) in alkaline water by the addition of water-soluble chiral compounds, such as ammonium salts, amines, and alcohols, thus providing a novel water-soluble chirality sensor.[641]

The double-helical **386** forms [3]pseudorotaxanes with β- and γ-CyDs having a twist-sense bias resulting from the chirality of the CyDs (Figure 98B), as evidenced by the ICDs, absorption, and ^{1}H NMR spectra.[642] The [3]pseudorotaxane with β-CyD reverts to the double helix upon the addition of

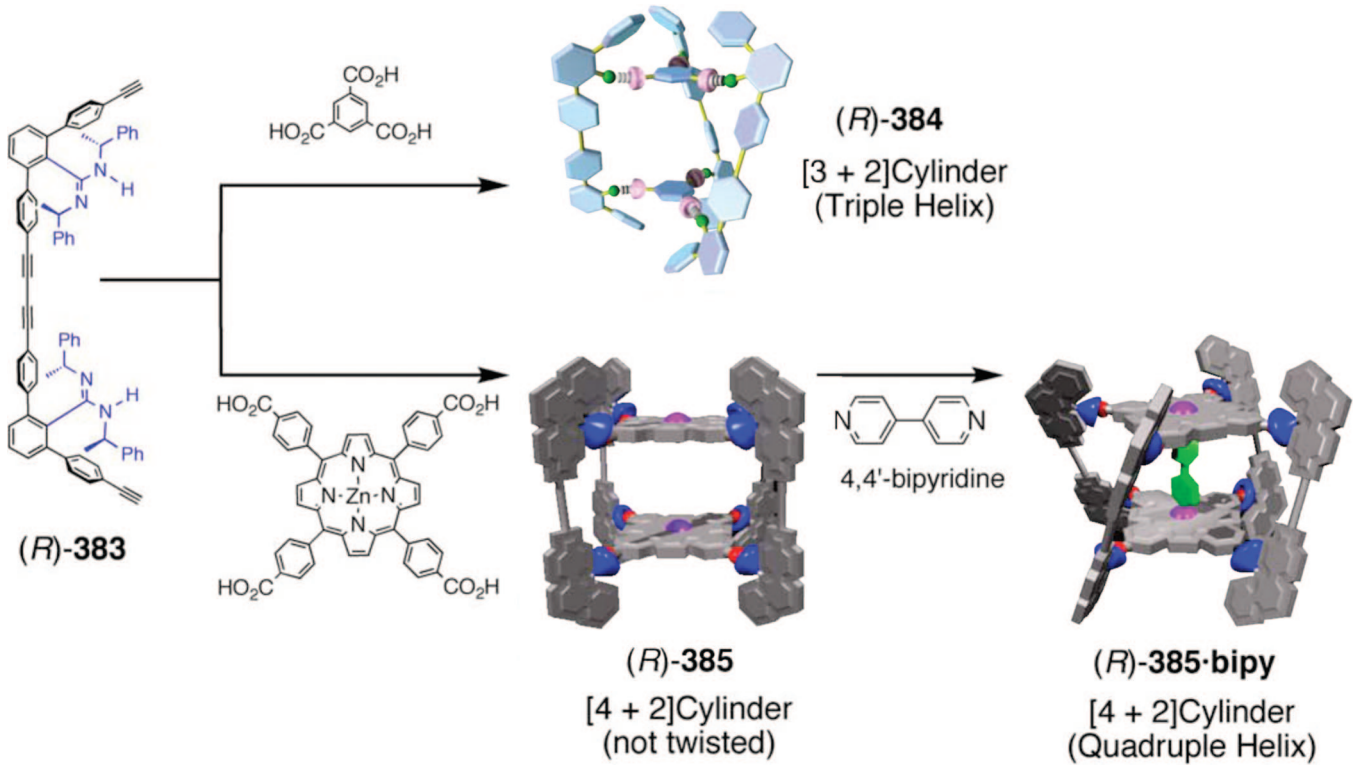

Figure 97. Schematic illustration of the formation of a [3 + 2] cylindrical complex ((*R*)-**384**), top) and of a [4 + 2] cylindrical complex ((*R*)-**385**), followed by sandwiching of 4,4′-bipyridine (bottom). (Reproduced with permission from ref 636. Copyright 2007 Wiley-VCH.)

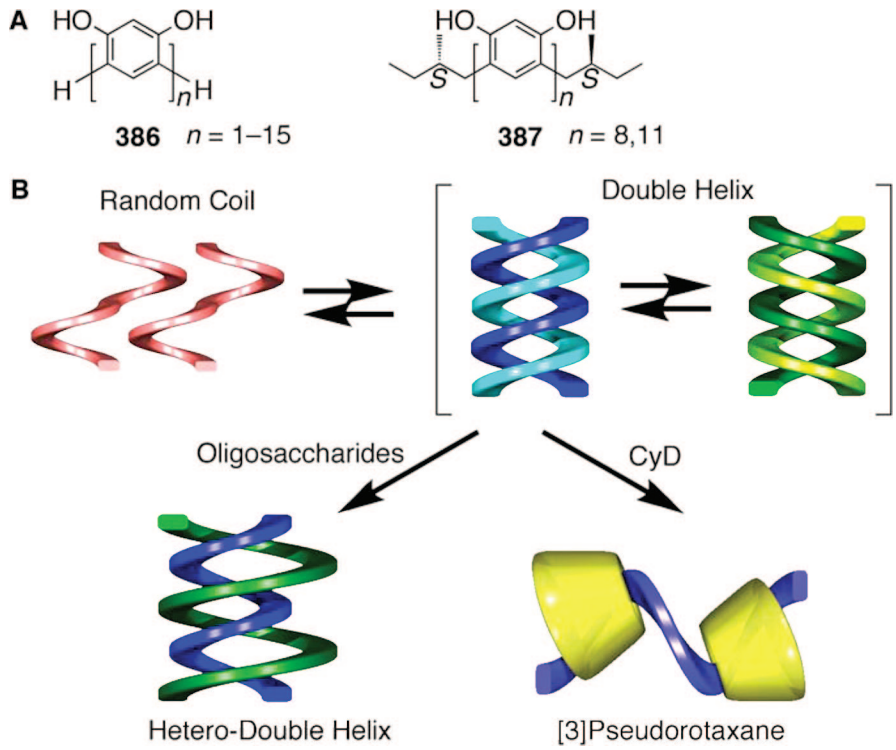

Figure 98. (A) Structural formulas of oligoresorcinols. (B) Schematic illustration of the double-helix formation of the oligoresorcinols and unwinding of the double helix followed by the [3]pseudorotaxane formation with cyclodextrins and the heterodouble-helix formation with linear oligosaccharides.

an adamantane derivative that forms an inclusion complex with the β-CyD. **386** also complexes with linear oligosaccharides, generating preferred one-handed heterodouble helices with a high stereoselectivity on the chain lengths and glycosidic linkage patterns.[643] The molecular recognition of oligosaccharides especially in water is still considered underdeveloped, as opposed to the well-established synthetic receptors for mono- and disaccharides. These results imply further possibilities and the importance of this conceptually new approach to saccharide recognition in water.

Poly(*m*-phenylene) derivatives bearing oligo(ethylene oxide) side chains at the 5-positions (**388**) have also been

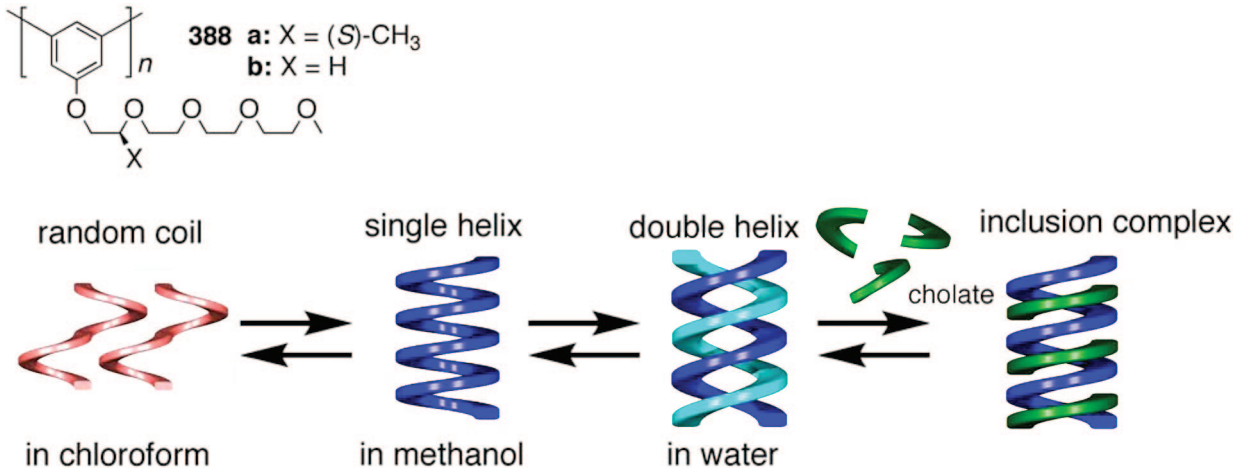

Figure 99. Schematic illustration of single-helix formation in methanol, double-helix formation in water of poly(*m*-phenylene)s bearing an oligo(ethylene oxide) side chain at the 5 position (**388**), and their inclusion complex formation with cholate in water. (Reproduced with permission from ref 645. Copyright 2009 The Royal Society of Chemistry.)

synthesized as a modification of the oligoresorcinols (Figure 99).[644,645] The poly(*m*-phenylene)s are soluble in chloroform owing to the oligo(ethylene oxide) side chains, where they take a random-coil conformation. In contrast to the oligoresorcinols, the poly(*m*-phenylene)s fold into a single-helical conformation in methanol through solvophobic interactions, as evidenced by the hypochromicity in the absorption spectra and upfield shifts in the ^{1}H NMR spectra. The poly(*m*-phenylene) bearing optically pure, chiral side chains (**388a**) adopts an excess one-handed helical conformation in methanol, of which the twist-sense bias is reversibly increased with decreasing temperature, indicating the dynamic nature of the single helix. Although **388a** is insoluble in water, the poly(*m*-phenylene) with achiral side chains (**388b**) is soluble in water, where it self-assembles into a double helix similar to the oligoresorcinols,[639,640] as supported by the hypochromicity in the absorption spectra and upfield shifts in the ^{1}H NMR spectra along with the DLS measurements. These results suggest that the poly(*m*-phenylene) is a useful structural motif for both single- and double-helical foldamers. Upon the addition of sodium cholate in water, the double-helical poly(*m*-phenylene) is transformed into single strands, which bind the cholate molecules to form an excess one-handed single helix.[645]

4.5. Miscellaneous

Yamaguchi and co-workers have reported that optically active acyclic ethynylhelicene oligomers (**389**) fold into a double-helical structure through solvophobic effects, of which the formation has been supported by ^{1}H NMR and CD analyses and VPO measurements (Chart 36).[646] The double-helix formation is highly dependent on the solvents; the double helices are favored in benzene, whereas they unfold into a monomeric random-coiled structure in chloroform. An interesting heterodouble-helix formation has also been observed between the pentamers bearing different substituents, a decyloxycarbonyl chain (**389a**) and an electron-withdrawing perfluorooctyl chain (**389b**).[647] Bis[hexa(ethynylhelicene)] derivatives with either a flexible hexadecamethylene linker (**390a**) or a rigid butadiyne linker (**390b**) also form an intramolecular double helix, as revealed by ^{1}H NMR and CD spectroscopies and VPO studies.[648] Upon heating in toluene, the intramolecular double helix is unfolded into a random coil, which folds into the double helix again when cooled. Interestingly, the folding rate is highly dependent on the concentration, implying the involvement of self-catalysis.

Inouye and co-workers have found that pyridine/pyridone alternate co-oligomers (**391**) self-assemble into a dimer, presumably a double helix, through hydrogen bonds, as evidenced by the ^{1}H NMR and VPO analyses.[649] Upon the addition of organosoluble monosaccharides, the duplexes are unraveled and bind the saccharides to form an excess one-handed single-helical inclusion complex, showing distinct Cotton effects in the absorption region of the π-conjugated oligomeric backbones.

Luh et al. reported an interesting structure analogue of DNA based on a complete synthetic skeleton.[650] A bis-norbornene derivative with a ferrocene linker has been subjected to ring-opening metathesis polymerization to yield a double-stranded polymer (**392**). STM measurements have shown several structures, of which a double helix with geometric parameters is very similar to those of the natural DNA, such as helical pitch. However, according to the MM calculations, the double-helical structure is less stable than the other structures, such as supercoiled and ladder structures. By incorporating a chiral ferrocene spacer, the resultant ladder polymers likely adopt an excess one-handed double-helical structure, supported by the CD spectra and STM images along with the MD simulations.[651] Using an analogous polynorbornene as the template, a kind of synthetic replication system, giving a complementary polymer, has been achieved.[652]

Noncyclic 2,6-bis(2-oxazolyl)pyridine (Pybox) derivatives are well-known ligands for catalytic asymmetric reactions.[653,654] Sada and co-workers have ingeniously constructed a supramolecular double-helical ladder (**393**), utilizing stable Pybox-secondary ammonium salt complexes,[655] of which the formation is driven by double hydrogen-bonding interactions.[656] An achiral poly(trimethylene iminium) salt forms a ladder polymer with a zinc porphyrin bearing two C_2-chiral bis(Pybox) ligands. Twisted by the chiral Pybox units, **393** adopts a preferred-handed double-helical conformation in solution, which has been confirmed by CD and AFM measurements.

As opposed to the ordinary helicates, of which the molecular strands are entwined together through metal cations, de Mendoza and co-workers have developed anion

Chart 36. Structural Formulas of the Miscellaneous Double-Helical Molecules

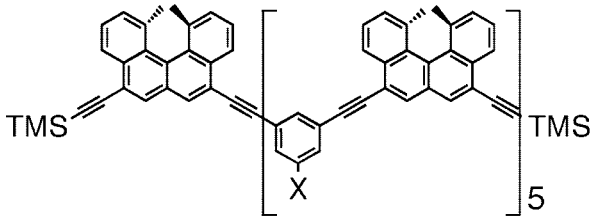

389 **a:** X = $CO_2{}^nC_{10}H_{21}$
b: X = $^nC_8F_{17}$

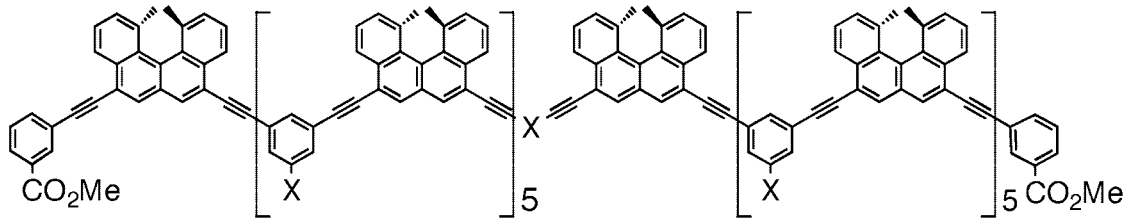

390 **a:** X =

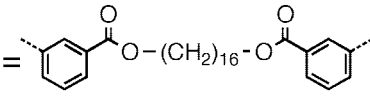

b: X =

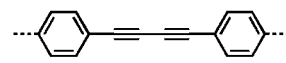

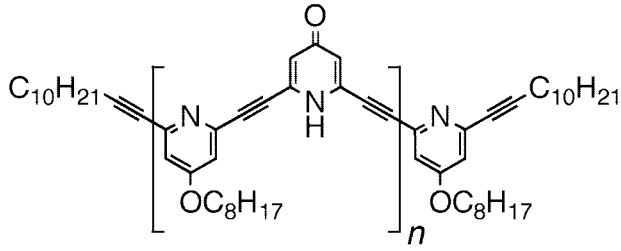

391

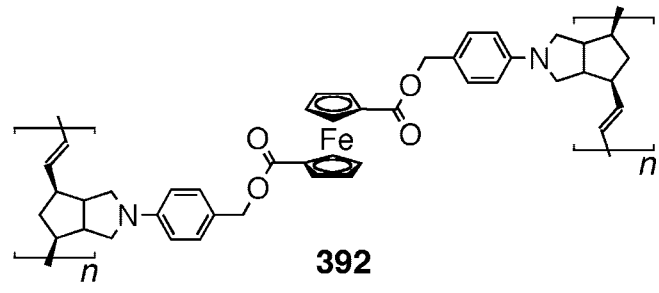

392

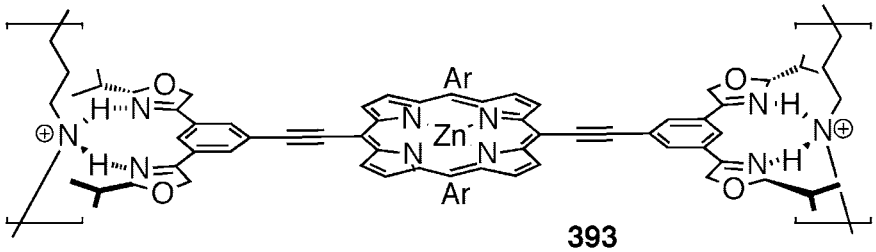

393

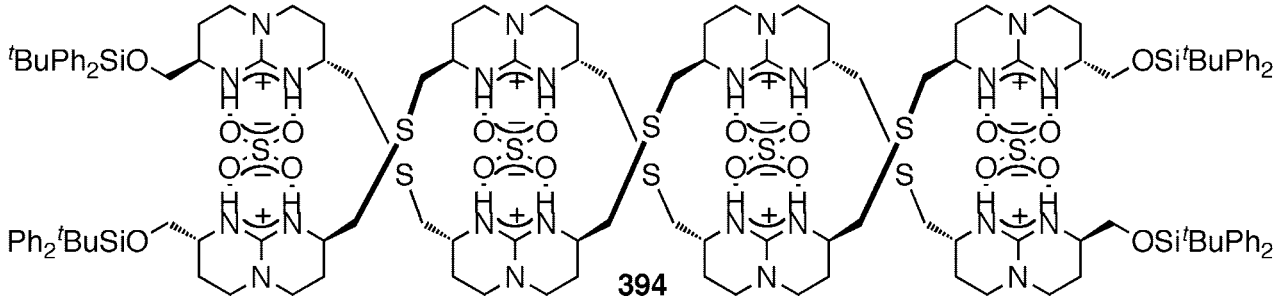

394

helicates (**394**) using sulfate anions to intertwine enantiomerically pure chiral bicyclic guanidinium salt strands.[657] The two guanidinium strands are forced to fold into a double-helical structure of the predictable handedness, which is imposed by the rigid guanidinium structure and confirmed by the ROESY and CD spectra along with MM calculations. Afterward, halide anions have been used for the self-assembly of organic molecular strands through hydrogen bonding interactions to form double helices in the solid state as well as in solution.[658,659]

DNA has been successfully utilized as a molecular glue to directly arrange gold nanoparticles (AuNPs) into periodic 3D crystalline lattices, demonstrating the potential of DNA as building blocks for 3D nanoengineering (Figure 100).[660,661] Recently, using DNA tile-mediated self-assembly, Yan and co-workers prepared various complex 3D geometric archi-

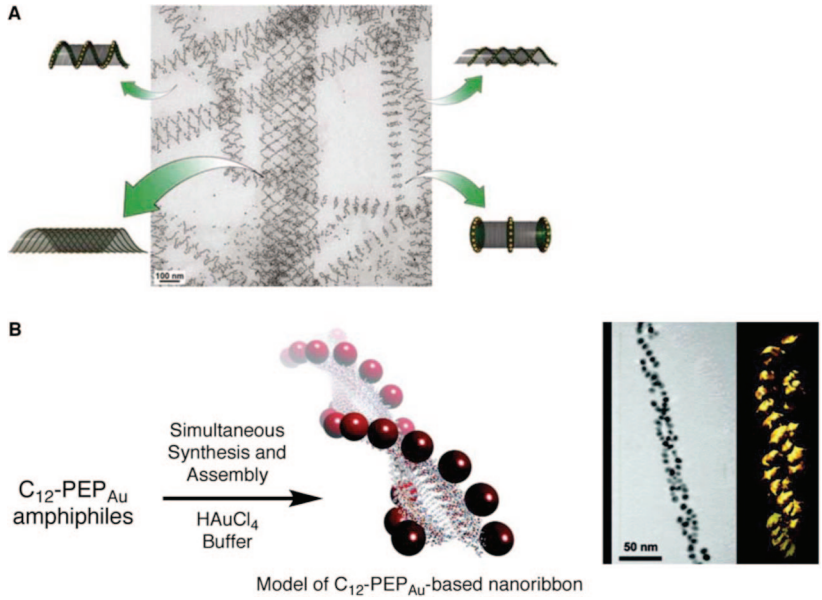

Figure 100. (A) TEM image of helical tubes formed from a DNA tile system carrying 5-nm AuNPs. (Reproduced with permission from ref 662. Copyright 2009 American Association for the Advancement of Science.) (B) C_{12}-PEPAu units assemble into left-handed twisted nanoribbons. (Reproduced with permission from ref 663. Copyright 2008 American Chemical Society.)

tectures of AuNPs, ranging in shape from stacked rings to single spirals, double spirals, and nested spirals.[662] Electron tomography has revealed the left-handed chirality for both the single- and double-stranded tubes, and unraveling transition of the double-helical tube into a single-helical one (Figure 100A). Rosi et al. prepared double helices of AuNPs using the self-assembly of oligopeptides with an affinity for AuNPs, followed by the peptide-based biomineralization of nanoparticles.[663] Electron tomography has disclosed that the nanoparticle double helices have a left-handed chirality, and their structures are highly regular and spatially complex (Figure 100B), exemplifying the utility of this methodology for rationally controlling the topology of nanoparticle superstructures with a controlled handedness.

5. Functions of Helical Polymers

The synthesis and structural elucidation of artificial helical polymers have been significantly developed, and a number of helical polymers with a controlled helical sense have been prepared to mimic biological helices, as mentioned in the previous sections. Applications of helical polymers, bioinspired by the sophisticated functions of biological helical polymers, however, still remain a challenge. In this section, potential applications of optically active helical polymers stimulated by enzymes that involve chiral recognition and asymmetric catalysis together with miscellaneous applications to sensory systems and advanced chiral materials for bio- and nanotechnologies are mainly described.

5.1. Chiral Recognition

The one-handed helical PTrMA (**2**) and poly-**9** prepared by the helix-sense-selective anionic polymerization using a chiral anionic initiator show an excellent chiral recognition for a variety of racemic compounds when used as a CSP for HPLC, and the CSPs of **2** and poly-**9** coated on a macroporous silica gel have been commercialized.[664−668] This was a significant milestone, demonstrating the practical usefulness of synthetic helical polymers, though this is an exceptional case. The PTrMA-based CSP, however, has a defect that the ester groups are slowly solvolyzed by methanol when used as an eluent for chiral HPLC, and the polymer gradually loses its helical conformation, leading to a loss of its chiral recognition ability. In contrast, the analogous amide derivative **15** is highly resistant to solvolysis in methanol, and the corresponding helical poly-**15** has the potential for a promising CSP. Optically active helical poly-**15**s with an almost 100% isotacticity were then prepared by the helix-sense-selective radical polymerization of **15** in the presence of (−)-menthol or (+)-neomenthol, and their chiral recognition abilities were evaluated using an enantioselective adsorption method. However, the chiral recognition ability of the polymers was very low compared to those of the one-handed helical PTrMA and poly-**9**, probably due to the low one-handedness of the polymers, judging from their low specific rotation values, although the helical sense excess has not yet been determined.[488]

Optically active cross-linked gels using the single-handed helical poly-**12** as a template have been synthesized by a template polymerization technique (Figure 101).[669] The gel, after removal of the template, retained the optical activity and preferentially adsorbed the same handed helical poly-**12** used as the template in the racemic poly-**12**. Moreover, the gel also showed a chiral recognition toward some racemates, such as *trans*-stilbene oxide (**405**, Chart 38) and enantioselectively adsorbed one of the enantiomers, while the gel showed no resolving power toward **405** before removal of the template helical polymer. These results strongly suggest that the chiral structure of the helical template is efficiently "imprinted"[670,671] in the gel and the observed resolution is likely based on the chiral structure imprinted in the gel. This may be the first example of molecular imprinting using a helical polymer as a template.[672]

Helical polyisocyanides also possess a chiral recognition ability, as evidenced by the fact that a mixture of right- and left-handed helical polyisocyanides was partially resolved by column chromatography using an optically active poly((−)-*sec*-butyl isocyanide) as a stationary phase.[22] When optically active poly(*tert*-butyl isocyanide) (**1**) prepared by the helix-sense-selective polymerization with an achiral nickel catalyst

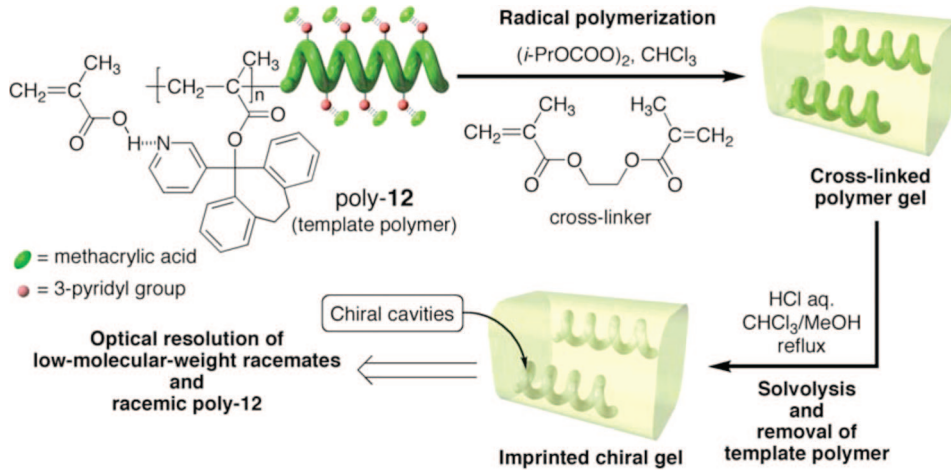

Figure 101. Schematic illustrations of the chiral gel synthesis by a molecular imprinting method using a one-handed helical polymethacrylate (poly-**12**) as template molecules. After cross-linking of methacrylic acid, noncovalent bonding to the pendant pyridyl groups of poly-**12** with a cross-linker and subsequent removal of the template polymer produce an imprinted chiral gel.

Chart 37

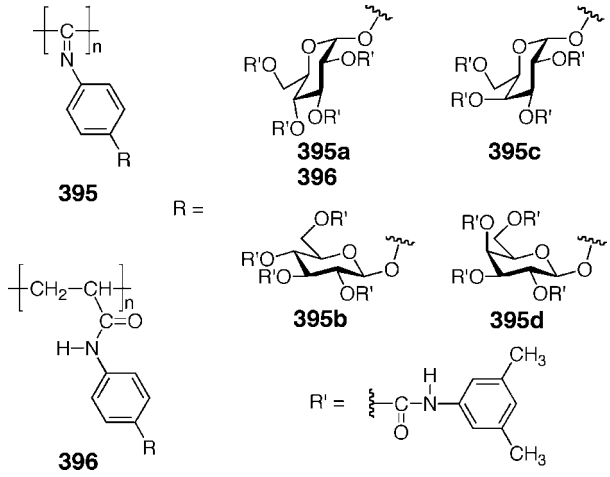

Chart 38

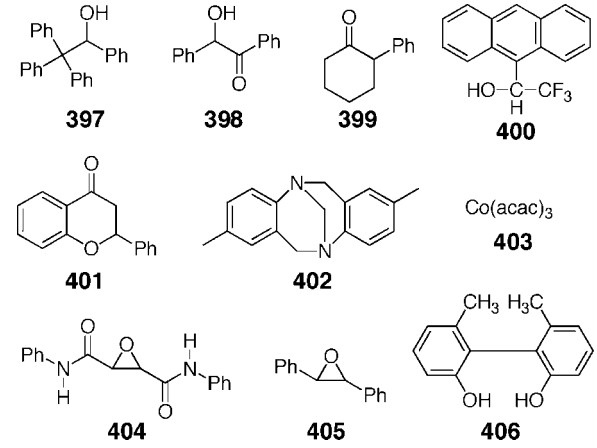

in the presence of (*R*)-phenylethylamine (**118**) was used as a CSP for HPLC, some racemates such as $Co(acac)_3$ (**403**, Chart 38) were partially resolved.[673]

The 3,5-dimethylphenylcarbamates of cellulose and amylose developed by Okamoto et al. are the most popular CSPs among a large variety of commercially available CSPs for HPLC.[664,667,674,675] Based on this observation, the 3,5-dimethylphenylcarbamate derivatives of the glucose- and galactose-carrying helical poly(phenyl isocyanide)s (**395**, Chart 37) have been prepared in order to investigate their chiral recognition abilities as CSPs for HPLC.[676] CD spectroscopy suggests a preference for the one helical sense in the helical polyisocyanides regulated by the pendant chiral sugar moieties. Ten different types of racemates with functional groups (Chart 38) were completely or partially resolved on the polymers depending on the stereostructure of the pendant sugars, whereas a nonhelical vinyl polymer bearing the same decorated sugar units (**396**) exhibited a lower chiral recognition, thus indicating the important role of the three-dimensionally regulated sugar arrays along the helical backbones of **395**. The CSPs of the galactose-carrying poly(phenyl isocyanide)s (**395c**, **395d**) showed a resolving ability for broader racemates than those of the glucose-type counterparts (**395a**, **395b**).

A stereoregular *cis-transoidal* PPA **87b** with a preferred-handed helical sense can also be used as a CSP for HPLC when coated on a macroporous silica gel, which resolved several racemates, such as **407**—**409**, **411**, as well as **398**, **400**, and **405**.[173] Interestingly, a stereoirregular PPA with a chemical structure identical to **87b**, prepared by a different synthetic route, showed a poor chiral recognition, thus indicating the indispensable role of the one-handed helical conformation induced by a stereoregular polymer backbone with chiral pendant groups for effective chiral recognition.[173]

A similar coated-type CSP derived from **87a** and a chemically bonded type CSP **410** have also been prepared. The latter CSP was made by polymerization of the corresponding chiral monomer with a rhodium catalyst in the presence of silica gel bearing phenylacetylene residues chemically bonded on a silica surface (Figure 102A) and can resolve completely some racemates, including **407** (Figure 102B). These two types of CSPs showed a relatively high and similar chiral recognition ability from each other,[677] indicating that the immobilized **87a** on the silica surface likely has a similar helical structure with a helical sense bias to that of the homopolymer **87a**.

Poly(*N*-propargylamide)s bearing L-ornithine and L-lysine pendant groups form a rather stable helical conformation of one particular handedness at high temperature and in the presence of methanol.[678] The copolymerization of the L-ornithine- and L-lysine-derived *N*-propargyamides with an achiral diacetylene, dipropargyl adipate, as a cross-linker using a rhodium catalyst produced optically active poly-

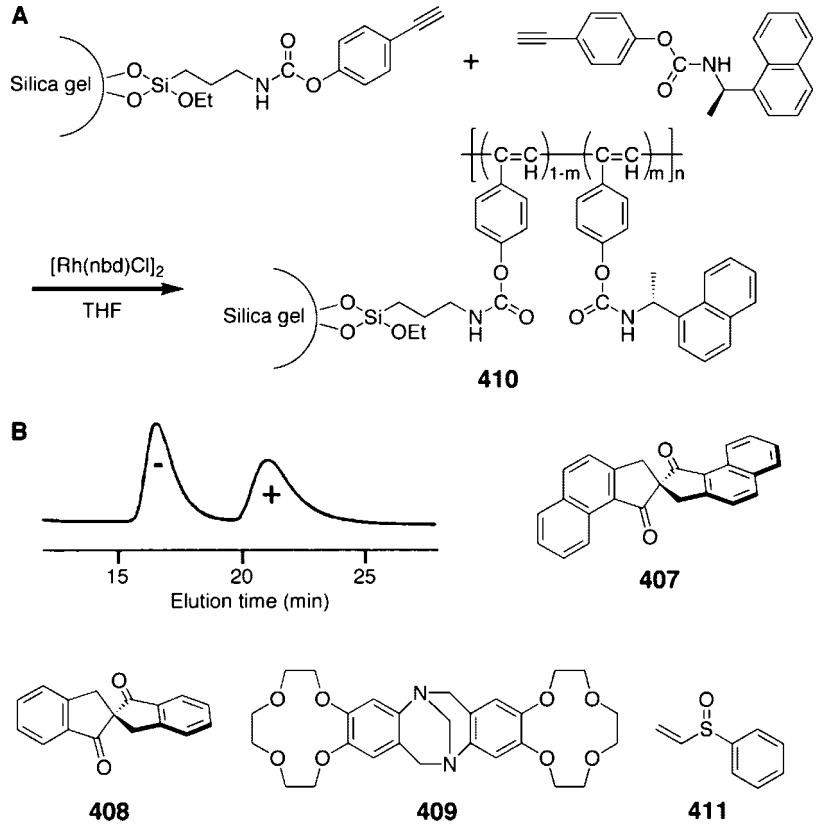

Figure 102. (A) Preparation of CSP **410**. (B) Separation of racemic **407** on CSP **410** (eluent, methanol; flow rate, 0.5 mL/min) and structures of racemates (**407**−**409** and **411**) resolved on CSP **410**.

Chart 39

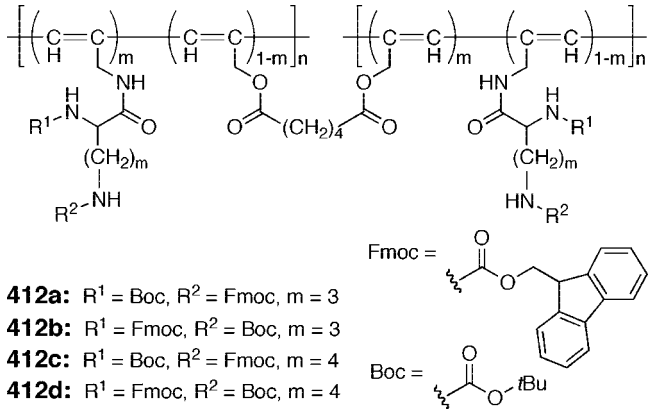

412a: R^1 = Boc, R^2 = Fmoc, m = 3
412b: R^1 = Fmoc, R^2 = Boc, m = 3
412c: R^1 = Boc, R^2 = Fmoc, m = 4
412d: R^1 = Fmoc, R^2 = Boc, m = 4

acetylene gels (**412**, Chart 39). The gels selectively adsorbed *N*-benzyloxycarbonyl L-Ala derivatives over the antipodes in THF.[679]

Other helical PPAs bearing chiral pinanyl groups such as **413**−**416** (Chart 40) have been prepared for use as solid membranes for separating the enantiomers of amino acids and chiral alcohols.[680,681] An optically active helical PPA (**116**) prepared by the helix-sense-selective polymerization of the corresponding achiral monomer using a rhodium-based chiral catalyst also exhibited an enantioselective permeability,[682] though the enantioselectivity was not as high as those of the pinanyl-bound helical PPAs. In order to improve the enantioselectivity and also create a metal-binding site in the membrane, hydrophilic *N*-(2-hydroxyethyl)aminomethyl groups being capable of chelating with Cu^{2+} ion are introduced on the pendant phenyl residues via the helix-sense-selective copolymerization (**417a**). The solid membrane derived from **417a** exhibited a better enantioselective permeability toward amino acids in water in the presence of Cu^{2+} ion (**417b**) than that of the original **417a** membrane.[683]

Chart 40

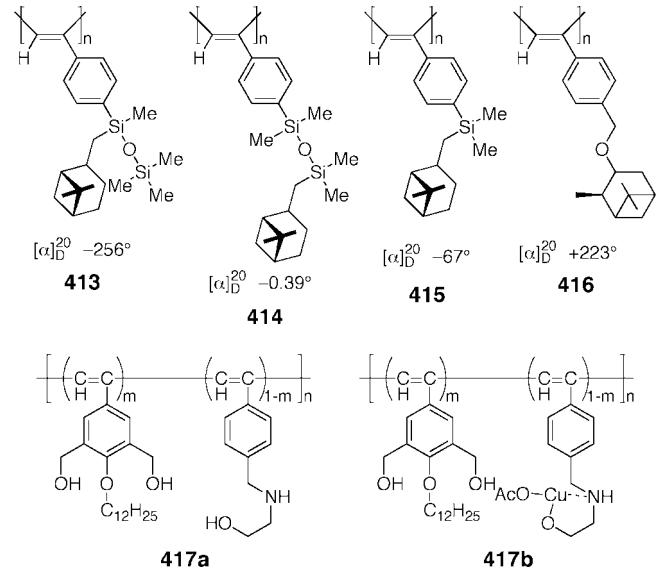

Optically active poly(diphenylacetylene) (*de*-**251**) and PPA (*de*-**252**) with a macromolecular helicity memory obtained by the *in situ* depinanylsilylation of the corresponding solid membranes (see Scheme 23 in section 2.7.2) can enrich enantiomers of tryptophan and phenylalanine in water during the permeation, or 2-butanol during pervaporation.[389,684] For example, the (*R*)-enriched 2-butanol of 58.6 and 80.5% ee preferentially permeated through the solid membranes of *de*-**251** and **251**, respectively. In addition, the permeation coefficient (*P*) of *de*-**251** for 2-butanol remarkably increased

Chart 41

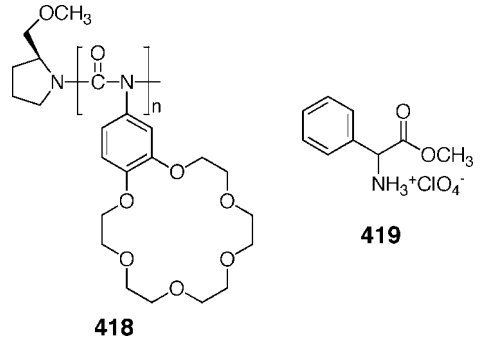

about 2 orders of magnitude over that of **251**.[684] These results suggest that the molecular-scale chiral space may be imprinted in the *de*-**251** during the depinanylsilylation, and such a chiral space likely contributes to the effective enantioselective permeation.

Poly(4′-isocyanatobenzo-18-crown-6) (**418**) is totally composed of achiral monomer units but forms an excess of the one helical conformation induced and chirally amplified by the optically active (*S*)-(2-methoxymethyl)pyrrolidine unit at the terminal end ("*domino effect*") (Chart 41).[685] Interestingly, the helical polymer exhibits a chiral discrimination toward racemic amino acid derivatives such as **419**, as supported by the enantioselective liquid−liquid extraction of one of the enantiomers. In sharp contrast, the unimer of **418** ($n = 1$) showed almost no enantioselectivity. Although the enantioselectivity of the polymer **418** was low, these results clearly demonstrate a supramolecular helical array of chiral or even achiral functional pendants with one particular handedness along the polymer backbone that appears to be a promising approach to the development of helical polymers with a chiral recognition ability.[685]

5.2. Asymmetric Catalysis

Optically active polymers that function as asymmetric catalysts are generally composed of small molecular chiral ligands covalently attached to or supported on achiral polymers, leading to polymer-supported asymmetric catalysts by which the enantioselectivities are totally governed by the immobilized chiral ligands while the polymers just work as supports.[686,687] However, if the support polymers could take a one-handed helical conformation, one may anticipate an intriguing synergistic effect of the helical chirality on the enantioselectivity, thereby leading to a more efficient asymmetric catalyst than the chiral ligand itself, although successful examples are quite rare. Another interesting approach is to employ rigid-rod one-handed helical polymers that possess no stereogenic centers except for a macromolecular helicity as a novel scaffold or template to spatially organize catalytic active, but achiral ligands, in a one-handed helical array along either the right- or left-handed twisted polymer backbone, which will provide an ideal and promising new class of asymmetric catalysts based on helical polymers.

Reggelin et al. took full advantage of the versatility and unique features of rigid-rod helical polymethacrylates developed by Okamoto[10,15] and have reported the first successful catalytic asymmetric C−C bond forming reaction using the helical polymethacrylates bearing one or two pyridyl groups as a chiral polymeric ligand (Scheme 28). The polymethacrylates were prepared by the helix-sense-selective polymerization or copolymerization with TrMA, affording

Scheme 28. Helical Polymer Catalysts Derived from Poly(triarylmethyl methacrylate)s (420−423)

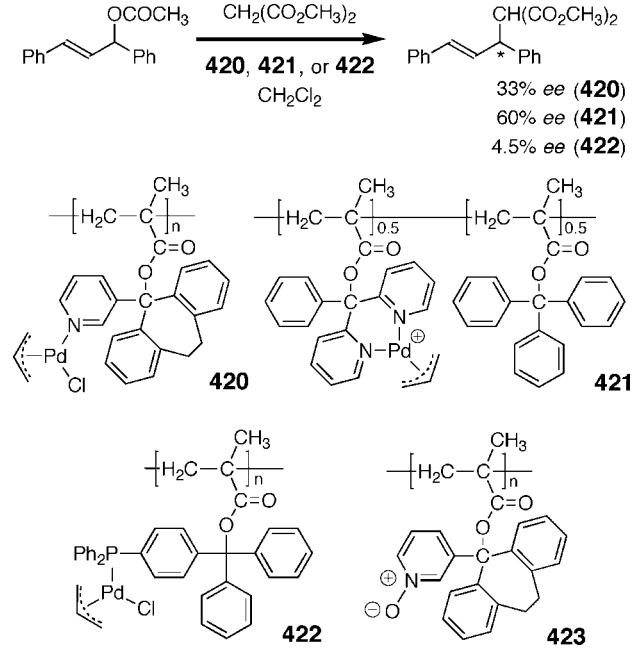

Scheme 29. Asymmetric Hydrosilylation with a Helical Poly(quinoxaline-2,3-diyl)-Based Chiral Ligand 424

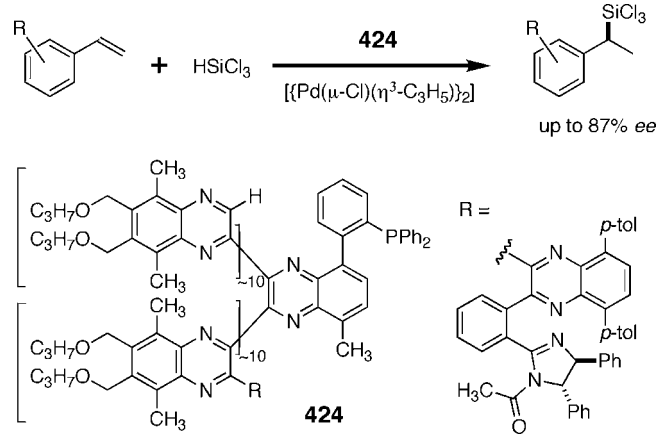

an isotactic, fully one-handed helical polymer and copolymer with a large specific rotation. Complexed with palladium, the resulting monodentate (**420**)[688] and bidentate (**421**)[689] palladium catalysts promoted the asymmetric allylic alkylation reaction, producing the substitution product with *ca.* 30 and 40−60% ee, respectively. Although the catalytic activity of the palladium phosphine complex (**422**)[689] was higher than those of **420** and **421**, the enantioselectivity was low (up to 4.5%), probably due to the low helix-sense excess of the polymer. An analogous pyridyl *N*-oxide substituted polymethacrylate (**423**) has also been employed as an organocatalyst for the asymmetric allylation of benzaldehyde, yielding the corresponding allylated products up to 19% ee.[690]

Optically active helical poly(quinoxaline-2,3-diyl)s (**424**) bearing metal-binding phosphino pendant groups have been synthesized by the helix-sense-selective living block copolymerization of *o*-diisocyanobenzenes using an optically active organopalladium complex (Scheme 29).[691] The obtained **424** has successfully been employed as a novel chiral polymer ligand for the palladium-catalyzed asymmetric hydrosilylation of substituted styrenes and showed a remark-

Scheme 30. Asymmetric Direct Aldol Reaction Mediated by a Poly(phenyl isocyanide) 425 with Macromolecular Helicity Memory

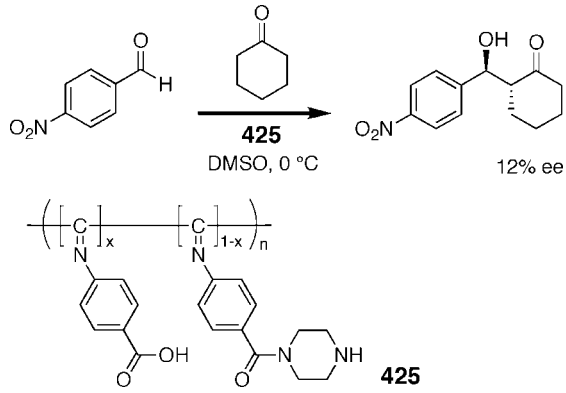

ably high enantioselectivity up to 87% ee. Importantly, this enantioselective reaction is totally promoted by the exceptionally stable helical structures with a high helix-sense excess of the polymer backbones.

Taking advantage of the "helicity induction and memory" effect described in section 2.7.1, an optically active helical polymer catalyst (**425**) having no additional chirality, except for the macromolecular helicity memory, has been prepared from poly(4-carboxyphenyl isocyanide) (**174**-H, Figure 42) with the helicity memory and piperazine (Scheme 30).[382] The bifunctional secondary amino and carboxylic acid pendants, arranged in a preferred-handed helical array along the polymer backbone, play an important role in the catalytic activity and enantioselectivity for the organocatalytic direct aldol reaction between aldehydes and ketones. The chiral information of the macromolecular helicity, memorized in the polymer backbone, is transferred to the asymmetric reaction, although its enantioselectivity was rather low (up to 12% ee).

An optically active PPA bearing achiral amino alcohol pendants (**417a**) prepared by the helix-sense-selective copolymerization using a rhodium catalyst in the presence of chiral amines mediated the asymmetric addition reaction of benzaldehyde with diethylzinc, giving a moderate enantioselectivity (*ca.* 20−30% ee).[692] In addition to static helical polymers, dynamic helical polymers with a predominantly one-handed helical conformation have also been used as a scaffold for the design and synthesis of other types of asymmetric helical polymer catalysts. Optically active or inactive monomers bearing specific substituents showing a catalytic activity or metal-binding ability are required to be homopolymerized (**426**−**428**) or copolymerized with chiral monomers (**429**) beforehand, respectively (Chart 42). A helical PPA (**426**) bearing optically active norephedrine units has been demonstrated as the first example of such a dynamic helical polymer that promoted the enantioselective addition of benzaldehyde with dialkylzinc to produce the nonracemic 1-phenylethanol of 30−49% ee.[693] An L-threonine-based helical poly(*N*-propargylamide) complexed with ruthenium (**427**) can catalyze an asymmetric hydrogen-transfer reaction of aromatic ketones to produce aromatic alcohols up to 36% ee.[694] The enantioselectivity was moderate but higher than that catalyzed by a ruthenium-complex with a monomer model (1.8% ee), indicating a kind of synergistic effect of the macromolecular helicity that enhanced the enantioselectivity.

Polypeptides and oligopeptides are know to efficiently catalyze the asymmetric epoxidation of α,β-unsaturated

Chart 42

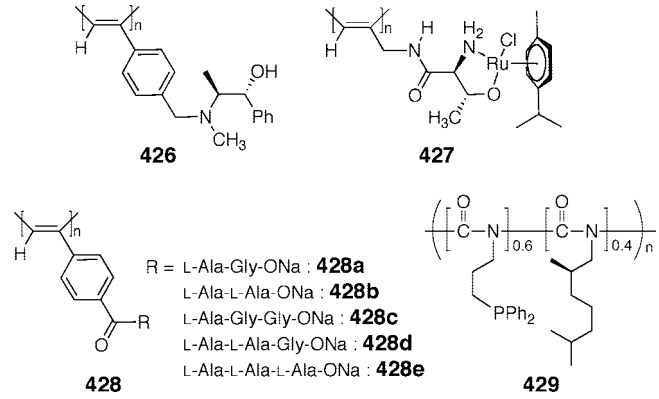

ketones, such as chalcone, with hydrogen peroxide in alkaline water, and the α-helical structures are considered to be essential for their high enantioselectivities.[695,696] Based on the organocatalytic activity of the peptides, a series of optically active PPAs (**428**) bearing oligopeptide pendants, from monomer to trimer, consisting of a combination of L-alanine (Ala) and glycine (Gly) residues (Chart 42) have been synthesized in order to investigate their asymmetric organocatalytic activities for the epoxidation of chalcone.[697] Among the helical PPAs, **428e** gave the highest enantioselectivity (34% ee), while the corresponding monomer showed almost no enantioselectivity (<2% ee), indicating that the helical structures of the PPAs in which the pendant oligopeptide residue is aligned in a one-handed helical array are indispensable for the effective asymmetric epoxidation. An optically active dynamic helical polyisocyanate composed of a chiral isocyanate and an achiral isocyanate bearing a phosphine pendant (60:40, mol/mol) (**429**) has also been employed as a helical polymer ligand for an asymmetric hydrogenation reaction.[689] Although the helical sense excess of **429** was not perfect, the polymer showed a low but apparent catalytic enantioselective activity in an asymmetric hydrogenation reaction when complexed with a rhodium catalyst, thus producing a hydrogenated product with a 14.5% ee.

Nucleic acids with specific sequences, such as ribozymes and deoxyribozymes, can catalyze reactions of nucleic acid substrates, although there is a fundamental limitation for applying them to modern organic asymmetric reactions.[698] Feringa, Roelfes, and co-workers have developed the first novel DNA-based asymmetric catalysis in which the chirality of the right-handed DNA-double helix plays a crucial role to be transferred to catalytic reactions (Figure 103).[699−705] The DNA complexes with the copper ligands bearing a DNA-intercalating acridine unit (**430**) promoted the Diels−Alder reaction of *ca.* 50% ee for the major (endo) isomer.[699] The drastic improvement in the enantioselectivity has been achieved when the bipyridine ligand (**431**) was employed in the Diels−Alder reaction,[700,701] the Michael reaction,[702] and the Friedel−Crafts reaction,[705] resulting in the corresponding products with an excellent enantioselectivity (up to 99% ee). The enantioselectivity and catalytic activity are dependent on the DNA-sequence.[703,705]

An optically active double-stranded helical dimer of **382a** composed of complementary strands, i.e., achiral amidine and carboxylic acid strands, bridged by achiral diphosphines has been prepared on the basis of the "helicity induction and memory" effect (Figure 96 in section 4.3). The totally artificial duplex has been found to be a versatile catalyst for

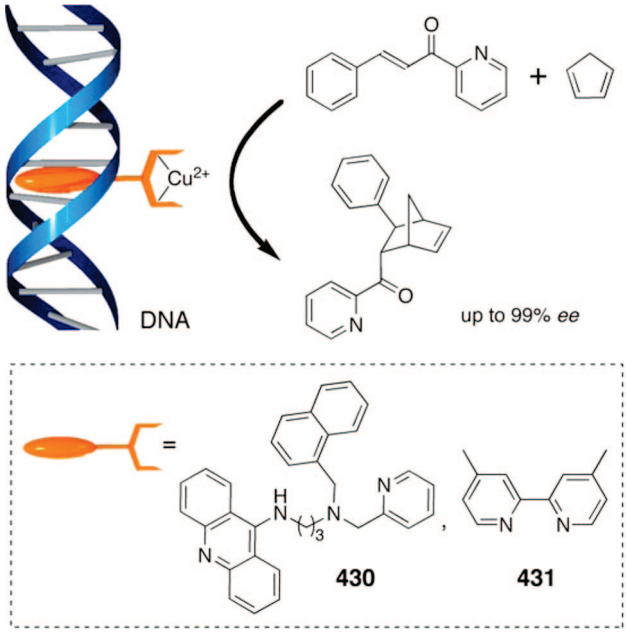

Figure 103. Schematic representation of the DNA-based copper-catalyzed asymmetric Diels−Alder reaction.

Scheme 31. Asymmetric Cyclopropanation of Styrene with Ethyl Diazoacetate Catalyzed by a Complementary Double-Helical Molecule with an Excess One-Handedness (382a)

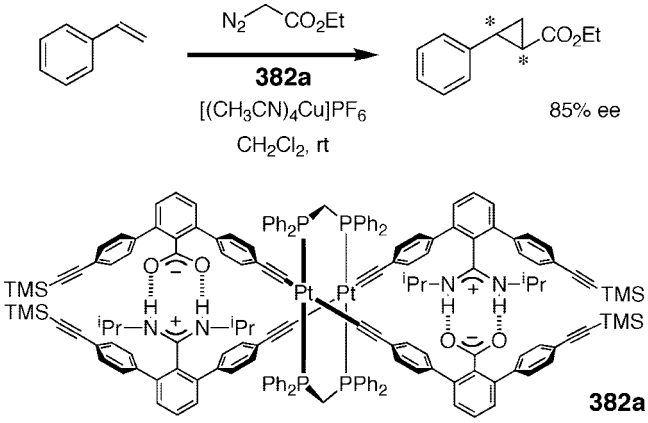

Chart 43

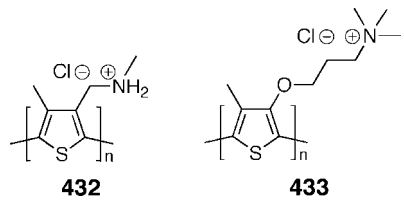

an asymmetric reaction (Scheme 31).[635] The alkynyl units on **382a** can accommodate metal ions such as Cu(I) in a tweezer-like fashion, and the double-helical **382a**/Cu(I) complex can catalyze the asymmetric cyclopropanation reaction of styrene with ethyl diazoacetate, thus producing an optically active cyclopropane up to 85% ee. The chiral space generated by the double-helical structure appears to be effective and indispensable for its high enantioselectivity. This approach provides a promising and conceptually new strategy in the broad field of supramolecular catalysis with a unique double-helical structure.

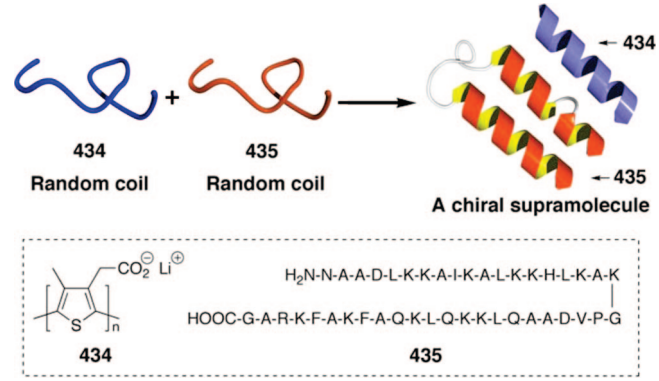

Figure 104. Schematic illustration of the supramolecular helical assembly induced by an achiral negatively charged polythiophene (**434**) and a positively charged random coil synthetic peptide (**435**).

5.3. Miscellaneous Applications

Several sensory systems using π-conjugated, water-soluble polythiophenes have been developed to detect biological macromolecules in water. A positively charged achiral polythiophene (**432**) (Chart 43) binds to a negatively charged DNA, and the complex showed induced Cotton effects in the polythiophene chromophore regions due to the induction of a helical ordering of **432** through electrostatic interactions with DNA as a chiral template in water.[706] This concept of an induction of helicity on achiral polythiophenes has been extended to sensing the helicity and conformational transition of a polysaccharide schizophyllan (SPG)[707] as well as the chirality of various nucleotides such as adenosine triphosphate (ATP)[708] by means of absorption and CD spectroscopic methods. The SPG/**433** complex showed the high quantum yield of circularly polarized luminescence not only in the solution state but also in the precipitated powder.[709] The chirality of **433**, induced by the complexation with SPG, was further immobilized through a sol−gel reaction with tetraethoxylsilane.[710]

A negatively charged, luminescent achiral polythiophene (**434**) assembles with a positively charged, synthetic peptide (**435**) with a random coil conformation in an aqueous solution, resulting in a supramolecular helix-bundle (Figure 104).[711] Interestingly, by mixing the two polymers in water, a preferred-handed helical conformation and a predominant α-helix are simultaneously induced in both polymers upon complexation via electrostatic interactions, as evidenced by the appearance of ICD in the π-conjugated chromophore region of **434** accompanied by a significant enhancement of the Cotton effect due to an α-helix formation. When optically active zwitterionic polythiophenes were used instead, their helically assembled structures and chiral properties can be detected by CD and emission spectra, leading to a novel sensory system for peptide helix bundles[712] and DNA hybridization.[713,714]

An interesting enantioselective discrimination of D- and L-phenylalanine (**436**) showing a visible color change has been achieved using optically active polyaniline-based thin films with a chiral memory (Figure 105).[393] The electrochemically polymerized emeraldine base form of polyaniline (**183a**, Chart 20) is known to exhibit an ICD in the main-chain chromophore region in solution and in the film when doped with chiral strong acids, such as (*R*)- or (*S*)-CSA, presumably due to the helical conformation with an excess handedness.[307] The (*R*)-CSA-doped polyaniline thin films

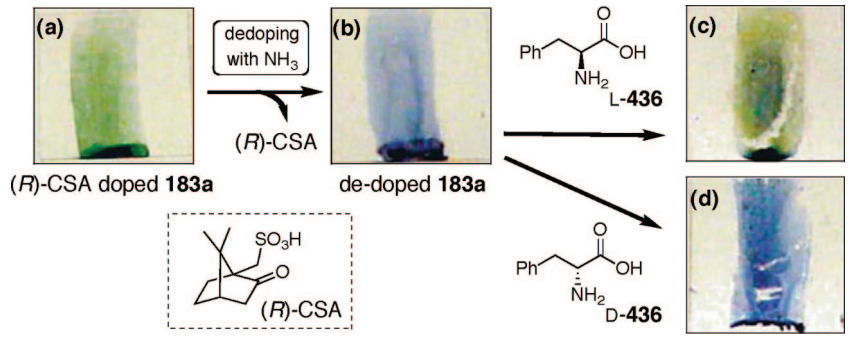

Figure 105. Schematic illustration of the enantioselective discrimination of D- and L-**436** by chiral polyaniline thin films: (a) a green (*R*)-CSA doped **183a** thin film; (b) a blue (*R*)-CSA dedoped **183a** thin film; (c) a dedoped **183a** thin film turns green after exposure to L-**436**; (d) a dedoped **183a** thin film stays blue after exposure to D-**436**. (Reproduced with permission from ref 393. Copyright 2003 Wiley-VCH.)

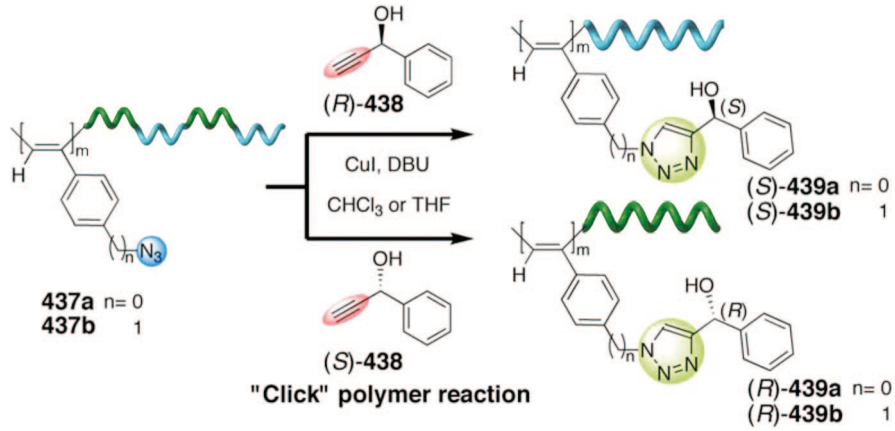

Figure 106. Schematic ilustration of the preferred-handed helix formation of **437** through click polymer reaction with optically active acetylenes (**438**).

retained their optical activity after removing the dopants; in other words, the polyaniline memorized the induced chirality in the thin films (see section 2.7.2).[392] The (*R*)-CSA dedoped polyaniline thin films further responded to the chirality of L- and D-**436** enantiomers and showed a different color change (green versus blue) by responding to the chirality of the amino acid. This chiral recognition mechanism remains unclear but is considered due to the formation of chiral cavities produced during the doping and dedoping processes with (*R*)-CSA, leading to the chirality-responsive thermochromism.

Taking advantage of a unique feature of the chirality-responsive helical polyacetylenes combined with the click reaction, a sensory system to detect the chirality of chiral acetylenes (**438**) has been constructed using optically inactive PPAs (**437**) bearing azide pendant groups (Figure 106).[715] The Cu-catalyzed click polymer reaction of the reactive azide groups of **437** with optically active acetylenes **438** produced helical PPAs (**439**) with a biased helical sense induced by the covalently bonded chiral pendant groups, thus showing characteristic ICDs whose Cotton effect signs can be used to sense the chirality of **438**.

The cholesteric phase (chiral nematic phase) of LCs has some intriguing optical properties, such as the selective reflection (Bragg reflection) of visible light, leading to brilliant colors if the cholesteric helical pitch coincides with the wavelength of visible light. Zentel et al. reported that optically active isocyanate terpolymers (**327** in Figure 64), a typical rigid-rod dynamic helical polyisocyanate, form lyotropic cholesteric structures with selective reflection in the visible range, and the cholesteric structure was frozen without loss of the optical quality by photopolymerization in styrene, thus yielding flexible polymer films with brilliant colors (Figure 107).[499,500] In the lyotropic cholesteric phases, the helical pitch of **327** increases with increasing temperature; thus, the wavelength of the selective reflection varies between 500 and 800 nm. After cross-linking, however, the selective reflection was frozen and no longer depended on the temperature. Therefore, the cross-linked films at various temperatures showed different colors depending on the temperature, and the angular dependence of the films displays an opalescent appearance (Figure 107B). This approach may be useful to develop advanced optoelectronic materials such as optical filters for large optical rotations or circular polarizers based on synthetic one-handed helical polymers.

As described in sections 2.1.1 and 2.5.2, a helical conformation with a preferred helical sense can be produced or induced in nonracemic solvents during the helix-sense-selective polymerization of bulky monomers or in dynamically racemic helical polyisocyanates and polysilanes, respectively, although chiral bias seems to be too weak to control the overall handedness of the helical polymers. Interestingly, when a chiral nematic phase was used as a polymerization solvent, Akagi and co-workers have found that helically twisted polyacetylene fibrils with either a clockwise or counterclockwise direction can be prepared by the polymerization of acetylene in chiral nematic LC phases (Figure 108).[716−718] (*R*)- or (*S*)-Binaphthyl derivatives having a mesogenic unit (**440**, **441**) combined with the nematic LC **442** and **443** induce a chiral nematic phase, in which the polymerization of acetylene with a homogeneous Ziegler−Natta catalyst proceeded to give hierarchically assembled helical fibrils consisting of multidomains with a spiral

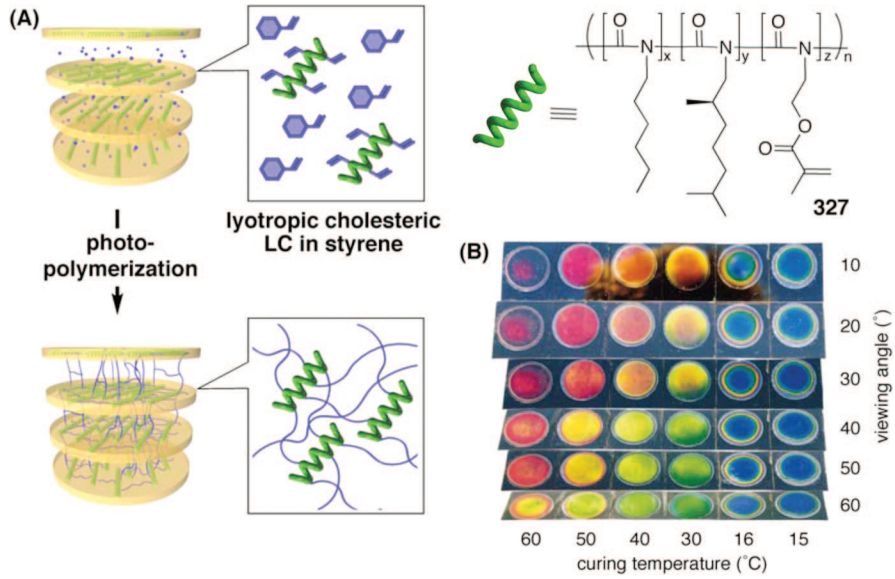

Figure 107. (A) Preparation of cholesteric networks through the photopolymerization of **327** with styrene. (B) Optical impression of the angular dependence of the films cross-linked at 15−60 °C. (Reproduced with permission from ref 500. Copyright 1999 American Chemical Society.)

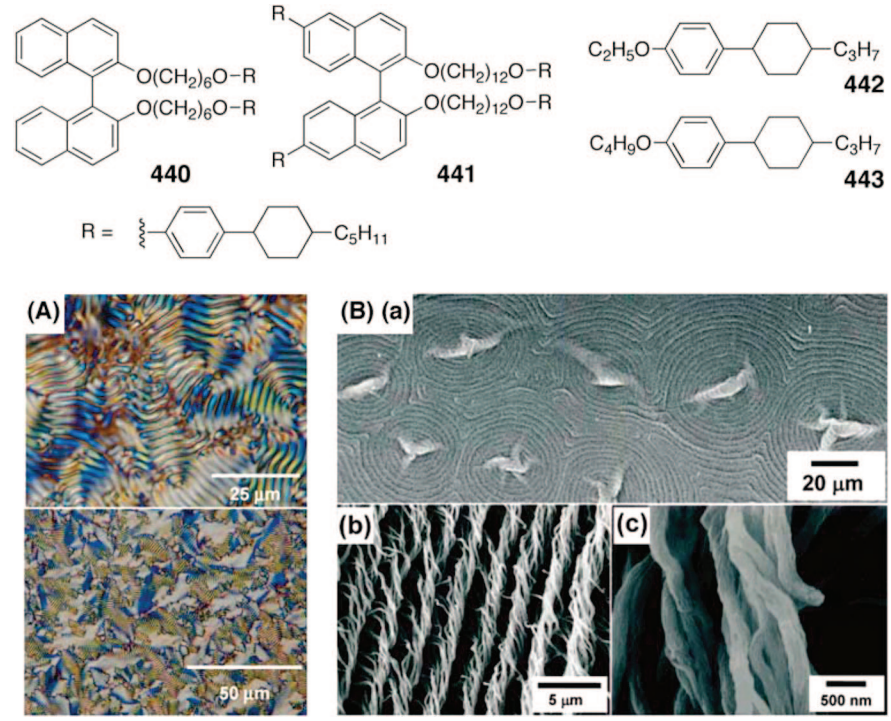

Figure 108. (A) Polarizing optical micrographs of the mixture of **442**, **443**, and (*S*)-**440** at 27 °C. (B) SEM images of helical polyacetylene films synthesized in the chiral nematic LC of (*R*)-**440**. (Reproduced with permission from ref 718. Copyright 2007 American Chemical Society.)

morphology, as observed by SEM; each domain is composed of a helically twisted fibril with a one-handed screw-sense (Figure 108B). Besides the helical polyacetylene fibrils, related helical fibrils composed of other π-conjugated polymers with a controlled spiral morphology have also been prepared by polymerization of the corresponding monomers in the chiral nematic phase used as an asymmetric induction field;[719,720] the details will be described elsewhere in this special issue.[721]

A versatile approach for chiroptical inversion switching and chiroptical memory with rewritable (RW) and write-once read-memory (WORM) modes has been developed by Fujiki et al., by taking advantage of the characteristic feature of temperature- and molecular weight-dependent helicity inversion of certain helical polysilanes (**266** in Figure 52) in the solid state (Figure 109).[722] A cast film of a low molecular weight **266** ($M_w = 1.3 \times 10^4$ and $M_w/M_n = 1.16$) on a quartz substrate reversibly switches between almost mirror-image CDs with the transition temperature (T_c) at approximately 47 °C upon heating followed by slow cooling (Figure 109A); this change can be repeated by the multiple heating−cooling cycles (Figure 109B), indicating the chiroptical inversion switch. On the other hand, when the film was rapidly quenched from above the T_c, the Cotton effect sign hardly switched, and as a consequence, the helical sense of **266** biased at high temperature is retained. This chiral

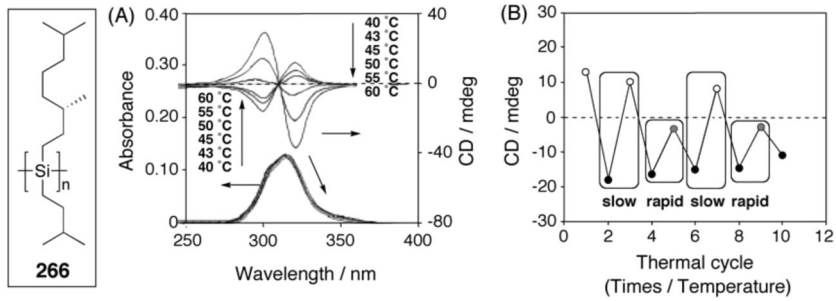

Figure 109. (A) UV and CD spectra of a **266** cast film upon heating. (B) Thermal-cycle responses of CD maxima intensities for the cast film. Thermal cycles were conducted by heating to 60 °C (filled circles), followed by either slow (open circles) or rapid (gray circles) cooling to 30 °C. Rapid cooling was achieved by dipping the film into ice water. Heating rate: 20 °C min^{-1}. (Reproduced with permission from ref 722. Copyright 2004 Wiley-VCH.)

memory effect can be further erased by heating to above the T_c, so that the chiroptical inversion switching and chiroptical memory with RW modes are possible using a low molecular weight **266** by controlling the cooling conditions in the solid film. Interestingly, when a higher molecular weight **266** ($M_w = 2.5 \times 10^4$ and $M_w/M_n = 1.16$) was used instead, the helix−helix transition took place only upon heating. This irreversible change in the CD signals suggests a possible nonerasable memory usable as the WORM mode.

Molecular springs with a switchable helical pitch (helical springs) triggered by external stimuli may undergo mechanical springlike motions that will provide intriguing potentials for constructing molecular nanomachines capable of expressing their motions to perform a mechanical operation on a macroscopic scale. Percec et al. have brought about the realization of such a system using self-organizable dendronized helical *cis*-PPAs such as **100** (Figure 110).[532] As described in sections 2.2.3 and 3.1.2, the *cis*-PPA **100** undergoes an unprecedented thermally induced *cisoid*-to-*transoid* conformational isomerism in bulk due to the bulky dendronized pendants that eliminate the typical 6π-electrocyclization that often occurs in other *cis*-PPAs (Figure 110A and B). This thermally induced conformational change is reversible and is accompanied by the springlike motion (extension and contraction) of the individual helical backbones cylindrically packed in bulk, as confirmed by XRD measurements of the extruded fibers. The molecular springlike motion is further amplified to convert the anisotropic thermal expansion along the column axis of the fibers, which allows the fiber to perform work in concert, as demonstrated with great interest by the lifting performance of a U.S. dime that weighs 250-times the weight of the fiber (Figure 110C and D).

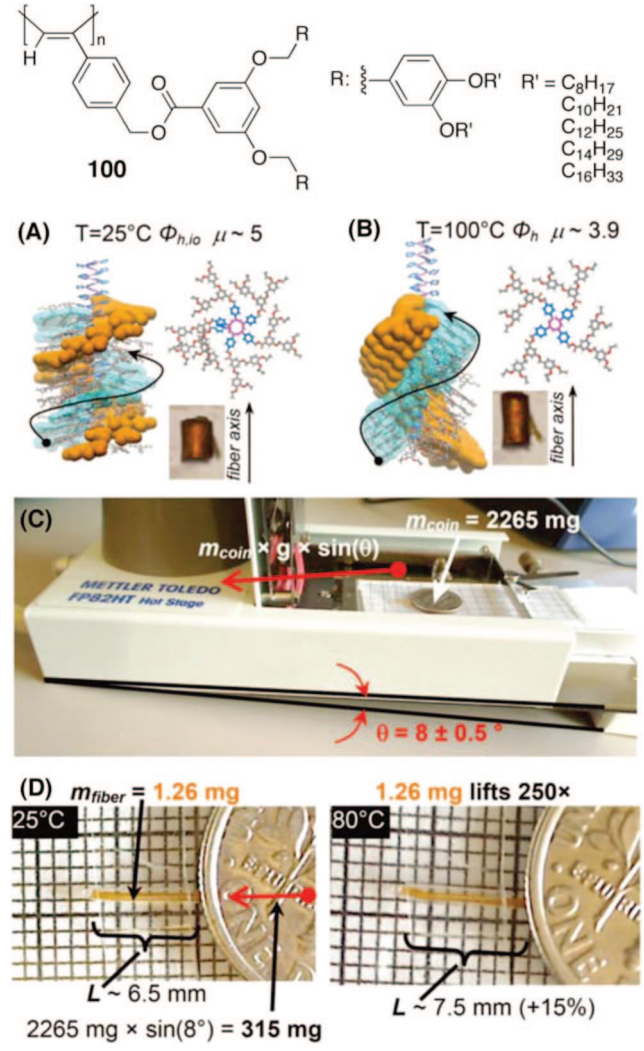

Figure 110. Nanomechanical function from thermoresponsible dendronized helical poly(phenylacetylene)s (**100**) through a *cis*−*cisoid* (A)-to-*cis*−*transoid* (B) conformational change of their polymer backbones at low and high temperatures, respectively. The oriented fiber can lift a dime on the inclined plane up an 8° of a Mettler hot stage (C) via the macroscopic scale expansion and contraction as shown in the expanded images at 25 and 80 °C of the oriented fiber (D), demonstrating that the fiber lifts 250-times its weight. (Reproduced with permission from ref 532. Copyright 2008 American Chemical Society.)

6. Conclusions and Outlook

The research area reviewed here has seen a remarkable amount of activity over the past decade, and a great number of single-stranded helical polymers with optical activity have been synthesized by the helix-sense-selective polymerization of new monomers with specific chiral catalysts or initiators, thus producing static helical polymers, or by the covalent and noncovalent bonding chiral interactions, yielding dynamic helical polymers. The static and dynamic helical polymers differ through their helix inversion barriers. As a consequence, the former helical conformations are locked during the polymerization under kinetic control, while the latter helical conformations are thermodynamically controlled. Along with the emerging research area of foldamers, foldamer motifs have been widely applied to the design and synthesis of novel helical polymers with a controlled helical sense, most of which possess a dynamic property in their helical conformations.

This review also shows that helical conformations of dynamic helical polymers can also be locked, as demon-

strated by the unique memory effect observed in dynamic helical poly(phenylacetylene)s and poly(phenyl isocyanide)s induced by chiral guest molecules. The memory effect has been proved to be valuable from a practical viewpoint such that a preferred-handed helical polymer can be obtained from commodity polymers, such as st-PMMA and st-PS. In addition, either static or dynamic helical polymers with an excess single-handedness can be prepared by the polymerization of monomers with the identical framework, but bearing different substituents.

The history of artificial helical polymers with optical activity is traced back to the 1970s. At that time, the elucidation of helical structures, in particular, their handedness and helical sense excess, appeared to be almost impossible. Recent significant developments in spectroscopic and microscopic instruments combined with the living polymerization techniques and computational approaches have made it possible to determine the helical structures of some helical polymers, including helical pitch, handedness, and helical sense excess, by direct observations of the individual helical polymer chains on substrates, which not only provides insight into the principles underlying the generation of helical conformations but also leads to further progress in helical polymers with specific structures and functions.

Apart from the breadth of single-stranded helical polymers and oligomers, the design and synthetic strategies for double-stranded helical polymers and oligomers remain limited, regardless of the natural model, the double-helical DNA. The complementary double-stranded oligomers and polymers with a controlled helix-sense will offer a promising approach to develop DNA-like helical systems for information storage and replication, one of the most sophisticated functions of DNA, but yet difficult to artificially realize at the present. However, the fact that the sequence-specific double-helix formation has been achieved in the totally artificial oligomeric strands through complementary amidinium-carboxylate salt bridges may lead to the first steps toward breaking nature's monopoly on self-replication and copy.

Inspired by the biological helices and functions, the helical architectures in synthetic polymers will give rise to emerging opportunities for applications to chiral materials with specific functionalities. In fact, some helical polymers have been successfully applied to the asymmetric catalysis and separation of enantiomers; some of them are commercialized as a CSP for HPLC. However, there are still gaps between natural and artificial helical polymers in terms of structures and functions. Biological helical polymers hierarchically assemble into supramolecular structures, such as the coiled-coil (helix bundle) superstructure and protein−DNA hybrids, which are responsible for their extraordinary functions. Therefore, with implications for biological helices, superstructures, and functions, not only mimicking biological helices but also developing supramolecular helical assemblies with a controlled helix-sense will be important and attractive future challenges, which will also provide a clue to the construction of advanced chiral materials.

7. Acknowledgments

We thank the Japan Science and Technology Agency (JST) and the Grant-in-Aid for Scientific Research (S) from the Japan Society for the Promotion of Science (JSPS) for financial support.

8. References

(1) Pauling, L.; Corey, R. B.; Branson, H. R. *Proc. Natl. Acad. Sci. U.S.A.* **1951**, *378*, 205.
(2) Watson, J. D.; Crick, F. H. C. *Nature* **1953**, *171*, 737.
(3) Saenger, W. *Principles of Nucleic Acid Structure*; Springer-Verlag: New York, 1984.
(4) Schulz, G. E.; Schirmer, R. H. *Principles of Protein Structure*; Springer-Verlag: New York, 1979.
(5) Natta, G.; Pino, P.; Corradini, P.; Danusso, F.; Mantica, E.; Mazzanti, G.; Moraglio, G. *J. Am. Chem. Soc.* **1955**, *77*, 1708.
(6) Tadokoro, H. *Structure of Crystalline Polymers*; Wiley: New York, 1979.
(7) Pino, P.; Lorenzi, G. P. *J. Am. Chem. Soc.* **1960**, *82*, 4745.
(8) Green, M. M.; Jha, S. K. *Chirality* **1997**, *9*, 424.
(9) Farina, M.; Peraldo, M.; Natta, G. *Angew. Chem., Int. Ed. Engl.* **1965**, *4*, 107.
(10) Okamoto, Y.; Nakano, T. *Chem. Rev.* **1994**, *94*, 349.
(11) Farina, M. *Top. Stereochem.* **1987**, *17*, 1.
(12) Wulff, G. *Angew. Chem., Int. Ed. Engl.* **1989**, *28*, 21.
(13) Pu, L. *Acta Polym.* **1997**, *48*, 116.
(14) Rowan, A. E.; Nolte, R. J. M. *Angew. Chem., Int. Ed.* **1998**, *37*, 63.
(15) Nakano, T.; Okamoto, Y. *Chem. Rev.* **2001**, *101*, 4013.
(16) Cornelissen, J. J. L. M.; Rowan, A. E.; Nolte, R. J. M.; Sommerdijk, N. A. J. M. *Chem. Rev.* **2001**, *101*, 4039.
(17) Green, M. M.; Peterson, N. C.; Sato, T.; Teramoto, A.; Cook, R.; Lifson, S. *Science* **1995**, *268*, 1860.
(18) Fujiki, M. *Macromol. Rapid Commun.* **2001**, *22*, 539.
(19) Maeda, K.; Yashima, E. *Top. Curr. Chem.* **2006**, *265*, 47.
(20) Yashima, E.; Maeda, K. In *Foldamers: Structure, Properties, and Applications*; Hecht, S., Huc, I., Eds.; Wiley-VCH: Weinheim, 2007.
(21) Sierra, T. In *Chirality at Nanoscale*; Amabilino, D., Ed.; Wiley: Weinheim, 2009.
(22) Nolte, R. J. M.; Van Beijnen, A. J. M.; Drenth, W. *J. Am. Chem. Soc.* **1974**, *96*, 5932.
(23) Okamoto, Y.; Suzuki, K.; Ohta, K.; Hatada, K.; Yuki, H. *J. Am. Chem. Soc.* **1979**, *101*, 4763.
(24) Yuki, H.; Okamoto, Y.; Okamoto, I. *J. Am. Chem. Soc.* **1980**, *102*, 6356.
(25) Corley, L. S.; Vogl, O. *Polym. Bull.* **1980**, *3*, 211.
(26) Ute, K.; Hirose, K.; Kashimoto, H.; Hatada, K.; Vogl, O. *J. Am. Chem. Soc.* **1991**, *113*, 6305.
(27) Ute, K.; Hirose, K.; Kashimoto, H.; Nakayama, H.; Hatada, K.; Vogl, O. *Polym. J.* **1993**, *25*, 1175.
(28) Green, M. M.; Andreola, C.; Munoz, B.; Reidy, M. P.; Zero, K. *J. Am. Chem. Soc.* **1988**, *110*, 4063.
(29) Yashima, E.; Maeda, K. *Macromolecules* **2008**, *41*, 3.
(30) Yashima, E.; Maeda, K.; Furusho, Y. *Acc. Chem. Res.* **2008**, *41*, 1166.
(31) Gellman, S. H. *Acc. Chem. Res.* **1998**, *31*, 173.
(32) Hill, D. J.; Mio, M. J.; Prince, R. B.; Hughes, T. S.; Moore, J. S. *Chem. Rev.* **2001**, *101*, 3893.
(33) Hamuro, Y.; Geib, S. J.; Hamilton, A. D. *J. Am. Chem. Soc.* **1996**, *118*, 7529.
(34) Berl, V.; Huc, I.; Khoury, R. G.; Krische, M. J.; Lehn, J. M. *Nature* **2000**, *407*, 720.
(35) *Foldamers: Structure, Properties, and Applications*; Hecht, S., Huc, I., Eds.; Wiley-VCH: Weinheim, 2007.
(36) Shimizu, T.; Masuda, M.; Minamikawa, H. *Chem. Rev.* **2005**, *105*, 1401.
(37) Keizer, H. M.; Sijbesma, R. P. *Chem. Soc. Rev.* **2005**, *34*, 226.
(38) You, C.-C.; Dobrawa, R.; Saha-Möller, C. R.; Würthner, F. *Top. Curr. Chem.* **2005**, *258*, 39.
(39) Ajayaghosh, A.; George, S. J.; Schenning, A. P. H. J. *Top. Curr. Chem.* **2005**, *258*, 83.
(40) Palmans, A. R. A.; Meijer, E. W. *Angew. Chem., Int. Ed.* **2007**, *46*, 8948.
(41) Aida, T.; Fukushima, T. *Philos. Trans. R. Soc. A* **2007**, *365*, 1539.
(42) Kim, H.-J.; Lim, Y.-B.; Lee, M. *J. Polym. Sci., Part A: Polym. Chem.* **2008**, *46*, 1925.
(43) Brunsveld, L.; Folmer, B. J. B.; Meijer, E. W.; Sijbesma, R. P. *Chem. Rev.* **2001**, *101*, 4071.
(44) Nielsen, P. E. *Acc. Chem. Res.* **1999**, *32*, 624.
(45) Cheng, R. P.; Gellman, S. H.; DeGrado, W. F. *Chem. Rev.* **2001**, *101*, 3219.
(46) Seebach, D.; Kimmerlin, T.; Sebesta, R.; Campo, M. A.; Beck, A. K. *Tetrahedron* **2004**, *60*, 7455.
(47) Brown, N. J.; Johansson, J.; Barron, A. E. *Acc. Chem. Res.* **2008**, *41*, 1409.
(48) Fowler, S. A.; Luechapanichkul, R.; Blackwell, H. E. *J. Org. Chem.* **2009**, *74*, 1440.
(49) Kizirian, J.-C. *Chem. Rev.* **2008**, *108*, 140.
(50) Nakano, T.; Shikisai, Y.; Okamoto, Y. *Polym. J.* **1996**, *28*, 51.

(51) Nakano, T.; Tsunematsu, K.; Okamoto, Y. *Chem. Lett.* **2002**, 42.
(52) Nakano, T.; Matsuda, A.; Okamoto, Y. *Polym. J.* **1996**, *28*, 556.
(53) Ishitake, K.; Satoh, K.; Kamigaito, M.; Okamoto, Y. *Angew. Chem., Int. Ed.* **2009**, *48*, 1991.
(54) Hoshikawa, N.; Hotta, Y.; Okamoto, Y. *J. Am. Chem. Soc.* **2003**, *125*, 12380.
(55) Amano, Y.; Okamoto, Y. *Polym. J.* **2005**, *37*, 629.
(56) Tsuji, M.; Azam, A.; Kamigaito, M.; Okamoto, Y. *Macromolecules* **2007**, *40*, 3518.
(57) Miyake, G. M.; Mariott, W. R.; Chen, E. Y. X. *J. Am. Chem. Soc.* **2007**, *129*, 6724.
(58) Miyake, G. M.; Chen, E. Y.-X. *Macromolecules* **2008**, *41*, 3405.
(59) Shiohara, K.; Habaue, S.; Okamoto, Y. *Polym. J.* **1998**, *30*, 249.
(60) Nakano, T.; Nakagawa, O.; Tsuji, M.; Tanikawa, M.; Yade, T.; Okamoto, Y. *Chem. Commun.* **2004**, 144.
(61) Mislow, K.; Bickart, P. *Isr. J. Chem.* **1977**, *15*, 1.
(62) Nakano, T.; Tanikawa, M.; Nakagawa, O.; Yade, T.; Sakamoto, T. *J. Polym. Sci., Part A: Polym. Chem.* **2009**, *47*, 239.
(63) Okamoto, Y.; Mohri, H.; Nakano, T.; Hatada, K. *J. Am. Chem. Soc.* **1989**, *111*, 5952.
(64) Mohri, H. Doctral Dissertation, Osaka University, 1989.
(65) Ute, K.; Asada, T.; Nabeshima, Y.; Hatada, K. *Acta Polym.* **1995**, *46*, 458.
(66) Millich, F. *Adv. Polym. Sci.* **1975**, *19*, 117.
(67) Nolte, R. J. M. *Chem. Soc. Rev.* **1994**, *23*, 11.
(68) Kamer, P. C. J.; Nolte, R. J. M.; Drenth, W. *J. Am. Chem. Soc.* **1988**, *110*, 6818.
(69) Deming, T. J.; Novak, B. M. *J. Am. Chem. Soc.* **1992**, *114*, 7926.
(70) Amabilino, D. B.; Serrano, J.-L.; Sierra, T.; Veciana, J. *J. Polym. Sci., Part A: Polym. Chem.* **2006**, *44*, 3161.
(71) Otten, M. B. J.; Metselaar, G. A.; Cornelissen, J. J. L. M.; Rown, A. E.; Nolte, R. J. M. In *Foldamers: Structure, Properties, and Applications*; Hecht, S., Huc, I., Eds.; Wiley-VCH: Weinheim, 2007.
(72) Cornelissen, J. J. L. M.; Donners, J. J. J. M.; de Gelder, R.; Graswinckel, W. S.; Metselaar, G. A.; Rowan, A. E.; Sommerdijk, N. A. J. M.; Nolte, R. J. M. *Science* **2001**, *293*, 676.
(73) Metselaar, G. A.; Adams, P. J. H. M.; Nolte, R. J. M.; Cornelissen, J. J. L. M.; Rowan, A. E. *Chem.—Eur. J.* **2007**, *13*, 950.
(74) Cornelissen, J. J. L. M.; Graswinckel, W. S.; Rowan, A. E.; Sommerdijk, N. A. J. M.; Nolte, R. J. M. *J. Polym. Sci., Part A: Polym. Chem.* **2003**, *41*, 1725.
(75) Samorí, P.; Ecker, C.; Gossl, I.; de Witte, P. A. J.; Cornelissen, J. J. L. M.; Metselaar, G. A.; Otten, M. B. J.; Rowan, A. E.; Nolte, R. J. M.; Rabe, J. P. *Macromolecules* **2002**, *35*, 5290.
(76) Wezenberg, S. J.; Metselaar, G. A.; Rowan, A. E.; Cornelissen, J. J. L. M.; Seebach, D.; Nolte, R. J. M. *Chem.—Eur. J.* **2006**, *12*, 2778.
(77) Metselaar, G. A.; Cornelissen, J. J. L. M.; Rowan, A. E.; Nolte, R. J. M. *Angew. Chem., Int. Ed.* **2005**, *44*, 1990.
(78) de Witte, P. A. J.; Castriciano, M.; Cornelissen, J. J. L. M.; Scolaro, L. M.; Nolte, R. J. M.; Rowan, A. E. *Chem.—Eur. J.* **2003**, *9*, 1775.
(79) Palermo, V.; Otten, M. B. J.; Liscio, A.; Schwartz, E.; de Witte, P. A. J.; Castriciano, M. A.; Wienk, M. M.; Nolde, F.; De Luca, G.; Cornelissen, J. J. L. M.; Janssen, R. A. J.; Mullen, K.; Rowan, A. E.; Nolte, R. J. M.; Samori, P. *J. Am. Chem. Soc.* **2008**, *130*, 14605.
(80) De Witte, P. A. J.; Hernando, J.; Neuteboom, E. E.; van Dijk, E. M. H. P.; Meskers, S. C. J.; Janssen, R. A. J.; van Hulst, N. F.; Nolte, R. J. M.; Garcia-Parajo, M. F.; Rowan, A. E. *J. Phys. Chem. B* **2006**, *110*, 7803.
(81) Hernando, J.; de Witte, P. A. J.; van Dijk, E.; Korterik, J.; Nolte, R. J. M.; Rowan, A. E.; Garcia-Parajo, M. F.; van Hulst, N. F. *Angew. Chem., Int. Ed.* **2004**, *43*, 4045.
(82) Foster, S.; Finlayson, C. E.; Keivanidis, P. E.; Huang, Y.-S.; Hwang, I.; Friend, R. H.; Otten, M. B. J.; Lu, L.-P.; Schwartz, E.; Nolte, R. J. M.; Rowan, A. E. *Macromolecules* **2009**, *42*, 2023.
(83) Schwartz, E.; Kitto, H. J.; de Gelder, R.; Nolte, R. J. M.; Rowan, A. E.; Cornelissen, J. J. L. M. *J. Mater. Chem.* **2007**, *17*, 1876.
(84) Kitto, H. J.; Schwartz, E.; Nijemeisland, M.; Koepf, M.; Cornelissen, J. J. L. M.; Rowan, A. E.; Nolte, R. J. M. *J. Mater. Chem.* **2008**, *18*, 5615.
(85) Kajitani, T.; Okoshi, K.; Sakurai, S.-i.; Kumaki, J.; Yashima, E. *J. Am. Chem. Soc.* **2006**, *128*, 708.
(86) Kajitani, T.; Okoshi, K.; Yashima, E. *Macromolecules* **2008**, *41*, 1601.
(87) Onitsuka, K.; Joh, T.; Takahashi, S. *Angew. Chem., Int. Ed. Engl.* **1992**, *31*, 851.
(88) Takei, F.; Hayashi, H.; Onitsuka, K.; Kobayashi, N.; Takahashi, S. *Angew. Chem., Int. Ed.* **2001**, *40*, 4092.
(89) Onouchi, H.; Okoshi, K.; Kajitani, T.; Sakurai, S.-i.; Nagai, K.; Kumaki, J.; Onitsuka, K.; Yashima, E. *J. Am. Chem. Soc.* **2008**, *130*, 229.
(90) Onitsuka, K.; Yabe, K.; Ohshiro, N.; Shimizu, A.; Okumura, R.; Takei, F.; Takahashi, S. *Macromolecules* **2004**, *37*, 8204.
(91) Onitsuka, K.; Yamamoto, M.; Mori, T.; Takei, F.; Takahashi, S. *Organometallics* **2006**, *25*, 1270.
(92) Onitsuka, K.; Mori, T.; Yamamoto, M.; Takei, F.; Takahashi, S. *Macromolecules* **2006**, *39*, 7224.
(93) Amabilino, D. B.; Ramos, E.; Serrano, J.-L.; Sierra, T.; Veciana, J. *J. Am. Chem. Soc.* **1998**, *120*, 9126.
(94) Amabilino, D. B.; Ramos, E.; Serrano, J.-L.; Sierra, T.; Veciana, J. *Polymer* **2005**, *46*, 1507.
(95) Tian, Y.; Kamata, K.; Yoshida, H.; Iyoda, T. *Chem.—Eur. J.* **2006**, *12*, 584.
(96) Kajitani, T.; Lin, H.; Nagai, K.; Okoshi, K.; Onouchi, H.; Yashima, E. *Macromolecules* **2009**, *42*, 560.
(97) Gomar-Nadal, E.; Veciana, J.; Rovira, C.; Amabilino, D. B. *Adv. Mater.* **2005**, *17*, 2095.
(98) Hida, N.; Takei, F.; Onitsuka, K.; Shiga, K.; Asaoka, S.; Iyoda, T.; Takahashi, S. *Angew. Chem., Int. Ed.* **2003**, *42*, 4349.
(99) Yamada, Y.; Kawai, T.; Abe, J.; Iyoda, T. *J. Polym. Sci., Part A: Polym. Chem.* **2002**, *40*, 399.
(100) Hasegawa, T.; Kondoh, S.; Matsuura, K.; Kobayashi, K. *Macromolecules* **1999**, *32*, 6595.
(101) Hasegawa, T.; Matsuura, K.; Ariga, K.; Kobayashi, K. *Macromolecules* **2000**, *33*, 2772.
(102) Suginome, M.; Ito, Y. *Adv. Polym. Sci.* **2004**, *17*, 77.
(103) Suginome, M.; Collet, S.; Ito, Y. *Org. Lett.* **2002**, *4*, 351.
(104) Ito, Y.; Kojima, Y.; Murakami, M.; Suginome, M. *Bull. Chem. Soc. Jpn.* **1997**, *70*, 2801.
(105) Suginome, M.; Noguchi, H.; Murakami, M. *Chem. Lett.* **2007**, *36*, 1036.
(106) Schlitzer, D. S.; Novak, B. M. *J. Am. Chem. Soc.* **1998**, *120*, 2196.
(107) Tang, H. Z.; Lu, Y. J.; Tian, G. L.; Capracotta, M. D.; Novak, B. M. *J. Am. Chem. Soc.* **2004**, *126*, 3722.
(108) Tang, H. Z.; Garland, E. R.; Novak, B. M.; He, J. T.; Polavarapu, P. L.; Sun, F. C.; Sheiko, S. S. *Macromolecules* **2007**, *40*, 3575.
(109) Tang, H.-Z.; Novak, B. M.; He, J.; Polavarapu, P. L. *Angew. Chem., Int. Ed.* **2005**, *44*, 7298.
(110) Tang, H. Z.; Boyle, P. D.; Novak, B. M. *J. Am. Chem. Soc.* **2005**, *127*, 2136.
(111) Green, M. M.; Park, J. W.; Sato, T.; Teramoto, A.; Lifson, S.; Selinger, R. L. B.; Selinger, J. V. *Angew. Chem., Int. Ed.* **1999**, *38*, 3138.
(112) Green, M. M.; Reidy, M. P.; Johnson, R. J.; Darling, G.; Oleary, D. J.; Willson, G. *J. Am. Chem. Soc.* **1989**, *111*, 6452.
(113) Jha, S. K.; Cheon, K.-S.; Green, M. M.; Selinger, J. V. *J. Am. Chem. Soc.* **1999**, *121*, 1665.
(114) Maeda, K.; Okamoto, Y. *Polym. J.* **1998**, *30*, 100.
(115) Teramoto, A. *Prog. Polym. Sci.* **2001**, *26*, 667.
(116) Lifson, S.; Andreola, C.; Peterson, N. C.; Green, M. M. *J. Am. Chem. Soc.* **1989**, *111*, 8850.
(117) Gu, H.; Nakamura, Y.; Sato, T.; Teramoto, A.; Green, M. M.; Andreola, C.; Peterson, N. C.; Lifson, S. *Macromolecules* **1995**, *28*, 1016.
(118) Ute, K.; Fukunishi, Y.; Jha, S. K.; Cheon, K. S.; Munoz, B.; Hatada, K.; Green, M. M. *Macromolecules* **1999**, *32*, 1304.
(119) Green, M. M.; Khatri, C.; Peterson, N. C. *J. Am. Chem. Soc.* **1993**, *115*, 4941.
(120) Green, M. M.; Garetz, B. A.; Munoz, B.; Chang, H. P.; Hoke, S.; Cooks, R. G. *J. Am. Chem. Soc.* **1995**, *117*, 4181.
(121) Patten, T. E.; Novak, B. M. *J. Am. Chem. Soc.* **1996**, *118*, 1906.
(122) Patten, T. E.; Novak, B. M. *J. Am. Chem. Soc.* **1991**, *113*, 5065.
(123) Lee, J. S.; Ryu, S. W. *Macromolecules* **1999**, *32*, 2085.
(124) Shin, Y.-D.; Kim, S.-Y.; Ahn, J.-H.; Lee, J.-S. *Macromolecules* **2001**, *34*, 2408.
(125) Ahn, J.-H.; Shin, Y.-D.; Nath, G. Y.; Park, S.-Y.; Rahman, M. S.; Samal, S.; Lee, J.-S. *J. Am. Chem. Soc.* **2005**, *127*, 4132.
(126) Matyjaszewski, K. *J. Inorg. Organomet. Polym.* **1992**, *2*, 5.
(127) Fujiki, M. *J. Am. Chem. Soc.* **1994**, *116*, 6017.
(128) Frey, H.; Moeller, M.; Matyjaszewski, K. *Macromolecules* **1994**, *27*, 1814.
(129) Fujiki, M.; Koe, J. R.; Terao, K.; Sato, T.; Teramoto, A.; Watanabe, J. *Polym. J.* **2003**, *35*, 297.
(130) Fujiki, M. *J. Organomet. Chem.* **2003**, *685*, 15.
(131) Kim, S.-Y.; Saxena, A.; Kwak, G.; Fujiki, M.; Kawakami, Y. *Chem. Commun.* **2004**, 538.
(132) Kawabe, T.; Naito, M.; Fujiki, M. *Polym. J.* **2008**, *40*, 317.
(133) Naito, M.; Nobusawa, K.; Onouchi, H.; Nakamura, M.; Yasui, K.-i.; Ikeda, A.; Fujiki, M. *J. Am. Chem. Soc.* **2008**, *130*, 16697.
(134) Motonaga, M.; Nakashima, H.; Katz, S.; Berry, D. H.; Imase, T.; Kawauchi, S.; Watanabe, J.; Fujiki, M.; Koe, J. R. *J. Organomet. Chem.* **2003**, *685*, 44.
(135) Ciardelli, F.; Benedetti, E.; Pieroni, O. *Makromol. Chem.* **1967**, *103*, 1.
(136) Ciardelli, F.; Lanzillo, S.; Pieroni, O. *Macromolecules* **1974**, *7*, 174.
(137) Tang, B. Z.; Kotera, N. *Macromolecules* **1989**, *22*, 4388.

(138) Yamaguchi, M.; Omata, K.; Hirama, M. *Chem. Lett.* **1992**, 2261.
(139) Moore, J. S.; Gorman, C. B.; Grubbs, R. H. *J. Am. Chem. Soc.* **1991**, *113*, 1704.
(140) Aoki, T.; Kokai, M.; Shinohara, K.-i.; Oikawa, E. *Chem. Lett.* **1993**, *22*, 2009.
(141) Yashima, E.; Huang, S. L.; Matsushima, T.; Okamoto, Y. *Macromolecules* **1995**, *28*, 4184.
(142) Li, B. S.; Cheuk, K. K. L.; Ling, L. S.; Chen, J. W.; Xiao, X. D.; Bai, C. L.; Tang, B. Z. *Macromolecules* **2003**, *36*, 77.
(143) Cheuk, K. K. L.; Lam, J. W. Y.; Lai, L. M.; Dong, Y. P.; Tang, B. Z. *Macromolecules* **2003**, *36*, 9752.
(144) Cheuk, K. K. L.; Li, B. S.; Lam, J. W. Y.; Xie, Y.; Tang, B. Z. *Macromolecules* **2008**, *41*, 5997.
(145) Cheuk, K. K. L.; Lam, J. W. Y.; Chen, J. W.; Lai, L. M.; Tang, B. Z. *Macromolecules* **2003**, *36*, 5947.
(146) Lai, L. M.; Lam, J. W. Y.; Qin, A. J.; Dong, Y. Q.; Tang, B. Z. *J. Phys. Chem. B* **2006**, *110*, 11128.
(147) Lai, L. M.; Lam, J. W. Y.; Tang, B. Z. *J. Polym. Sci., Part A: Polym. Chem.* **2006**, *44*, 2117.
(148) Lai, L. M.; Lam, J. W. Y.; Cheuk, K. K. L.; Sung, H. H. Y.; Williams, I. D.; Tang, B. Z. *J. Polym. Sci., Part A: Polym. Chem.* **2005**, *43*, 3701.
(149) Liu, J. H.; Yan, J. J.; Chen, E. Q.; Lam, J. W. Y.; Dong, Y. P.; Liang, D. H.; Tang, B. Z. *Polymer* **2008**, *49*, 3366.
(150) Lam, J. W. Y.; Tang, B. Z. *Acc. Chem. Res.* **2005**, *38*, 745.
(151) Okoshi, K.; Sakajiri, K.; Kumaki, J.; Yashima, E. *Macromolecules* **2005**, *38*, 4061.
(152) Otsuka, I.; Hongo, T.; Nakade, H.; Narumi, A.; Sakai, R.; Satoh, T.; Kaga, H.; Kakuchi, T. *Macromolecules* **2007**, *40*, 8930.
(153) Cheuk, K. K. L.; Lam, J. W. Y.; Li, B. S.; Xie, Y.; Tang, B. Z. *Macromolecules* **2007**, *40*, 2633.
(154) Matsuura, K.; Furuno, S.-i.; Kobayashi, K. *Chem. Lett.* **1998**, *27*, 847.
(155) Takata, T.; Ishiwari, F.; Sato, T.; Seto, R.; Koyama, Y. *Polym. J.* **2008**, *40*, 846.
(156) Nomura, R.; Nakako, H.; Masuda, T. *J. Mol. Catal. A: Chem.* **2002**, *190*, 197.
(157) Suzuki, Y.; Shiotsuki, M.; Sanda, F.; Masuda, T. *Chem.—Asian J.* **2008**, *3*, 2075.
(158) Zhao, H. C.; Sanda, F.; Masuda, T. *J. Polym. Sci., Part A: Polym. Chem.* **2005**, *43*, 5168.
(159) Tabei, J.; Sanda, F.; Masuda, T. *Kobunshi Ronbunshu* **2006**, *63*, 286.
(160) Nomura, R.; Tabei, J.; Nishiura, S.; Masuda, T. *Macromolecules* **2003**, *36*, 561.
(161) Deng, J.; Luo, X.; Zhao, W.; Yang, W. *J. Polym. Sci., Part A: Polym. Chem.* **2008**, *46*, 4112.
(162) Deng, J.; Chen, B.; Luo, X.; Yang, W. *Macromolecules* **2009**, *42*, 933.
(163) Zhou, J.-L.; Chen, X.-F.; Fan, X.-H.; Lu, C.-X.; Zhou, Q.-F. *J. Polym. Sci., Part A: Polym. Chem.* **2006**, *44*, 6047.
(164) Zhang, Z.; Deng, J.; Zhao, W.; Wang, J.; Yang, W. *J. Polym. Sci., Part A: Polym. Chem.* **2007**, *45*, 500.
(165) Zhang, Z. G.; Deng, J. P.; Li, J. W.; Yang, W. T. *Polym. J.* **2008**, *40*, 436.
(166) Mitsuyama, M.; Kondo, K. *Macromol. Chem. Phys.* **2000**, *201*, 1613.
(167) Lai, L. M.; Lam, J. W. Y.; Tang, B. Z. *J. Polym. Sci., Part A: Polym. Chem.* **2006**, *44*, 6190.
(168) Simionescu, C. I.; Percec, V.; Dumitrescu, S. *J. Polym. Sci., Part A: Polym. Chem.* **1977**, *15*, 2497.
(169) Furlani, A.; Napoletano, C.; Russo, M. V.; Feast, W. J. *Polym. Bull.* **1986**, *16*, 311.
(170) Tabata, M.; Yang, W.; Yokota, K. *Polym. J.* **1990**, *22*, 1105.
(171) Kishimoto, Y.; Eckerle, P.; Miyatake, T.; Ikariya, T.; Noyori, R. *J. Am. Chem. Soc.* **1994**, *116*, 12131.
(172) Simionescu, C. I.; Percec, V. *Prog. Polym. Sci.* **1982**, *8*, 133.
(173) Yashima, E.; Huang, S.; Okamoto, Y. *J. Chem. Soc., Chem. Commun.* **1994**, 1811.
(174) Percec, V.; Obata, M.; Rudick, J. G.; De, B. B.; Glodde, M.; Bera, T. K.; Magonov, S. N.; Balagurusamy, V. S. K.; Heiney, P. A. *J. Polym. Sci., Part A: Polym. Chem.* **2002**, *40*, 3509.
(175) Schenning, A. P. H. J.; Fransen, M.; Meijer, E. W. *Macromol. Rapid Commun.* **2002**, *23*, 265.
(176) Percec, V.; Rudick, J. G.; Peterca, M.; Wagner, M.; Obata, M.; Mitchell, C. M.; Cho, W. D.; Balagurusamy, V. S. K.; Heiney, P. A. *J. Am. Chem. Soc.* **2005**, *127*, 15257.
(177) Percec, V.; Rudick, J. G.; Peterca, M.; Staley, S. R.; Wagner, M.; Obata, M.; Mitchell, C. M.; Cho, W. D.; Balagurusamy, V. S. K.; Lowe, J. N.; Glodde, M.; Weichold, O.; Chung, K. J.; Ghionni, N.; Magonov, S. N.; Heiney, P. A. *Chem.—Eur. J.* **2006**, *12*, 5731.
(178) Percec, V.; Peterca, M.; Rudick, J. G.; Aqad, E.; Imam, M. R.; Heiney, P. A. *Chem.—Eur. J.* **2007**, *13*, 9572.
(179) Percec, V.; Aqad, E.; Peterca, M.; Rudick, J. G.; Lemon, L.; Ronda, J. C.; De, B. B.; Heiney, P. A.; Meijer, E. W. *J. Am. Chem. Soc.* **2006**, *128*, 16365.
(180) Rudick, J. G.; Percec, V. *New J. Chem.* **2007**, *31*, 1083.
(181) Percec, V.; Rudick, J. G.; Peterca, M.; Aqad, E.; Imam, M. R.; Heiney, P. A. *J. Polym. Sci., Part A: Polym. Chem.* **2007**, *45*, 4974.
(182) Rudick, J. G.; Percec, V. *Acc. Chem. Res.* **2008**, *41*, 1641.
(183) Rudick, J. G.; Percec, V. *Macromol. Chem. Phys.* **2008**, *209*, 1759.
(184) Kong, X. X.; Lam, J. W. Y.; Tang, B. Z. *Macromolecules* **1999**, *32*, 1722.
(185) Karim, S. M. A.; Nomura, R.; Masuda, T. *J. Polym. Sci., Part A: Polym. Chem.* **2001**, *39*, 3130.
(186) Percec, V.; Rudick, J. G.; Nombel, P.; Buchowicz, W. *J. Polym. Sci., Part A: Polym. Chem.* **2002**, *40*, 3212.
(187) Morino, K.; Asari, T.; Maeda, K.; Yashima, E. *J. Polym. Sci., Part A: Polym. Chem.* **2004**, *42*, 4711.
(188) Percec, V.; Rudick, J. G. *Macromolecules* **2005**, *38*, 7241.
(189) Percec, V.; Rudick, J. G.; Aqad, E. *Macromolecules* **2005**, *38*, 7205.
(190) Nomura, R.; Fukushima, Y.; Nakako, H.; Masuda, T. *J. Am. Chem. Soc.* **2000**, *122*, 8830.
(191) Ashida, Y.; Sato, T.; Morino, K.; Maeda, K.; Okamoto, Y.; Yashima, E. *Macromolecules* **2003**, *36*, 3345.
(192) Morino, K.; Maeda, K.; Okamoto, Y.; Yashima, E.; Sato, T. *Chem.—Eur. J.* **2002**, *8*, 5112.
(193) Sakurai, S.-i.; Ohsawa, S.; Nagai, K.; Okoshi, K.; Kumaki, J.; Yashima, E. *Angew. Chem., Int. Ed.* **2007**, *46*, 7605.
(194) Gu, H.; Sato, T.; Teramoto, A.; Varichon, L.; Green, M. M. *Polym. J.* **1997**, *29*, 77.
(195) Okamoto, N.; Mukaida, F.; Gu, H.; Nakamura, Y.; Sato, T.; Teramoto, A.; Green, M. M.; Andreola, C.; Peterson, N. C.; Lifson, S. *Macromolecules* **1996**, *29*, 2878.
(196) Yoshiba, K.; Hama, R.; Teramoto, A.; Nakamura, N.; Maeda, K.; Okamoto, Y.; Sato, T. *Macromolecules* **2006**, *39*, 3435.
(197) Terao, K.; Terao, Y.; Teramoto, A.; Nakamura, N.; Fujiki, M.; Sato, T. *Macromolecules* **2001**, *34*, 6519.
(198) Teramoto, A.; Terao, K.; Terao, Y.; Nakamura, N.; Sato, T.; Fujiki, M. *J. Am. Chem. Soc.* **2001**, *123*, 12303.
(199) Tabei, J.; Shiotsuki, M.; Sato, T.; Sanda, F.; Masuda, T. *Chem.—Eur. J.* **2005**, *11*, 3591.
(200) Kobayashi, S.; Morino, K.; Yashima, E. *Chem. Commun.* **2007**, 2351.
(201) Aoki, T.; Kaneko, T.; Maruyama, N.; Sumi, A.; Takahashi, M.; Sato, T.; Teraguchi, M. *J. Am. Chem. Soc.* **2003**, *125*, 6346.
(202) Katagiri, H.; Kaneko, T.; Teraguchi, M.; Aoki, T. *Chem. Lett.* **2008**, *37*, 390.
(203) Nishimura, T.; Ichikawa, Y.; Hayashi, T.; Onishi, N.; Shiotsuki, M.; Masuda, T. *Organometallics* **2009**, *28*, 4890.
(204) Hadano, S.; Kishimoto, T.; Hattori, T.; Tanioka, D.; Teraguchi, M.; Aoki, T.; Kaneko, T.; Namikoshi, T.; Marwanta, E. *Macromol. Chem. Phys.* **2009**, *210*, 717.
(205) Umeda, Y.; Kaneko, T.; Teraguchi, M.; Aoki, T. *Chem. Lett.* **2005**, *34*, 854.
(206) Murata, H.; Miyajima, D.; Nishide, H. *Macromolecules* **2006**, *39*, 6331.
(207) Jia, H.; Teraguchi, M.; Aoki, T.; Abe, Y.; Kaneko, T.; Hadano, S.; Namikoshi, T.; Marwanta, E. *Macromolecules* **2009**, *42*, 17.
(208) Tang, B. Z.; Xu, H. Y. *Macromolecules* **1999**, *32*, 2569.
(209) Yuan, W. Z.; Sun, J. Z.; Dong, Y. Q.; Haussler, M.; Yang, F.; Xu, H. P.; Qin, A. J.; Lam, J. W. Y.; Zheng, Q.; Tang, B. Z. *Macromolecules* **2006**, *39*, 8011.
(210) Nelson, J. C.; Saven, J. G.; Moore, J. S.; Wolynes, P. G. *Science* **1997**, *277*, 1793.
(211) Prince, R. B.; Barnes, S. A.; Moore, J. S. *J. Am. Chem. Soc.* **2000**, *122*, 2758.
(212) Tanatani, A.; Mio, M. J.; Moore, J. S. *J. Am. Chem. Soc.* **2001**, *123*, 1792.
(213) Ray, C. R.; Moore, J. S. *Adv. Polym. Sci.* **2005**, *177*, 91.
(214) Zhao, X.; Schanze, K. S. *Langmuir* **2006**, *22*, 4856.
(215) Kaneko, T.; Yoshimoto, S.; Hadano, S.; Teraguchi, M.; Aoki, T. *Polyhedron* **2007**, *26*, 1825.
(216) Shinohara, K.; Aoki, T.; Kaneko, T.; Oikawa, E. *Polymer* **2001**, *42*, 351.
(217) Sanji, T.; Sato, Y.; Kato, N.; Tanaka, M. *Macromolecules* **2007**, *40*, 4747.
(218) Liu, R.; Sanda, F.; Masuda, T. *Macromolecules* **2008**, *41*, 5089.
(219) van Gorp, J. J.; Vekemans, J.; Meijer, E. W. *Chem. Commun.* **2004**, 60.
(220) Sinkeldam, R. W.; van Houtem, M.; Pieterse, K.; Vekemans, J.; Meijer, E. W. *Chem.—Eur. J.* **2006**, *12*, 6129.
(221) Sinkeldam, R. W.; Hoeben, F. J. M.; Pouderoijen, M. J.; De Cat, I.; Zhang, J.; Furukawa, S.; De Feyter, S.; Vekemans, J.; Meijer, E. W. *J. Am. Chem. Soc.* **2006**, *128*, 16113.
(222) Yamaguchi, K.; Matsumura, G.; Kagechika, H.; Azumaya, I.; Ito, Y.; Itai, A.; Shudo, K. *J. Am. Chem. Soc.* **1991**, *113*, 5474.

(223) Azumaya, I.; Kagechika, H.; Yamaguchi, K.; Shudo, K. *Tetrahedron* **1995**, *51*, 5277.
(224) Tanatani, A.; Yokoyama, A.; Azumaya, I.; Takakura, Y.; Mitsui, C.; Shiro, M.; Uchiyama, M.; Muranaka, A.; Kobayashi, N.; Yokozawa, T. *J. Am. Chem. Soc.* **2005**, *127*, 8553.
(225) Mikami, K.; Tanatani, A.; Yokoyama, A.; Yokozawa, T. *Macromolecules* **2009**, *42*, 3849.
(226) Yamazaki, K.; Yokoyama, A.; Yokozawa, T. *Macromolecules* **2006**, *39*, 2432.
(227) Johnson, J. A.; Finn, M. G.; Koberstein, J. T.; Turro, N. J. *Macromol. Rapid Commun.* **2008**, *29*, 1052.
(228) Binder, W. H.; Sachsenhofer, R. *Macromol. Rapid Commun.* **2008**, *29*, 952.
(229) Fournier, D.; Hoogenboom, R.; Schubert, U. S. *Chem. Soc. Rev.* **2007**, 1369.
(230) Lutz, J.-F. *Angew. Chem., Int. Ed.* **2007**, *46*, 1018.
(231) Meudtner, R. M.; Hecht, S. *Macromol. Rapid Commun.* **2008**, *29*, 347.
(232) Kobayashi, S.; Itomi, K.; Morino, K.; Iida, H.; Yashima, E. *Chem. Commun.* **2008**, 3019.
(233) Iwasaki, T.; Kohinata, Y.; Nishide, H. *Org. Lett.* **2005**, *7*, 755.
(234) Iwasaki, T.; Tsukahara, Y.; Nishide, H. *Chem. Lett.* **2005**, *34*, 164.
(235) Zhang, H.-C.; Pu, L. *Macromolecules* **2004**, *37*, 2695.
(236) Bouman, M. M.; Havinga, E. E.; Janssen, R. A. J.; Meijer, E. W. *Mol. Cryst. Liq. Cryst.* **1994**, *256*, 439.
(237) Bouman, M. M.; Meijer, E. W. *Adv. Mater.* **1995**, *7*, 385.
(238) Langeveld-Voss, B. M. W.; Janssen, R. A. J.; Christiaans, M. P. T.; Meskers, S. C. J.; Dekkers, H.; Meijer, E. W. *J. Am. Chem. Soc.* **1996**, *118*, 4908.
(239) Bidan, G.; Guillerez, S.; Sorokin, V. *Adv. Mater.* **1996**, *8*, 157.
(240) Ochiai, K.; Tabuchi, Y.; Rikukawa, M.; Sanui, K.; Ogata, N. *Thin Solid Films* **1998**, *327*−*329*, 454.
(241) Langeveld-Voss, B. M. W.; Christiaans, M. P. T.; Janssen, R. A. J.; Meijer, E. W. *Macromolecules* **1998**, *31*, 6702.
(242) Langeveld-Voss, B. M. W.; Waterval, R. J. M.; Janssen, R. A. J.; Meijer, E. W. *Macromolecules* **1999**, *32*, 227.
(243) Langeveld-Voss, B. M. W.; Janssen, R. A. J.; Meijer, E. W. *J. Mol. Struct.* **2000**, *521*, 285.
(244) Goto, H.; Yashima, E. *J. Am. Chem. Soc.* **2002**, *124*, 7943.
(245) Grenier, C. R. G.; George, S. J.; Joncheray, T. J.; Meijer, E. W.; Reynolds, J. R. *J. Am. Chem. Soc.* **2007**, *129*, 10694.
(246) Andersson, M. R.; Ekeblad, P. O.; Hjertberg, T.; Wennerström, O.; Inganäs, O. *Polym. Commun.* **1991**, *32*, 546.
(247) Nilsson, K. P. R.; Andersson, M. R.; Inganäs, O. *J. Phys.: Condens. Matter* **2002**, *14*, 10011.
(248) Nilsson, K. P. R.; Olsson, J. D. M.; Konradsson, P.; Inganäs, O. *Macromolecules* **2004**, *37*, 6316.
(249) Zhang, Z. B.; Fujiki, M.; Motonaga, M.; Nakashima, H.; Torimitsu, K.; Tang, H. Z. *Macromolecules* **2002**, *35*, 941.
(250) Tang, H. Z.; Fujiki, M.; Sato, T. *Macromolecules* **2002**, *35*, 6439.
(251) Zhang, Z. B.; Motonaga, M.; Fujiki, M.; McKenna, C. E. *Macromolecules* **2003**, *36*, 6956.
(252) Vanormelingen, W.; Van den Bergh, K.; Verbiest, T.; Koeckelberghs, G. *Macromolecules* **2008**, *41*, 5582.
(253) Yeh, M.-Y.; Luh, T.-Y. *Chem.*−*Asian J.* **2008**, *3*, 1620.
(254) Piguet, C.; Bernardinelli, G.; Hopfgartner, G. *Chem. Rev.* **1997**, *97*, 2005.
(255) Kim, H.-J.; Zin, W.-C.; Lee, M. *J. Am. Chem. Soc.* **2004**, *126*, 7009.
(256) Kim, H.-J.; Lee, J.-H.; Lee, M. *Angew. Chem., Int. Ed.* **2005**, *44*, 5810.
(257) Jung, O.-S.; Kim, Y. J.; Lee, Y.-A.; Park, J. K.; Chae, H. K. *J. Am. Chem. Soc.* **2000**, *122*, 9921.
(258) Kim, H.-J.; Lee, E.; Park, H.-S.; Lee, M. *J. Am. Chem. Soc.* **2007**, *129*, 10994.
(259) Wackerly, J. W.; Moore, J. S. *Macromolecules* **2006**, *39*, 7269.
(260) Zhao, D. H.; Moore, J. S. *Org. Biomol. Chem.* **2003**, *1*, 3471.
(261) Yashima, E.; Maeda, K.; Nishimura, T. *Chem.*−*Eur. J.* **2004**, *10*, 43.
(262) Yashima, E.; Matsushima, T.; Okamoto, Y. *J. Am. Chem. Soc.* **1995**, *117*, 11596.
(263) Tsukube, H.; Shinoda, S. *Chem. Rev.* **2002**, *102*, 2389.
(264) Hembury, G. A.; Borovkov, V. V.; Inoue, Y. *Chem. Rev.* **2008**, *108*, 1.
(265) Yashima, E.; Matsushima, T.; Okamoto, Y. *J. Am. Chem. Soc.* **1997**, *119*, 6345.
(266) Onouchi, H.; Maeda, K.; Yashima, E. *J. Am. Chem. Soc.* **2001**, *123*, 7441.
(267) Onouchi, H.; Kashiwagi, D.; Hayashi, K.; Maeda, K.; Yashima, E. *Macromolecules* **2004**, *37*, 5495.
(268) Kamikawa, Y.; Kato, T.; Onouchi, H.; Kashiwagi, D.; Maeda, K.; Yashima, E. *J. Polym. Sci., Part A: Polym. Chem.* **2004**, *42*, 4580.
(269) Onouchi, H.; Hasegawa, T.; Kashiwagi, D.; Ishiguro, H.; Maeda, K.; Yashima, E. *Macromolecules* **2005**, *38*, 8625.
(270) Onouchi, H.; Hasegawa, T.; Kashiwagi, D.; Ishiguro, H.; Maeda, K.; Yashima, E. *J. Polym. Sci., Part A: Polym. Chem.* **2006**, *44*, 5039.
(271) Miyagawa, T.; Furuko, A.; Maeda, K.; Katagiri, H.; Furusho, Y.; Yashima, E. *J. Am. Chem. Soc.* **2005**, *127*, 5018.
(272) Hasegawa, T.; Maeda, K.; Ishiguro, H.; Yashima, E. *Polym. J.* **2006**, *38*, 912.
(273) Yashima, E.; Nimura, T.; Matsushima, T.; Okamoto, Y. *J. Am. Chem. Soc.* **1996**, *118*, 9800.
(274) Kawamura, H.; Maeda, K.; Okamoto, Y.; Yashima, E. *Chem. Lett.* **2001**, 58.
(275) Yashima, E.; Maeda, Y.; Okamoto, Y. *Chem. Lett.* **1996**, 955.
(276) Yashima, E.; Maeda, Y.; Matsushima, T.; Okamato, Y. *Chirality* **1997**, *9*, 593.
(277) Maeda, K.; Okada, S.; Yashima, E.; Okamoto, Y. *J. Polym. Sci., Part A: Polym. Chem.* **2001**, *39*, 3180.
(278) Nagai, K.; Maeda, K.; Takeyama, Y.; Sakajiri, K.; Yashima, E. *Macromolecules* **2005**, *38*, 5444.
(279) Nonokawa, R.; Yashima, E. *J. Am. Chem. Soc.* **2003**, *125*, 1278.
(280) Nonokawa, R.; Yashima, E. *J. Polym. Sci., Part A: Polym. Chem.* **2003**, *41*, 1004.
(281) Nonokawa, R.; Oobo, M.; Yashima, E. *Macromolecules* **2003**, *36*, 6599.
(282) Kawamura, H.; Ishikawa, M.; Maeda, K.; Yashima, E. *Chem. Lett.* **2003**, *32*, 1086.
(283) Goto, H.; Morino, K.; Morishita, T.; Maeda, K.; Yashima, E. *Kobunshi Ronbunshu* **2006**, *63*, 325.
(284) Maeda, K.; Tamaki, S.; Tamura, K.; Yashima, E. *Chem.*−*Asian J.* **2008**, *3*, 614.
(285) Manning, G. S. *Acc. Chem. Res.* **1979**, *12*, 443.
(286) Saito, M. A.; Maeda, K.; Onouchi, H.; Yashima, E. *Macromolecules* **2000**, *33*, 4616.
(287) Goto, H.; Zhang, H. Q.; Yashima, E. *J. Am. Chem. Soc.* **2003**, *125*, 2516.
(288) Morino, K.; Oobo, M.; Yashima, E. *Macromolecules* **2005**, *38*, 3461.
(289) Maeda, K.; Hatanaka, K.; Yashima, E. *Mendeleev Commun.* **2004**, 231.
(290) Dei, S.; Matsumoto, A. *Macromol. Chem. Phys.* **2009**, *210*, 11.
(291) Yashima, E.; Goto, H.; Okamoto, Y. *Polym. J.* **1998**, *30*, 69.
(292) Maeda, K.; Goto, H.; Yashima, E. *Macromolecules* **2001**, *34*, 1160.
(293) Tabei, J.; Nomura, R.; Sanda, F.; Masuda, T. *Macromolecules* **2003**, *36*, 8603.
(294) Maeda, K.; Yamamoto, N.; Okamoto, Y. *Macromolecules* **1998**, *31*, 5924.
(295) Sakai, R.; Satoh, T.; Kakuchi, R.; Kaga, H.; Kakuchi, T. *Macromolecules* **2003**, *36*, 3709.
(296) Sakai, R.; Satoh, T.; Kakuchi, R.; Kaga, H.; Kakuchi, T. *Macromolecules* **2004**, *37*, 3996.
(297) Ishikawa, M.; Maeda, K.; Yashima, E. *J. Am. Chem. Soc.* **2002**, *124*, 7448.
(298) Yashima, E.; Maeda, K.; Yamanaka, T. *J. Am. Chem. Soc.* **2000**, *122*, 7813.
(299) Dellaportas, P.; Jones, R. G.; Holder, S. J. *Macromol. Rapid Commun.* **2002**, *23*, 99.
(300) Nakashima, H.; Koe, J. R.; Torimitsu, K.; Fujiki, M. *J. Am. Chem. Soc.* **2001**, *123*, 4847.
(301) Holder, S. J.; Achilleos, M.; Jones, R. G. *J. Am. Chem. Soc.* **2006**, *128*, 12418.
(302) Li, J.; Schuster, G. B.; Cheon, K. S.; Green, M. M.; Selinger, J. V. *J. Am. Chem. Soc.* **2000**, *122*, 2603.
(303) Saxena, A.; Guo, G.; Fujiki, M.; Yang, Y.; Ohira, A.; Okoshi, K.; Naito, M. *Macromolecules* **2004**, *37*, 3081.
(304) Ichimura, K. *Chem. Rev.* **2000**, *100*, 1847.
(305) Sannigrahi, B.; McGeady, P.; Khan, I. M. *Macromol. Biosci.* **2004**, *4*, 999.
(306) Vera, F.; Almuzara, C.; Orera, I.; Barberá, J.; Oriol, L.; Serrano, J. L.; Sierra, T. *J. Polym. Sci., Part A: Polym. Chem.* **2008**, *46*, 5528.
(307) Majidi, M. R.; Kanemaguire, L. A. P.; Wallace, G. G. *Polymer* **1995**, *36*, 3597.
(308) Strounina, E. V.; Kane-Maguire, L. A. P.; Wallace, G. G. *Polymer* **2006**, *47*, 8088.
(309) Moriuchi, T.; Shen, X.; Hirao, T. *Tetrahedron* **2006**, *62*, 12237.
(310) Yashima, E.; Goto, H.; Okamoto, Y. *Macromolecules* **1999**, *32*, 7942.
(311) Maeda, K.; Morioka, K.; Yashima, E. *Macromolecules* **2007**, *40*, 1349.
(312) Arnt, L.; Tew, G. N. *Macromolecules* **2004**, *37*, 1283.
(313) Inouye, M.; Waki, M.; Abe, H. *J. Am. Chem. Soc.* **2004**, *126*, 2022.
(314) Waki, M.; Abe, H.; Inouye, M. *Chem.*−*Eur. J.* **2006**, *12*, 7839.
(315) Hanan, G. S.; Lehn, J. M.; Kyritsakas, N.; Fischer, J. *J. Chem. Soc., Chem. Commun.* **1995**, 765.
(316) Petitjean, A.; Nierengarten, H.; van Dorsselaer, A.; Lehn, J. M. *Angew. Chem., Int. Ed.* **2004**, *43*, 3695.
(317) Petitjean, A.; Cuccia, L. A.; Schmutz, M.; Lehn, J. M. *J. Org. Chem.* **2008**, *73*, 2481.

(318) Hou, J. L.; Shao, X. B.; Chen, G. J.; Zhou, Y. X.; Jiang, X. K.; Li, Z. T. *J. Am. Chem. Soc.* **2004**, *126*, 12386.
(319) Li, Z.-T.; Hou, J.-L.; Li, C. *Acc. Chem. Res.* **2008**, *41*, 1343.
(320) Maurizot, V.; Dolain, C.; Huc, I. *Eur. J. Org. Chem.* **2005**, 1293.
(321) Kolomiets, E.; Berl, V.; Lehn, J. M. *Chem.—Eur. J.* **2007**, *13*, 5466.
(322) Oh, K.; Jeong, K. S.; Moore, J. S. *Nature* **2001**, *414*, 889.
(323) Zhao, D. H.; Moore, J. S. *J. Am. Chem. Soc.* **2002**, *124*, 9996.
(324) Hecht, S.; Khan, A. *Angew. Chem., Int. Ed.* **2003**, *42*, 6021.
(325) Haraguchi, S.; Hasegawa, T.; Numata, M.; Fujiki, M.; Uezu, K.; Sakurai, K.; Shinkai, S. *Org. Lett.* **2005**, *7*, 5605.
(326) Sanji, T.; Kato, N.; Kato, M.; Tanaka, M. *Angew. Chem., Int. Ed.* **2005**, *44*, 7301.
(327) Li, C.; Numata, M.; Bae, A.-H.; Sakurai, K.; Shinkai, S. *J. Am. Chem. Soc.* **2005**, *127*, 4548.
(328) Sanji, T.; Kato, N.; Tanaka, M. *Org. Lett.* **2006**, *8*, 235.
(329) Feringa, B. L.; van Delden, R. A. *Angew. Chem., Int. Ed.* **1999**, *38*, 3419.
(330) Eelkema, R.; Feringa, B. L. *Org. Biomol. Chem.* **2006**, *4*, 3729.
(331) Pijper, D.; Feringa, B. L. *Soft Matter* **2008**, *4*, 1349.
(332) Mateos-Timoneda, M. A.; Crego-Calama, M.; Reinhoudt, D. N. *Chem. Soc. Rev.* **2004**, *33*, 363.
(333) Praveen, V. K.; Babu, S. S.; Vijayakumar, C.; Varghese, R.; Ajayaghosh, A. *Bull. Chem. Soc. Jpn.* **2008**, *81*, 1196.
(334) Yamamoto, T.; Fukushima, T.; Aida, T. *Adv. Polym. Sci.* **2008**, 1.
(335) Gao, G. Z.; Sanda, F.; Masuda, T. *Macromolecules* **2003**, *36*, 3938.
(336) Nomura, R.; Tabei, J.; Masuda, T. *Macromolecules* **2002**, *35*, 2955.
(337) Tabei, J.; Nomura, R.; Masuda, T. *Macromolecules* **2002**, *35*, 5405.
(338) Maeda, K.; Okamoto, Y. *Macromolecules* **1998**, *31*, 1046.
(339) Takei, F.; Onitsuka, K.; Takahashi, S. *Polym. J.* **2000**, *32*, 524.
(340) Takei, F.; Onitsuka, K.; Takahashi, S. *Polym. J.* **1999**, *31*, 1029.
(341) Okamoto, Y.; Nishikawa, M.; Nakano, T.; Yashima, E.; Hatada, K. *Macromolecules* **1995**, *28*, 5135.
(342) Prince, R. B.; Moore, J. S.; Brunsveld, L.; Meijer, E. W. *Chem.—Eur. J.* **2001**, *7*, 4150.
(343) Morino, K.; Watase, N.; Maeda, K.; Yashima, E. *Chem.—Eur. J.* **2004**, *10*, 4703.
(344) Podlech, J. *Angew. Chem., Int. Ed.* **1999**, *38*, 477.
(345) Nishino, H.; Kosaka, A.; Hembury, G. A.; Shitomi, H.; Onuki, H.; Inoue, Y. *Org. Lett.* **2001**, *3*, 921.
(346) Nishimura, T.; Takatani, K.; Sakurai, S.-i.; Maeda, K.; Yashima, E. *Angew. Chem., Int. Ed.* **2002**, *41*, 3602.
(347) Nishimura, T.; Maeda, K.; Ohsawa, S.; Yashima, E. *Chem.—Eur. J.* **2005**, *11*, 1181.
(348) Ohsawa, S.; Maeda, K.; Yashima, E. *Macromolecules* **2007**, *40*, 9244.
(349) Nishimura, T.; Ohsawa, S.; Maeda, K.; Yashima, E. *Chem. Commun.* **2004**, 646.
(350) Nishimura, T.; Tsuchiya, K.; Ohsawa, S.; Maeda, K.; Yashima, E.; Nakamura, Y.; Nishimura, J. *J. Am. Chem. Soc.* **2004**, *126*, 11711.
(351) Venkatraman, J.; Shankaramma, S. C.; Balaram, P. *Chem. Rev.* **2001**, *101*, 3131.
(352) Pengo, B.; Formaggio, F.; Crisma, M.; Toniolo, C.; Bonora, G. M.; Broxterman, Q. B.; Kamphuis, J.; Saviano, M.; Iacovino, R.; Rossi, F.; Benedetti, E. *J. Chem. Soc., Perkin Trans. 2* **1998**, 1651.
(353) Inai, Y.; Komori, H.; Ousaka, N. *Chem. Rec.* **2007**, *7*, 191.
(354) Ousaka, N.; Inai, Y. *J. Org. Chem.* **2009**, *74*, 1429.
(355) Inai, Y.; Tagawa, K.; Takasu, A.; Hirabayashi, T.; Oshikawa, T.; Yamashita, M. *J. Am. Chem. Soc.* **2000**, *122*, 11731.
(356) Inai, Y.; Ousaka, N.; Okabe, T. *J. Am. Chem. Soc.* **2003**, *125*, 8151.
(357) Okamoto, Y.; Matsuda, M.; Nakano, T.; Yashima, E. *Polym. J.* **1993**, *25*, 391.
(358) Okamoto, Y.; Matsuda, M.; Nakano, T.; Yashima, E. *J. Polym. Sci., Part A: Polym. Chem.* **1994**, *32*, 309.
(359) Maeda, K.; Matsuda, M.; Nakano, T.; Okamoto, Y. *Polym. J.* **1995**, *27*, 141.
(360) Obata, K.; Kabuto, C.; Kira, M. *J. Am. Chem. Soc.* **1997**, *119*, 11345.
(361) Obata, K.; Kira, M. *Macromolecules* **1998**, *31*, 4666.
(362) Sanji, T.; Takase, K.; Sakurai, H. *J. Am. Chem. Soc.* **2001**, *123*, 12690.
(363) Sanji, T.; Takase, K.; Sakurai, H. *Bull. Chem. Soc. Jpn.* **2004**, *77*, 1607.
(364) Sanji, T.; Takase, K.; Sakurai, H. *Polym. Bull.* **2007**, *59*, 169.
(365) Abe, H.; Murayama, D.; Kayamori, F.; Inouye, M. *Macromolecules* **2008**, *41*, 6903.
(366) Naidu, V. R.; Kim, M. C.; Suk, J.-m.; Kim, H.-J.; Lee, M.; Sim, E.; Jeong, K.-S. *Org. Lett.* **2008**, *10*, 5373.
(367) Hu, H.-Y.; Xiang, J.-F.; Yang, Y.; Chen, C.-F. *Org. Lett.* **2008**, *10*, 1275.
(368) King, E. D.; Tao, P.; Sanan, T. T.; Hadad, C. M.; Parquette, J. R. *Org. Lett.* **2008**, *10*, 1671.
(369) Clayden, J.; Lemiègre, L.; Morris, G. A.; Pickworth, M.; Snape, T. J.; Jones, L. H. *J. Am. Chem. Soc.* **2008**, *130*, 15193.
(370) Ute, K.; Kinoshita, R.; Matsui, K.-i.; Miyatake, N.; Hatada, K. *Chem. Lett.* **1992**, *21*, 1337.
(371) Monde, K.; Miura, N.; Hashimoto, M.; Taniguchi, T.; Inabe, T. *J. Am. Chem. Soc.* **2006**, *128*, 6000.
(372) Yashima, E.; Maeda, K.; Okamoto, Y. *Nature* **1999**, *399*, 449.
(373) Maeda, K.; Morino, K.; Okamoto, Y.; Sato, T.; Yashima, E. *J. Am. Chem. Soc.* **2004**, *126*, 4329.
(374) Onouchi, H.; Miyagawa, T.; Furuko, A.; Maeda, K.; Yashima, E. *J. Am. Chem. Soc.* **2005**, *127*, 2960.
(375) Furusho, Y.; Kimura, T.; Mizuno, Y.; Aida, T. *J. Am. Chem. Soc.* **1997**, *119*, 5267.
(376) Sugasaki, A.; Ikeda, M.; Takeuchi, M.; Robertson, A.; Shinkai, S. *J. Chem. Soc., Perkin Trans. 1* **1999**, 3259.
(377) Prins, L. J.; De Jong, F.; Timmerman, P.; Reinhoudt, D. N. *Nature* **2000**, *408*, 181.
(378) Kubo, Y.; Ohno, T.; Yamanaka, J.; Tokita, S.; Iida, T.; Ishimaru, Y. *J. Am. Chem. Soc.* **2001**, *123*, 12700.
(379) Rosaria, L.; D'Urso, A.; Mammana, A.; Purrello, R. *Chirality* **2008**, *20*, 411.
(380) Ishikawa, M.; Maeda, K.; Mitsutsuji, Y.; Yashima, E. *J. Am. Chem. Soc.* **2004**, *126*, 732.
(381) Hase, Y.; Mitsutsuji, Y.; Ishikawa, M.; Maeda, K.; Okoshi, K.; Yashima, E. *Chem.—Asian J.* **2007**, *2*, 755.
(382) Miyabe, T.; Hase, Y.; Iida, H.; Maeda, K.; Yashima, E. *Chirality* **2009**, *21*, 44.
(383) Maeda, K.; Ishikawa, M.; Yashima, E. *J. Am. Chem. Soc.* **2004**, *126*, 15161.
(384) Ousaka, N.; Inai, Y.; Kuroda, R. *J. Am. Chem. Soc.* **2008**, *130*, 12266.
(385) Yu, Z.; Wan, X.; Zhang, H.; Chen, X.; Zhou, Q. *Chem. Commun.* **2003**, 974.
(386) Decher, G. *Science* **1997**, *277*, 1232.
(387) Maeda, K.; Matsushita, Y.; Ezaka, M.; Yashima, E. *Chem. Commun.* **2005**, 4152.
(388) Teraguchi, M.; Masuda, T. *Macromolecules* **2002**, *35*, 1149.
(389) Teraguchi, M.; Mottate, K.; Kim, S. Y.; Aoki, T.; Kaneko, T.; Hadano, S.; Masuda, T. *Macromolecules* **2005**, *38*, 6367.
(390) Buono, A. M.; Immediata, I.; Rizzo, P.; Guerra, G. *J. Am. Chem. Soc.* **2007**, *129*, 10992.
(391) Guadagno, L.; Raimondo, M.; Silvestre, C.; Immediata, I.; Rizzo, P.; Guerra, G. *J. Mater. Chem.* **2008**, *18*, 567.
(392) Guo, H.; Knobler, C. M.; Kaner, R. B. *Synth. Met.* **1999**, *101*, 44.
(393) Huang, J. X.; Egan, V. M.; Guo, H. L.; Yoon, J. Y.; Briseno, A. L.; Rauda, I. E.; Garrell, R. L.; Knobler, C. M.; Zhou, F. M.; Kaner, R. B. *Adv. Mater.* **2003**, *15*, 1158.
(394) Kusuyama, H.; Takase, M.; Higashihata, Y.; Tseng, H.-T.; Chatani, Y.; Tadokoro, H. *Polymer* **1982**, *23*, 1256.
(395) Kawauchi, T.; Kumaki, J.; Kitaura, A.; Okoshi, K.; Kusanagi, H.; Kobayashi, K.; Sugai, T.; Shinohara, H.; Yashima, E. *Angew. Chem., Int. Ed.* **2008**, *47*, 515.
(396) Spěváček, J.; Schneider, B. *Adv. Colloid Interface Sci.* **1987**, *27*, 81.
(397) te Nijenhuis, K. *Adv. Polym. Sci.* **1997**, *130*, 67.
(398) Hatada, K.; Kitayama, T. *Polym. Int.* **2000**, *49*, 11.
(399) Kawauchi, T.; Kitaura, A.; Kumaki, J.; Kusanagi, H.; Yashima, E. *J. Am. Chem. Soc.* **2008**, *130*, 11889.
(400) Kumaki, J.; Kawauchi, T.; Okoshi, K.; Kusanagi, H.; Yashima, E. *Angew. Chem., Int. Ed.* **2007**, *46*, 5348.
(401) Mizuno, Y.; Aida, T.; Yamaguchi, K. *J. Am. Chem. Soc.* **2000**, *122*, 5278.
(402) Alam, M. A.; Tsuda, A.; Sei, Y.; Yamaguchi, K.; Aida, T. *Tetrahedron* **2008**, *64*, 8264.
(403) Toyofuku, K.; Alam, M. A.; Tsuda, A.; Fujita, N.; Sakamoto, S.; Yamaguchi, K.; Aida, T. *Angew. Chem., Int. Ed.* **2007**, *46*, 6476.
(404) Ikeda, C.; Yoon, Z. S.; Park, M.; Inoue, H.; Kim, D.; Osuka, A. *J. Am. Chem. Soc.* **2005**, *127*, 534.
(405) Brunsveld, L.; Schenning, A. P. H. J.; Broeren, M. A. C.; Janssen, H. M.; Vekemans, J. A. J. M.; Meijer, E. W. *Chem. Lett.* **2000**, 292.
(406) Lightfoot, M. P.; Mair, F. S.; Pritchard, R. G.; Warren, J. E. *Chem. Commun.* **1999**, 1945.
(407) Wilson, A. J.; Masuda, M.; Sijbesma, R. P.; Meijer, E. W. *Angew. Chem., Int. Ed.* **2005**, *44*, 2275.
(408) Onouchi, H.; Miyagawa, T.; Morino, K.; Yashima, E. *Angew. Chem., Int. Ed.* **2006**, *45*, 2381.
(409) Miyagawa, T.; Yamamoto, M.; Muraki, R.; Onouchi, H.; Yashima, E. *J. Am. Chem. Soc.* **2007**, *129*, 3676.
(410) Hannah, K. C.; Armitage, B. A. *Acc. Chem. Res.* **2004**, *37*, 845.
(411) Pohl, F. M.; Jovin, T. M. *J. Mol. Biol.* **1972**, *67*, 375.
(412) Bradbury, E. M.; Carpenter, B. G.; Goldman, H. *Biopolymers* **1968**, *6*, 837.
(413) Toriumi, H.; Saso, N.; Yasumoto, Y.; Sasaki, S.; Uematsu, I. *Polym. J.* **1979**, *11*, 977.
(414) Sasaki, S.; Yasumoto, Y.; Uematsu, I. *Macromolecules* **1981**, *14*, 1797.
(415) Watanabe, J.; Okamoto, S.; Abe, A. *Liq. Cryst.* **1993**, *15*, 259.

(416) Abe, A.; Okamoto, S.; Kimura, N.; Tamura, K.; Onigawara, H.; Watanabe, J. *Acta Polym.* **1993**, *44*, 54.
(417) Watanabe, J.; Okamoto, S.; Satoh, K.; Sakajiri, K.; Furuya, H.; Abe, A. *Macromolecules* **1996**, *29*, 7084.
(418) Sakajiri, K.; Saeki, S.; Kawauchi, S.; Watanabe, J. *Polym. J.* **2000**, *32*, 803.
(419) Abe, A.; Hiraga, K.; Imada, Y.; Hiejima, T.; Furuya, H. *Peptide Sci.* **2005**, *80*, 249.
(420) Ha, S. C.; Lowenhaupt, K.; Rich, A.; Kim, Y.-G.; Kim, K. K. *Nature* **2005**, *437*, 1183.
(421) Ute, K.; Oka, K.; Okamoto, Y.; Hatada, K.; Xi, F.; Vogl, O. *Polym. J.* **1991**, *23*, 1419.
(422) Tabei, J.; Nomura, R.; Sanda, F.; Masuda, T. *Macromolecules* **2004**, *37*, 1175.
(423) Tabei, J.; Nomura, R.; Masuda, T. *Macromolecules* **2003**, *36*, 573.
(424) Nakako, H.; Nomura, R.; Masuda, T. *Macromolecules* **2001**, *34*, 1496.
(425) Hino, K.; Maeda, K.; Okamoto, Y. *J. Phys. Org. Chem.* **2000**, *13*, 361.
(426) Maeda, K.; Okamoto, Y. *Macromolecules* **1998**, *31*, 5164.
(427) Tang, K.; Green, M. M.; Cheon, K. S.; Selinger, J. V.; Garetz, B. A. *J. Am. Chem. Soc.* **2003**, *125*, 7313.
(428) Cheon, K. S.; Selinger, J. V.; Green, M. M. *Angew. Chem., Int. Ed.* **2000**, *39*, 1482.
(429) Ohira, A.; Kunitake, M.; Fujiki, M.; Naito, M.; Saxena, A. *Chem. Mater.* **2004**, *16*, 3919.
(430) Koe, J. R.; Fujiki, M.; Motonaga, M.; Nakashima, H. *Chem. Commun.* **2000**, 389.
(431) Fujiki, M. *J. Am. Chem. Soc.* **2000**, *122*, 3336.
(432) Sanda, F.; Terada, K.; Masuda, T. *Macromolecules* **2005**, *38*, 8149.
(433) Tabei, J.; Nomura, R.; Shiotsuki, M.; Sanda, F.; Masuda, T. *Macromol. Chem. Phys.* **2005**, *206*, 323.
(434) Sakurai, S.-i.; Okoshi, K.; Kumaki, J.; Yashima, E. *J. Am. Chem. Soc.* **2006**, *128*, 5650.
(435) Zhao, H. C.; Sanda, F.; Masuda, T. *Macromol. Chem. Phys.* **2005**, *206*, 1653.
(436) Zhao, H. C.; Sanda, F.; Masuda, T. *Polymer* **2005**, *46*, 2841.
(437) Fujiki, M.; Koe, J. R.; Motonaga, M.; Nakashima, H.; Terao, K.; Teramoto, A. *J. Am. Chem. Soc.* **2001**, *123*, 6253.
(438) Maeda, K.; Kamiya, N.; Yashima, E. *Chem.—Eur. J.* **2004**, *10*, 4000.
(439) Okamoto, Y.; Nakano, T.; Ono, E.; Hatada, K. *Chem. Lett.* **1991**, 525.
(440) Otsuka, I.; Sakai, R.; Satoh, T.; Kakuchi, R.; Kaga, H.; Kakuchi, T. *J. Polym. Sci., Part A: Polym. Chem.* **2005**, *43*, 5855.
(441) Otsuka, I.; Sakai, R.; Kakuchi, R.; Satoh, T.; Kakuchi, T. *Eur. Polym. J.* **2008**, *44*, 2971.
(442) Fukushima, T.; Takachi, K.; Tsuchihara, K. *Macromolecules* **2008**, *41*, 6599.
(443) Ueno, A.; Anzai, J.-i.; Osa, T.; Kadoma, Y. *Bull. Chem. Soc. Jpn.* **1979**, *52*, 549.
(444) Ueno, A.; Takahashi, K.; Anzai, J.; Osa, T. *J. Am. Chem. Soc.* **1981**, *103*, 6410.
(445) Pieroni, O.; Fissi, A.; Angelini, N.; Lenci, F. *Acc. Chem. Res.* **2001**, *34*, 9.
(446) Mayer, S.; Zentel, R. *Prog. Polym. Sci.* **2001**, *26*, 1973.
(447) Maxein, G.; Zentel, R. *Macromolecules* **1995**, *28*, 8438.
(448) Pijper, D.; Feringa, B. L. *Angew. Chem., Int. Ed.* **2007**, *46*, 3693.
(449) Feringa, B. L.; van Delden, R. A.; Koumura, N.; Geertsema, E. M. *Chem. Rev.* **2000**, *100*, 1789.
(450) Pijper, D.; Jongejan, M. G. M.; Meetsma, A.; Feringa, B. L. *J. Am. Chem. Soc.* **2008**, *130*, 4541.
(451) Yashima, E.; Maeda, Y.; Okamoto, Y. *J. Am. Chem. Soc.* **1998**, *120*, 8895.
(452) Morino, K.; Maeda, K.; Yashima, E. *Macromolecules* **2003**, *36*, 1480.
(453) Yashima, E.; Maeda, K.; Sato, O. *J. Am. Chem. Soc.* **2001**, *123*, 8159.
(454) Maeda, K.; Mochizuki, H.; Watanabe, M.; Yashima, E. *J. Am. Chem. Soc.* **2006**, *128*, 7639.
(455) Inai, Y.; Ishida, Y.; Tagawa, K.; Takasu, A.; Hirabayashi, T. *J. Am. Chem. Soc.* **2002**, *124*, 2466.
(456) Waki, M.; Abe, H.; Inouye, M. *Angew. Chem., Int. Ed.* **2007**, *46*, 3059.
(457) Miyake, H.; Kamon, H.; Miyahara, I.; Sugimoto, H.; Tsukube, H. *J. Am. Chem. Soc.* **2008**, *130*, 792.
(458) Miyake, H.; Yoshida, K.; Sugimoto, H.; Tsukube, H. *J. Am. Chem. Soc.* **2004**, *126*, 6524.
(459) Meudtner, R. M.; Hecht, S. *Angew. Chem., Int. Ed.* **2008**, *47*, 4926.
(460) Jiang, H.; Dolain, C.; Leger, J. M.; Gornitzka, H.; Huc, I. *J. Am. Chem. Soc.* **2004**, *126*, 1034.
(461) Nafie, L. A.; Freedman, T. B. In *Circular Dichroism: Principles and Applications*, 2nd ed.; Berova, N., Nakanishi, K., Woody, R. W., Eds.; Wiley-VCH: New York, 2000.
(462) Keiderling, T. A. In *Circular Dichroism: Principles and Applications*, 2nd ed.; Berova, N., Nakanishi, K., Woody, R. W., Eds.; Wiley-VCH: New York, 2000.
(463) Pauling, L.; Corey, R. B. *Proc. Natl. Acad. Sci. U.S.A.* **1951**, *37*, 241.
(464) Schlüter, A. D.; Rabe, J. P. *Angew. Chem., Int. Ed.* **2000**, *39*, 864.
(465) Sheiko, S. S.; Moller, M. *Chem. Rev.* **2001**, *101*, 4099.
(466) Shmueli, U.; Traub, W.; Rosenheck, K. *J. Polym. Sci., Part A-2: Polym. Phys.* **1969**, *7*, 515.
(467) Miller, R. D.; Farmer, B. L.; Fleming, W.; Sooriyakumaran, R.; Rabolt, J. *J. Am. Chem. Soc.* **1987**, *109*, 2509.
(468) Klemann, B.; West, R.; Koutsky, J. A. *Macromolecules* **1993**, *26*, 1042.
(469) Schilling, F. C.; Lovinger, A. J.; Zeigler, J. M.; Davis, D. D.; Bovey, F. A. *Macromolecules* **1989**, *22*, 3055.
(470) KariKari, E. K.; Greso, A. J.; Farmer, B. L.; Miller, R. D.; Rabolt, J. F. *Macromolecules* **1993**, *26*, 3937.
(471) Watanabe, J.; Kamee, H.; Fujiki, M. *Polym. J.* **2001**, *33*, 495.
(472) Okoshi, K.; Kamee, H.; Suzaki, G.; Tokita, M.; Fujiki, M.; Watanabe, J. *Macromolecules* **2002**, *35*, 4556.
(473) Oka, H.; Suzaki, G.; Edo, S.; Suzuki, A.; Tokita, M.; Watanabe, J. *Macromolecules* **2008**, *41*, 7783.
(474) Vogl, O.; Jaycox, G. D.; Kratky, C.; Simonsick, W. J.; Hatada, K. *Acc. Chem. Res.* **1992**, *25*, 408.
(475) Ute, K.; Fukunishi, Y.; Niimi, R.; Iwakura, T.; Hatada, K. *Polym. Prepr. Jpn.* **1996**, *45*, 3284.
(476) Ito, Y.; Ohara, T.; Shima, R.; Suginome, M. *J. Am. Chem. Soc.* **1996**, *118*, 9188.
(477) Aharoni, S. M. *Macromolecules* **1979**, *12*, 94.
(478) Aharoni, S. M. *J. Polym. Sci., Polym. Phys. Ed.* **1979**, *17*, 683.
(479) Metselaar, G. A.; Wezenberg, S. J.; Cornelissen, J. J. L. M.; Nolte, R. J. M.; Rowan, A. E. *J. Polym. Sci., Part A: Polym. Chem.* **2007**, *45*, 981.
(480) Okoshi, K.; Nagai, K.; Kajitani, T.; Sakurai, S.-i.; Yashima, E. *Macromolecules* **2008**, *41*, 7752.
(481) Aharoni, S. M. *J. Macromol. Sci.: Phys.* **1982**, *B21*, 105.
(482) Bieglé, A.; Mathis, A.; Galin, J.-C. *Macromol. Chem. Phys.* **2000**, *201*, 113.
(483) Kajitani, T.; Onouchi, H.; Sakurai, S.-i.; Nagai, K.; Okoshi, K.; Onitsuka, K.; Yashima, E. Unpublished results.
(484) Kim, J.; Novak, B. M.; Waddon, A. J. *Macromolecules* **2004**, *37*, 1660.
(485) Kim, J.; Novak, B. M.; Waddon, A. J. *Macromolecules* **2004**, *37*, 8286.
(486) Tian, G. L.; Lu, Y. J.; Novak, B. M. *J. Am. Chem. Soc.* **2004**, *126*, 4082.
(487) Ito, Y.; Ihara, E.; Uesaka, T.; Murakami, M. *Macromolecules* **1992**, *25*, 6711.
(488) Hoshikawa, N.; Yamamoto, C.; Hotta, Y.; Okamoto, Y. *Polym. J.* **2006**, *38*, 1258.
(489) Okoshi, K.; Saxena, A.; Fujiki, M.; Suzaki, G.; Watanabe, J.; Tokita, M. *Mol. Cryst. Liq. Cryst.* **2004**, *419*, 57.
(490) Okoshi, K.; Saxena, A.; Naito, M.; Suzaki, G.; Tokita, M.; Watanabe, J.; Fujiki, M. *Liq. Cryst.* **2004**, *31*, 279.
(491) Okoshi, K.; Suzuki, A.; Tokita, M.; Fujiki, M.; Watanabe, J. *Macromolecules* **2009**, *42*, 3443.
(492) Weber, P.; Guillon, D.; Skoulios, A.; Miller, R. D. *J. Phys. (Paris)* **1989**, *50*, 793.
(493) Weber, P.; Guillon, D.; Skoulios, A.; Miller, R. D. *Liq. Cryst.* **1990**, *8*, 825.
(494) Asuke, T.; West, R. *Macromolecules* **1991**, *24*, 343.
(495) Klemann, B. M.; West, R.; Koutsky, J. A. *Macromolecules* **1996**, *29*, 198.
(496) Aharoni, S. M. *J. Polym. Sci., Polym. Phys. Ed.* **1980**, *18*, 1303.
(497) Sato, T.; Sato, Y.; Umemura, Y.; Teramoto, A.; Nagamura, Y.; Wagner, J.; Weng, D. X.; Okamoto, Y.; Hatada, K.; Green, M. M. *Macromolecules* **1993**, *26*, 4551.
(498) Green, M. M.; Zanella, S.; Gu, H.; Sato, T.; Gottarelli, G.; Jha, S. K.; Spada, G. P.; Schoevaars, A. M.; Feringa, B.; Teramoto, A. *J. Am. Chem. Soc.* **1998**, *120*, 9810.
(499) Maxein, G.; Keller, H.; Novak, B. M.; Zentel, R. *Adv. Mater.* **1998**, *10*, 341.
(500) Maxein, G.; Mayer, S.; Zentel, R. *Macromolecules* **1999**, *32*, 5747.
(501) Maeda, K.; Takeyama, Y.; Sakajiri, K.; Yashima, E. *J. Am. Chem. Soc.* **2004**, *126*, 16284.
(502) Nagai, K.; Sakajiri, K.; Maeda, K.; Okoshi, K.; Sato, T.; Yashima, E. *Macromolecules* **2006**, *39*, 5371.
(503) Okoshi, K.; Sakurai, S.-i.; Ohsawa, S.; Kuniaki, J.; Yashima, E. *Angew. Chem., Int. Ed.* **2006**, *45*, 8173.
(504) Okoshi, K.; Kajitani, T.; Nagai, K.; Yashima, E. *Macromolecules* **2008**, *41*, 258.
(505) Yamakawa, H. *Modern Theory of Polymer Solutions*; Harper and Row: New York, 1971.
(506) Yamakawa, H. *Helical Wormlike Chains in Polymer Solutions*; Springer: Berlin, 1997.
(507) Sato, T.; Teramoto, A. *Adv. Polym. Sci.* **1996**, *126*, 85.

(508) Khokhlov, A. R.; Semenov, A. N. *Physica A* **1981**, *108*, 546.
(509) Khokhlov, A. R.; Semenov, A. N. *Physica A* **1982**, *112*, 605.
(510) Samorí, P.; Ecker, C.; Gossl, I.; de Witte, P. A. J.; Cornelissen, J. J. L. M.; Metselaar, G. A.; Otten, M. B. J.; Rowan, A. E.; Nolte, R. J. M.; Rabe, J. P. *Macromolecules* **2002**, *35*, 5290.
(511) Green, M. M.; Gross, R. A.; Schilling, F. C.; Zero, K.; Crosby, C. *Macromolecules* **1988**, *21*, 1839.
(512) Nieh, M.-P.; Goodwin, A. A.; Stewart, J. R.; Novak, B. M.; Hoagland, D. A. *Macromolecules* **1998**, *31*, 3151.
(513) Terao, K.; Terao, Y.; Teramoto, A.; Nakamura, N.; Fujiki, M.; Sato, T. *Macromolecules* **2001**, *34*, 4519.
(514) Terao, K.; Terao, Y.; Teramoto, A.; Nakamura, N.; Terakawa, I.; Sato, T.; Fujiki, M. *Macromolecules* **2001**, *34*, 2682.
(515) Natsume, T.; Wu, L.; Sato, T.; Terao, K.; Teramoto, A.; Fujiki, M. *Macromolecules* **2001**, *34*, 7899.
(516) Cotts, P. M. *J. Polym. Sci., Part B: Polym. Phys.* **1994**, *32*, 771.
(517) Cotts, P. M.; Ferline, S.; Dagli, G.; Pearson, D. S. *Macromolecules* **1991**, *24*, 6730.
(518) Conio, G.; Bianchi, E.; Ciferri, A.; Krigbaum, W. R. *Macromolecules* **1984**, *17*, 856.
(519) Itou, T.; Chikiri, H.; Teramoto, A.; Aharoni, S. M. *Polym. J.* **1988**, *20*, 143.
(520) Murakami, H.; Norisuye, T.; Fujita, H. *Macromolecules* **1980**, *13*, 345.
(521) Kuwata, M.; Murakami, H.; Norisuye, T.; Fujita, H. *Macromolecules* **1984**, *17*, 2731.
(522) Gu, H.; Nakamura, Y.; Sato, T.; Teramoto, A.; Green, M. M.; Andreola, C. *Polymer* **1999**, *40*, 849.
(523) Green, M. M.; Gross, R. A.; Crosby, C.; Schilling, F. C. *Macromolecules* **1987**, *20*, 992.
(524) Yen, C.-C.; Tokita, M.; Park, B.; Takezoe, H.; Watanabe, J. *Macromolecules* **2006**, *39*, 1313.
(525) Saito, T.; Iso, N.; Mizuno, H.; Onda, N.; Yamato, H.; Odashima, H. *Biopolymers* **1982**, *21*, 715.
(526) Kashiwagi, Y.; Norisuye, T.; Fujita, H. *Macromolecules* **1981**, *14*, 1220.
(527) Yanaki, T.; Norisuye, T.; Fujita, H. *Macromolecules* **1980**, *13*, 1462.
(528) Godfrey, J. E.; Eisenberg, H. *Biophys. Chem.* **1976**, *5*, 301.
(529) Sato, T.; Norisuye, T.; Fujita, H. *Polym. J.* **1984**, *16*, 341.
(530) Hase, Y.; Ishikawa, M.; Muraki, R.; Maeda, K.; Yashima, E. *Macromolecules* **2006**, *39*, 6003.
(531) Hase, Y.; Nagai, K.; Iida, H.; Maeda, K.; Ochi, N.; Sawabe, K.; Sakajiri, K.; Okoshi, K.; Yashima, E. *J. Am. Chem. Soc.* **2009**, *131*, 10719.
(532) Percec, V.; Rudick, J. G.; Peterca, M.; Heiney, P. A. *J. Am. Chem. Soc.* **2008**, *130*, 7503.
(533) Harada, N.; Nakanishi, K. *Circular Dichroic Spectroscopy-Exciton Coupling in Organic Stereochemistry*; University Science Books: Mill Valley, CA, 1983.
(534) Nakanish, K.; Berova, N. In *Circular Dichroism: Principles and Applications*, 2nd ed.; Nakanishi, K., Berova, N., Woody, R. W., Eds.; Wiley-VCH: New York, 2000.
(535) Tabei, J.; Shiotsuki, M.; Sanda, F.; Masuda, T. *Macromolecules* **2005**, *38*, 9448.
(536) Cornelissen, J. J. L. M.; Sommerdijk, N. A. J. M.; Nolte, R. J. M. *Macromol. Chem. Phys.* **2002**, *203*, 1625.
(537) Beijnen, A. J. M. V.; Nolte, R. J. M.; Drenth, W.; Hezemans, A. M. F. *Tetrahedron* **1976**, *32*, 2017.
(538) Suzuki, Y.; Tabei, J.; Shiotsuki, M.; Inai, Y.; Sanda, F.; Masuda, T. *Macromolecules* **2008**, *41*, 1086.
(539) Kaneko, T.; Umeda, Y.; Yamamoto, T.; Teraguchi, M.; Aoki, T. *Macromolecules* **2005**, *38*, 9420.
(540) Buffeteau, T.; Ducasse, L.; Poniman, L.; Delsuc, N.; Huc, I. *Chem. Commun.* **2006**, 2714.
(541) Ratner, B. D.; Tsukruk, V. V. *Scanning Probe Microscopy of Polymers*; American Chemical Society: Washington, DC, 1998.
(542) Maaloum, M. *Eur. Biophys. J.* **2003**, *32*, 585.
(543) Hansma, H. G.; Laney, D. E.; Bezanilla, M.; Sinsheimer, R. L.; Hansma, P. K. *Biophys. J.* **1995**, *68*, 1672.
(544) Maeda, Y.; Matsumoto, T.; Tanaka, H.; Kawai, T. *Jpn. J. Appl. Phys.* **1999**, *38*, L1211.
(545) Tanaka, H.; Hamai, C.; Kanno, T.; Kawai, T. *Surf. Sci.* **1999**, *432*, L611.
(546) Shinohara, K.; Yasuda, S.; Kato, G.; Fujita, M.; Shigekawa, H. *J. Am. Chem. Soc.* **2001**, *123*, 3619.
(547) Sakurai, S.-i.; Ohira, A.; Suzuki, Y.; Fujito, R.; Nishimura, T.; Kunitake, M.; Yashima, E. *J. Polym. Sci., Part A: Polym. Chem.* **2004**, *42*, 4621.
(548) Sakurai, S.-i.; Kuroyanagi, K.; Morino, K.; Kunitake, M.; Yashima, E. *Macromolecules* **2003**, *36*, 9670.
(549) Sakurai, S.-i.; Kuroyanagi, K.; Nonokawa, R.; Yashima, E. *J. Polym. Sci., Part A: Polym. Chem.* **2004**, *42*, 5838.
(550) Kumaki, J.; Sakurai, S.-i.; Yashima, E. *Chem. Soc. Rev.* **2009**, *38*, 737.
(551) Sakurai, S.-i.; Okoshi, K.; Kumaki, J.; Yashima, E. *Angew. Chem., Int. Ed.* **2006**, *45*, 1245.
(552) Drenth, W.; Nolte, R. J. M. *Acc. Chem. Res.* **1979**, *12*, 30.
(553) Millich, F. *J. Polym Sci., Macromol. Rev.* **1980**, *15*, 207.
(554) Millich, F.; Hellmuth, E. W.; Huang, S. Y. *J. Polym. Sci.: Polym. Chem. Ed.* **1975**, *13*, 2143.
(555) Wu, Z.-Q.; Nagai, K.; Banno, M.; Okoshi, K.; Onitsuka, K.; Yashima, E. *J. Am. Chem. Soc.* **2009**, *131*, 6708.
(556) Kusanagi, H.; Tadokoro, H.; Chatani, Y. *Macromolecules* **1976**, *9*, 531.
(557) Kumaki, J.; Kawauchi, T.; Yashima, E. *J. Am. Chem. Soc.* **2005**, *127*, 5788.
(558) Kusuyama, H.; Miyamoto, N.; Chatani, Y.; Tadokoro, H. *Polym. Commun.* **1983**, *24*, 119.
(559) Sugaya, H.; Sakai, Y. *Contrib. Nephrol.* **1998**, *125*, 1.
(560) Schomaker, E.; Challa, G. *Macromolecules* **1989**, *22*, 3337.
(561) Brinkhuis, R. H. G.; Schouten, A. J. *Macromolecules* **1992**, *25*, 2725.
(562) Kumaki, J.; Kawauchi, T.; Ute, K.; Kitayama, T.; Yashima, E. *J. Am. Chem. Soc.* **2008**, *130*, 6373.
(563) Jahnke, E.; Lieberwirth, I.; Severin, N.; Rabe, J. P.; Frauenrath, H. *Angew. Chem., Int. Ed.* **2006**, *45*, 5383.
(564) Lee, C. C.; Grenier, C.; Meijer, E. W.; Schenning, A. P. H. J. *Chem. Soc. Rev.* **2009**, *38*, 671.
(565) Gunari, N.; Cong, Y.; Zhang, B.; Fischer, K.; Janshoff, A.; Schmidt, M. *Macromol. Rapid Commun.* **2008**, *29*, 821.
(566) Jiménez, J. L.; Nettleton, E. J.; Bouchard, M.; Robinson, C. V.; Dobson, C. M.; Saibil, H. R. *Proc. Natl. Acad. Sci., U. S. A.* **2002**, *99*, 9196.
(567) Ionescu-Zanetti, C.; Khurana, R.; Gillespie, J. R.; Petrick, J. S.; Trabachino, L. C.; Minert, L. J.; Carter, S. A.; Fink, A. L. *Proc. Natl. Acad. Sci., U. S. A.* **1999**, *96*, 13175.
(568) Koga, T.; Matsuoka, M.; Higashi, N. *J. Am. Chem. Soc.* **2005**, *127*, 17596.
(569) Krappe, U.; Stadler, R.; Voigt-Martin, I. *Macromolecules* **1995**, *28*, 4558.
(570) Elbs, H.; Drummer, C.; Abetz, V.; Krausch, G. *Macromolecules* **2002**, *35*, 5570.
(571) Ho, R.-M.; Chiang, Y.-W.; Tsai, C.-C.; Lin, C.-C.; Ko, B.-T.; Huang, B.-H. *J. Am. Chem. Soc.* **2004**, *126*, 2704.
(572) Chiang, Y.-W.; Ho, R.-M.; Ko, B.-T.; Lin, C.-C. *Angew. Chem., Int. Ed.* **2005**, *44*, 7969.
(573) Chiang, Y.-W.; Ho, R.-M.; Thomas, E. L.; Burger, C.; Hsiao, B. S. *Adv. Funct. Mater.* **2009**, *19*, 448.
(574) Tseng, W.-H.; Chen, C.-K.; Chiang, Y.-W.; Ho, R.-M.; Akasaka, S.; Hasegawa, H. *J. Am. Chem. Soc.* **2009**, *131*, 1356.
(575) Cornelissen, J. J. L. M.; Fischer, M.; Sommerdijk, N. A. J. M.; Nolte, R. J. M. *Science* **1998**, *280*, 1427.
(576) Malashkevich, V. N.; Kammerer, R. A.; Efimov, V. P.; Schulthess, T.; Engel, J. *Science* **1996**, *274*, 761.
(577) Schlaad, H.; Krasia, T.; Antonietti, M. *J. Am. Chem. Soc.* **2004**, *126*, 11307.
(578) Li, C. Y.; Cheng, S. Z. D.; Ge, J. J.; Bai, F.; Zhang, J. Z.; Mann, I. K.; Chien, L. C.; Harris, F. W.; Lotz, B. *J. Am. Chem. Soc.* **2000**, *122*, 72.
(579) Li, C. Y.; Yan, D.; Cheng, S. Z. D.; Bai, F.; He, T.; Chien, L. C.; Harris, F. W.; Lotz, B. *Macromolecules* **1999**, *32*, 524.
(580) Lotz, B.; Cheng, S. Z. D. *Polymer* **2005**, *46*, 577.
(581) Li, C. Y.; Cheng, S. Z. D.; Weng, X.; Ge, J. J.; Bai, F.; Zhang, J. Z.; Calhoun, B. H.; Harris, F. W.; Chien, L.-C.; Lotz, B. *J. Am. Chem. Soc.* **2001**, *123*, 2462.
(582) Li, B. S.; Cheuk, K. K. L.; Salhi, F.; Lam, J. W. Y.; Cha, J. A. K.; Xiao, X. D.; Bai, C. L.; Tang, B. Z. *Nano Lett.* **2001**, *1*, 323.
(583) Yan, Y.; Yu, Z.; Huang, Y. W.; Yuan, W. X.; Wei, Z. X. *Adv. Mater.* **2007**, *19*, 3353.
(584) Yan, Y.; Deng, K.; Yu, Z.; Wei, Z. *Angew. Chem., Int. Ed.* **2009**, *48*, 2003.
(585) Constable, E. C. *Tetrahedron* **1992**, *48*, 10013.
(586) Albrecht, M. *Chem. Rev.* **2001**, *101*, 3457.
(587) Huc, I. *Eur. J. Org. Chem.* **2004**, 17.
(588) Amemiya, R.; Yamaguchi, M. *Org. Biomol. Chem.* **2008**, *6*, 26.
(589) Haldar, D.; Schmuck, C. *Chem. Soc. Rev.* **2009**, *38*, 363.
(590) Lehn, J. M.; Rigault, A.; Siegel, J.; Harrowfield, J.; Chevrier, B.; Moras, D. *Proc. Natl. Acad. Sci. U. S. A.* **1987**, *84*, 2565.
(591) Koert, U.; Harding, M. M.; Lehn, J. M. *Nature* **1990**, *346*, 339.
(592) Zarges, W.; Hall, J.; Lehn, J. M.; Bolm, C. *Helv. Chim. Acta* **1991**, *74*, 1843.
(593) Woods, C. R.; Benaglia, M.; Cozzi, F.; Siegel, J. S. *Angew. Chem., Int. Ed. Engl.* **1996**, *35*, 1830.
(594) Annunziata, R.; Benaglia, M.; Cinquini, M.; Cozzi, F.; Woods, C. R.; Siegel, J. S. *Eur. J. Org. Chem.* **2001**, 173.

(595) Orita, A.; Nakano, T.; An, D. L.; Tanikawa, K.; Wakamatsu, K.; Otera, J. *J. Am. Chem. Soc.* **2004**, *126*, 10389.
(596) Hasenknopf, B.; Lehn, J. M. *Helv. Chim. Acta* **1996**, *79*, 1643.
(597) Kramer, R.; Lehn, J. M.; Marquis-Rigault, A. *Proc. Natl. Acad. Sci. U. S. A.* **1993**, *90*, 5394.
(598) Allouche, L.; Marquis, A.; Lehn, J.-M. *Chem.—Eur. J.* **2006**, *12*, 7520.
(599) Smith, V. C. M.; Lehn, J.-M. *Chem. Commun.* **1996**, 2733.
(600) Hasenknopf, B.; Lehn, J.-M.; Baum, G.; Fenske, D. *Proc. Natl. Acad. Sci. U. S. A.* **1996**, *93*, 1397.
(601) Marquis, A.; Smith, V.; Harrowfield, J.; Lehn, J.-M.; Herschbach, H.; Sanvito, R.; Leize-Wagner, E.; Van Dorsselaer, A. *Chem.—Eur. J.* **2006**, *12*, 5632.
(602) Bell, T. W.; Jousselin, H. *Nature* **1994**, *367*, 441.
(603) Psillakis, E.; Jeffery, J. C.; McCleverty, J. A.; Ward, M. D. *Chem. Commun.* **1997**, 479.
(604) Dietrich-Buchecker, C.; Sauvage, J.-P. *Chem. Commun.* **1999**, 615.
(605) Katagiri, H.; Miyagawa, T.; Furusho, Y.; Yashima, E. *Angew. Chem., Int. Ed.* **2006**, *45*, 1741.
(606) Williams, A. F.; Piguet, C.; Bernardinelli, G. *Angew. Chem., Int. Ed. Engl.* **1991**, *103*, 1490.
(607) Charbonniere, L. J.; Bernardinelli, G.; Piguet, C.; Sargeson, A. M.; Williams, A. F. *J. Chem. Soc., Chem. Commun.* **1994**, 1419.
(608) Kramer, R.; Lehn, J. M.; De Cian, A.; Fischer, J. *Angew. Chem., Int. Ed. Engl.* **1993**, *32*, 703.
(609) Dietrich-Buchecker, C. O.; Sauvage, J. P. *Angew. Chem., Int. Ed. Engl.* **1989**, *28*, 189.
(610) Dietrich-Buchecker, C. O.; Guilhem, J.; Pascard, C.; Sauvage, J. P. *Angew. Chem., Int. Ed. Engl.* **1990**, *29*, 1154.
(611) Dietrich-Buchecker, C. O.; Sauvage, J.-P.; De Cian, A.; Fischer, J. *J. Chem. Soc., Chem. Commun.* **1994**, 2231.
(612) Rapenne, G.; Dietrich-Buchecker, C.; Sauvage, J.-P. *J. Am. Chem. Soc.* **1996**, *118*, 10932.
(613) Dietrich-Buchecker, C.; Rapenne, G.; Sauvage, J.-P.; De Cian, A.; Fischer, J. *Chem.—Eur. J.* **1999**, *5*, 1432.
(614) Berl, V.; Huc, I.; Khoury, R. G.; Lehn, J.-M. *Chem.—Eur. J.* **2001**, *7*, 2810.
(615) Jiang, H.; Maurizot, V.; Huc, I. *Tetrahedron* **2004**, *60*, 10029.
(616) Haldar, D.; Jiang, H.; Leger, J.-M.; Huc, I. *Angew. Chem., Int. Ed.* **2006**, *45*, 5483.
(617) Haldar, D.; Jiang, H.; Leger, J.-M.; Huc, I. *Tetrahedron* **2007**, *63*, 6322.
(618) Dolain, C.; Zhan, C.; Leger, J.-M.; Daniels, L.; Huc, I. *J. Am. Chem. Soc.* **2005**, *127*, 2400.
(619) Zhan, C.; Leger, J.-M.; Huc, I. *Angew. Chem., Int. Ed.* **2006**, *45*, 4625.
(620) Berni, E.; Kauffmann, B.; Bao, C.; Lefeuvre, J.; Bassani, D. M.; Huc, I. *Chem.—Eur. J.* **2007**, *13*, 8463.
(621) Gan, Q.; Bao, C.; Kauffmann, B.; Grelard, A.; Xiang, J.; Liu, S.; Huc, I.; Jiang, H. *Angew. Chem., Int. Ed.* **2008**, *47*, 1715.
(622) Shirude, P. S.; Gillies, E. R.; Ladame, S.; Godde, F.; Shin-ya, K.; Huc, I.; Balasubramanian, S. *J. Am. Chem. Soc.* **2007**, *129*, 11890.
(623) Gillies, E. R.; Deiss, F.; Staedel, C.; Schmitter, J.-M.; Huc, I. *Angew. Chem., Int. Ed.* **2007**, *46*, 4081.
(624) Prins, L. J.; Reinhoudt, D. N.; Timmerman, P. *Angew. Chem., Int. Ed.* **2001**, *40*, 2382.
(625) Sanford, A. R.; Yamato, K.; Yang, X.; Yuan, L.; Han, Y.; Gong, B. *Eur. J. Biochem.* **2004**, *271*, 1416.
(626) Tanaka, Y.; Katagiri, H.; Furusho, Y.; Yashima, E. *Angew. Chem., Int. Ed.* **2005**, *44*, 3867.
(627) Li, J.; Wisner, J. A.; Jennings, M. C. *Org. Lett.* **2007**, *9*, 3267.
(628) Maeda, T.; Furusho, Y.; Sakurai, S.-I.; Kumaki, J.; Okoshi, K.; Yashima, E. *J. Am. Chem. Soc.* **2008**, *130*, 7938.
(629) Furusho, Y.; Tanaka, Y.; Maeda, T.; Ikeda, M.; Yashima, E. *Chem. Commun.* **2007**, 3174.
(630) Furusho, Y.; Tanaka, Y.; Yashima, E. *Org. Lett.* **2006**, *8*, 2583.
(631) Ikeda, M.; Tanaka, Y.; Hasegawa, T.; Furusho, Y.; Yashima, E. *J. Am. Chem. Soc.* **2006**, *128*, 6806.
(632) Kim, H.-J.; Lee, E.; Kim, M. G.; Kim, M.-C.; Lee, M.; Sim, E. *Chem.—Eur. J.* **2008**, *14*, 3883.
(633) Yang, Y.; Chen, T.; Xiang, J.-F.; Yan, H.-J.; Chen, C.-F.; Wan, L.-J. *Chem.—Eur. J.* **2008**, *14*, 5742.
(634) Ito, H.; Furusho, Y.; Hasegawa, T.; Yashima, E. *J. Am. Chem. Soc.* **2008**, *130*, 14008.
(635) Hasegawa, T.; Furusho, Y.; Katagiri, H.; Yashima, E. *Angew. Chem., Int. Ed.* **2007**, *46*, 5885.
(636) Katagiri, H.; Tanaka, Y.; Furusho, Y.; Yashima, E. *Angew. Chem., Int. Ed.* **2007**, *46*, 2435.
(637) Kobayashi, N.; Sasaki, S.; Abe, M.; Watanabe, S.; Fukumoto, H.; Yamamoto, T. *Macromolecules* **2004**, *37*, 7986.
(638) Williams, D. J.; Colquhoun, H. M.; O'Mahoney, C. A. *J. Chem. Soc., Chem. Commun.* **1994**, 1643.
(639) Goto, H.; Katagiri, H.; Furusho, Y.; Yashima, E. *J. Am. Chem. Soc.* **2006**, *128*, 7176.
(640) Goto, H.; Furusho, Y.; Miwa, K.; Yashima, E. *J. Am. Chem. Soc.* **2009**, *131*, 4710.
(641) Goto, H.; Furusho, Y.; Yashima, E. *Chem. Commun.* **2009**, 1650.
(642) Goto, H.; Furusho, Y.; Yashima, E. *J. Am. Chem. Soc.* **2007**, *129*, 109.
(643) Goto, H.; Furusho, Y.; Yashima, E. *J. Am. Chem. Soc.* **2007**, *129*, 9168.
(644) Ben, T.; Goto, H.; Miwa, K.; Goto, H.; Morino, K.; Furusho, Y.; Yashima, E. *Macromolecules* **2008**, *41*, 4506.
(645) Ben, T.; Furusho, Y.; Goto, H.; Miwa, K.; Yashima, E. *Org. Biomol. Chem.* **2009**, *7*, 2509.
(646) Sugiura, H.; Nigorikawa, Y.; Saiki, Y.; Nakamura, K.; Yamaguchi, M. *J. Am. Chem. Soc.* **2004**, *126*, 14858.
(647) Amemiya, R.; Saito, N.; Yamaguchi, M. *J. Org. Chem.* **2008**, *73*, 7137.
(648) Sugiura, H.; Amemiya, R.; Yamaguchi, M. *Chem.—Asian J.* **2008**, *3*, 244.
(649) Abe, H.; Machiguchi, H.; Matsumoto, S.; Inouye, M. *J. Org. Chem.* **2008**, *73*, 4650.
(650) Yang, H.-C.; Lin, S.-Y.; Yang, H.-C.; Lin, C.-L.; Tsai, L.; Huang, S.-L.; Chen, I. W.-P.; Chen, C.-h.; Jin, B.-Y.; Luh, T.-Y. *Angew. Chem., Int. Ed.* **2006**, *45*, 726.
(651) Yang, H.-C.; Lee, S.-L.; Chen, C.-h.; Lin, N.-T.; Yang, H.-C.; Jin, B.-Y.; Luh, T.-Y. *Chem. Commun.* **2008**, 6158.
(652) Lin, N.-T.; Lin, S.-Y.; Lee, S.-L.; Chen, C.-h.; Hsu, C.-H.; Hwang, L. P.; Xie, Z.-Y.; Chen, C.-H.; Huang, S.-L.; Luh, T.-Y. *Angew. Chem., Int. Ed.* **2007**, *46*, 4481.
(653) Ghosh, A. K.; Mathivanan, P.; Cappiello, J. *Tetrahedron: Asymmetry* **1998**, *9*, 1.
(654) Nishiyama, H.; Sakaguchi, H.; Nakamura, T.; Horihata, M.; Kondo, M.; Itoh, K. *Organometallics* **1989**, *8*, 846.
(655) Sugimoto, T.; Suzuki, T.; Shinkai, S.; Sada, K. *J. Am. Chem. Soc.* **2007**, *129*, 270.
(656) Sada, K.; Sugimoto, T.; Tani, T.; Tateishi, Y.; Yi, T.; Shinkai, S.; Maeda, H.; Tohnai, N.; Miyata, M. *Chem. Lett.* **2003**, *32*, 758.
(657) Sánchez-Quesada, J.; Seel, C.; Prados, P.; de Mendoza, J.; Dalcol, I.; Giralt, E. *J. Am. Chem. Soc.* **1996**, *118*, 277.
(658) Coles, S. J.; Frey, J. G.; Gale, P. A.; Hursthouse, M. B.; Light, M. E.; Navakhun, K.; Thomas, G. L. *Chem. Commun.* **2003**, 568.
(659) Keegan, J.; Kruger, P. E.; Nieuwenhuyzen, M.; O'Brien, J.; Martin, N. *Chem. Commun.* **2001**, 2192.
(660) Nykypanchuk, D.; Maye, M. M.; van der Lelie, D.; Gang, O. *Nature* **2008**, *451*, 549.
(661) Park, S. Y.; Lytton-Jean, A. K. R.; Lee, B.; Weigand, S.; Schatz, G. C.; Mirkin, C. A. *Nature* **2008**, *451*, 553.
(662) Sharma, J.; Chhabra, R.; Cheng, A.; Brownell, J.; Liu, Y.; Yan, H. *Science* **2009**, *323*, 112.
(663) Chen, C.-L.; Zhang, P.; Rosi, N. L. *J. Am. Chem. Soc.* **2008**, *130*, 13555.
(664) Okamoto, Y.; Yashima, E. *Angew. Chem., Int. Ed.* **1998**, *37*, 1020.
(665) Nakano, T. *J. Chromatogr., A* **2001**, *906*, 205.
(666) Yamamoto, C.; Okamoto, Y. *Bull. Chem. Soc. Jpn.* **2004**, *77*, 227.
(667) Okamoto, Y.; Ikai, T. *Chem. Soc. Rev.* **2008**, *37*, 2593.
(668) Okamoto, Y. *J. Polym. Sci., Part A: Polym. Chem.* **2009**, *47*, 1731.
(669) Nakano, T.; Satoh, Y.; Okamoto, Y. *Macromolecules* **2001**, *34*, 2405.
(670) Haupt, K.; Mosbach, K. *Chem. Rev.* **2000**, *100*, 2495.
(671) Wulff, G. *Chem. Rev.* **2002**, *102*, 1.
(672) Habaue, S.; Satonaka, T.; Nakano, T.; Okamoto, Y. *Polymer* **2004**, *45*, 5095.
(673) Yamagishi, A.; Tanaka, I.; Taniguchi, M.; Takahashi, M. *J. Chem. Soc., Chem. Commun.* **1994**, 1113.
(674) Yashima, E. *J. Chromatogr., A* **2001**, *906*, 105.
(675) Yashima, E.; Yamamoto, C.; Okamoto, Y. *Synlett* **1998**, 344.
(676) Tsuchida, A.; Hasegawa, T.; Kobayashi, K.; Yamamoto, C.; Okamoto, Y. *Bull. Chem. Soc. Jpn.* **2002**, *75*, 2681.
(677) Yashima, E.; Matsushima, T.; Nimura, T.; Okamoto, Y. *Korean Polym. J.* **1996**, *4*, 139.
(678) Liu, R. Y.; Sanda, F.; Masuda, T. *Polymer* **2007**, *48*, 6510.
(679) Liu, R. Y.; Sanda, F.; Masuda, T. *J. Polym. Sci., Part A: Polym. Chem.* **2008**, *46*, 4175.
(680) Aoki, T.; Fukuda, T.; Shinohara, K. I.; Kaneko, T.; Teraguchi, M.; Yagi, M. *J. Polym. Sci., Part A: Polym. Chem.* **2004**, *42*, 4502.
(681) Aoki, T.; Kaneko, T. *Polym. J.* **2005**, *37*, 717.
(682) Tanioka, D.; Takahashi, M.; Teraguchi, M.; Kaneko, T.; Aoki, T. *Polym. Prepr. Jpn.* **2001**, *50*, 3092.
(683) Hadano, S.; Teraguchi, M.; Kaneko, T.; Aoki, T. *Chem. Lett.* **2007**, *36*, 220.
(684) Teraguchi, M.; Suzuki, J.; Kaneko, T.; Aoki, T.; Masuda, T. *Macromolecules* **2003**, *36*, 9694.
(685) Sakai, R.; Otsuka, I.; Satoh, T.; Kakuchi, R.; Kaga, H.; Kakuchi, T. *J. Polym. Sci., Part A: Polym. Chem.* **2006**, *44*, 325.

(686) Benaglia, M.; Puglisi, A.; Cozzi, F. *Chem. Rev.* **2003**, *103*, 3401.
(687) Lu, J.; Toy, P. H. *Chem. Rev.* **2009**, *109*, 815.
(688) Reggelin, M.; Schultz, M.; Holbach, M. *Angew. Chem., Int. Ed.* **2002**, *41*, 1614.
(689) Reggelin, M.; Doerr, S.; Klussmann, M.; Schultz, M.; Holbach, M. *Proc. Natl. Acad. Sci., U. S. A.* **2004**, *101*, 5461.
(690) Müller, C. A.; Hoffart, T.; Holbach, M.; Reggelin, M. *Macromolecules* **2005**, *38*, 5375.
(691) Yamamoto, T.; Suginome, M. *Angew. Chem., Int. Ed.* **2009**, *48*, 539.
(692) Hara, T.; Teraguchi, M.; Kaneko, T.; Aoki, T. *Polym. Prep. Jpn.* **2004**, *53*, 2926.
(693) Yashima, E.; Maeda, Y.; Okamoto, Y. *Polym. J.* **1999**, *31*, 1033.
(694) Sanda, F.; Araki, H.; Masuda, T. *Chem. Lett.* **2005**, *34*, 1642.
(695) Juliá, S.; Masana, J.; Vega, J. C. *Angew. Chem., Int. Ed. Engl.* **1980**, *19*, 929.
(696) Davie, E. A. C.; Mennen, S. M.; Xu, Y.; Miller, S. J. *Chem. Rev.* **2007**, *107*, 5759.
(697) Maeda, K.; Tanaka, K.; Morino, K.; Yashima, E. *Macromolecules* **2007**, *40*, 6783.
(698) Silverman, S. K. *Org. Biomol. Chem.* **2004**, *2*, 2701.
(699) Roelfes, G.; Feringa, B. L. *Angew. Chem., Int. Ed.* **2005**, *44*, 3230.
(700) Roelfes, G.; Boersma, A. J.; Feringa, B. L. *Chem. Commun.* **2006**, 635.
(701) Boersma, A. J.; Feringa, B. L.; Roelfes, G. *Org. Lett.* **2007**, *9*, 3647.
(702) Coquière, D.; Feringa, B.; Roelfes, G. *Angew. Chem., Int. Ed.* **2007**, *46*, 9308.
(703) Boersma, A. J.; Klijn, J. E.; Feringa, B. L.; Roelfes, G. *J. Am. Chem. Soc.* **2008**, *130*, 11783.
(704) Oltra, N. S.; Roelfes, G. *Chem. Commun.* **2008**, 6039.
(705) Boersma, A. J.; Feringa, B. L.; Roelfes, G. *Angew. Chem., Int. Ed.* **2009**, *48*, 3346.
(706) Ewbank, P. C.; Nuding, G.; Suenaga, H.; McCullough, R. D.; Shinkai, S. *Tetrahedron Lett.* **2001**, *42*, 155.
(707) Li, C.; Numata, M.; Hasegawa, T.; Sakurai, K.; Shinkai, S. *Chem. Lett.* **2005**, *34*, 1354.
(708) Li, C.; Numata, M.; Takeuchi, M.; Shinkai, S. *Chem.—Asian J.* **2006**, *1*−*2*, 95.
(709) Haraguchi, S.; Numata, M.; Li, C.; Nakano, Y.; Fujiki, M.; Shinkai, S. *Chem. Lett.* **2009**, *38*, 254.
(710) Haraguchi, S.; Numata, M.; Kaneko, K.; Shinkai, S. *Bull. Chem. Soc. Jpn.* **2008**, *81*, 1002.
(711) Nilsson, K. P. R.; Rydberg, J.; Baltzer, L.; Inganäs, O. *Proc. Natl. Acad. Sci., U. S. A.* **2004**, *101*, 11197.
(712) Nilsson, K. P. R.; Rydberg, J.; Baltzer, L.; Inganäs, O. *Proc. Natl. Acad. Sci., U. S. A.* **2003**, *100*, 10170.
(713) Nilsson, K. P. R.; Inganäs, O. *Nat. Mater.* **2003**, *2*, 419.
(714) Ho, H.-A.; Najari, A.; Leclerc, M. *Acc. Chem. Res.* **2008**, *41*, 168.
(715) Itomi, K.; Kobayashi, S.; Morino, K.; Iida, H.; Yashima, E. *Polym. J.* **2009**, *41*, 108.
(716) Akagi, K.; Piao, G.; Kaneko, S.; Sakamaki, K.; Shirakawa, H.; Kyotani, M. *Science* **1998**, *282*, 1683.
(717) Akagi, K.; Guo, S.; Mori, T.; Goh, M.; Piao, G.; Kyotani, M. *J. Am. Chem. Soc.* **2005**, *127*, 14647.
(718) Goh, M.; Kyotani, M.; Akagi, K. *J. Am. Chem. Soc.* **2007**, *129*, 8519.
(719) Goto, H.; Akagi, K. *Angew. Chem., Int. Ed.* **2005**, *44*, 4322.
(720) Goto, H.; Akagi, K. *J. Polym. Sci., Part A: Polym. Chem.* **2006**, *44*, 1042.
(721) Akagi, K. *Chem. Rev.*, in press.
(722) Ohira, A.; Okoshi, K.; Fujiki, M.; Kunitake, M.; Naito, M.; Hagihara, T. *Adv. Mater.* **2004**, *16*, 1645.

CR900162Q